Brackish Groundwater in the Lipan Aquifer Area, Texas

by Mark C. Robinson, P.G. • Matthew L. Webb • Jean Broce Perez • Alan G. Andrews

Report 384
January 2018

Texas Water Development Board
www.twdb.texas.gov

ERRATA - July 10, 2020

Page 96 –

Replace:

5. Calculate resistivity of water equivalent (R_{we}).
   There are several invasion zone correction formulas that could be used based on the type of geophysical logs used. The following formula shows no correction:

$$\mathbf{R_{we} = R_{mf\_Tf} / (R_{xo}/R_o)}$$

$\mathbf{R_{we}}$ = Resistivity water equivalent (units: ohms-meter)

With:

5. Calculate resistivity of the water (R_w).
   There are several invasion zone correction formulas that could be used based on the type of geophysical logs used. The following formula shows no correction:

$$\mathbf{R_w = R_{mf\_Tf} / (R_{xo}/R_o)}$$

$\mathbf{R_w}$ = Resistivity of water (units: ohms-meter)

Page 97 –

Replace:

6. Calculate resistivity of water from resistivity of water equivalent based on groundwater type correction factor (R_{we_cor}).

$$\mathbf{R_w = R_{we\_cor} \cdot R_{we}}$$

$\mathbf{R_{we}}$ = Resistivity water equivalent (units: ohm-meter)
$\mathbf{R_{we\_cor}}$ = Groundwater type correction factor (units: dimensionless)
$\mathbf{R_w}$ = Resistivity of water (units: ohm-meter)

Note: The following **Rwe_cor** values can be used for water types:

- $\mathbf{R_{we\_cor}}$ = 1.33, for average sodium bicarbonate (Estepp, 2010).
- $\mathbf{R_{we\_cor}}$ = 1.75, for high sodium bicarbonate (Alger, 1966).
- $\mathbf{R_{we\_cor}}$ = 1.1, for average sodium sulfate (Estepp, 2010).
- $\mathbf{R_{we\_cor}}$ = 1.0, for sodium chloride solutions (Estepp, 2010).

For this study, $\mathbf{R_{we\_cor}} = 1$, therefore $\mathbf{R_w} = \mathbf{R_{we}}$.

With:

6. No correction is required for groundwater type with the Alger-Harrison Method (Alger and Harrison, 1989).

Page 139 –

Add:

Alger, R.P., and Harrison, C.W., 1989, Improved fresh water assessment in sand aquifers utilizing geophysical well logs: The Log Analyst, v. 30, no. 1, p. 31-44.

Texas Water Development Board

Report 384

Brackish Groundwater in the Lipan Aquifer Area, Texas

by
Mark C. Robinson, P.G.
Matthew L. Webb
Jean Broce Perez
Alan G. Andrews, P.G.

January 2018

Texas Water Development Board

Geoscientist Seal

The contents of this report (including figures and tables) document the work of the following licensed Texas geoscientist:

Mark C. Robinson, P.G. No. 5649

Mr. Robinson was responsible for working on all aspects of the project and preparing the report. The seal appearing on this document was authorized on December 6, 2017, by

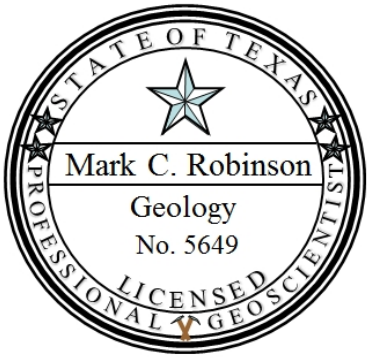

Mark C. Robinson

The contents of this report (including figures and tables) document the work of the following licensed Texas geoscientist:

Alan G. Andrews, P.G. No. 11758

Mr. Andrews created raster surfaces and maps of the hydrostratigraphic units discussed in the report, carried out calculations to determine total dissolved solids concentrations, and compiled the GIS data package associated with the report. The seal appearing on this document was authorized on December 6, 2017, by

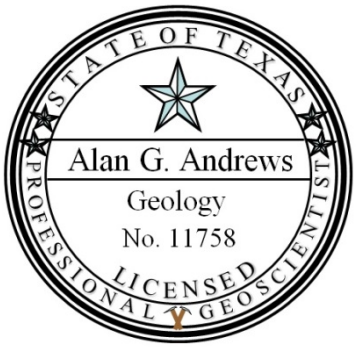

Alan G. Andrews

Cover photo courtesy of Andrea Croskrey

"Yates Formation outcrop, northern Tom Green County, Texas"

Texas Water Development Board

Kathleen Jackson
Member

Peter Lake
Member

To provide leadership, information, education, and support for planning, financial assistance, and outreach for the conservation and responsible development of water for Texas.

Published and distributed by the
Texas Water Development Board
P.O. Box 13231, Capitol Station
Austin, Texas 78711-3231

2018
(Printed on recycled paper)

This page is intentionally blank.

Table of Contents

List of Figures

List of Tables

1. Executive summary

Brackish groundwater is an abundant resource in Texas and recognized as an important supply to meet future water demands. The Texas Water Development Board (TWDB) funded a study that estimated more than 2.7 billion acre-feet of brackish groundwater (with a total dissolved solids concentration of 1,000 to 10,000 milligrams per liter) is available in the state. However, the study was, by design, broad in scope and narrow in its assessment of groundwater quality. To improve on the 2003 study, the TWDB requested and received funding from the 81st Texas Legislature in 2009 to implement the Brackish Resources Aquifer Characterization System (BRACS) program to more thoroughly characterize the brackish aquifers.

The goals of the BRACS program are to (1) map and characterize the brackish parts of the major and minor aquifers of the state in greater detail using existing water well reports, geophysical well logs, and available aquifer data and (2) build datasets that can be used for groundwater exploration and replicable numerical groundwater flow models to estimate aquifer productivity. Since the program's inception, the TWDB completed five internal studies and presently has three ongoing studies. Additionally, the Texas Legislature has appropriated in total $2.1 million to the TWDB to fund three research projects in 2010 and seven aquifer projects in 2015. Continued funding to support work for House Bill 30 was vetoed during the 85th Texas Legislature session, but internal staff continues to work on aquifer studies.

The TWDB chose to study the Lipan Aquifer because of recent severe drought conditions in the area and the growing demand for water in the region. According to the TWDB Precipitation and Lake Evaporation website, the long-term regional annual precipitation in the TWDB-designated precipitation quadrangle number 607, which corresponds to the study area, is 21 inches. However, in 2011, only 6.9 inches of precipitation was reported. Data from the TWDB Water Data for Texas website indicates storage in the four surface water reservoirs that serve San Angelo decreased to less than 13 percent of capacity and, despite high statewide precipitation in 2014 and 2015, surface storage in the area had only increased to 19 percent by 2016.

The Lipan Aquifer, centered around Tom Green County in west central Texas, is one of the 21 minor aquifers in Texas. The study area is 3,850 square miles in size and encompasses the majority of Tom Green County and parts of Coke, Concho, Glasscock, Irion, Runnels, Schleicher, and Sterling counties. It lies entirely within the Region F Regional Water Planning Area and Groundwater Management Area 7 and contains parts of six groundwater conservation districts.

According to the 2016 Region F Regional Water Plan (Freese and Nichols and LBG-Guyton Associates, 2015), Tom Green, Runnels, and Concho counties currently use, or are expected to use, water from the Lipan Aquifer. The Lipan Aquifer currently supplies approximately 23 percent of the total water demand for the area. Annual water demands for these counties are forecast to increase from 81,796 acre-feet to 143,444 acre-feet between 2010 and 2070, while existing drought of record water supplies are forecast to be 85,612 acre-feet by decade 2070. This results in a 57,832 acre-foot need for new water supply by decade 2070.

The Lipan Aquifer is composed of a diverse set of geological units capable of producing brackish groundwater with total dissolved solids between 1,000 and 9,999 milligrams per liter,

defined as slightly saline to moderately saline groundwater. We found that a thin cover of less than 200 feet of Quaternary and Neogene sediments and up to 400 feet of Cretaceous limestone overlie a series of westerly dipping geological formations composed of Permian limestone, dolomite, shale, and siltstone. Groundwater can be found in the weathered portions of most of the Permian formations and throughout younger geological units where wells have been drilled below the static water level.

The Lipan Aquifer has approximately 6.22 million acre-feet of groundwater that can be quantified within three salinity zones: (1) 0.17 million acre-feet of fresh groundwater (0 to 999 milligrams per liter of total dissolved solids), (2) 4.44 million acre-feet of slightly saline groundwater (1,000 to 2,999 milligrams per liter of total dissolved solids), and (3) 1.61 million acre-feet of moderately saline groundwater (3,000 to 9,999 milligrams per liter of total dissolved solids). With the available data, we could not accurately define the bottom depth of very saline groundwater zone (10,000 to 34,999 milligrams per liter of total dissolved solids), but it is expected to be between 500 and 900 feet below ground surface.

The fresh water zone is restricted to the Quaternary-Neogene and Cretaceous formations. The slightly and moderately saline zones transect all Permian formations. A significant portion of any brackish groundwater in the Lipan Aquifer study area is within weathered Permian formations overlain by Cretaceous formations. Although there are only a few instances where water wells have been completed into Permian formations in these areas, the development of brackish groundwater in these areas may represent an untapped resource for entities interested in brackish groundwater desalination.

The TWDB did not designate brackish groundwater production zones in the Lipan Aquifer. House Bill 30 (84th Texas Legislature, 2015) requirements precluded designation because the Lipan Aquifer does not have hydrogeologic barriers separating fresh and brackish groundwater and brackish groundwater is currently serving as a significant source for municipal, domestic, or agricultural purposes.

In order to supply Texas resource planners and policy makers with reliable tools for assessing the aquifer response associated with groundwater use over a 50-year planning period, the Texas Legislature instituted the Groundwater Availability Modeling (GAM) program during the 76th Legislative Session in 1999. In 2005, House Bill 1763 mandated that groundwater conservation districts evaluate and develop the desired future conditions for aquifers within their groundwater management areas, from which managed available groundwater is to be estimated. The Lipan Aquifer GAM was developed in 2005 to meet these objectives. Based upon the hydrogeology detailed in this study, a future GAM can be designed with more accurate predictive capabilities.

We found that despite the large numbers of wells drilled for water and hydrocarbons over the last 70 years within the study area, there are very few records on the water quality and aquifer hydraulic properties of the brackish groundwater intervals. Future efforts to obtain this information from wells drilled through the brackish groundwater formations would be extremely useful in more accurately quantifying this resource.

Study deliverables include a peer-reviewed report, Geographic Information System map files, BRACS Database and data dictionary, and water well and geophysical well log files. All data used for the study is readily available to the public and downloadable from the TWDB website.

2. Introduction

Mapping of Texas' saline water resources dates back to 1956 with the U.S. Geological Survey conducting a high-level study to outline the occurrence, quantity, and quality of saline waters in the state (Winslow and Kister, 1956). The study was part of a national effort to identify new sources for water-scarce areas. In 1970, the TWDB funded a more detailed study "to make a reconnaissance and inventory of the principal saline aquifers in Texas that discussed the salinity, the productivity, and the geology of the aquifers" (Core Laboratories, 1972). In 2003, the TWDB funded a study to map the brackish aquifers and calculate the volume of brackish (slightly to moderately saline) groundwater available in these aquifers (LBG-Guyton Associates, 2003). The study was done to support the regional water planning process and help identify alternative sources to meet water demands. It estimated there is approximately 2.7 billion acre-feet of brackish groundwater in the aquifers in the state (LBG-Guyton Associates, 2003). While the study demonstrated that brackish groundwater is an important resource, it also highlighted the need for detailed aquifer studies.

In 2009, the 81st Texas Legislature provided funding to the TWDB to establish the Brackish Resources Aquifer Characterization System (BRACS). The goal of the program is to map and characterize the brackish portions of the aquifers in Texas in sufficient detail to provide useful information and data to regional water planning groups and other entities interested in using brackish groundwater as a water supply. The TWDB completed the first pilot study on the Pecos Valley Aquifer in West Texas to establish the methods of data analysis for future studies.

In 2010, with legislative funding, the TWDB funded three research projects totaling $449,500 to support the BRACS program (Table 2-1). The first project identified geophysical well logs that could be used to map the geologic structure of aquifers and estimate the salinity of groundwater across Texas. The logs were then scanned into digital images and entered into a database. The BRACS Database now has more than 52,000 logs available (TWDB, 2016a). The second project compiled a bibliography of more than 7,500 reports, articles, and graduate research papers with an emphasis on Texas geologic formations containing brackish groundwater into a relational database. This database serves as a source of reference for evaluating existing geologic information for a project area. The third project assessed computer software capable of modeling different densities of groundwater found in brackish aquifers. A project report and a modeling code selection tool were developed to help users select the appropriate software.

In 2015, the 84th Texas Legislature passed House Bill 30, directing the TWDB to conduct studies to identify and designate brackish groundwater production zones in the state. The legislation directed the TWDB to make designations in four aquifers—the Carrizo-Wilcox Aquifer located between the Colorado River and the Rio Grande, the Gulf Coast Aquifer and sediments bordering that aquifer, the Blaine Aquifer, and the Rustler Aquifer—and to report the designations to the legislature by December 1, 2016. The TWDB selected three additional brackish aquifers (the Trinity, Blossom, and Nacatoch aquifers) to study. The legislation further requires the TWDB to identify and designate brackish groundwater production zones in the remaining aquifers in the state before December 1, 2022. For information on House Bill 30 requirements refer to Section 4. With the passing of House Bill 30, the TWDB funded seven aquifer projects totaling $1.7 million (Table 2-1).

Table 2-1. TWDB-funded projects of the BRACS program.

Report title	Short description	Contractor	Study type	Year funded	Grant amount
Geophysical Well Log Data Collection Project	Geophysical well logs from brackish aquifers in the state were collected from multiple sources, digitized, and entered into a database.	Bureau of Economic Geology	Research	2010	$300,000
Brackish Groundwater Bibliography Project	The project developed a comprehensive bibliography of Texas brackish aquifers.	INTERA, Inc.	Research	2010	$99,500
An Assessment of Modeling Approaches to Brackish Aquifers in Texas	The study assessed groundwater modeling approaches for brackish aquifers.	INTERA, Inc.	Research	2010	$50,000
Identification of Potential Brackish Groundwater Production Areas – Carrizo Aquifer	The project mapped and characterized the aquifer and evaluated the aquifer for potential production areas.	Bureau of Economic Geology	Research	2016	$181,446
Identification of Potential Brackish Groundwater Production Areas – Gulf Coast Aquifer	The project mapped and characterized the aquifer and evaluated the aquifer for potential production areas.	INTERA, Inc.	Research	2016	$500,000
Brackish Groundwater in the Blaine Aquifer System, North Central Texas	The project mapped and characterized the aquifer and evaluated the aquifer for potential production areas.	Daniel B. Stephens & Associates, Inc.	Research	2016	$200,000
Identification of Potential Brackish Groundwater Production Areas – Rustler Aquifer	The project mapped and characterized the aquifer and evaluated the aquifer for potential production areas.	INTERA, Inc.	Research	2016	$200,000
Identification of Potential Brackish Groundwater Production Areas – Blossom Aquifer	The project will map and characterize the aquifer and evaluate the aquifer for potential production areas.	LBG-Guyton	Research	2016	$50,000
Identification of Potential Brackish Groundwater Production Areas – Nacatoch Aquifer	The project will map and characterize the aquifer and evaluate the aquifer for potential production areas.	LBG-Guyton	Research	2016	$150,000
Identification of Potential Brackish Groundwater Production Areas – Trinity Aquifer	The project will map and characterize the aquifer and evaluate the aquifer for potential production areas.	Southwest Research Institute	Research	2016	$400,000

The TWDB has completed five internal studies (Figure 2-1) and presently has three ongoing studies (Figure 2-2). The five completed studies include the Pecos Valley Aquifer in West Texas (Meyer and others, 2012), the Queen City and Sparta aquifers in Atascosa and McMullen counties (Wise, 2014), the Gulf Coast Aquifer in the Corpus Christi area (Meyer, 2012), the Lower Rio Grande Valley (Meyer and others, 2014), and the Lipan Aquifer. The ongoing study for the Wilcox, Carrizo, Queen City, Sparta, and Yegua aquifers in Central Texas (collectively called the Upper Coastal Plain Aquifers) is in the initial stages of analysis. The other two ongoing studies for the Dockum and Edwards-Trinity Plateau aquifers began the initial phase of data collection in the spring of 2017.

For each BRACS study, the TWDB staff collects as much geological, geophysical, and water-well data as is available in the public domain and uses the information to map and characterize both the vertical and horizontal extent of the aquifers in great detail. Groundwater is classified into five salinity classes (Table 2-2): fresh, slightly saline, moderately saline, very saline, and

brine (Winslow and Kister, 1956). The volume of groundwater in each salinity class is estimated based on the three-dimensional mapping of the salinity zones. All project information is entered into the BRACS Database that the TWDB developed to store and analyze the information. The BRACS Database is a Microsoft Access database that is described in a detailed BRACS Database Data Dictionary (Meyer, 2017), which are both downloadable from the TWDB website (www.twdb.texas.gov/innovativewater/bracs/database.asp).

Table 2-2. Groundwater salinity classification used in the study (Winslow and Kister, 1956). Colors used in this table for each salinity classification are consistent throughout the report and GIS datasets.

Groundwater salinity classification	Total dissolved solids concentration (units: milligrams per liter)
Fresh	0 to 999
Slightly saline	1,000 to 2,999
Moderately saline	3,000 to 9,999
Very saline	10,000 to 34,999
Brine	Greater than 35,000

The project deliverables, both the report and data, are available to the public on the TWDB website. The report is organized into various chapters. The data includes raw data in numerous digital formats and processed data in the form of GIS datasets. Digital geophysical well logs used for the studies are available upon request or downloadable from the TWDB Water Data Interactive website (www2.twdb.texas.gov/apps/waterdatainteractive/groundwaterdataviewer).

Information produced from these studies is not intended to serve as a substitute for site-specific evaluations of local aquifer characteristics and groundwater conditions for desalination projects. During design and development of a well field, an entity will need to determine the productivity of the brackish aquifer using monitoring and production wells and groundwater modeling. It is important to note that existing TWDB groundwater models are designed for regional assessment and are not applicable to well field analysis. These models are not constructed to analyze the effect of salinity on groundwater flow and in general should not be used for estimating withdrawal of saline water. Other significant factors an entity should evaluate before developing brackish groundwater are groundwater quantity and quality changes and potential subsidence.

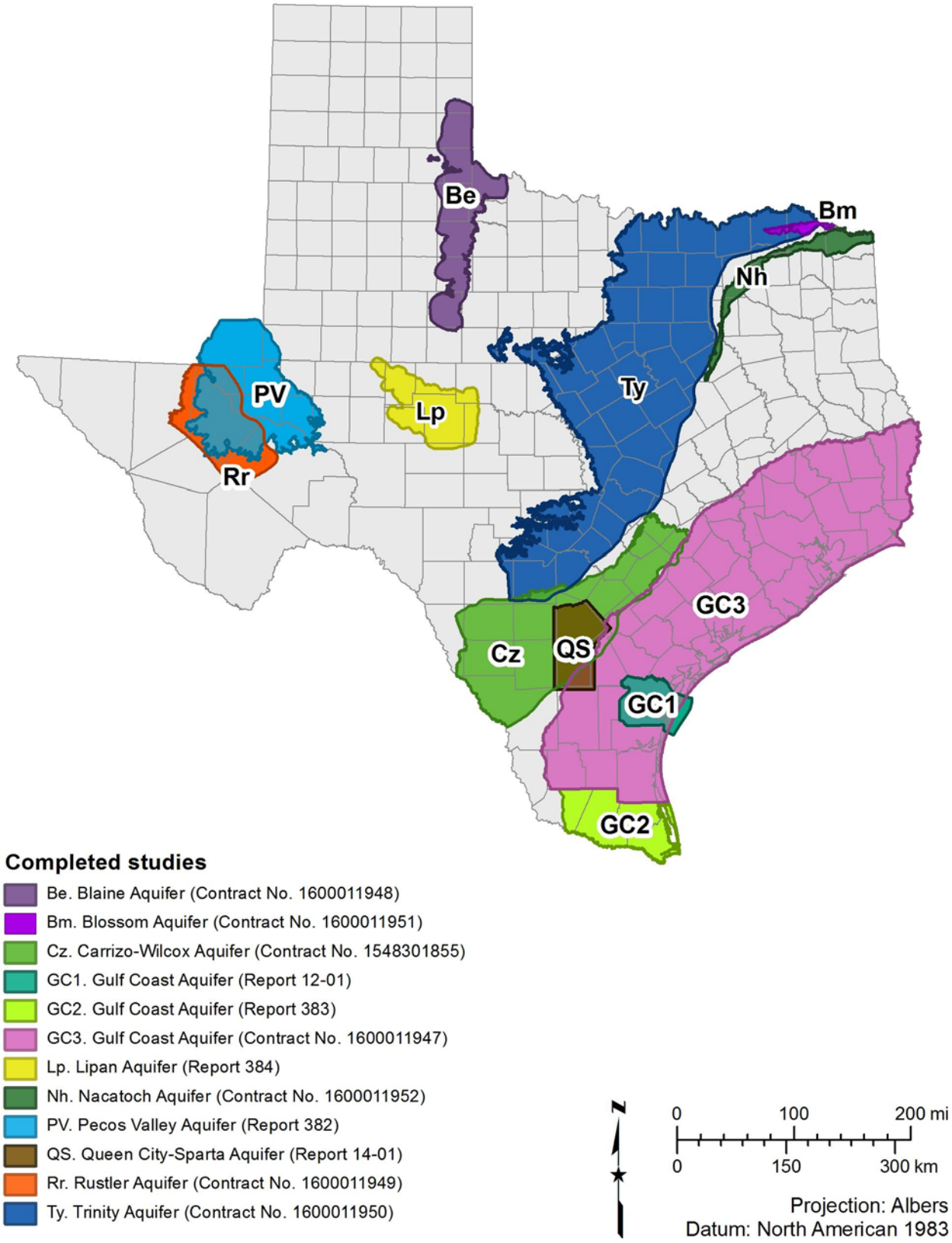

Figure 2-1. Completed studies of the BRACS program.

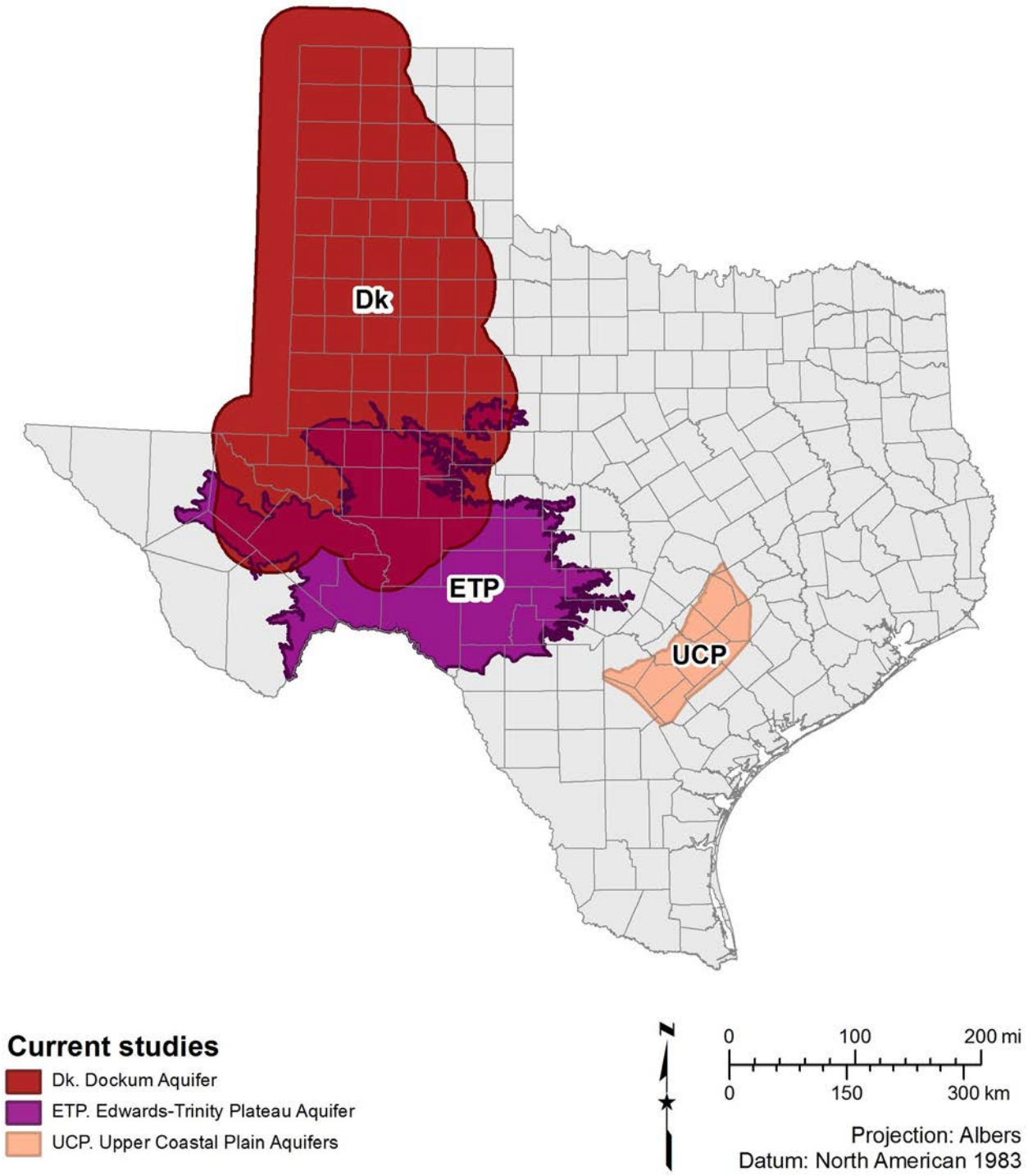

Figure 2-2. Ongoing studies of the BRACS program.

3. Study area

The Lipan Aquifer is one of the 21 minor aquifers in Texas and is centered around Tom Green County in west central Texas. The Lipan Aquifer study area encompasses parts of Coke, Concho, Glasscock, Irion, Runnels, Schleicher, Sterling, and Tom Green counties that are underlain by the Lipan Aquifer. The study area is defined as the area overlying the TWDB-defined extent of the Lipan Aquifer (TWDB, 2007b) and an additional four-mile buffer zone (Figure 3-1). This area encompasses 3,850 square miles. The aquifer consists of Quaternary and Neogene sediments at or near the surface and underlying hydrologically connected Permian formations. Ground-surface elevations range from approximately 2,800 feet to 1,600 feet above mean sea level.

The study area lies entirely within the Region F Regional Water Planning Area and Groundwater Management Area 7 and contains parts of six groundwater conservation districts: (1) Coke County Underground Water Conservation District, (2) Glasscock Groundwater Conservation District, (3) Irion County Water Conservation District, (4) Lipan-Kickapoo Water Conservation District, (5) Plateau Underground Water Conservation and Supply District, and (6) Sterling County Underground Water Conservation District (Figure 3-2).

Cities and the boundaries of the larger public water supply systems in the study area are presented in Figure 3-3. A cross-reference between the public water supply system name, map identification number, and public water supply identification number assigned by the Texas Commission on Environmental Quality is provided in Table 3-1. The public water supply name or identification number can be used to query public water system data from the Texas Commission on Environmental Quality website using the Texas Drinking Water Watch. Source of the water system boundaries is a 2011 study contracted by the TWDB (HDR, 2011) using 2010 data; not all public water supply systems are present in this dataset, and water system boundaries may have changed since this project was completed.

There are no existing desalination facilities in the study area. The 2017 State Water Plan contains two recommended water management strategies proposing to use brackish groundwater in the study area. The water user groups include the City of San Angelo and the Concho Rural Water Supply Corporation (TWDB, 2016c).

Two major (Edwards-Trinity Plateau and Ogallala) and two minor (Dockum and Lipan) aquifers are present in the study area (Figure 3-4). Many of the water wells investigated in the study produce water from the Edwards-Trinity Plateau Aquifer, which overlies the Lipan Aquifer on the south, west, and much of the north perimeter. Some water wells also produce water from the Dockum Aquifer to the west, but to a lesser extent. These wells are used in the study for various purposes, but only data from wells producing from the Lipan Aquifer are included for aquifer performance and water quality evaluation.

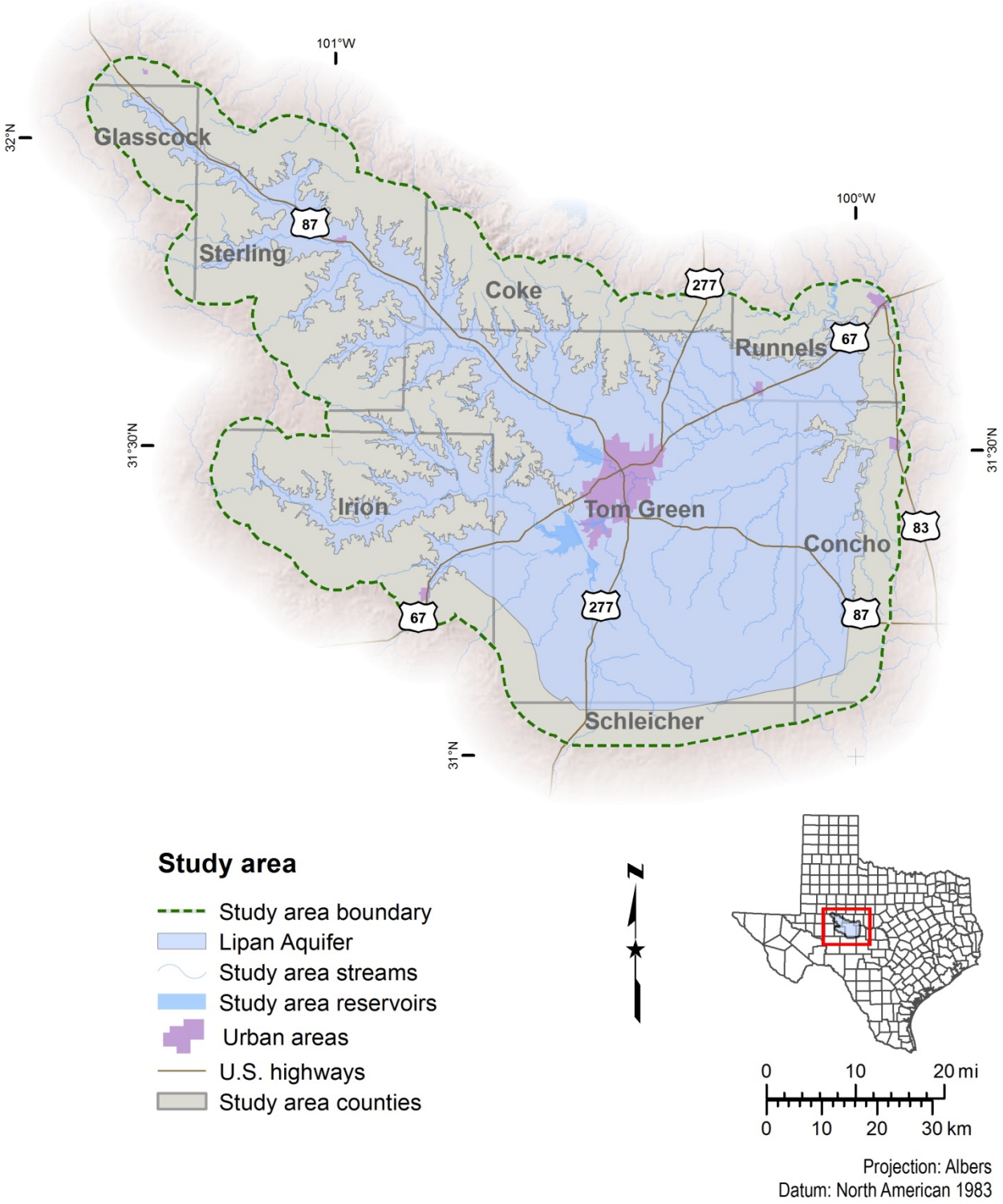

Figure 3-1. **Study area boundary based on the TWDB-established extent of the Lipan Aquifer and a four-mile buffer.**

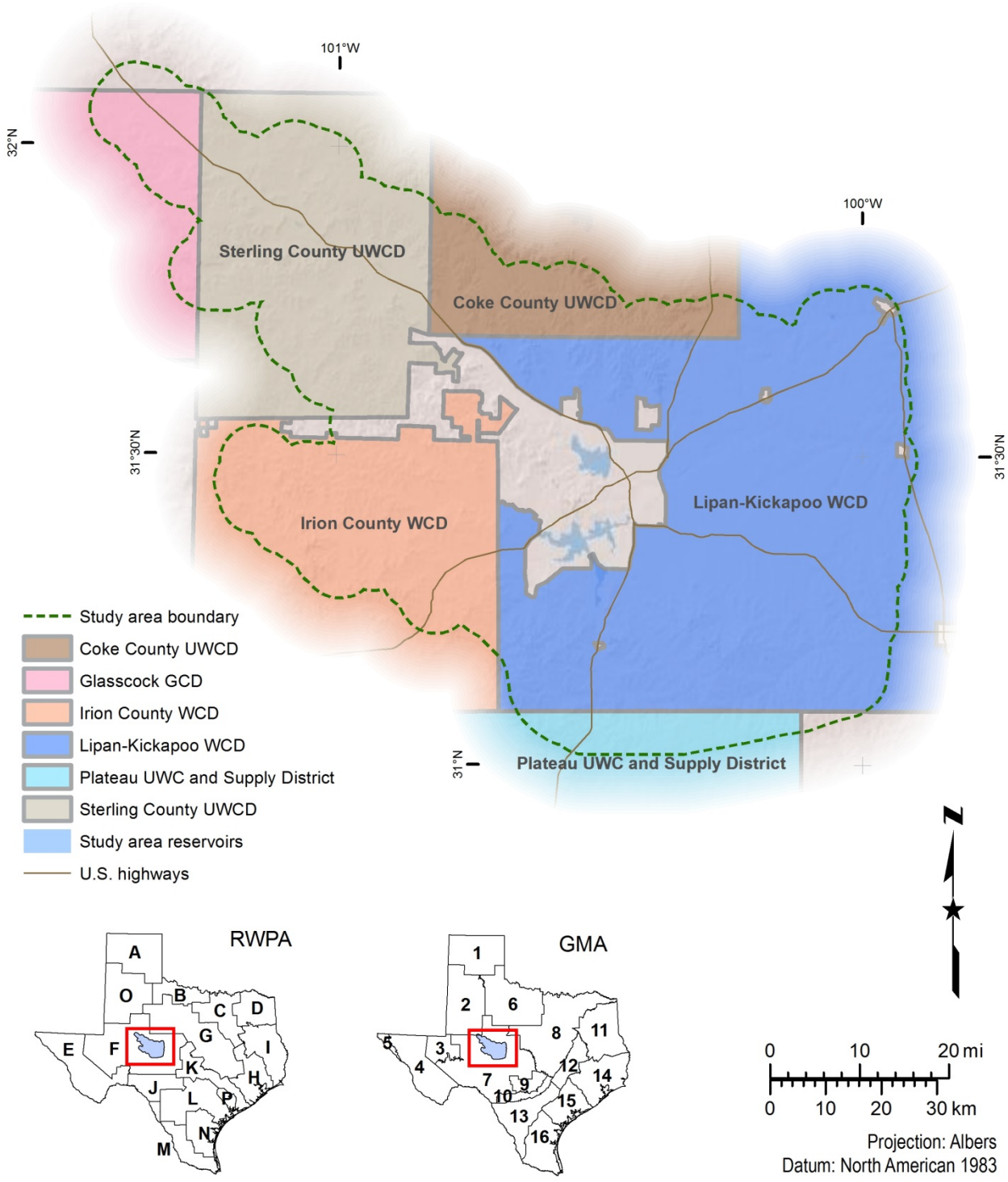

Figure 3-2. **Administrative boundaries within the Lipan Aquifer study area. GCD = groundwater conservation district; GMA = groundwater management area; RWPA = regional water planning area; UWC = underground water conservation; UWCD = underground water conservation; WCD = water conservation district.**

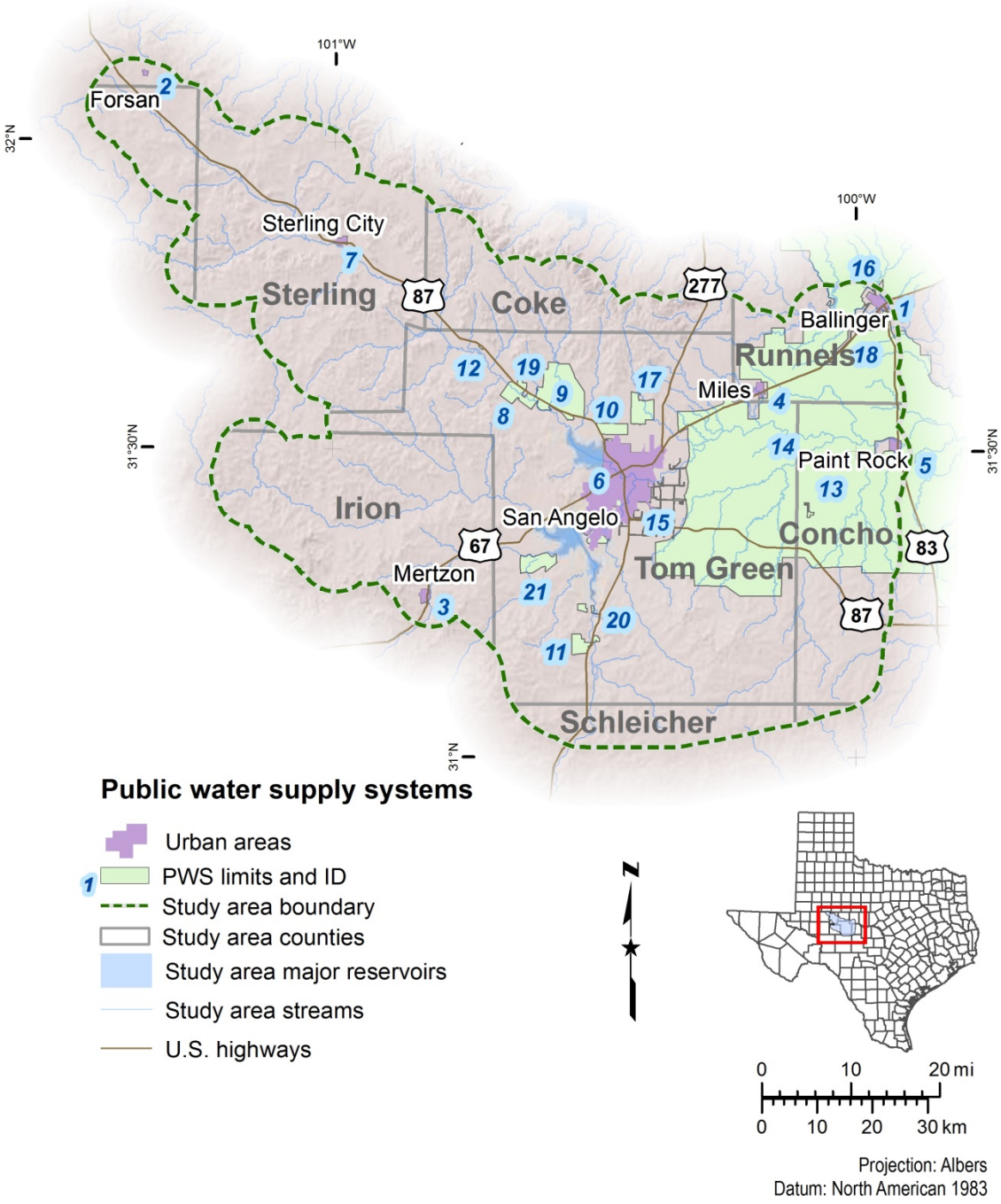

Figure 3-3. **City and public water supply system boundaries within the Lipan Aquifer study area. Table 3-1 is a cross-reference of public water system map number and name. City boundaries from Texas Natural Resources Information System Geographic Information System file. Public water system boundaries are from HDR (2011). ID = identification number, refers to map number used; PWS = public water system.**

Table 3-1 **Public water system cross-reference table that relates the map ID number and the public water supply system name and identification number (PWS ID) used in Figure 3-3. The Texas Commission on Environmental Quality official public water supply system names and assigned ID numbers are used in this table.**

Map ID	PWS ID	Public water system name
1	2000001	City of Ballinger
2	1140011	City of Forsan
3	1180002	City of Mertzon
4	2000002	City of Miles
5	480012	City of Paint Rock
6	2260001	City of San Angelo
7	2160001	City of Sterling City
8	2260067	Concho Rural Water Deer Valley Est
9	2260008	Concho Rural Water Grape Creek
10	2260020	Concho Rural Water North Concho Lake Est
11	2260093	Concho Rural Water The Oaks
12	2260060	Concho Rural Water Water Valley
13	480011	Eola WSC
14	480015	Millersview-Doole WSC
15	2260107	Millersview-Doole WSC Tyler Terrace
16	2000005	North Runnels WSC
17	2260101	Red Creek MUD
18	2000004	Rowena WSC
19	2260003	Tom Green County FWSD 1 Carlsbad
20	2260004	Tom Green County FWSD 2 Christoval
21	2260052	Tom Green County FWSD 3

Notes: Est = Estates; FWSD = Fresh Water Supply District; ID = identification number; MUD = Municipal Utility District; PWS = public water system; WSC = Water Supply Corporation.

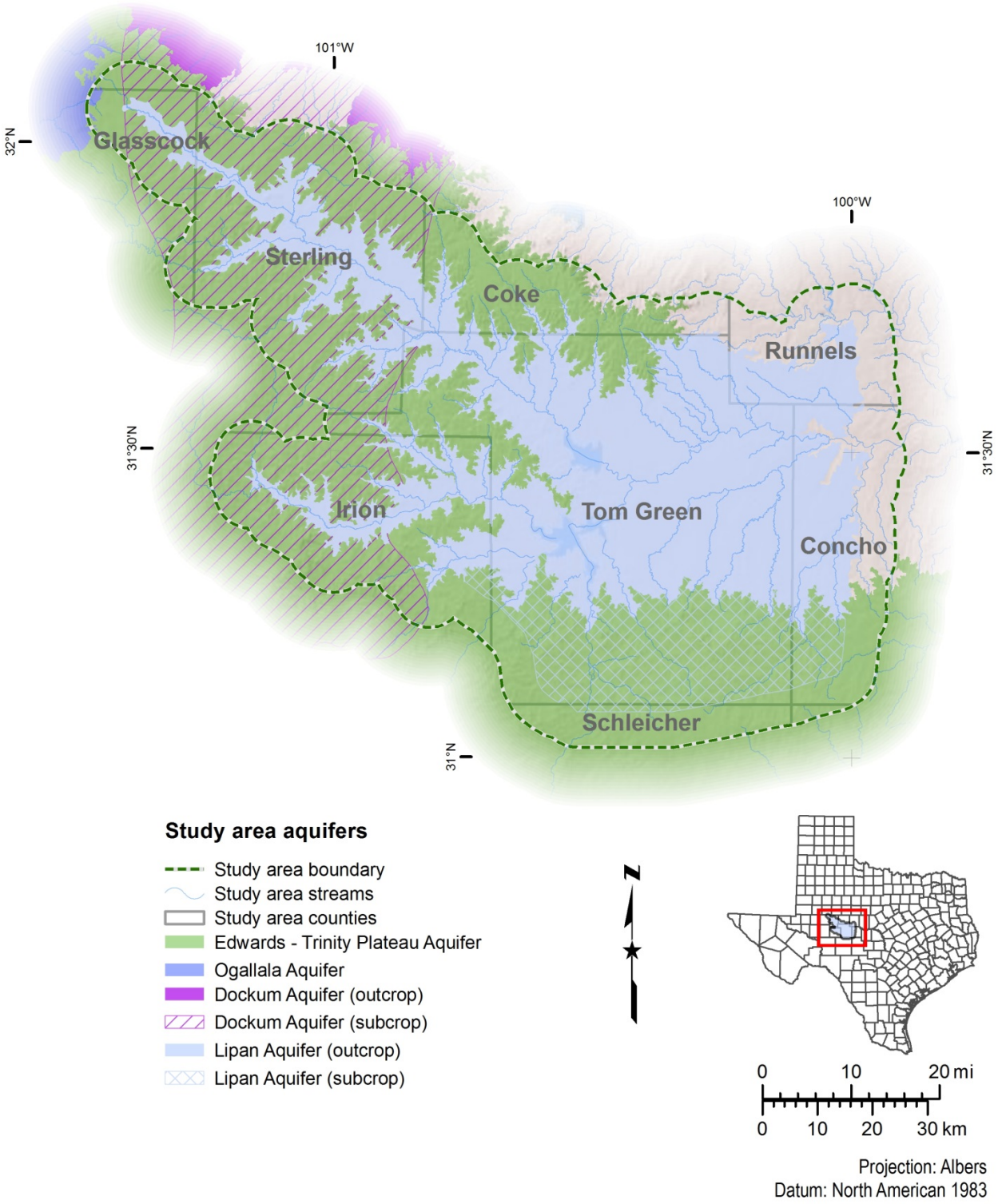

Figure 3-4. **Major and minor aquifers in the Lipan Aquifer study area.**

4. Region F Regional Water Planning Area summary

The Region F Regional Water Planning Area encompasses all of 32 counties in West Texas. The study area lies completely within Region F and includes most of Tom Green County and portions of Coke, Concho, Glasscock, Runnels, Schleicher, and Sterling counties. In this section the historical pumpage and demand, estimated future demand and needs, and recommended water management strategies are limited only to those counties where the Lipan Aquifer is an active or future source of supply. The source of data is the 2016 Region F Water Plan (Freese and Nichols and LBG-Guyton Associates, 2015) used to develop the current 2017 State Water Plan (TWDB, 2016c).

The 2016 Region F Water Plan reports existing water supplies from the Lipan Aquifer only in Tom Green, Concho, and Runnels counties. Lipan Aquifer groundwater pumping was reported at 28,242 acre-feet in 2010. Pumping from all groundwater sources was reported at 53,650 acre-feet in 2010. The Lipan Aquifer provided approximately 53 percent of all groundwater in the counties where it was an active water source during that period.

Tom Green, Concho, and Runnels counties' total water use for 2010 was 81,796 acre-feet. Groundwater from all sources supplied 66 percent of the water, and specifically the Lipan Aquifer provided 35 percent of groundwater sources. Irrigation and municipal categories were the top sources of water use, accounting for 67 percent and 26 percent, respectively. County-other, manufacturing, mining, steam-electric, and livestock categories comprised the remaining 7 percent of the water use.

By decade 2070, annual water demand is forecast to increase by 75 percent to 143,444 acre-feet while available supply is estimated to decrease to 85,612 acre-feet per year. This difference in supply and demand will result in a need for 57,832 acre-feet of additional water supply. There are two recommended water management strategies for groundwater desalination that will help meet the water shortage where the source may be brackish groundwater from the Lipan Aquifer. The water user groups and project sponsors are the City of San Angelo and the Concho Rural Water Supply Corporation.

For the City of San Angelo, the strategy and its supporting project are called "Desalination of other aquifer supplies in Tom Green County – San Angelo" in the Region F Water Plan. The difference between a water management strategy and project is that a strategy is a plan to meet a water need and the project is the infrastructure required to implement the strategy. The proposed water source is the Permian formations of the Lipan Aquifer. The plan envisions a 7-million-gallon-per-day desalination plant located northwest of the city generating 3,750 acre-feet of new supply annually beginning in decade 2050. The capital cost of the project is $58 million, and unit water cost for the strategy is $1,985 per acre-foot during the capital cost amortization period.

The decision to include the desalination strategy was influenced by an LBG-Guyton Associates (2008) study to evaluate the local Whitehorse and Clearfork groups as potential brackish water sources. Two wells were drilled into the Whitehorse Group. One well produced no water, and the second well produced only 10 gallons per minute so the formation was dropped from consideration. The well completed in the Clearfork Group produced 45 gallons per minute, and

the team recommended further investigation. Further details of these results are discussed in Section 6 of this report.

The Concho Rural Water Supply Corporation also plans to develop brackish groundwater. The strategy and its supporting project are called “Desalination of other aquifer supplies in Tom Green County – Concho Rural WSC” in the Region F Water Plan. They estimate producing 150 acre-feet of new water supply per year starting in decade 2020. While not specifically noted, the Lipan Aquifer may be the potential source, depending on their initial studies and testing. The estimated capital cost of the project is $5.1 million, and unit water cost for the strategy is $3,505 per acre-foot during the capital cost amortization period.

5. Previous investigations

One of the earliest geological investigations of the study area was completed by Henderson (1928), which provides references to still earlier works from the late 1890s. Henderson does an excellent job of describing the character and extent of outcrops available for study in Tom Green County. Other works by Beede and Waite (1918) and Beede and Bentley (1918) provide similar studies for Runnels and Coke counties, respectively. All of these early studies make mention of the modest groundwater availability for the region.

The Texas Board of Water Engineers (1941) compiled basic data on 630 water wells from Tom Green County. This was followed by Willis (1954) who provided the first comprehensive study of the groundwater resources for the Tom Green County portion of the Lipan Aquifer. This work reviewed 648 water well records and 235 water sample analyses to generate a relatively thorough description of the shallow groundwater resources. Willis considered that all of the Lipan Flat alluvial sediments were Quaternary in age and assigned them to the Leona Formation. The Willis study represents the starting point for this and all other studies of the Lipan Aquifer.

Lee (1986) published a detailed analysis of the groundwater resources of the Lipan Aquifer. Lee's study utilized basic information from 283 water wells of which 280 provided specific-conductance measurements as a method to determine water quality. Lee used the hydrogeologic model introduced by Willis as a template for assigning the groundwater properties to specific stratigraphic formations. Lee generally confirms the previous work performed by Willis and additionally concludes that continued growth in groundwater demand could create declines in water levels of the Lipan Aquifer.

Richter and others (1990) performed a detailed study to determine the sources of salinization in the Concho River watershed. They made extensive use of water samples taken from water wells, oil wells, and test borings. Water samples from this report that could be accurately located spatially and vertically were loaded into the BRACS Database and used in this study. They concluded that the major sources of high salinity in the Lipan Aquifer are brines from deeper Permian formations discharging into shallow aquifer units.

LBG-Guyton Associates (2003; 2004; 2005; 2008) and Freese and Nichols (2006) prepared a series of reports on the availability of brackish groundwater for the TWDB. The first of these, published in 2003, was a statewide analysis designed to be a regional planning tool that briefly mentioned the Lipan Aquifer. In 2004, an evaluation of the brackish groundwater resources for the Region F Regional Water Planning Group estimated that 1.25 million acre-feet of groundwater is available in the Lipan Aquifer. The 2005 report focused specifically on evaluating the Triassic and Permian brackish groundwater resources near the city of San Angelo and was included in its entirety in the 2006 report as appendix B. The 2006 report was written as an initial feasibility assessment in preparation for drilling and possibly developing a brackish groundwater well field close to the city of San Angelo.

LGB-Guyton's report in 2008 details the results of a three-well drilling program designed to find potential sources of brackish groundwater in proximity to the city of San Angelo. Although some valuable data was generated during the drilling of these wells, the project did not manage to identify a significant source of brackish groundwater capable of supporting a desalinization

plant. Water quality samples from depths of 615 and 675 feet in one well (BRACS well identification number 51449) had total dissolved solids concentrations of 7,040 and 8,140 milligrams per liter, respectively. A deeper sample taken at 903 feet had a total dissolved solids concentration of 65,800 milligrams per liter. We determined that the samples from 615 and 675 feet were actually taken in the San Angelo Formation rather than the Clear Fork Group as stated in the report. The sample from 903 feet was obtained from the Clear Fork Group. They performed a well test in the interval of 505 to 687 feet that yielded (1) a water quality sample with a total dissolved solids concentration of 3,990 milligrams per liter, (2) a maximum sustained well yield of 45 gallons per minute, and (3) a transmissivity of 200 gallons per day per foot. The report provided no explanation for the relatively low total dissolved solids concentration measured during the well test.

Additionally, LBG-Guyton Associates (2004) constructed a groundwater availability model for the Lipan Aquifer. The groundwater availability model used a single 400-foot-thick layer to simulate and model groundwater flow. The model is intended to be used for regional planning purposes and cannot be applied to individual wells or localized areas.

The Bureau of Economic Geology has published a comprehensive set of geologic map sheets at a scale of 1:250,000. Four of these map sheets include portions of the study area: (1) Big Spring (Eifler and others, 1974), (2) Brownwood (Kier and others, 1976), (3) San Angelo (Eifler, 1976), and (4) Sonora (McKalips and others, 1981). The digitized version of these maps created by the U.S. Geological Survey, in cooperation with the Texas Natural Resources Information System in 2007 (TWDB, 2007a), were used to generate the surface geology map.

6. Data collection and analysis

One of the primary objectives of the study is to gather available well data from existing water well reports, geophysical well logs, water chemistry samples, and aquifer tests. This information augments existing well information contained in the TWDB Groundwater Database (TWDB, 2016b). No single agency has complete information on all water wells or oil and gas wells in Texas. Therefore, a number of existing collections that contain publicly available paper and digital information were evaluated. Because many of the datasets and analysis features did not fit into the structure of the existing TWDB Groundwater Database, the information was loaded into the BRACS Database. Each well that was added to the BRACS Database shows the source of the information and all applicable well identification numbers.

Another equally important objective is to make the information and datasets gathered for the study readily available to the public. Thus, all of the information collected is non-confidential. The information includes raw data such as water well reports and digital geophysical well logs in numerous digital formats, processed data such as lithology, simplified lithologic descriptions, stratigraphic picks, water chemistry, and interpreted results in the form of GIS datasets.

With these goals in mind, we collected well data from several sources:

- Abilene Geological Society
- Bureau of Economic Geology Geophysical Log Facility
- Bureau of Economic Geology Report of Investigations 19 (Richter and others, 1990),
- Texas Commission on Environmental Quality water well image files and public drinking water files
- Texas Department of Licensing and Regulation Submitted Driller's Report Database
- Railroad Commission of Texas paper and digital geophysical well logs and the Underground Injection Control Database
- Texas Water Development Board Groundwater Database, BRACS Database, paper well reports, paper geophysical log collection, groundwater availability model studies, and written reports
- U.S. Geological Survey geophysical well logs

A total of 6,995 well records were collected within the study area, which included 5,520 water wells (Figure 6-1), 1,316 oil and/or gas wells (Figure 6-2), and 159 other types of wells (Figure 6-3). We appended information from 4,681 wells to the BRACS Database (Table 6-1). Of these well records, 394 have a state well number and 530 have Q-logs from the Groundwater Advisory Unit of the Railroad Commission of Texas, which were also added to the geophysical well log collection. An additional 2,314 well records are present in the TWDB Groundwater Database.

Table 6-1. Sources of BRACS Database well control data. Source names correspond to the field name SOURCE_WELL_DATA in the table called tblWell_Location in the BRACS Database.

Source of data	Sample count
Abilene Geological Society published report	7
BEG paper/digital geophysical logs	568
BEG Report of Investigations 191	68
LBG Brackish GW for San Angelo study	3
LBG Lipan GAM study well data	1,838
RRC digital geophysical logs	75
RRC GAU Q-log paper/digital geophysical logs	530
TCEQ PWS water wells	14
TCEQ water well images	2
TDLR digital water well reports	1,208
TWDB aquifer test information	2
TWDB geophysical logs	48
TWDB Groundwater Database	286
TWDB published reports	19
USGS geophysical logs	13

Notes: BEG = Bureau of Economic Geology; GAM = groundwater availability model; GAU = Groundwater Advisory Unit; GW = groundwater; LBG = LBG-Guyton Associates; PWS = public water supply; RRC = Railroad Commission of Texas; TCEQ = Texas Commission on Environmental Quality; TDLR = Texas Department of Licensing and Regulation; USGS = U.S. Geological Survey.

This represents only a fraction of all the wells installed in the study area. Information about many other wells was either unavailable, incomplete, limited in scope, of poor quality, confidential, or did not meet the requirements of the study. The additional information mentioned above is available from public and private sources:

- TWDB Groundwater Database for additional water quality data
- Submitted Driller's Report Database for well reports newer than 2001
- Water Well Report Viewer of the Texas Commission on Environmental Quality for well reports older than 2001
- Railroad Commission of Texas for digital geophysical well logs
- Bureau of Economic Geology for paper and digital geophysical well logs and miscellaneous records
- Lipan-Kickapoo Water Conservation District for well records

We did not verify the location of every well that was obtained from other agency datasets unless there appeared to be a problem, such as a mismatch in the geology. When locations had to be verified or digital locations were not available, the GIS files of the Original Texas Land Survey and linen maps from the Groundwater Advisory Unit of the Railroad Commission of Texas were used as a base map. The location legal description noted on the log header was used to plot the

wells in GIS to determine the latitude and longitude coordinates. Users of our study data should be aware that well locations may need verification. Because the TWDB Groundwater Database and the Texas Department of Licensing and Regulation Submitted Driller's Report Database are updated on a daily basis, users should also be aware that in the future there may be information available in these databases in addition to that present in the BRACS Database.

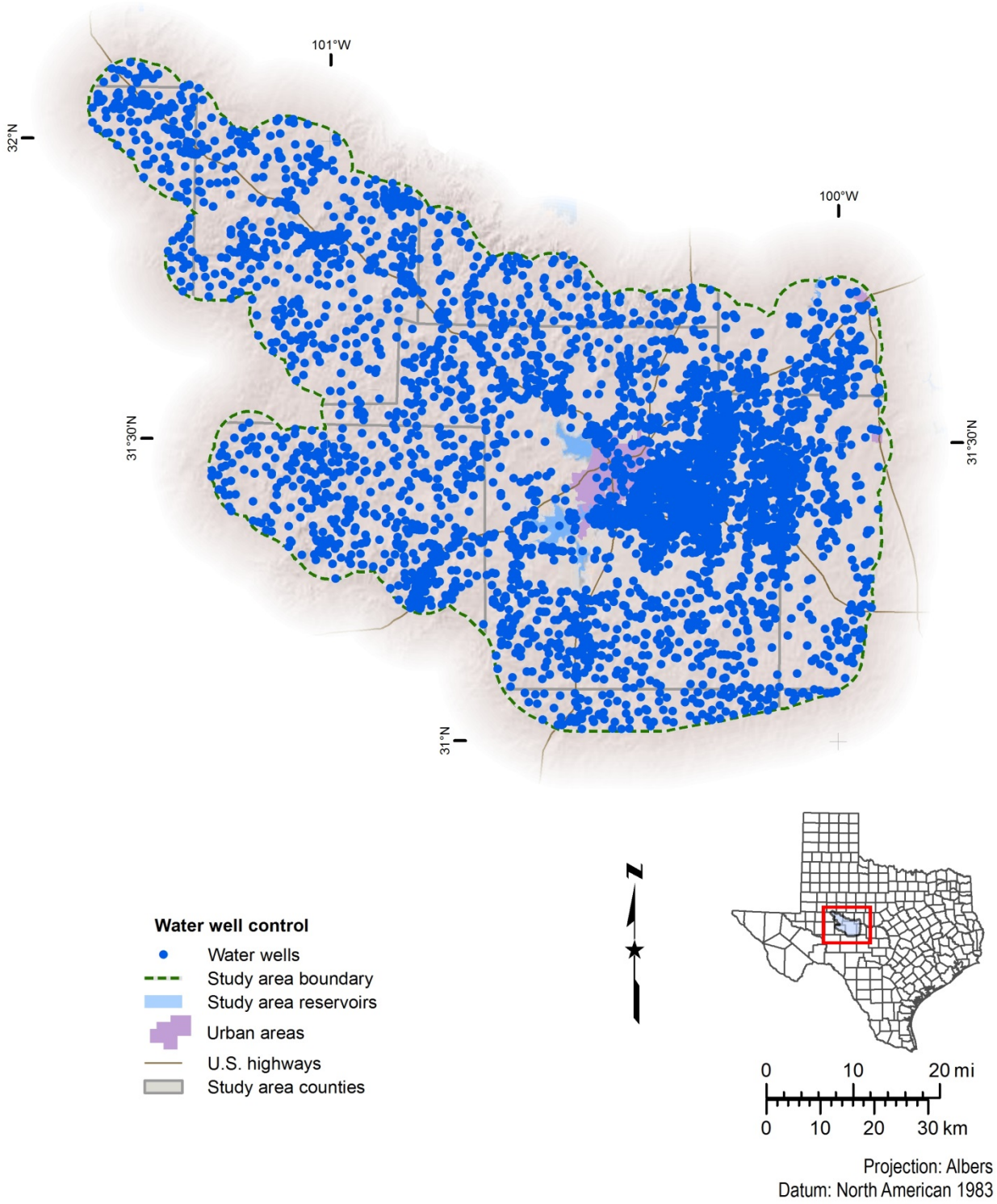

Figure 6-1. **Water well control in the Lipan Aquifer study area. The water well control consists of 5,520 wells; 3,296 have been assigned a well identification number in the TWDB BRACS Database; 2,558 wells have been assigned a state well number in the TWDB Groundwater Database; and 334 have assigned well identifiers in both databases.**

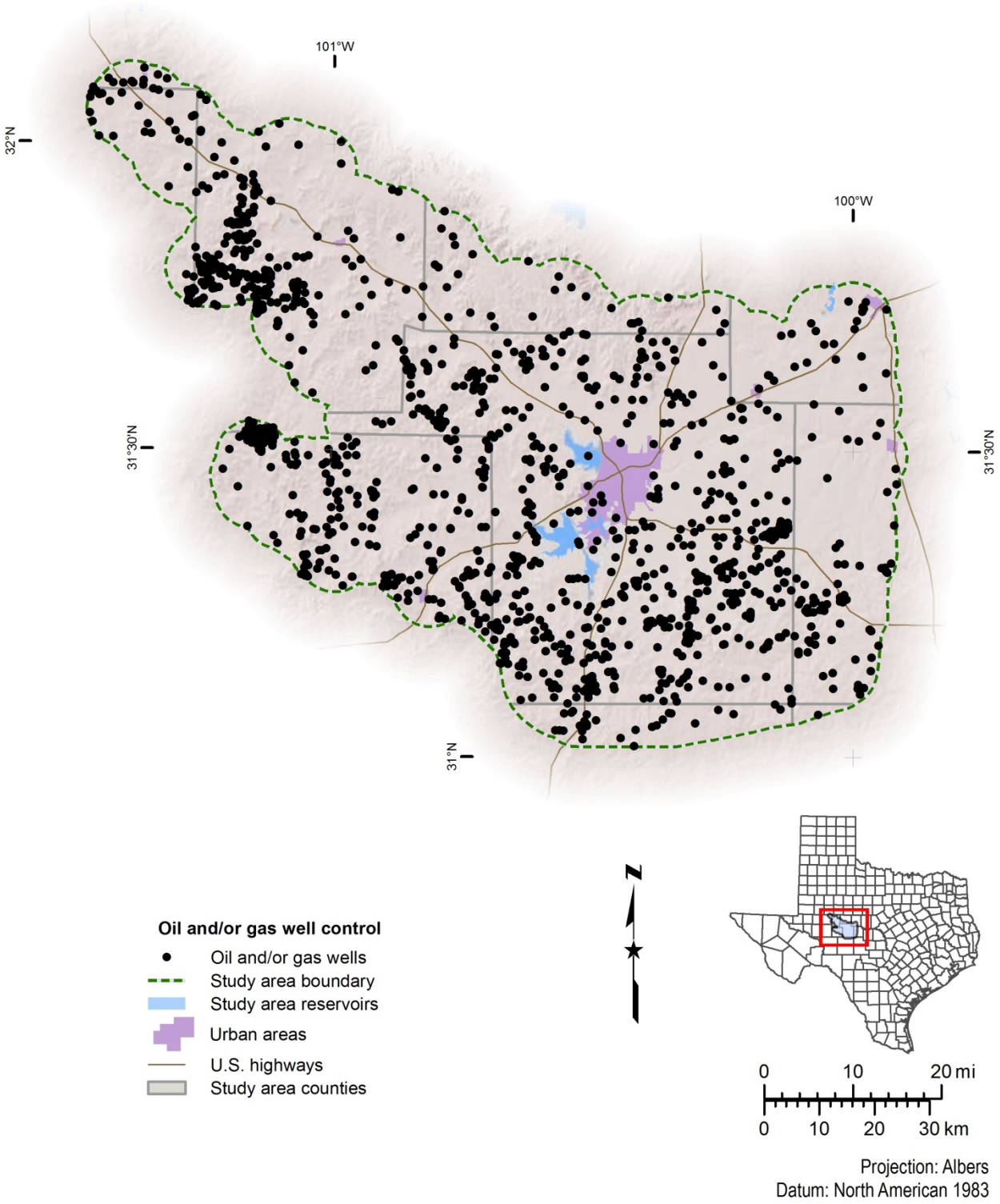

Figure 6-2. **Oil and/or gas well control in the Lipan Aquifer study area. The oil and/or gas well control consists of 1,316 wells; 1,226 have been assigned a well identification number in the TWDB BRACS Database; 134 wells have been assigned a state well number in the TWDB Groundwater Database; and 44 have assigned well identifiers in both databases.**

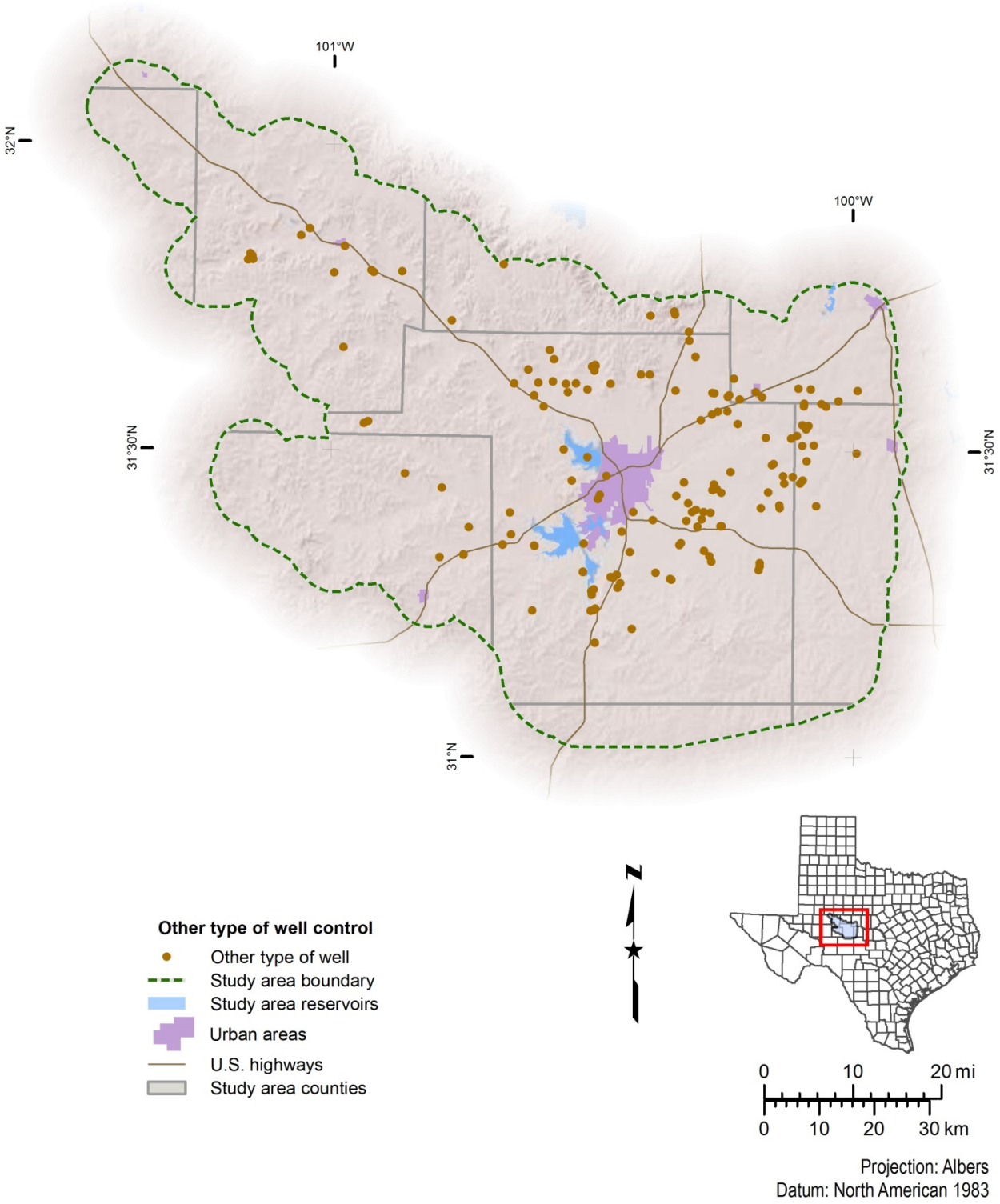

Figure 6-3. **Well control identified as other in the Lipan Aquifer study area. The other type of well control consists of observation, test, geothermal, and other uses. There are 159 wells of this type in the study area. All have assigned well identification numbers in the TWDB BRACS Database.**

7. Hydrogeology

The geology of the study area is unique and provides a fascinating picture of the geologic history of this portion of Central Texas. The study area is located upon the Eastern Shelf of the Permian Basin of Texas and encompasses a large portion of the Concho River Basin and its tributaries. The study area is centered in the Lipan Flat region located in Tom Green and western Concho counties but extends into portions of Coke, Glasscock, Irion, Runnels, and Schleicher counties. The oldest rocks evaluated in this study belong to the Lueders Formation from the Leonardian Stage of North America and are assigned to the middle to lower Permian. The youngest rocks are the recent Holocene and Pleistocene deposits that blanket the Concho River valley, the Lipan Flat, and the surrounding hillsides (Figure 7-1 and Table 7-1).

Within the study area, groundwater is produced from the Quaternary and Neogene sediments, Triassic Dockum Group, Cretaceous Trinity Group, and the weathered Permian units that are generally within 200 feet of the ground surface. The Trinity and Dockum aquifers in the study area will be addressed in future TWDB studies and are not discussed as part of this study.

Hydrocarbon production is present throughout the study area, and many of the Permian aquifer units can also be hydrocarbon bearing, for example the San Andres Formation in the Water Valley Field located in northwest Tom Green County. There have also been historical reports of shallow hydrocarbon occurrences that are within 100 feet of the surface west and south of San Angelo (Udden and Phillips, 1911; LGB-Guyton, 2008).

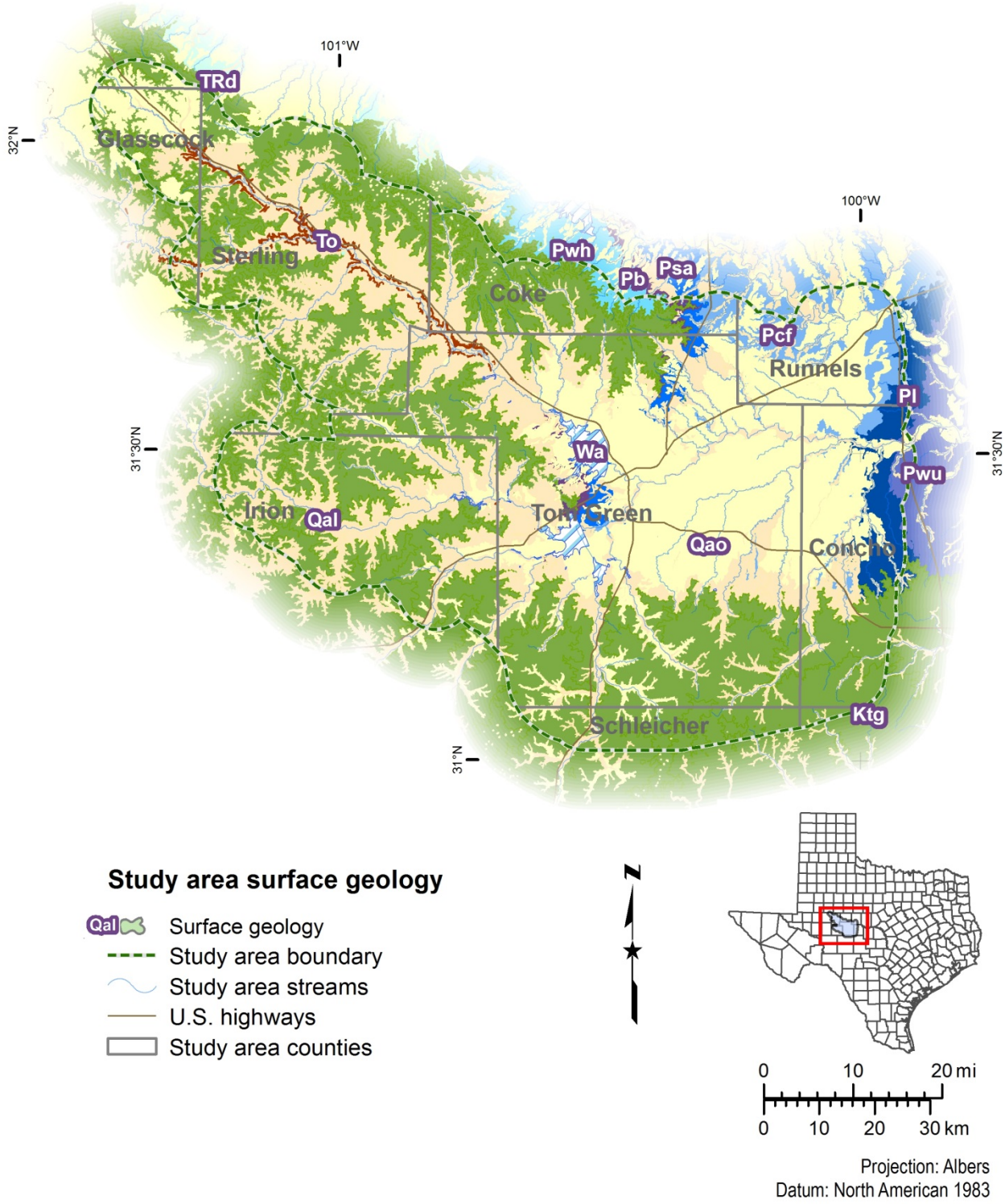

Figure 7-1. **Surface geology in the Lipan Aquifer study area. Modified from the TWDB (2007a). The formation labels are defined in Table 7-1.**

Table 7-1. Surface geology formation labels and names cross referenced. Labels and names from TWDB (2007a).

Symbol	Formation label	Formation name
	Qal	Quaternary alluvium
	Qao	Quaternary deposits
	To	Ogallala Formation
	Ktg	Trinity Group
	TRd	Dockum Group
	Pwh	Whitehorse Group
	Pb	San Andres (Blaine) Formation
	Psa	San Angelo Formation
	Pcf	Clear Fork Group
	Pl	Lueders Formation
	Pwu	Wichita undivided
	Wa	Water

7.1 Structure

The study area is located on a structural feature known as the Eastern Shelf, which is an extensive paleo-high that forms the eastern limit of the Midland Basin (Figure 7.1-1). The Eastern Shelf existed throughout the Permian Period and was an area of fluvial and shallow marine deposition as sediments from the eastern land mass were transported into the Midland Basin.

The Permian Basin is a broad structural low formed prior to the Middle Pennsylvanian Period approximately 300 million years before present. During periods of major sea level regressions, there were episodes of erosion and non-deposition which resulted in the creation of several major unconformities that exist between the formations from the (1) Permian and Triassic, (2) Triassic and Cretaceous, and (3) Cretaceous and Neogene (Tertiary) time periods.

We found that the Permian units dip from east to west across the study area. The oldest Permian formation studied was the Lueders Formation, which dips at an approximate rate of 57 feet per mile in the study area. The Clear Fork Group dips at a rate of 45 feet per mile in the study area. The Pease River Group dips at a rate of approximately 35 feet per mile in the study area. The Whitehorse Group dips at a rate of approximately 25 feet per mile in the study area. The Ochoan Series dips at a rate of 10 feet per mile in the study area. The surface upon which the Trinity Group was deposited (that also represents the top of the Dockum Group in places) dips towards the southeast at a rate of approximately 8 feet per mile in the study area.

We did not identify any large-scale faulting within the study area, although deformation and faulting of the Permian and Triassic formations during the Laramide Orogeny undoubtedly occurred. Extensional tectonics during the Cenozoic caused localized fault displacements and fracturing that is evidenced in study area outcrops.

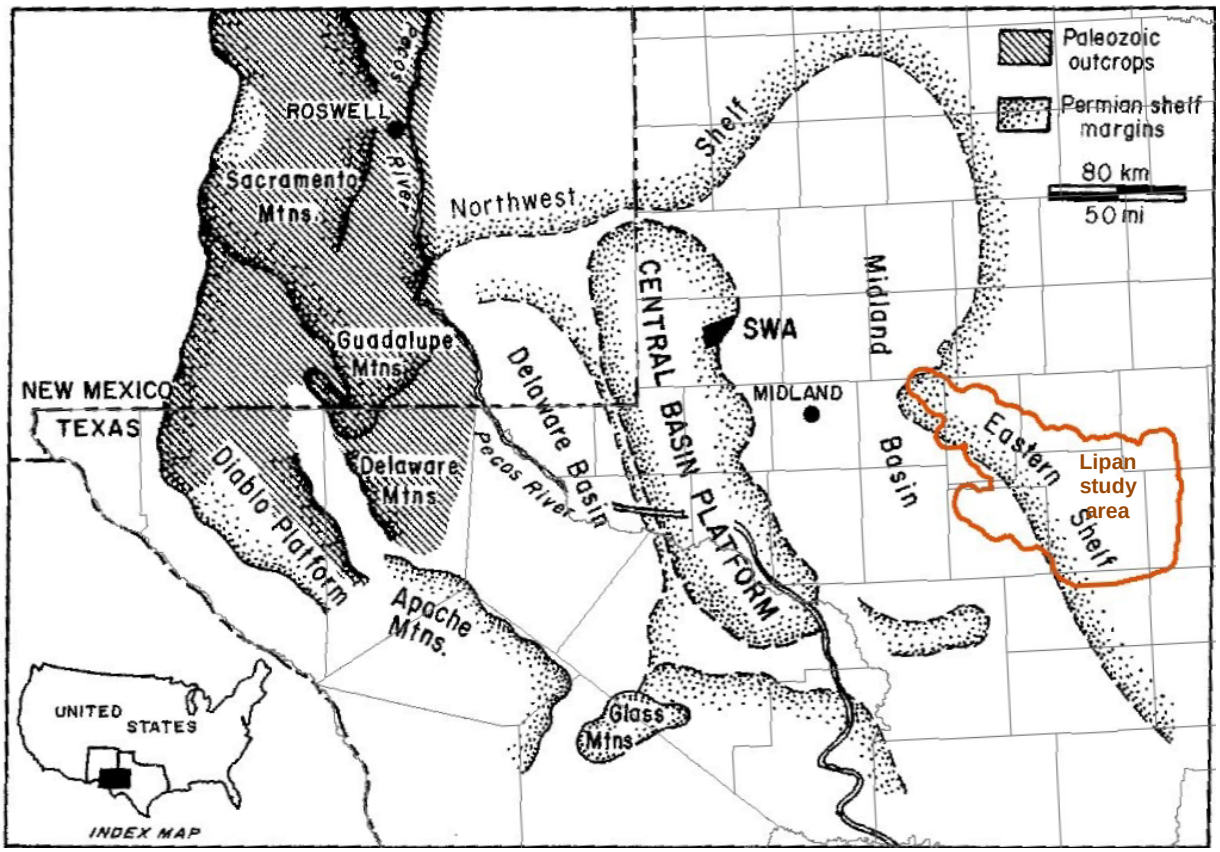

Figure 7.1-1. Structural provinces of the Permian Basin (modified from Stueber and others, 1998). The Lipan Aquifer study area is outlined in brown.

7.2 Stratigraphy

We correlated 1,549 geophysical well logs and water well reports to better understand the distribution of strata capable of containing brackish groundwater beneath the study area. The correlation framework is based upon previously published type logs, cross sections, and studies that used geophysical well logs. The Lueders Formation, which was the oldest unit correlated, was found at a depth of over 5,200 feet in Glasscock County along the western edge of the study area and outcrops in Concho County along the eastern edge of the study area. The youngest stratigraphic unit correlated is the Quaternary and Neogene sediments, which overlies all other geological units in the study area and has a total thickness of up to 150 feet.

The study area is extensive and stretches over 110 miles from northwest to southeast and 60 miles from northeast to southwest. Additionally, the study area overlies Permian formations that span the transition from the shallow marine to fluvial depositional facies of the Eastern Shelf to the marine slope and shore-face deposits of the Midland Basin. As a result, we faced significant challenges in correlating stratigraphic surfaces across the study area, including (1) changing lithology, (2) changes in unit thickness, and (3) limited data control. This was a significant issue primarily for the Lueders Formation, Clear Fork Group, San Angelo Formation, and San Andres Formation, which have the furthest easternmost extents. Permian formations of the Whitehorse Group and younger units are relatively consistent in terms of stratigraphic character within the study area (Figure 7.2-1).

Geologic period	Epoch and age (millions of years before present)	Regional series	Geologic group	Stratigraphic unit	
				Midland Basin	Eastern Shelf
Quarternary	Holocene (0.01-present)			alluvium	alluvium
	Pleistocene (2.6-0.01)			Pleistocene	Leona
Neogene (Tertiary)	Pliocene (5.33-2.6)			Pliocene	Ogallala
					unconformity
Cretaceous	Early (145.0-100.5)	Comanchean	Fredericksburg	Fredericksburg	Edwards Limestone Fort Terrett
			Trinity	Trinity Sand	Antlers Sand
					unconformity
Triassic	Upper (237.0-201.3)		Dockum	Dockum	Dockum
					unconformity
Permian	Lopingian (260-252)	Ochoan		Dewey Lake Rustler Salado Castille	Dewey Lake Rustler Salado
					unconformity
	Guadalupian (272-260)	Guadalupian	Whitehorse	Tansill Yates Seven Rivers Queen Grayburg	Tansill Yates Seven Rivers Queen Grayburg
			Pease River	San Andres	San Andres (Blaine) San Angelo
					unconformity
	Cisuralian (299-272)	Leonardian	Clear Fork	Clear Fork *undifferentiated*	**Choza**: Upper Choza; Tubb member **Vale**: Bullwagon Dolomite; Vale shale **Arroyo**: *Standpipe Limestone*; Arroyo
			Wichita - Albany	Wichita *undifferentiated*	Lueders

Lipan Aquifer units

Figure 7.2-1. Stratigraphic column of geological units identified within the Lipan Aquifer study area. Geologic epochs and ages are defined by the International Commission on Stratigraphy Chronostratigraphic Chart (modified from Gradstein and others, 2012). Geological units that produce water in the Lipan Aquifer are highlighted.

The majority of the geophysical well logs used were from wells drilled to explore for or produce oil and gas. These logs date from the 1940s to the present and represent a progression of down-hole well logging tool technologies. The earliest geophysical well logs were known as "electric logs" and were based upon the original logging tools first developed by Emil Schlumberger in 1927. These types of logs record the electrical resistivity response from fluid in the rocks to both an induced current and a natural electrical potential. Beginning in the late 1940s, logging tools were introduced that measured the natural gamma radiation of formation rocks as well as their response to a radioactive source. For purposes of stratigraphic correlation during this study the principle well logs used were the gamma ray, spontaneous potential, and deep resistivity.

The correlation process required the use of scanned images of well logs that had been loaded to the BRACS Database. These well logs come from a multitude of sources including the Railroad Commission of Texas and the Bureau of Economic Geology. Correlations were recorded digitally in an ESRI ArcGIS® map layer so that they could be displayed as sub-sea elevations posted at the well locations. This process helped avoid data entry errors and allowed for the continuous review of the correlations as they were interpreted.

All recent oil wells and most of the older oil wells set casing to a depth below the base of fresh water in order to protect shallow fresh water aquifers and ensure the stability of the well bore. Depending upon location and prevailing regulations, this casing would generally extend 200 to 500 feet below ground surface. This creates a problem for well logging because electric well logs require an uncased fluid-filled hole for them to properly record the electrical properties of the rocks. This restriction does not apply to the nuclear well logging tools, like the gamma ray log, which are able to record meaningful data virtually to the surface, although consideration must be made for the effects of the casing and annular cement on the amplitude of the recorded values.

We prepared three-dimensional GIS surfaces of the top of the formations in units of feet for (1) below ground surface and (2) elevation referenced to mean sea level. We also prepared isochore maps showing formation thickness (see Appendix 20.1 for all formation surfaces). Examples of stratigraphic picks from geophysical well logs used to determine formation boundaries are shown in Section 8.4.

7.2.1 Permian

Upper Permian formations total 3,600 feet thick within the study area and dip towards the northwest at an average of 50 feet per mile. Permian formations outcrop across the study area except for the western fourth where they are overlain with up to 1,200 feet of Triassic, Cretaceous, and younger geological formations. These outcrops of Permian formations represent some of the most southerly exposures of a broad north-south trending band that stretches across Central Texas. After deposition of the Permian formations, a long period of erosion and non-deposition occurred that lasted until the deposition of the Late Triassic Dockum Group (Hill, 1972). During this long period of subaerial exposure, the Permian formations were leveled off and a zone of alteration and weathering formed. We believe that this altered zone contains increased porosity and permeability, allowing the Permian rocks to act as aquifers in the study area. The Permian subcrop that represents the paleo-outcrop expression of the formations prior to Cretaceous deposition is shown in Figure 7.2-2.

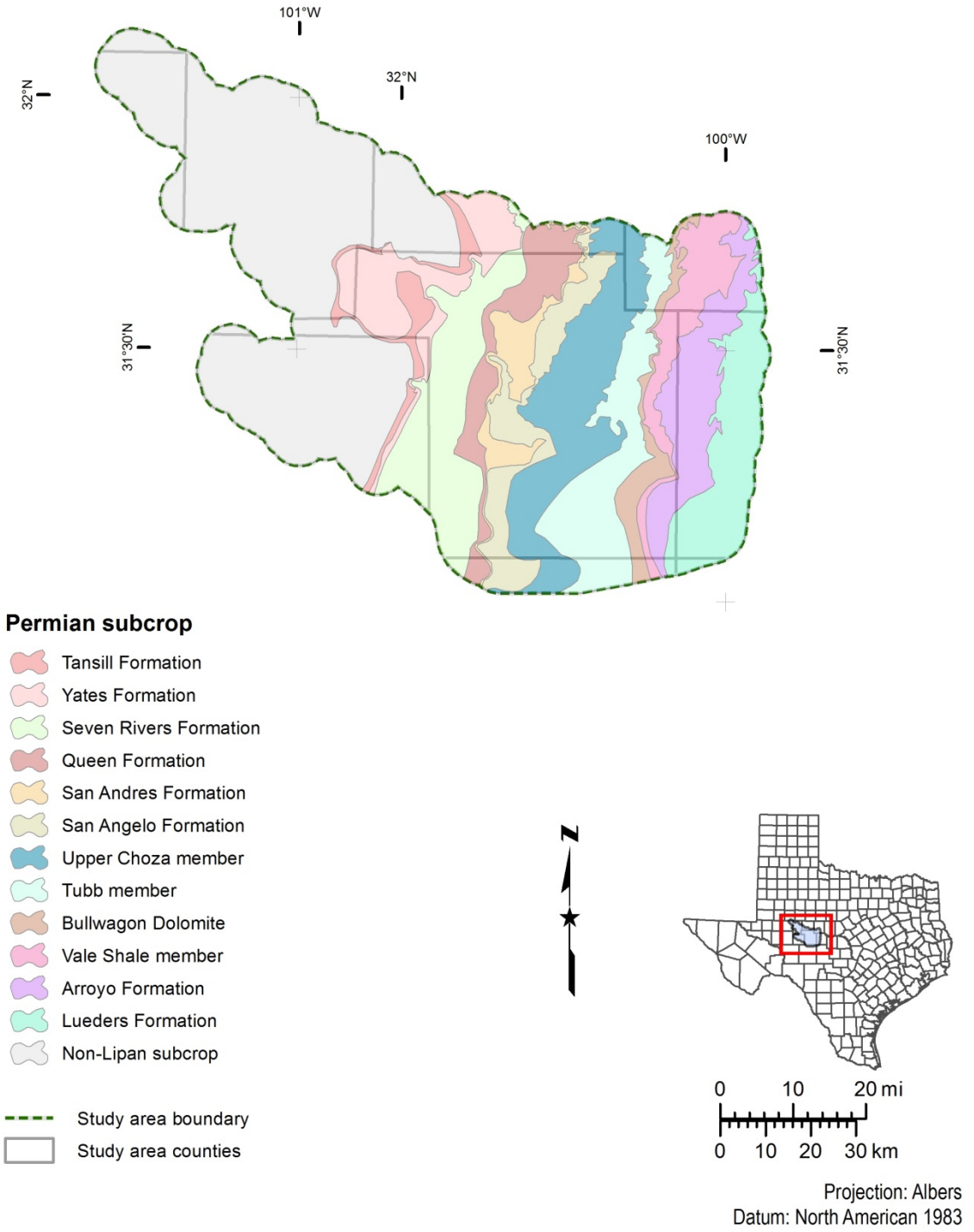

Figure 7.2-2. Permian subcrop in the Lipan study area. Shaded areas indicate where Permian formations either outcrop or subcrop below overlying Quaternary and Neogene sediments or Cretaceous formations. The Grayburg Formation subcrops below the Queen Formation so it is not shown.

Lueders Formation, Wichita-Albany Group

The oldest correlated surface was the top of the Lueders Formation, which outcrops in western Concho County. In north central Texas, the Lueders Limestone (named for a small town on the Clear Fork of the Brazos River in eastern Jones County) has been accepted as the top of the Wichita Division (Wrather, 1917).

The Lueders Formation is thought to have been deposited during a time of relatively high sea-level and is composed of interbedded gray to tan limestone and calcareous mudstone. The Lueders Formation has numerous shallow-marine fossils (Beede and Waite, 1918). The Lueders Formation transitions from predominantly limestone in the east to predominantly shale in the west. This transition reflects a facies change from nearshore shallow water deposition on the Eastern Shelf to a slope and basinal depositional environment in the west. In Concho County groundwater has been produced from the Lueders Formation with higher volumes and lower salinity from shallow wells that are in close proximity to the Concho River.

Arroyo Formation, Clear Fork Group

The base of the Clear Fork Group is represented by the Arroyo Formation, which is composed of limestone, dolomite, and shale. The uppermost member of the Arroyo Formation in the eastern portion of the study area is the Standpipe Limestone, which outcrops in Runnels County just north of the study area. The Standpipe Limestone is a 10- to 15-foot thick tan to light-gray marly limestone (Sellards, 1932) that is not continuous across the study area and not separated from the Arroyo Formation in this study. The Arroyo Formation changes dramatically from east to west across the study area from predominantly limestone in the east to predominantly shale in the west. This transition reflects a facies change from nearshore shallow water deposition on the Eastern Shelf to a slope and basinal environment in the west. The overall thickness of the Arroyo Formation also changes dramatically across the study area from 250 feet in western Concho County to just over 1,000 feet in Irion County. Shallow wells have produced small to moderate quantities of slightly saline water from this formation.

Vale Shale member, Vale Formation, Clear Fork Group

We have divided the Vale Formation of the Clear Fork Group into two units because of their distinctly different lithologic properties: (1) the Bullwagon Dolomite and (2) the Vale Shale member. The Vale Shale member is defined as that portion of the Vale Formation from the base of the Bullwagon Dolomite to the top of the Arroyo Formation. The Vale Shale member is composed predominantly of reddish silty shale, shale, and minor carbonate beds. It has been locally referred to as the “big red” and is generally too fine-grained to be a significant source of water (Willis, 1954). The Vale Shale member maintains a fairly constant thickness of 100 to 200 feet throughout the study area.

Bullwagon Dolomite, Vale Formation, Clear Fork Group

The Bullwagon Dolomite is formally a part of the Vale Formation but will be discussed as a unique stratigraphic unit in this study. The Bullwagon Dolomite is composed of two distinct massive dolomite strata separated by a shale parting and takes its name from Bullwagon Creek in Taylor County (Wrather, 1917). The Bullwagon Dolomite is 50 to 90 feet thick and has been previously identified as a water-bearing interval (Willis, 1954). The significant level of

fracturing in the Bullwagon Dolomite and potential for dissolution of calcareous material adjacent to the fractures as it weathers has increased the porosity and permeability of this unit and enhanced its aquifer characteristics. We determined that this weathering process has had a significant impact on those portions of the formation within about 300 feet of the ground surface.

Tubb member, Choza Formation, Clear Fork Group

We determined that the lower portion of the Choza Formation of the Clear Fork Group represented a significant depositional unit separated by a distinct correlative surface. The informal stratigraphic name of Tubb (Muzzullo, 1982; Ruppel and Ward, 2013) was used to identify this distinct Choza Formation member. The Tubb member is identified by a regional flooding event that resulted in a 20- to 50-foot shaly interval whose base marks the top of the Tubb member. Much of the rest of the Tubb member is similar to the overlying Upper Choza member and is composed of alternating fine-grained silty-sand, shale, and dolomitic limestone. Shallow wells have produced significant quantities of slightly saline water from this formation.

Upper Choza member, Choza Formation, Clear Fork Group

The Choza Formation is the upper unit of the Clear Fork Group. It is composed of silty red shale and dolomitic limestone beds deposited during a time when the area was submerged due to a sea level transgression. The shale and dolomitic beds are thin and highly interbedded (Beede and Bentley, 1918; Ruppel and Ward, 2013) indicating shallow marine carbonate shelf deposition. We have separated the Choza Formation into the Upper Choza member and the underlying Tubb member in order to determine if their aquifer properties differ significantly. The Upper Choza member is 200 to 500 feet thick within the study area. Shallow wells in the Upper Choza member produce water ranging from slightly to moderately saline.

San Angelo Formation, Pease River Group

The San Angelo Formation unconformably overlies the Clear Fork Group and is composed of sandstone, shale, and conglomerate within the study area (Sellards, 1932). The San Angelo Formation is 100 to 400 feet thick in the study area and outcrops within the City of San Angelo. A 10- to 20-foot thick basal conglomerate produces highly mineralized groundwater with total dissolved solids of 800 to 52,000 parts per million in limited quantities (Willis, 1954). Water quality samples collected in wells used by this study found the range of total dissolved solids to be 673 to 8,140 milligrams per liter.

San Andres Formation, Pease River Group

The San Andres Formation is composed of more than 400 feet of interbedded dolomitic sand, shale, anhydrite, gypsum, and halite. The sedimentary character of the San Andres Formation is indicative of an evaporite shelf deposit with high-frequency cyclical-deposition of beds indicating a shallow marine environment. This formation does not produce significant quantities of groundwater in the study area.

Grayburg Formation, Whitehorse Group

The Grayburg Formation forms a wedge of fine-grained sandstone interbedded with shale, anhydrite, dolomite, and thin beds of halite. The Grayburg Formation has a total thickness of

more than 500 feet in the far western edge of the study area. This formation does not produce significant quantities of groundwater in the study area.

Queen Formation, Whitehorse Group

The Queen Formation is composed of fine-grained sandstone, siltstone, shale, and silty anhydrite. This formation is present in the western half of the study area and is 100 to 150 feet thick. The Queen Formation may be capable of producing small quantities of saline water within the study area from the fine-grained sandstones and siltstones.

Seven Rivers Formation, Whitehorse Group

The Seven Rivers Formation is 100 to 400 feet thick within the study area. The upper 10 to 20 feet of the Seven Rivers Formation is an anhydrite unit that can be easily identified on most geophysical well logs and represents a significant regional correlation. This unit is composed of fine-grained sandstone, shale, and anhydrite. This formation has produced small quantities of fresh to moderately saline groundwater within the study area.

Yates Formation, Whitehorse Group

Two significant anhydrite beds bracket the Yates Formation, which is generally 100 to 150 feet thick within the study area. The Yates Formation is composed of red, fine-grained, sandstone beds with thin layers of shale and limestone interspersed (Mear, 1963). The fine-grained sand beds have produced small amounts of moderately saline water from shallow wells within the study area.

Tansill Formation, Whitehorse Group

In the study area, the Tansill Formation is an anhydrite interval almost 75 feet thick. Because of its lithology, it can be easily identified in the subsurface on most geophysical well logs. The Tansill Formation does not have significant water-bearing potential in the study area but is an important and useful regional stratigraphic unit for correlation and mapping purposes.

Rustler-Salado formations, Ochoan Series

We have combined both the Rustler and the underlying Salado formations as a single mappable unit. These formations are composed of sandy anhydrite and anhydrite beds that are almost 400 feet thick in the far western portions of the study area. This unit does not have significant water-bearing capabilities in the study area.

Dewey Lake Formation, Ochoan Series

The Dewey Lake Formation consists of silty shale and overlies the Rustler Formation in the western portion of the study area. The Dewey Lake Formation reached a maximum thickness of 200 feet in the study area. The Dewey Lake Formation does not have significant water-bearing potential within the study area.

7.2.2 Triassic

The Dockum Group is present in the western portion of the study area and lies unconformably upon the Permian Dewey Lake Formation. The Dockum Group outcrops north and west of the study area but, other than one anomalous outcrop just south of Sterling City, is not exposed in the study area. In the study area, the Dockum Group is composed of the Santa Rosa Sandstone and the underlying Tecovas Shale which are commonly mapped together and designated as the Lower Dockum. The Dockum Group reaches a maximum thickness of 1,100 feet in the western portion of the study area. The Dockum Group is a known aquifer, and its brackish water potential will be addressed in a separate study.

7.2.3 Cretaceous

Early Cretaceous limestone, shale, and sandstone of the Edwards and Trinity groups unconformably overlie older units and form abrupt cliffs and canyons south, west, and north of the Lipan Flat that is located in the central and eastern sections of Tom Green County. These rocks reach a combined thickness of more than 400 feet and are known to contain fresh water. Four water quality samples in south Tom Green County contained brackish water. However, they are not considered part of the Lipan Aquifer and their brackish water potential will be addressed in future TWDB studies. We believe that cross-formational flow occurs from these Cretaceous formations into the underlying aquifers (Beach and others, 2004).

7.2.4 Quaternary and Neogene (Tertiary)

Previous workers have assigned the post-Cretaceous sediments that represent a significant part of the Lipan Aquifer to the Quaternary Leona Formation. The assignment of these deposits to the Leona Formation was done by Willis (1954). The Leona Formation was initially defined by Hill and Vaughn (1889) for Pleistocene terrace deposits in Uvalde and Zavala counties. Henderson (1928) assigned a Pleistocene age to the terrace gravel exposed along the banks of the Concho River because of the presence of two macro fossils found loose in creek beds. Subsequently, Plummer (1932) placed all Texas Pleistocene terraces into the Leona Formation. Willis cites both Plummer and Henderson in his decision to assign the coarse-grained conglomerate and gravel exposed along the Concho River to the Leona Formation.

Descriptions of the Pleistocene terrace deposits by Hill and Vaughn (1889) at the type location for the Leona describe them as "…fine calcareous silt at the surface, and grades downward into coarse gravel." Plummer (1932) states that the Leona Formation is composed of red to reddish-gray silt and fine gravel. The coarse-grained terrace deposits in Tom Green County are markedly different. Henderson (1928) describes them as coarse conglomerates cemented with hard, sandy, siliceous-calcareous cement. Additionally, neither Henderson (1928) nor any subsequent study presented any definitive fossil evidence that documents a clear Pleistocene age to the conglomerates described.

During the course of this study, hundreds of water well reports from the TWDB Groundwater Database and the Texas Department of Licensing and Regulation Submitted Driller's Report Database were reviewed in order to build an accurate map of the thickness of sediment overlying the Permian formations. These drillers' water well reports (Figure 7.2-3) provide a general, non-technical description of the sediment and rock encountered during the drilling of a well. The

descriptions are based upon the cuttings returned to the ground surface during rotary method drilling. We observed numerous descriptions of the sediment in the Lipan Flat where a conglomerate is overlain by a relatively thick "white limestone," which in turn is overlain by silty sand and clay.

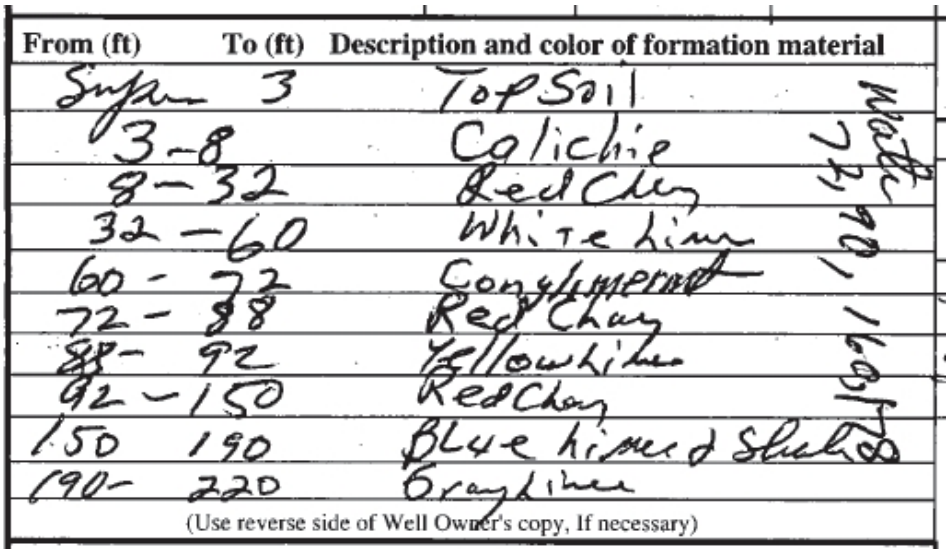

From (ft)	To (ft)	Description and color of formation material
Surface	3	Top Soil
3	8	Caliche
8	32	Red Clay
32	60	White Lime
60	72	Conglomerate
72	88	Red Clay
88	92	Yellow Lime
92	150	Red Clay
150	190	Blue lime & Shale
190	220	Gray Lime

(Use reverse side of Well Owner's copy, If necessary)

Figure 7.2-3. Example of a drillers' water well report (state well number 43-38-515).

We believe that the "white limestone" unit is most likely a mature caliche, defined as a calcareous deposit formed at or near the ground surface that may be a paleosol indicator. The caliche zone is commonly found 10 to 50 feet below ground surface and is 15 to 50 feet thick. An isochore map of the caliche unit is shown in Figure 7.2-4. This thick section of mature caliche is unlikely to have formed during the Pleistocene because there would not be sufficient time for the formation of such a significant thickness of caliche (Seni, 1980).

Frequently, an interval described in drillers' water well reports as a conglomerate or coarse gravel as much as 100 feet thick underlies the caliche layer. The conglomerate unit at the base of the Quaternary and Neogene interval is an important water-bearing unit for the Lipan Aquifer. The thick caliche unit overlying the conglomerate can locally act as a barrier to the vertical downward flow of groundwater, creating shallow perched aquifers. This conclusion is supported by drillers' water well reports that frequently note the presence of water-bearing sediment directly above the caliche unit and then again in the deeper conglomerates.

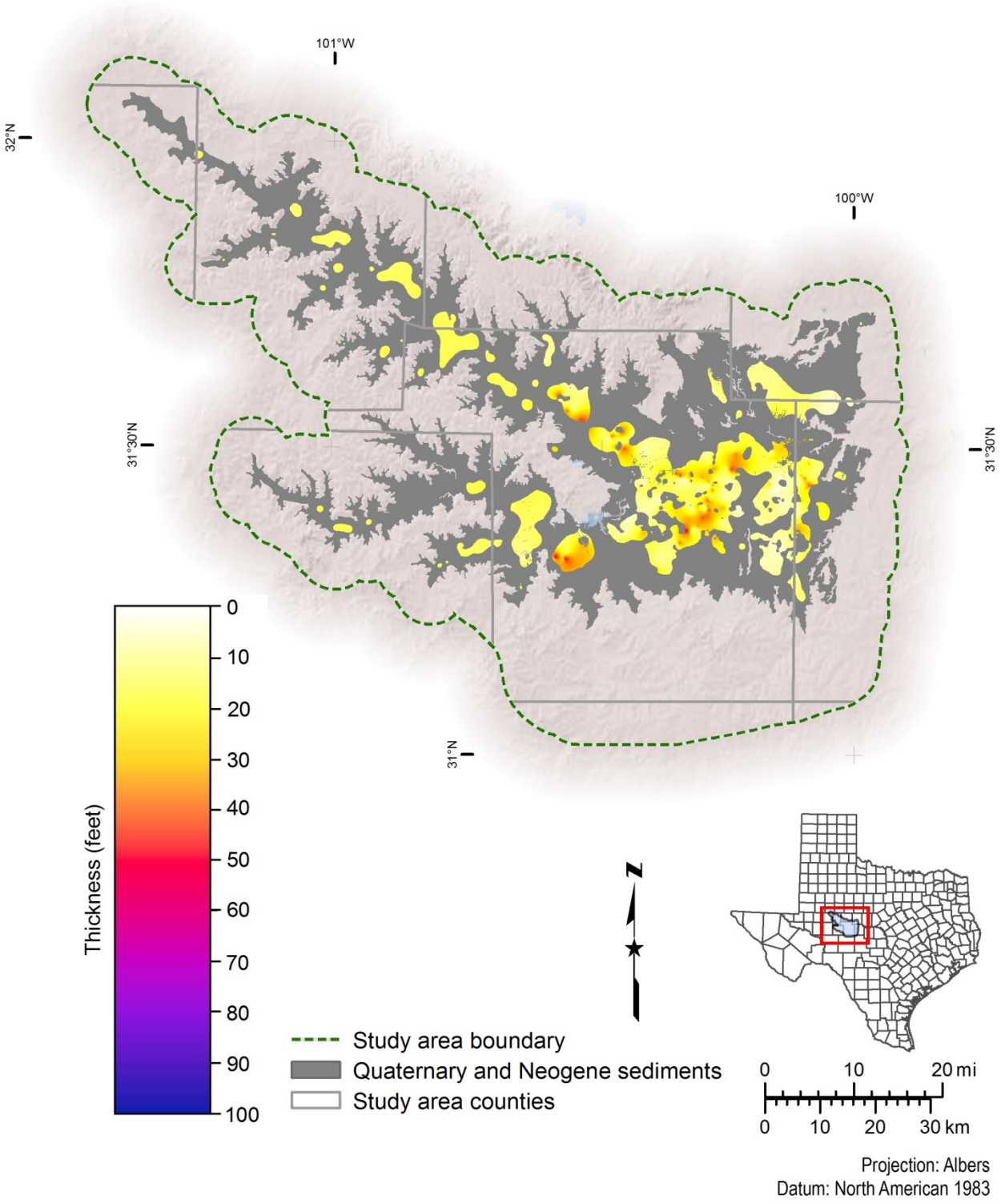

Figure 7.2-4. **Isochore map of the caliche zone. Thickness values are in feet. The dark gray area denotes the areal extent of the Quaternary and Neogene sediments.**

We believe that the basal 50 to 120 feet of sediment deposited in the Lipan Flat and surrounding areas are most likely Neogene (Late Tertiary) age and possibly time-correlative with the Ogallala Formation. The caliche zone that immediately overlies the basal conglomerate was probably formed during the latest Neogene time period and is equivalent to the caprock commonly associated with the Ogallala Formation. After deposition, the Neogene sediment was eroded by area streams forming canyons and ravines across the Lipan Flat. These depressions were subsequently filled with fine-grained sand, silt, and clay that were eroded from the surrounding Permian and Cretaceous outcrops creating the current geomorphic profile.

We determined that only the upper most alluvial sediments with a maximum thickness of 50 feet were deposited during the Quaternary and should be assigned to the Leona Formation.

7.3 Stratigraphic type logs

A series of type logs were generated (Figure 7.3-1 through Figure 7.3-13) to illustrate the stratigraphic correlations made throughout the study area. Because of the size of the study area and the geologic changes in the geological formations across this distance, two sets of type logs were generated—one for the western and one for the eastern study area. Note that the Trinity and Dockum groups and the Dewey Lake, Rustler, Tansill, and Yates formations are not represented in the eastern type logs because they are present only in the western portion of the study area. A type log may have one or more correlations marked on the geophysical well log depending upon the thickness of the geological formations that are being delineated.

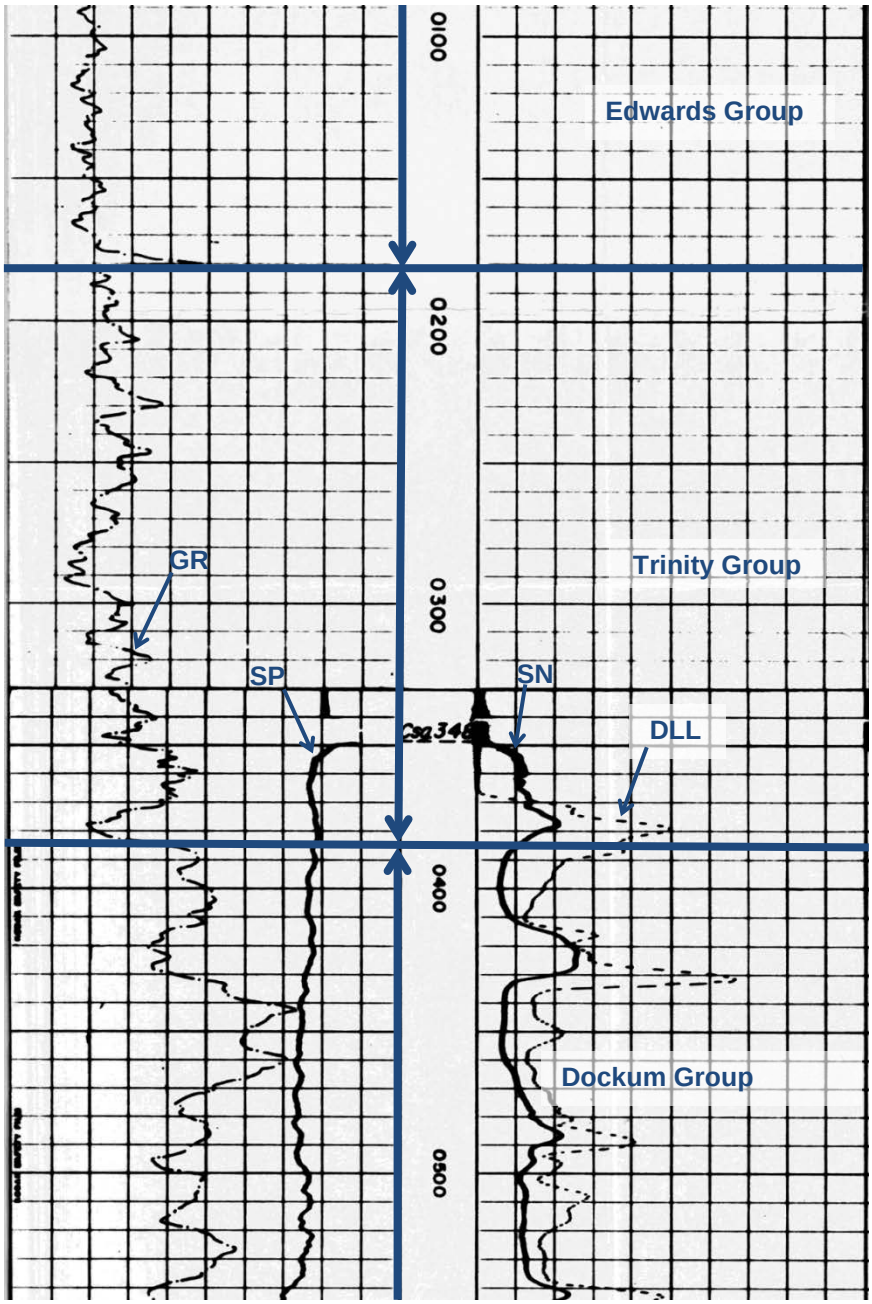

Figure 7.3-1. **Western correlations for the Trinity Group and Dockum Group on BRACS Database well identification number 37978. The spontaneous potential and gamma ray tools are shown in the left track, depth (in feet below ground surface) is shown in the middle track, and the normal and deep lateral resistivity tools are shown in the right track. DLL = deep lateral resistivity, GR = gamma ray, SN = short normal resistivity, SP = spontaneous potential.**

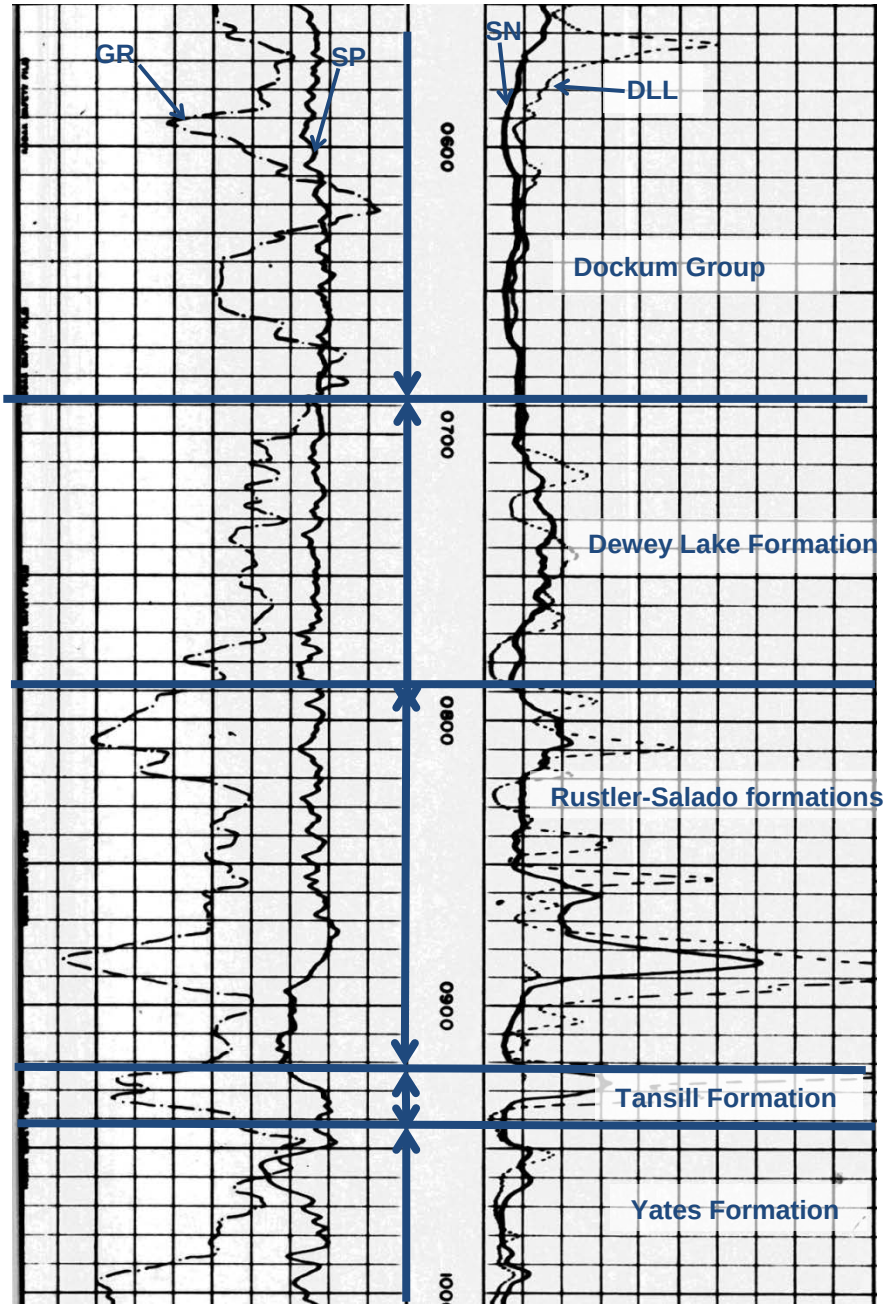

Figure 7.3-2. **Western correlations for the Dockum Group, Dewey Lake Formation, Rustler-Salado formations, Tansill Formation, and Yates Formation on BRACS Database well identification number 37978. The spontaneous potential and gamma ray tools are shown in the left track, depth (in feet below ground surface) is shown in the middle track, and the normal and deep lateral resistivity tools are shown in the right track. DLL = deep lateral resistivity, GR = gamma ray, SN = short normal resistivity, SP = spontaneous potential.**

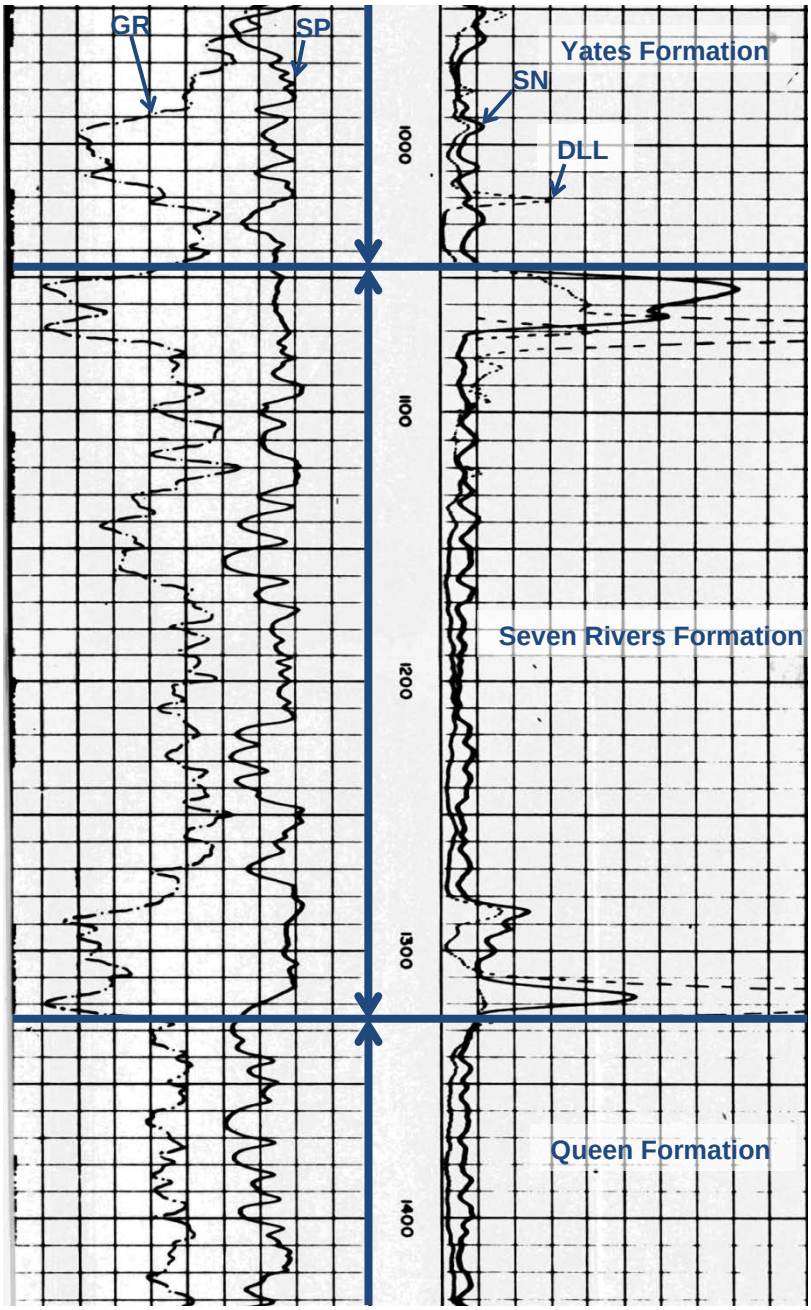

Figure 7.3-3. **Western correlations for the Yates Formation, Seven Rivers Formation, and Queen Formation on BRACS Database well identification number 37978. The spontaneous potential and gamma ray tools are shown in the left track, depth (in feet below ground surface) is shown in the middle track, and the normal and deep lateral resistivity tools are shown in the right track. DLL = deep lateral resistivity, GR = gamma ray, SN = short normal resistivity, SP = spontaneous potential.**

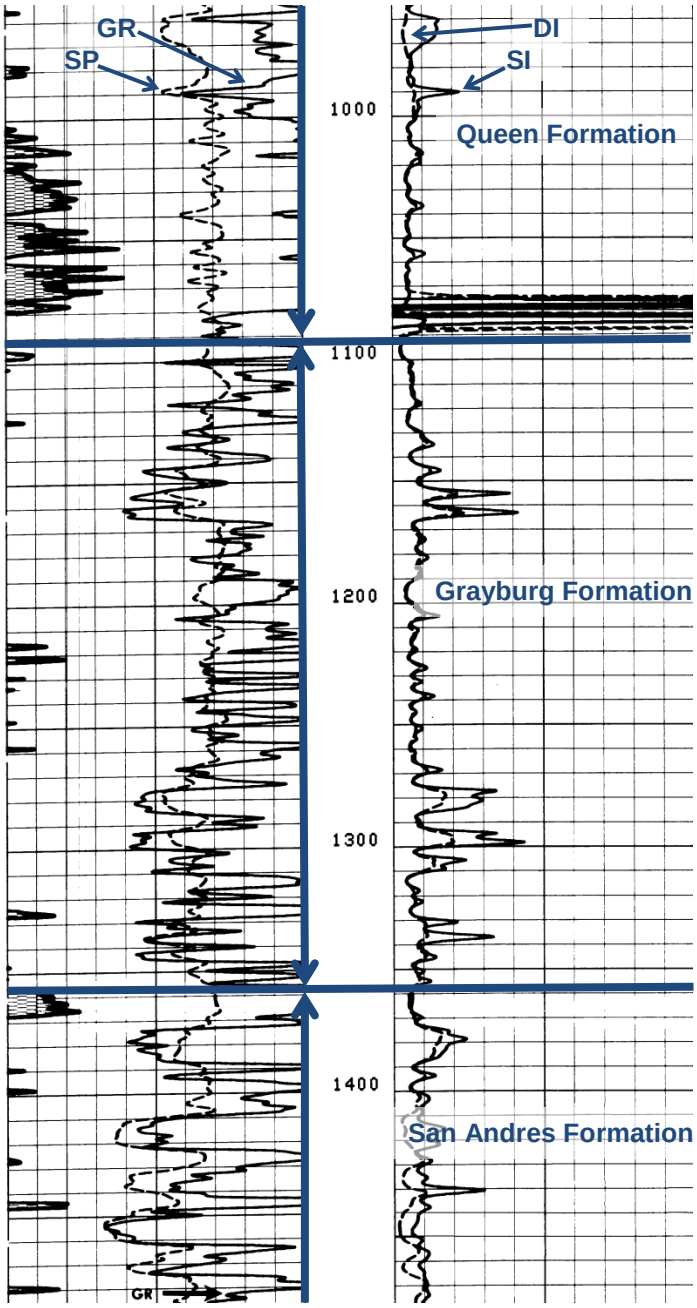

Figure 7.3-4. **Western correlations for the Queen Formation, Grayburg Formation, and San Andres Formation on BRACS Database well identification number 35123. The spontaneous potential and gamma ray tools are shown in the left track, depth (in feet below ground surface) is shown in the middle track, and the shallow and deep induction tools are shown in the right track. DI = deep induction, GR = gamma ray, SI = short induction, SP = spontaneous potential.**

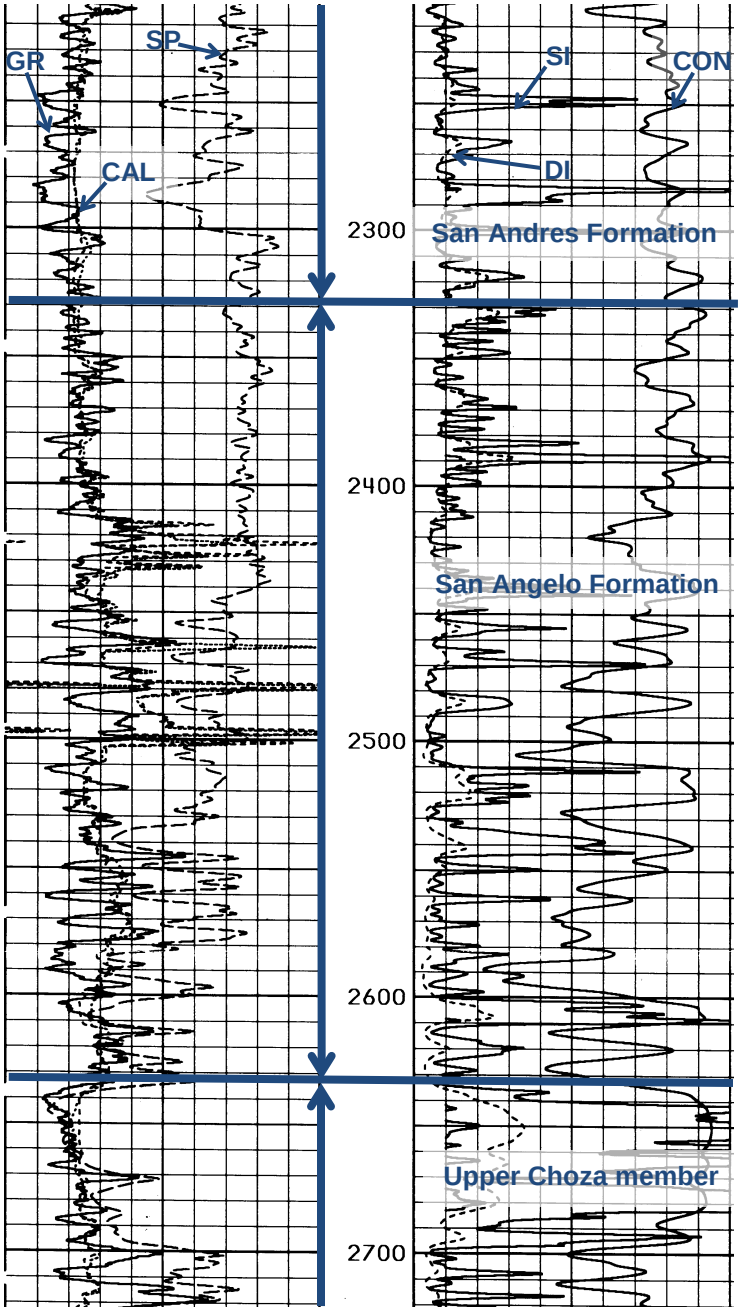

Figure 7.3-5. **Western correlations for the San Andres Formation, San Angelo Formation, and Upper Choza member on BRACS Database well identification number 28112. The caliper, spontaneous potential, and gamma ray tools are shown in the left track, depth (in feet below ground surface) is shown in the middle track, and the shallow and deep induction and conductivity tools are shown in the right track. CAL = caliper, CON = conductivity, DI = deep induction, GR = gamma ray, SI = short induction, SP = spontaneous potential.**

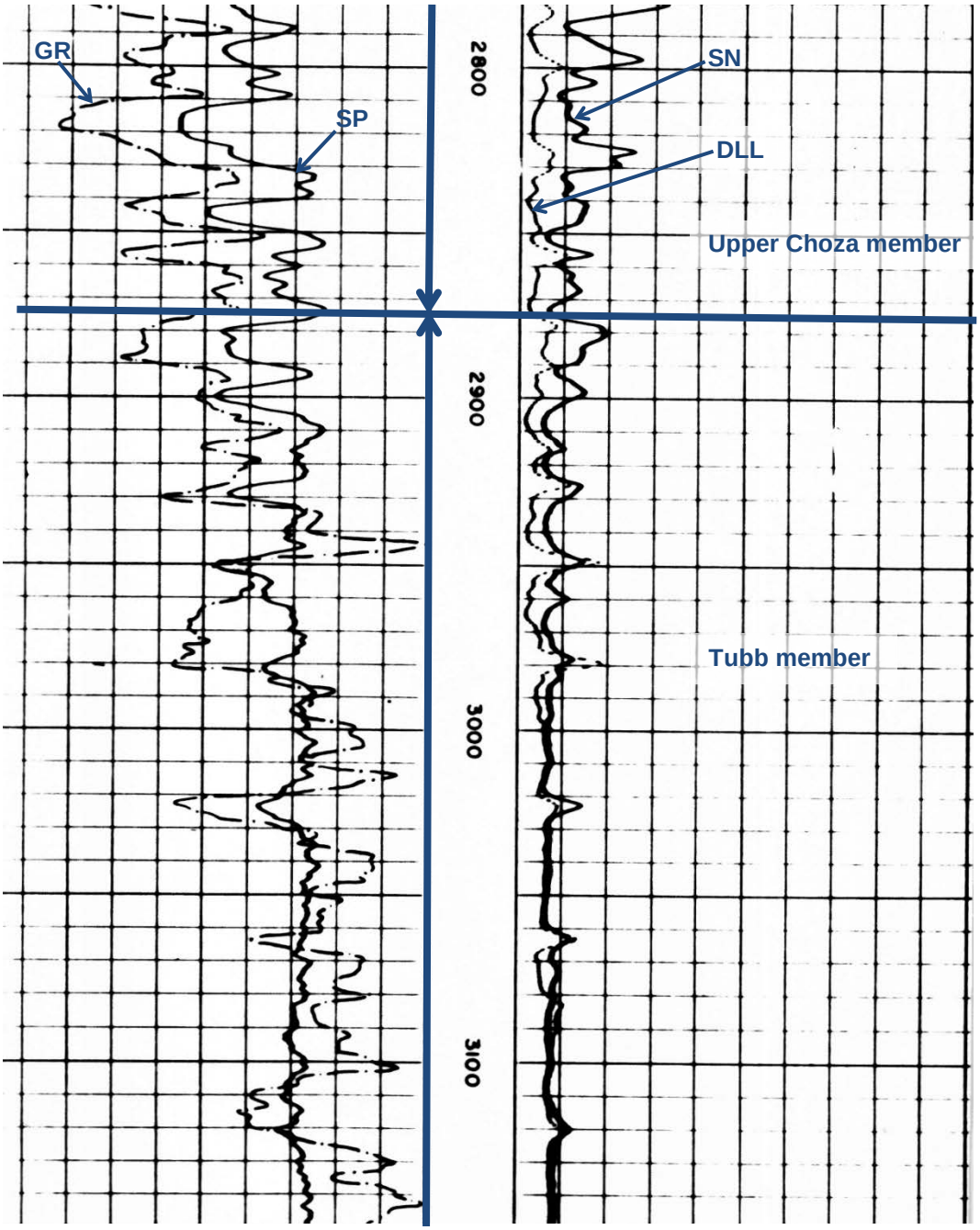

Figure 7.3-6. **Western correlations for the Upper Choza member and Tubb member on BRACS Database well identification number 37978. The spontaneous potential and gamma ray tools are shown in the left track, depth (in feet below ground surface) is shown in the middle track, and the normal and deep lateral resistivity tools are shown in the right track. DLL = deep lateral resistivity, GR = gamma ray, SN = short normal resistivity, SP = spontaneous potential.**

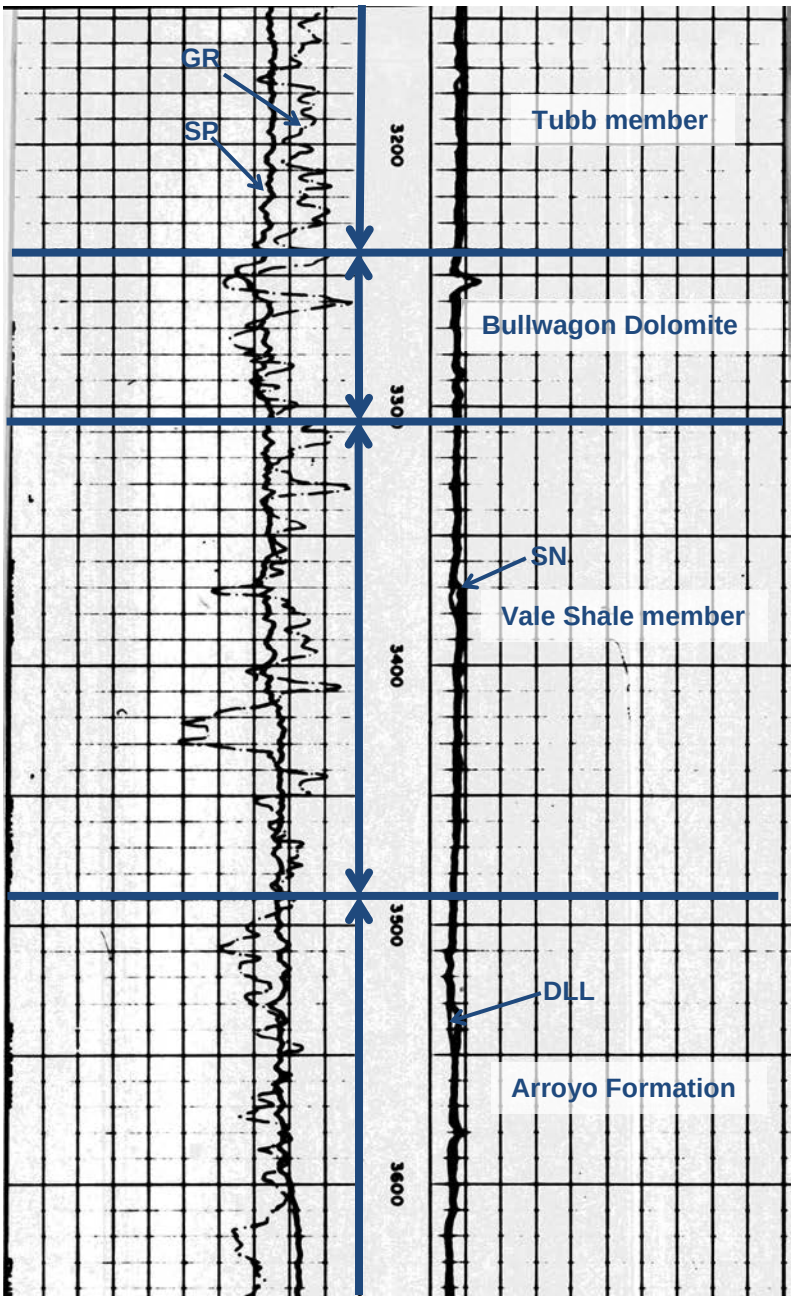

Figure 7.3-7. **Western correlations for the Tubb member, Bullwagon Dolomite, Vale Shale member, and Arroyo Formation on BRACS Database well identification number 37978. The spontaneous potential and gamma ray tools are shown in the left track, depth (in feet below ground surface) is shown in the middle track, and the normal and deep lateral resistivity tools are shown in the right track. DLL = deep lateral resistivity, GR = gamma ray, SN = short normal resistivity, SP = spontaneous potential.**

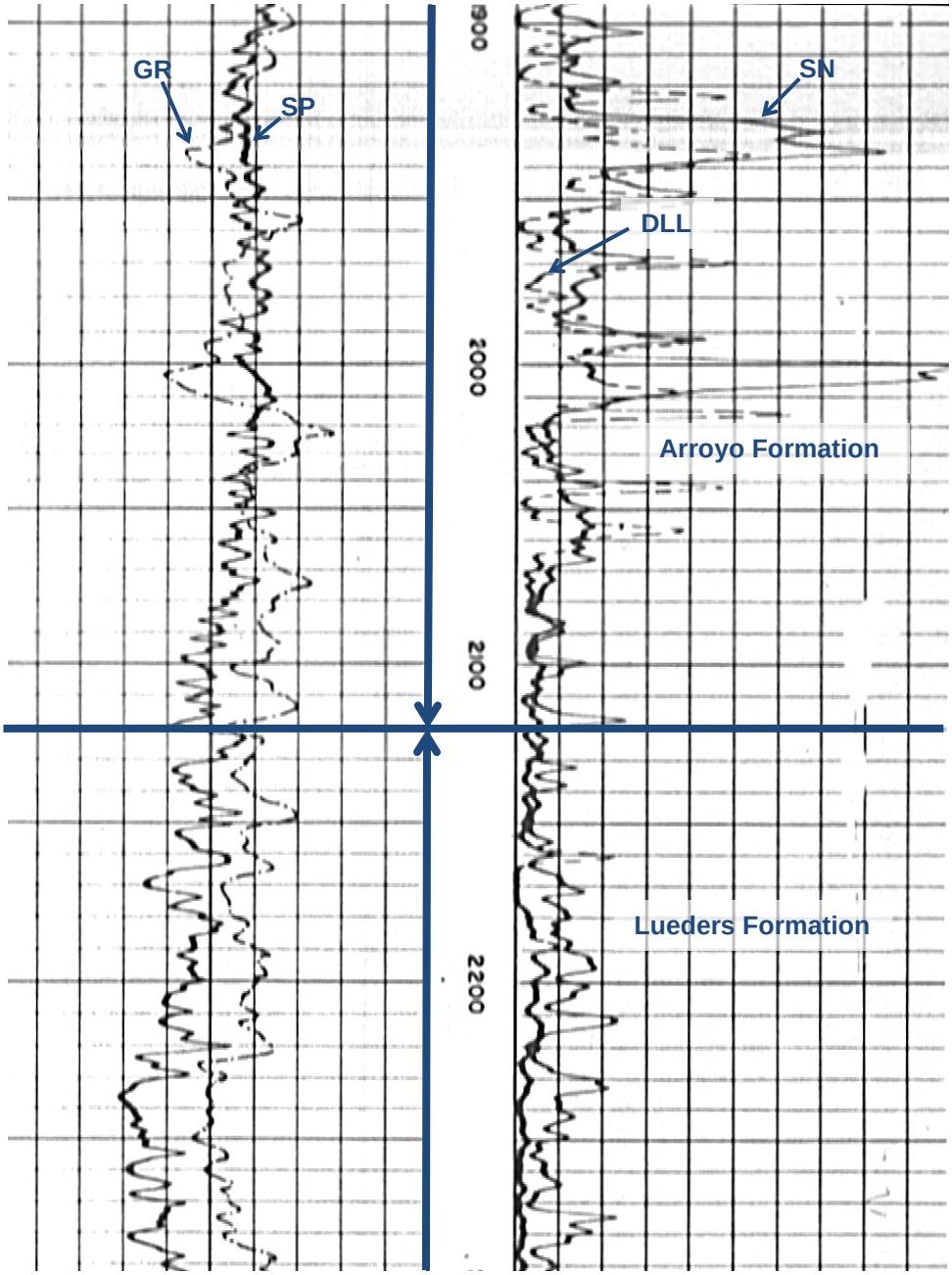

Figure 7.3-8. **Western correlations for the Arroyo Formation and Lueders Formation on BRACS Database well identification number 25724. The spontaneous potential and gamma ray tools are shown in the left track, depth (in feet below ground surface) is shown in the middle track, and the normal and deep lateral resistivity tools are shown in the right track. DLL = deep lateral resistivity, GR = gamma ray , SN = short normal resistivity, SP=spontaneous potential.**

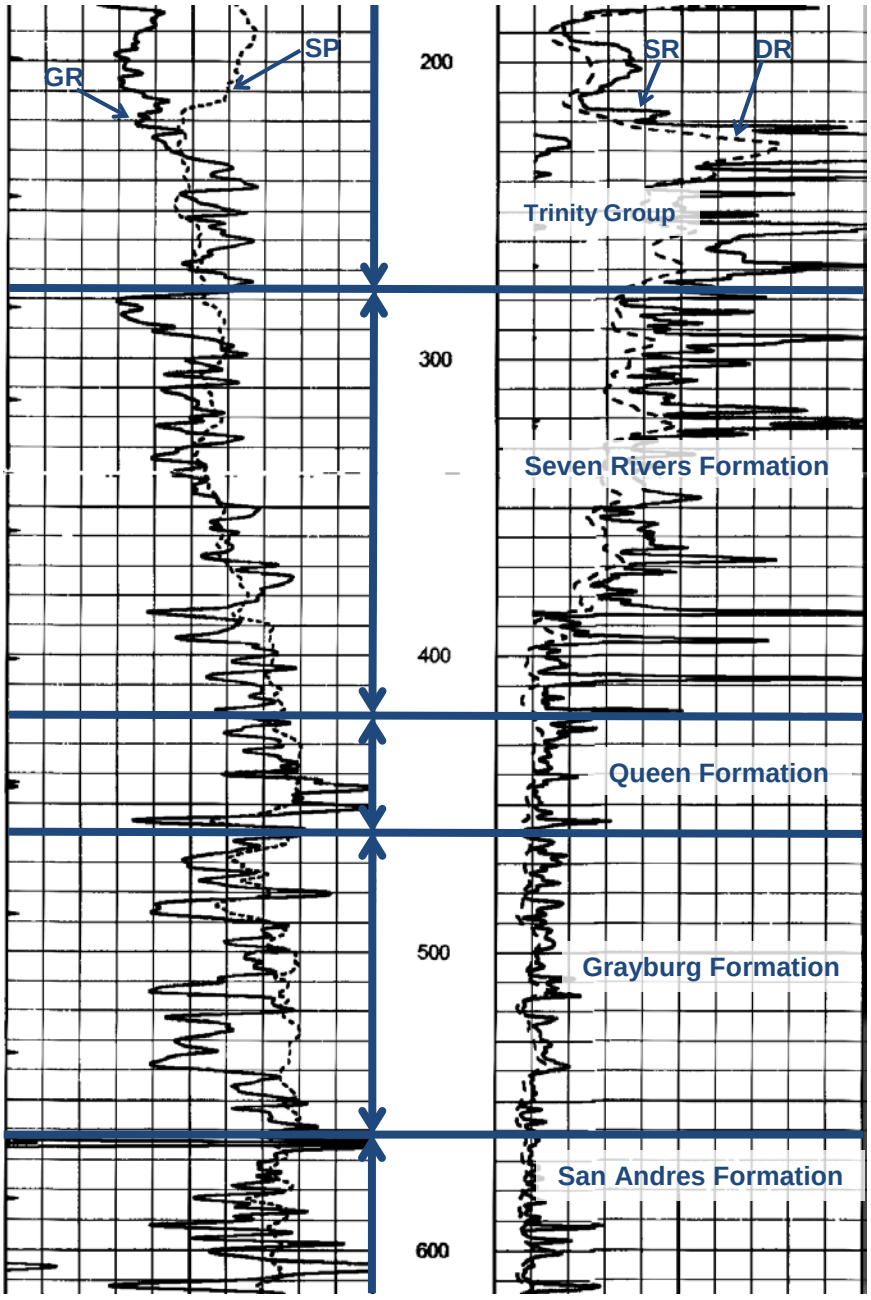

Figure 7.3-9. **Eastern correlations for the Trinity Group, Seven Rivers Formation, Queen Formation, Grayburg Formation, and San Andres Formation on BRACS Database well identification number 55930. The spontaneous potential and gamma ray tools are shown in the left track, depth (in feet below ground surface) is shown in the middle track, and the shallow and deep resistivity tools are shown in the right track. DR = deep induction resistivity, GR = gamma ray, SP = spontaneous potential, SR = shallow resistivity.**

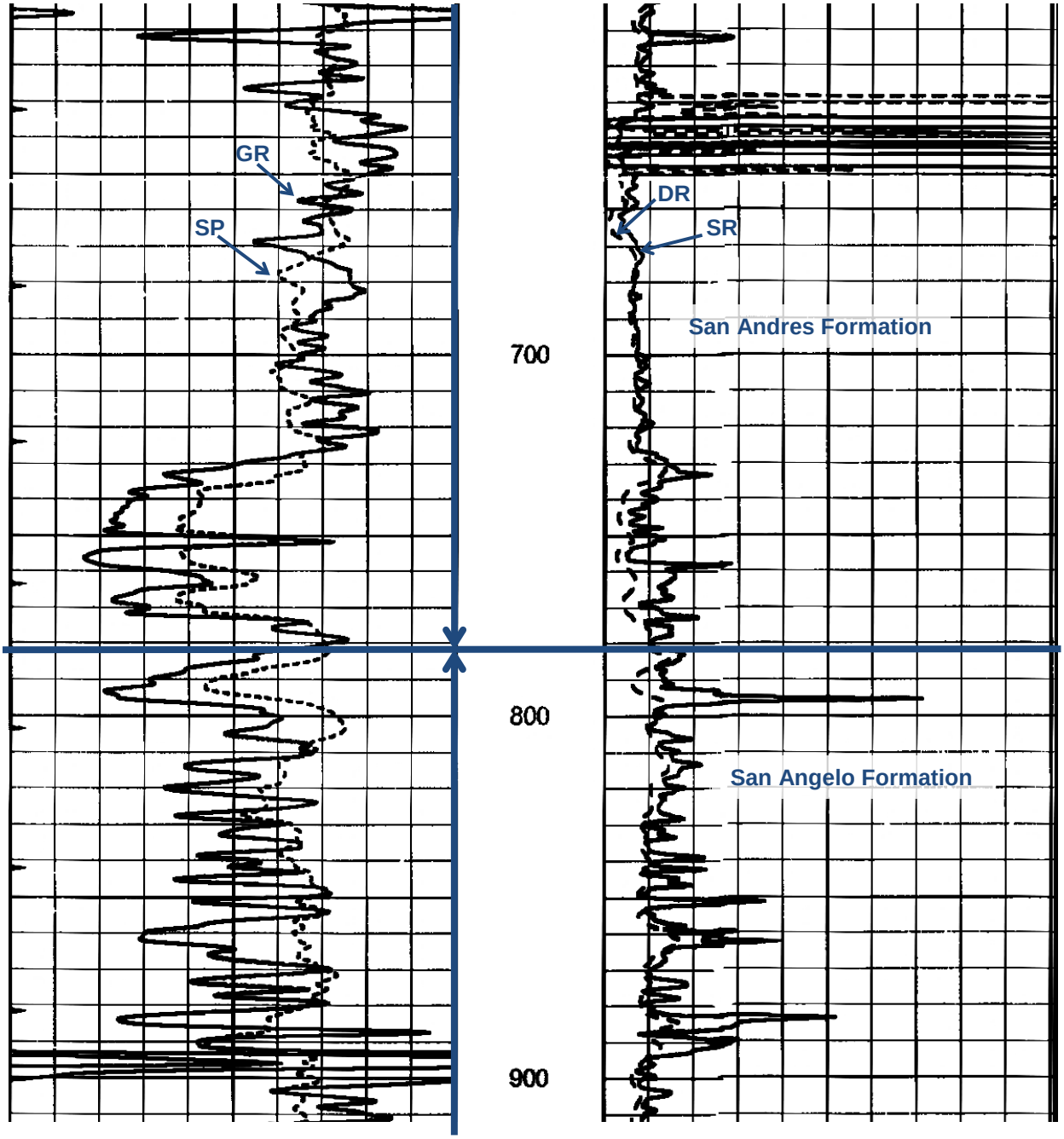

Figure 7.3-10. **Eastern correlations for the San Andres Formation and San Angelo Formation on BRACS Database well identification number 55930. The spontaneous potential and gamma ray tools are shown in the left track, depth (in feet below ground surface) is shown in the middle track, and the shallow and deep resistivity tools are shown in the right track. DR = deep induction resistivity, GR = gamma ray, SP = spontaneous potential, SR = shallow resistivity.**

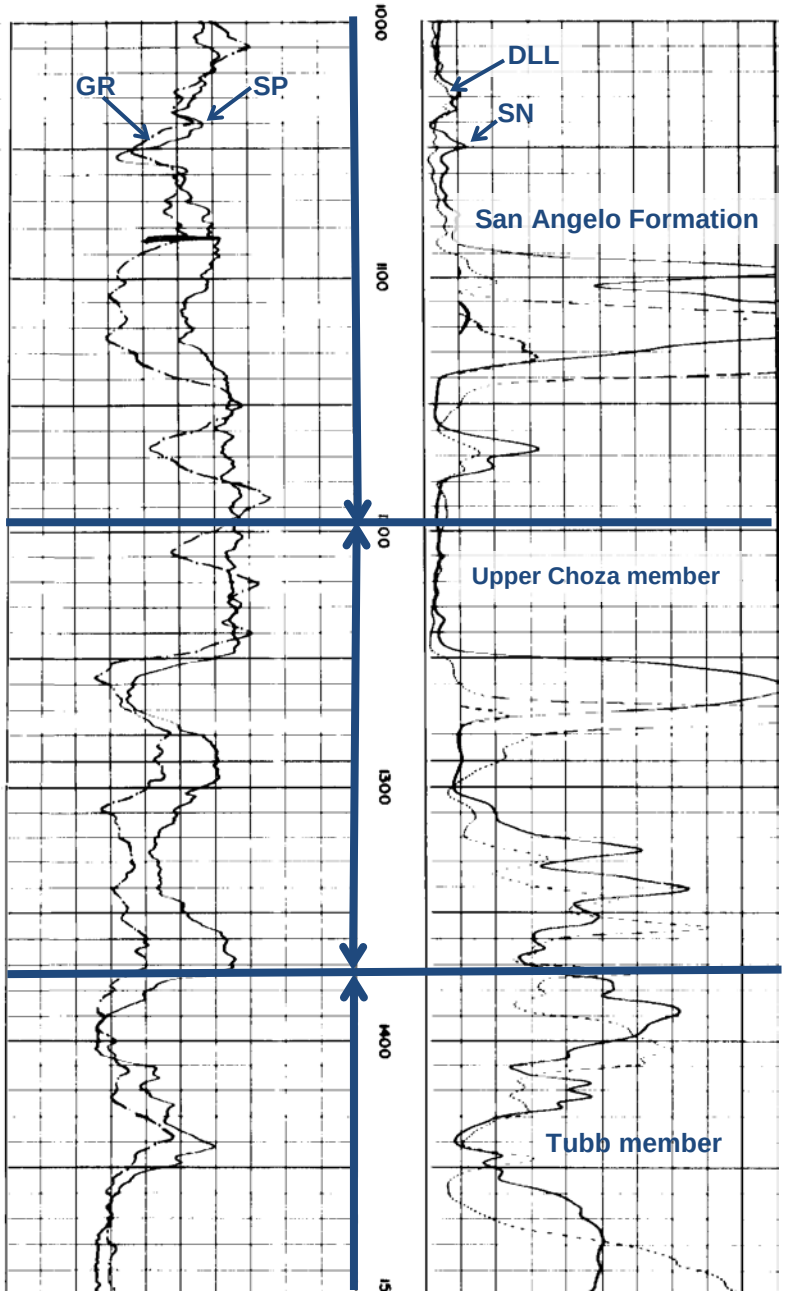

Figure 7.3-11. **Eastern correlations for the San Angelo Formation, Upper Choza member, and Tubb Formation on BRACS Database well identification number 55235. The spontaneous potential and gamma ray tools are shown in the left track, depth (in feet below ground surface) is shown in the middle track, and the short normal and deep lateral resistivity tools are shown in the right track. DLL = deep lateral resistivity, GR = gamma ray, SN = short normal resistivity, SP = spontaneous potential.**

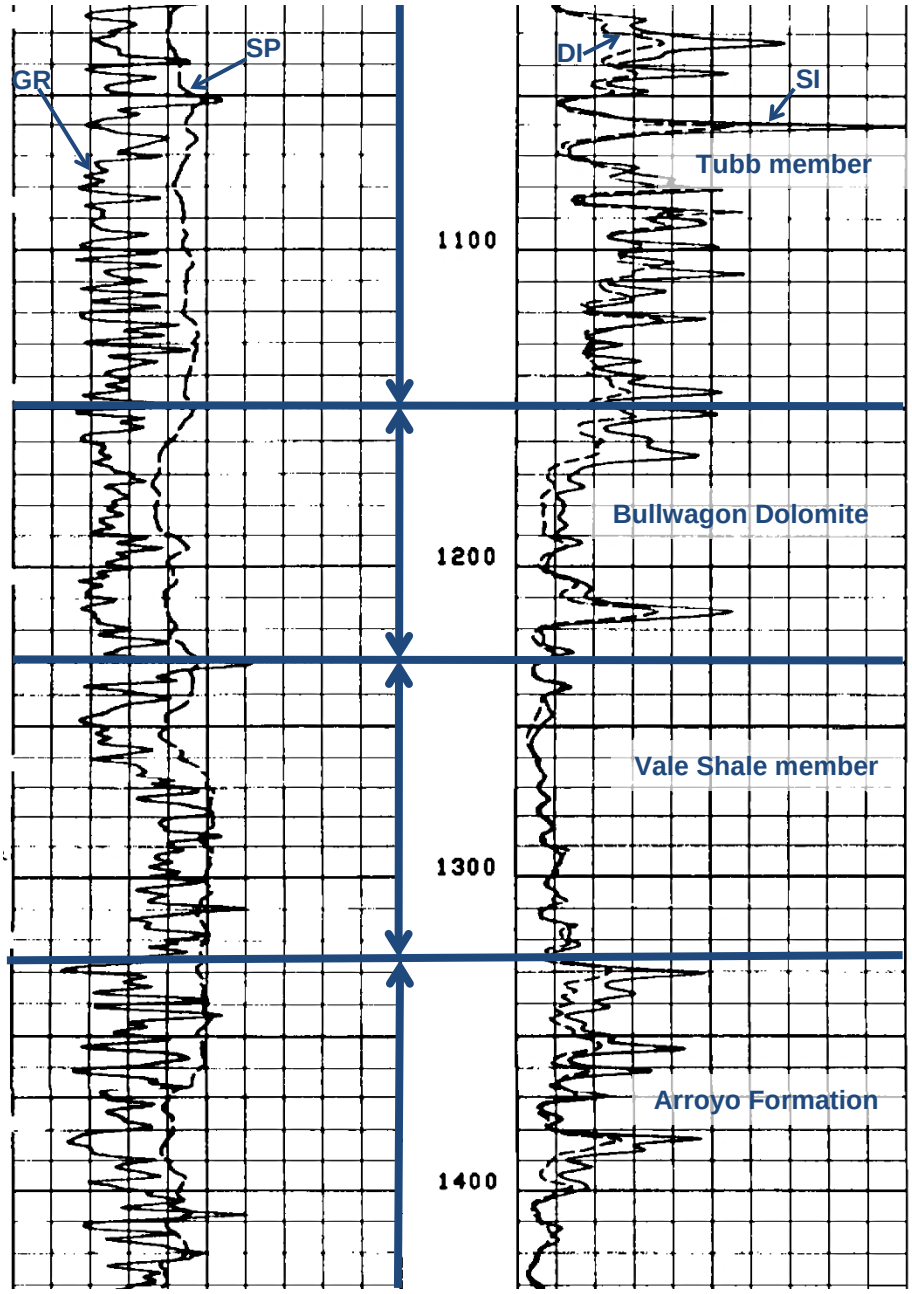

Figure 7.3-12. **Eastern correlations for the Tubb member, Bullwagon Dolomite, Vale Shale member, and Arroyo Formation on BRACS Database well identification number 55756. The spontaneous potential and gamma ray tools are shown in the left track, depth (in feet below ground surface) is shown in the middle track, and the short normal and deep induction tools are shown in the right track. DI = deep induction, GR = gamma ray, SI = short induction, SP = spontaneous potential.**

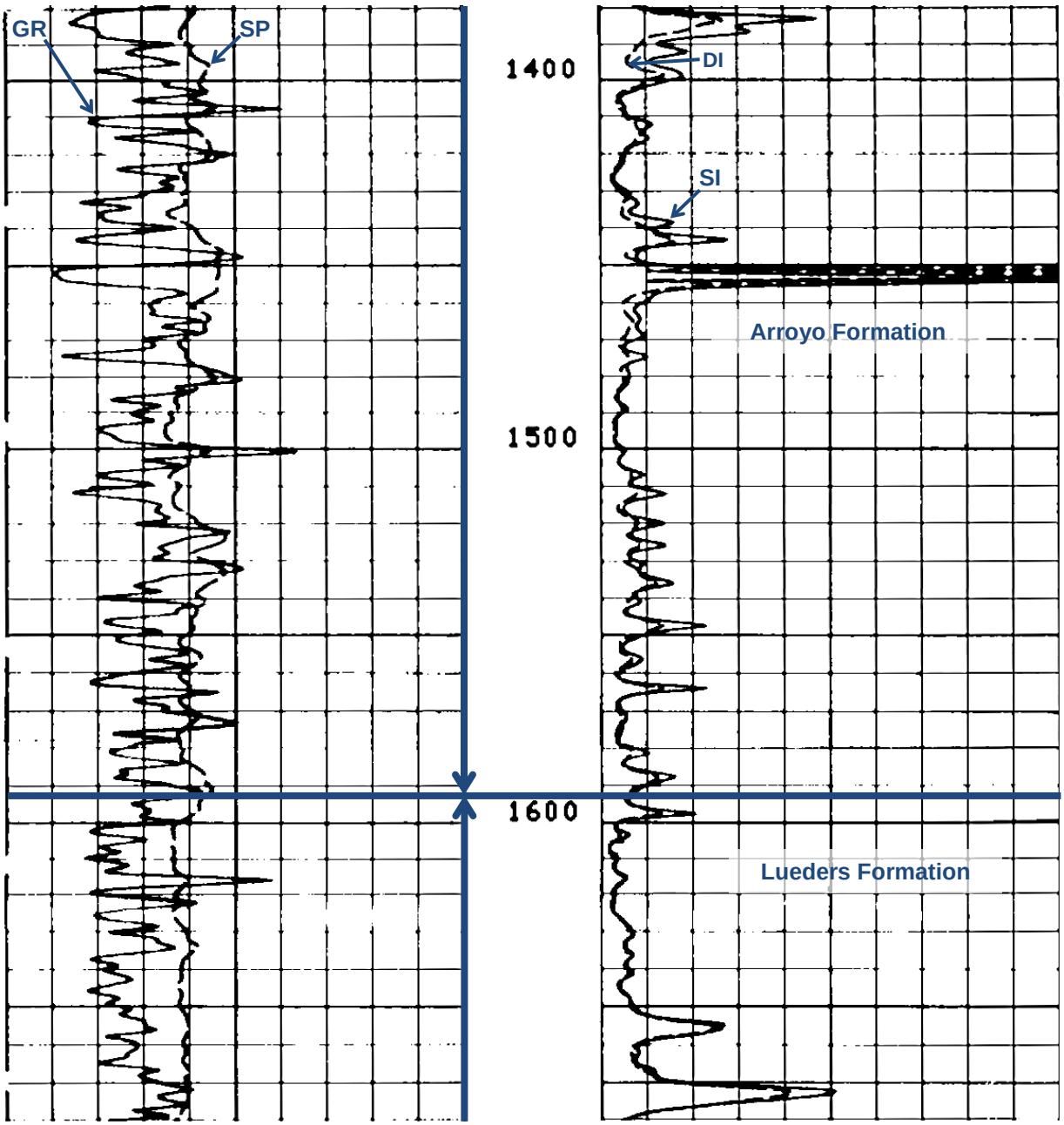

Figure 7.3-13. Eastern correlations for the Arroyo Formation and Lueders Formation on BRACS Database well identification number 55756. The spontaneous potential and gamma ray tools are shown in the left track, depth (in feet below ground surface) is shown in the middle track, and the short normal and deep induction tools are shown in the right track. DI = deep induction, GR = gamma ray, SI = short induction, SP = spontaneous potential.

7.4 Study area cross sections

We constructed six structural cross sections to illustrate the structural and stratigraphic relationships of the geological formations interpreted in the study area. Using a set of Python® scripts developed in ArcGIS® at the U.S. Geological Survey (Thoms, 2005), we constructed cross section profiles that used the GIS elevation surfaces created from the well log correlations made during the course of this study. These cross sections span the entire study area (Figure 7.4-1), providing a powerful aid in understanding the nature of the geologic contact between the various units. A vertical to horizontal exaggeration of 100 was utilized to visualize some of the thinner correlated formations. The cross reference list of codes and associated stratigraphic units is presented in Table 7.4-1**.**

Cross section A-A' transects the study area in a northwest to southeast direction (Figure 7.4-2). The cross section is oriented in the general direction of the structural dip of the Permian formations. Note the onlapping of the Seven Rivers, Queen, and Grayburg formations onto the San Andres Formation.

Cross section B-B' transects the study area in a northwest to southeast direction (Figure 7.4-3). The cross section is oriented in the general direction of the structural dip of the Permian formations. Note the onlapping of the Seven Rivers, Queen, and Grayburg formations onto the San Andres Formation. The Dewey Lake Formation is clearly shown lying unconformably on the Rustler-Salado, Tansill, and Yates formations.

Cross section C-C' transects the study area in a northwest to southeast direction (Figure 7.4-4). The cross section is oriented in the general direction of the structural dip of the Permian formations. Note the onlapping of the Seven Rivers, Queen, and Grayburg formations onto the San Andres Formation. The Dewey Lake Formation is clearly shown lying unconformably on the Rustler-Salado, Tansill, and Yates formations.

Cross section D-D' transects the study area in a southwest to northeast direction (Figure 7.4-5). The cross section is oriented in the general direction of the structural strike of the Permian formations. The Dewey Lake Formation is clearly shown lying unconformably on the Rustler-Salado, Tansill, Yates, and Seven Rivers formations.

Cross section E-E' transects the study area in a southwest to northeast direction (Figure 7.4-6). The cross section is oriented in the general direction of the structural strike of the Permian formations. Note the onlapping of the Seven Rivers, Queen, and Grayburg formations onto the San Andres Formation. The San Angelo and San Andres formations outcrop near the center of the cross section line.

Cross section F-F' transects the study area in a southwest to northeast direction (Figure 7.4-7). The cross section is oriented in the general direction of the structural strike of the Permian formations.

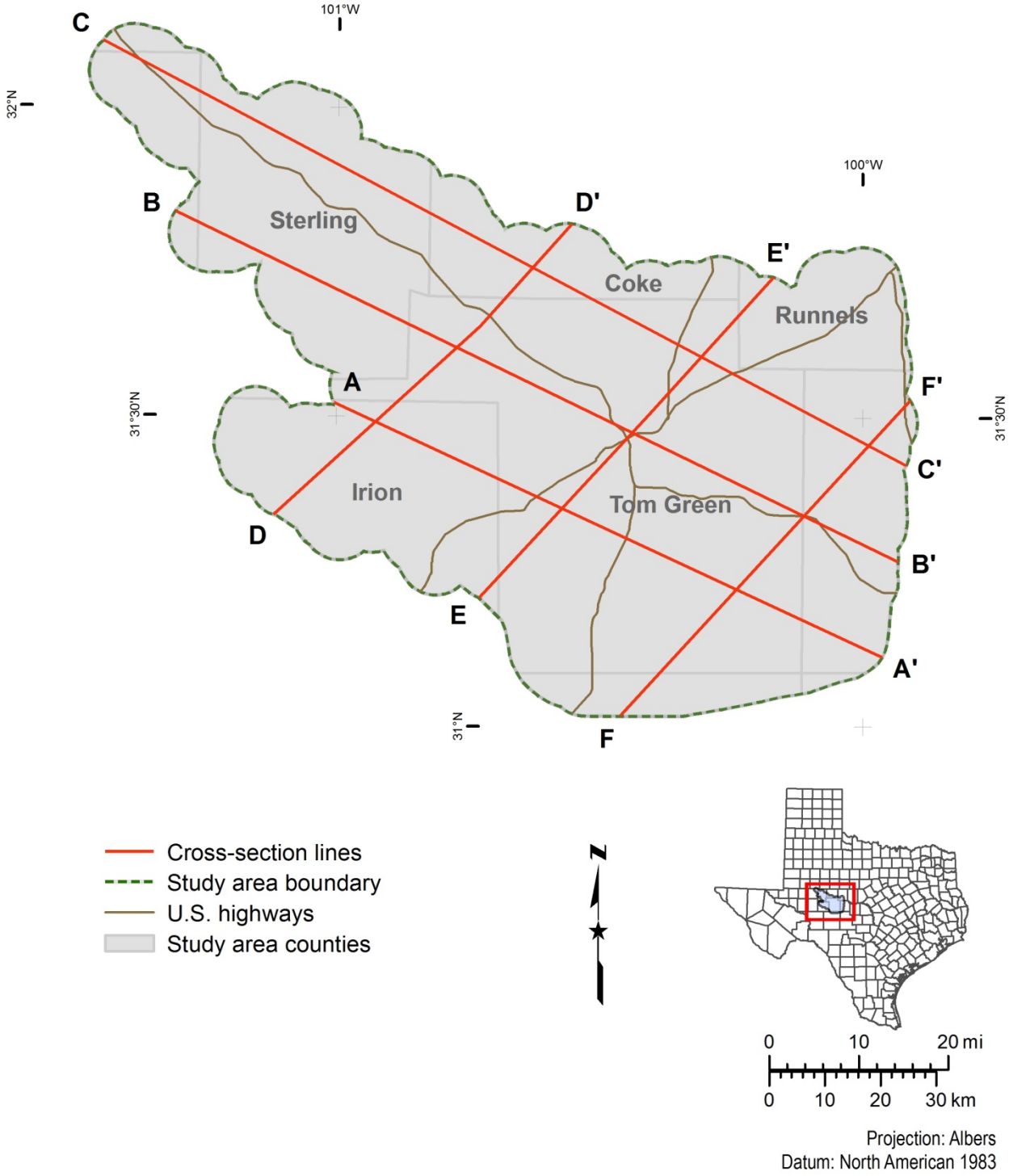

Figure 7.4-1. Location of cross section lines in the Lipan Aquifer study area.

Table 7.4-1. **List of aquifer codes with stratigraphic units referenced in Figure 7.4-2 through Figure 7.4-7. The list is organized from youngest to oldest units.**

Aquifer code	Stratigraphic unit
QT	Quaternary and Neogene sediments
TG	Trinity Group
LD	Dockum Group
DL	Dewey Lake Formation
RSC	Rustler-Salado formations
TA	Tansill Formation
YA	Yates Formation
SR	Seven Rivers Formation
Q	Queen Formation
GY	Grayburg Formation
SA	San Andres Formation
SG	San Angelo Formation
CH	Upper Choza member
TB	Tubb member
BW	Bullwagon Dolomite
VL	Vale Shale member
AY	Arroyo Formation
LE	Lueders Formation and older formations

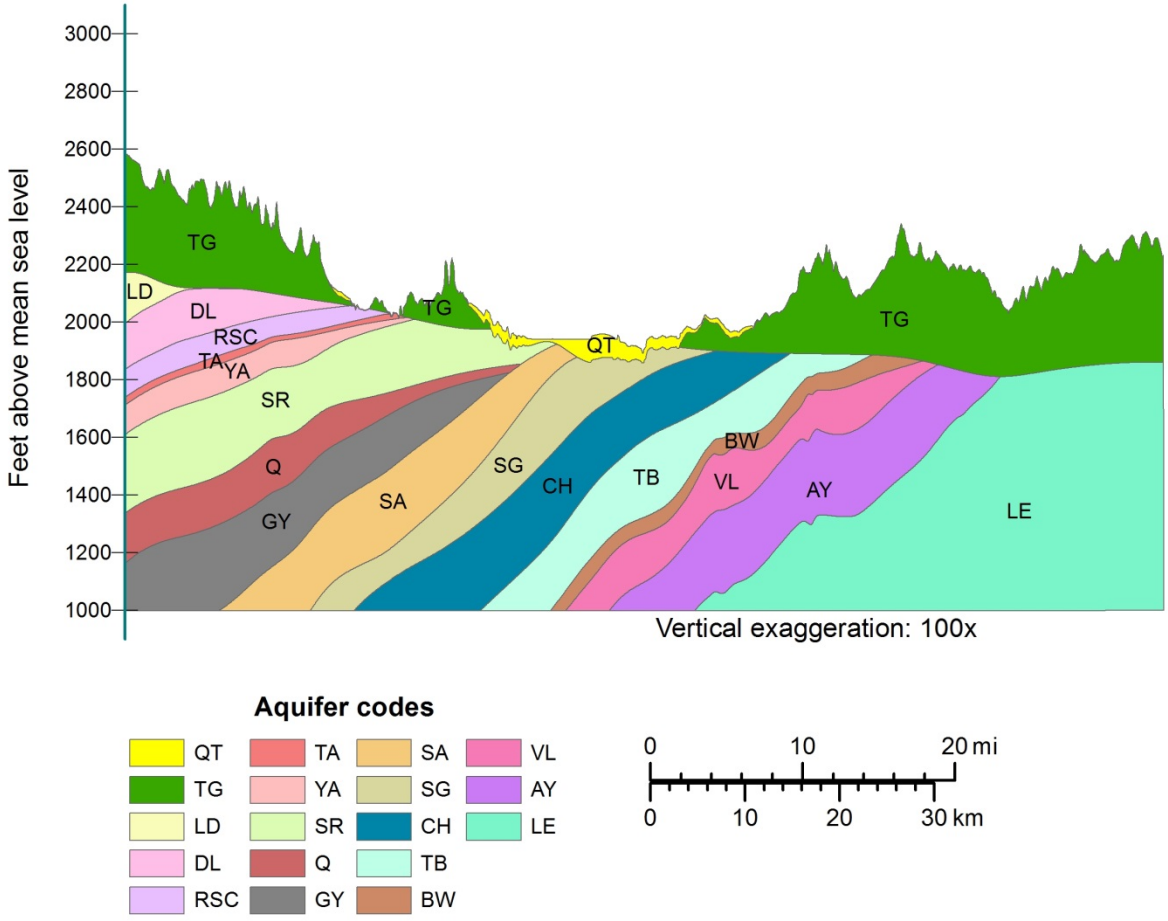

Figure 7.4-2. Cross section A-A'. Refer to Figure 7.4-1 for cross section location and Table 7.4-1 for aquifer code descriptions.

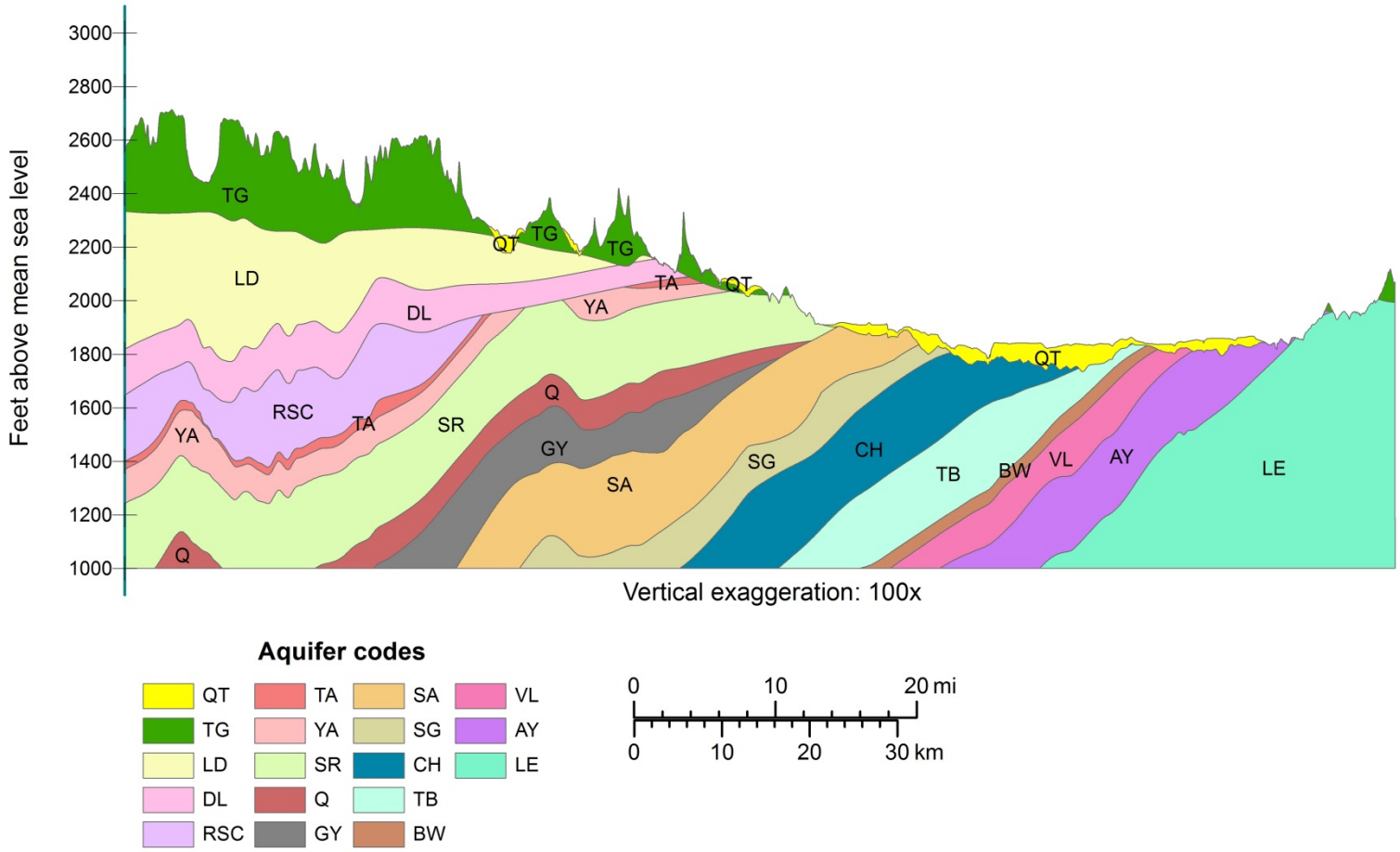

Figure 7.4-3. Cross section B-B'. Refer to Figure 7.4-1 for cross section location and Table 7.4-1 for aquifer code descriptions.

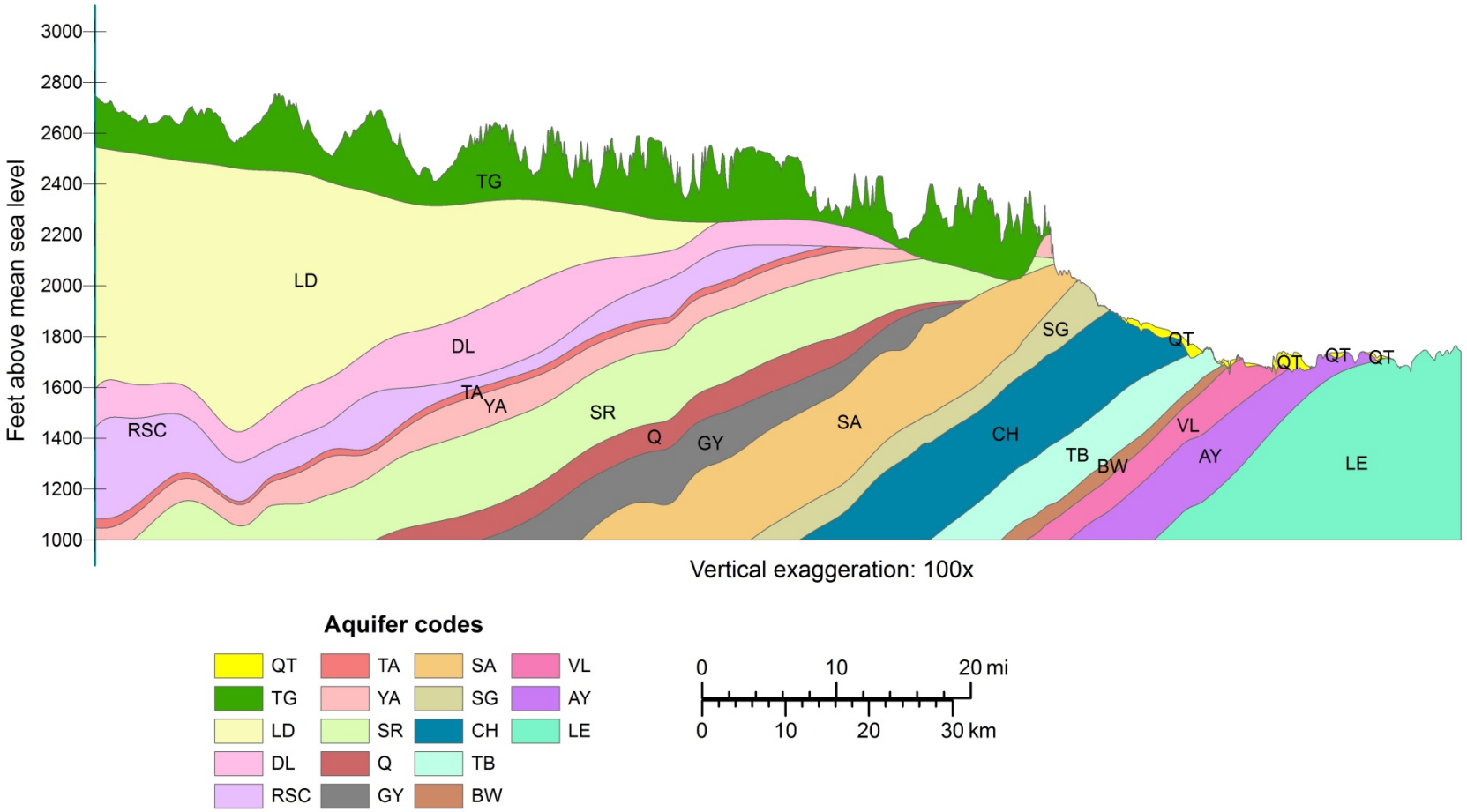

Figure 7.4-4. Cross section C-C'. Refer to Figure 7.4-1 for cross section location and Table 7.4-1 for aquifer code descriptions.

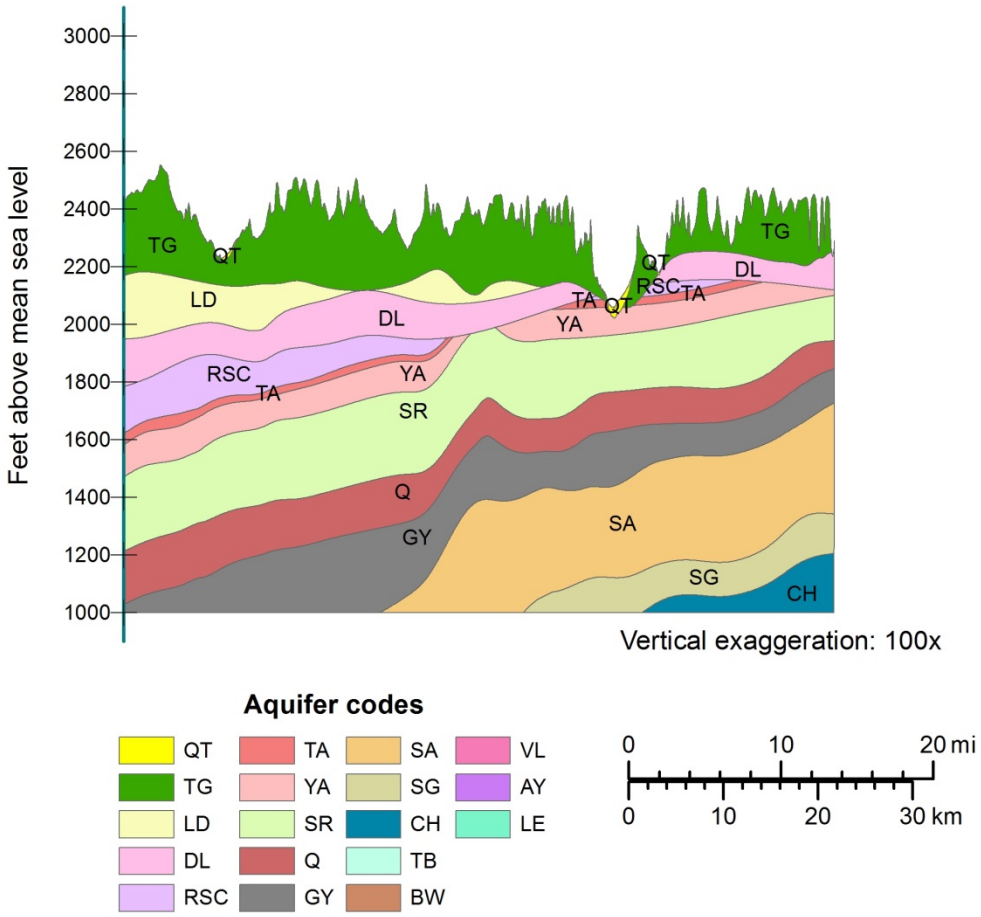

Figure 7.4-5. Cross section D-D'. Refer to Figure 7.4-1 for cross section location and Table 7.4-1 for aquifer code descriptions.

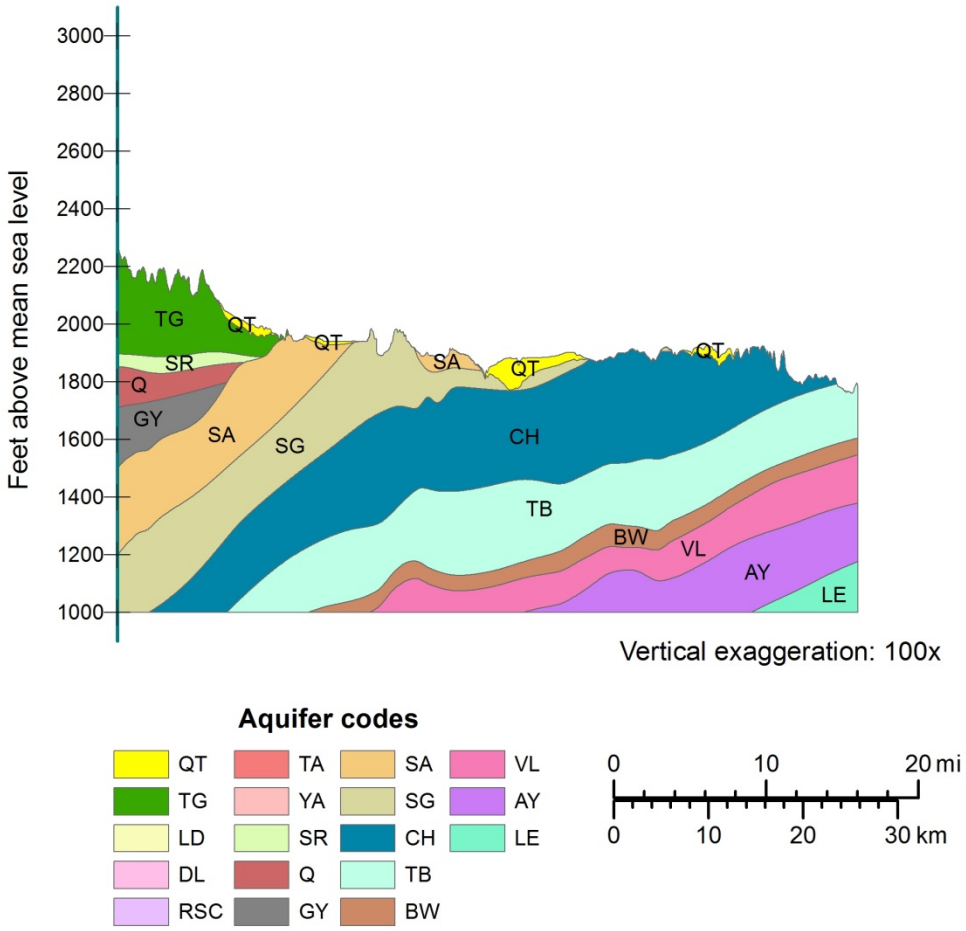

Figure 7.4-6. **Cross section E-E'. Refer to Figure 7.4-1 for cross section location and Table 7.4-1 for aquifer code descriptions. The San Angelo and San Andres formations outcrop near the center of the cross section line.**

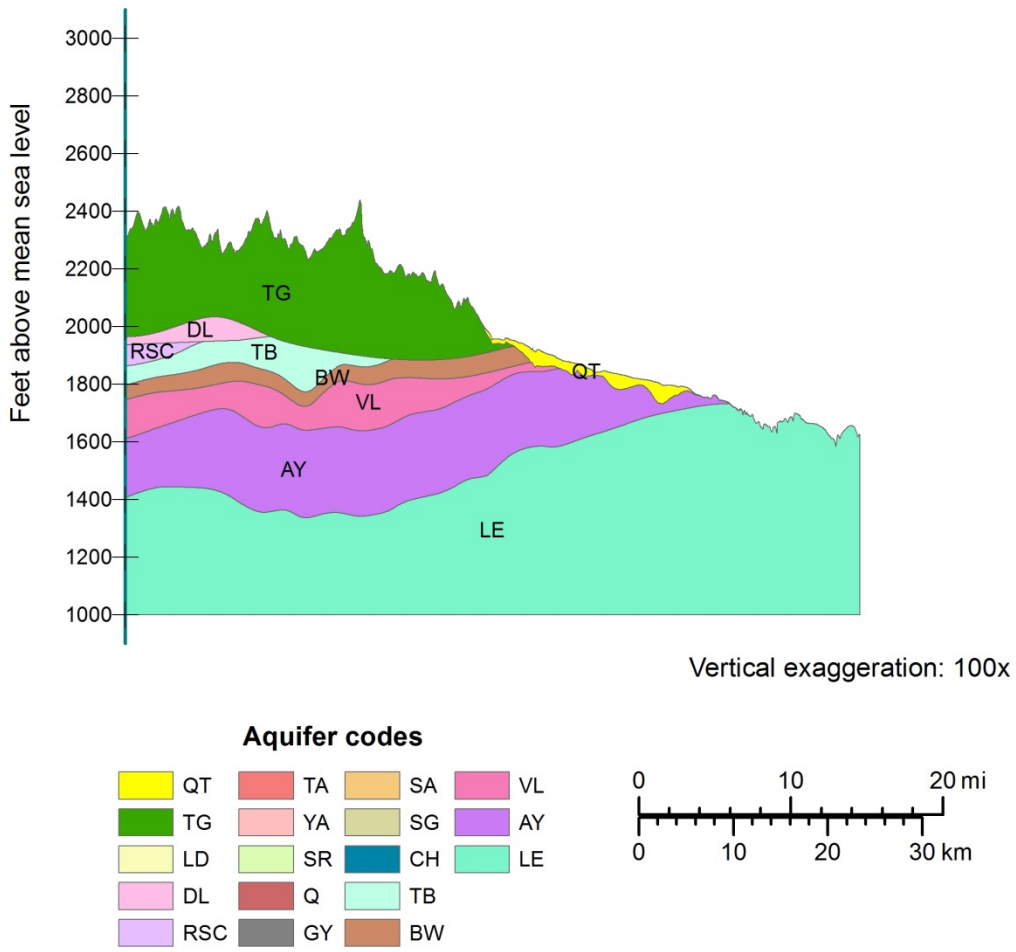

Figure 7.4-7. Cross section F-F'. Refer to Figure 7.4-1 for cross section location and Table 7.4-1 for aquifer code descriptions.

8. Aquifer determination

Water wells in the TWDB Groundwater Database have aquifer codes assigned to them. Over the 25 years that the database has been in existence, different staff members have used a variety of information to assign aquifer codes in the database. In the study area there has been significant variability in the assignment of these aquifer codes because of the complex relationship between the overlying Quaternary and Neogene sediments and the underlying Permian formations. The stratigraphic correlations that we have made during the course of this study created new subdivisions of the Clear Fork Group that have not previously been used at the TWDB.

A uniform dataset was created that would allow us to compare water quality, static water level, and aquifer test information within an individual stratigraphic unit or across a group of units. In order to complete this task we used GIS and conducted database queries of many different tables to analyze the data and compile it into a study aquifer determination table in Microsoft® Access®.

In the analysis, each stratigraphic unit was included in the study area: Quaternary and Neogene sediments, Trinity Group, Dockum Group, Rustler-Salado formations, Tansill Formation, Yates Formation, Seven Rivers Formation, Queen Formation, Grayburg Formation, San Andres Formation, San Angelo Formation, Upper Choza member, Tubb member, Bullwagon Dolomite, Vale Shale member, Arroyo Formation, and Lueders Formation.

The first step was to select all TWDB Groundwater Database wells and BRACS Database wells within the study area and insert them into the aquifer determination table named tblBRACS_Lipan_AquiferDetermination. There are 6,995 wells in this table: 2,708 with a state well number, 4,681 with a BRACS Database well number, and 394 that have both numbers.

We extracted the depth-to-surface value for each interpreted stratigraphic unit (for example, San Angelo Formation top depth) at each well site using the ArcGIS® tool (Spatial Analyst®, Extraction, Extract Value to Point). These extracted values were then used to update the aquifer determination table in Microsoft® Access®. The spatial intersection of the (1) top and bottom of the well screen interval, (2) well depth, or (3) total depth of a well with the top and bottom surfaces of the geological units was made for each well in the table. The intersection precedence, if present, was well screen, well depth, and total depth of hole. Well screens that straddled more than one stratigraphic unit had each stratigraphic unit assigned to it. If well screen information was not available, the well depth or total depth of the hole was used. In these cases, all stratigraphic units were selected based on the depth and formation top and bottom depths and an "X" was added to the beginning of the list of stratigraphic codes to indicate that no screen information was available.

Queries were written in Structured Query Language, and the analysis was processed using four programs written using Visual Basic for Applications® in Microsoft® Access®. All of the wells were processed together in a series of steps. Results were checked with the raw data and queried for consistency and accuracy and when necessary the Visual Basic for Applications® code was corrected and the data reprocessed. This selection process determined and recorded the aquifer(s) for each well. Wells with no screened interval and no total depth available were not assigned aquifers.

The well information stored in the database was extracted and geo-referenced in ArcGIS® to spatially display the information. This step was used to verify the logic of the Structured Query Language and to identify and correct errors. The patterns of aquifer usage across the study area can thus be evaluated, although care needs to be exercised when using wells whose aquifer(s) were assigned only on the basis of well depth or total depth of hole.

With the results of the aquifer determination analysis we were able to assign a standardized set of aquifer codes for groundwater quality samples, aquifer test results, and salinity calculations. Throughout this report the aquifer codes assigned were used to classify data and analyses in a uniform and consistent manner.

The newly assigned aquifer codes were compared to aquifer assignments of wells in the TWDB Groundwater Database and to water sample data in published reports. In many cases, the aquifer codes previously assigned to a well were different from our aquifer determination result. We reviewed many of these, reexamining the water well report lithology, well screen, and formation surface datasets and concluded that the aquifer codes assigned in this study represent an accurate classification. In the future we may apply the BRACS aquifer determinations for the aquifer designations in the TWDB Groundwater Database.

Wells with aquifer test information were assessed using the aquifer determination results and then compared with the source of the data in published reports. In several cases, the aquifer assigned to a well in the published report was different from the aquifer determination result. After reexamining the water well report lithology, well screen, and formation surface datasets, we concluded that errors in past reports have persisted and been carried over into more recent studies.

While the analysis tool was written specifically for this study area, the methodology can be applied anywhere in the state. However, the dataset and series of custom queries must be developed for each specific study area.

9. Aquifer hydraulic properties

The hydraulic properties of an aquifer refer to characteristics that allow water to flow through the aquifer. Hydraulic properties include transmissivity, hydraulic conductivity, specific yield, specific capacity, drawdown, pumping rate (well yield), and storage coefficient. Lithology, cementation, fracturing, structural framework, and juxtaposition of adjacent geological formations all influence the flow of water within and between aquifers.

We compiled hydraulic properties for 1,341 wells containing 1,433 analyses completed in the study area. This data is contained in the BRACS Database in the table called tblBRACS_AquiferTestInformation and in the custom study area table called tblBRACS_Lipan_Aquifer_Test. Our analysis was limited to the Quaternary and Neogene sediments and nine Permian stratigraphic units that are known to be composed of lithologies that have aquifer characteristics conducive to groundwater storage and flow, resulting in 10 total target units. The Cretaceous and Triassic formations in the area will be considered separately in future studies. We also excluded wells that we determined may have produced water from multiple Permian formations. This approach was used to isolate hydraulic characteristics to a known Permian formation and/or its overlying Quaternary and Neogene sediments. This exclusion process reduced available data to 379 wells containing 396 analyses. This selected subset of available data is in the BRACS Database in the table called tblBRACS_Lipan_Aquifer_Test_Select. Locations of these wells are presented in Figure 9-1.

The spatial distribution of wells with aquifer test data and displayed with symbol colors based on geological formation clearly shows a pattern of clustering in a southwest to northeast orientation that reflects the subcrop structural dip of the Permian formations, with progressively younger formations displayed from southeast to northwest (Figure 9-1). Hydraulic property data was not available for the Queen Formation. Available data for the nine remaining geological units evaluated for water production are shown in Table 9-1.

The sources of aquifer test information include (1) TWDB aquifer test spreadsheet, (2) the remarks table in the TWDB Groundwater Database, (3) published reports (LBG-Guyton Associates, 2008), and (4) the Texas Department of Licensing and Regulation Submitted Driller's Report Database (2016). Additional information may be available in the TWDB paper well reports.

We found no hydraulic conductivity or specific yield data for wells located within the study area that met the criteria noted above. There was one well, BRACS well identification number 51961 (state well number 43-149-03), which was completed in the Upper Choza member and reported a transmissivity of 1,100 gallons per day per foot.

Users of the hydraulic property data presented in our study should evaluate the data in the proper context. We obtained many of the well yields from tests conducted decades ago, and many well yields are from domestic small-capacity wells that may not be indicative of what a properly designed, large capacity well may be capable of producing.

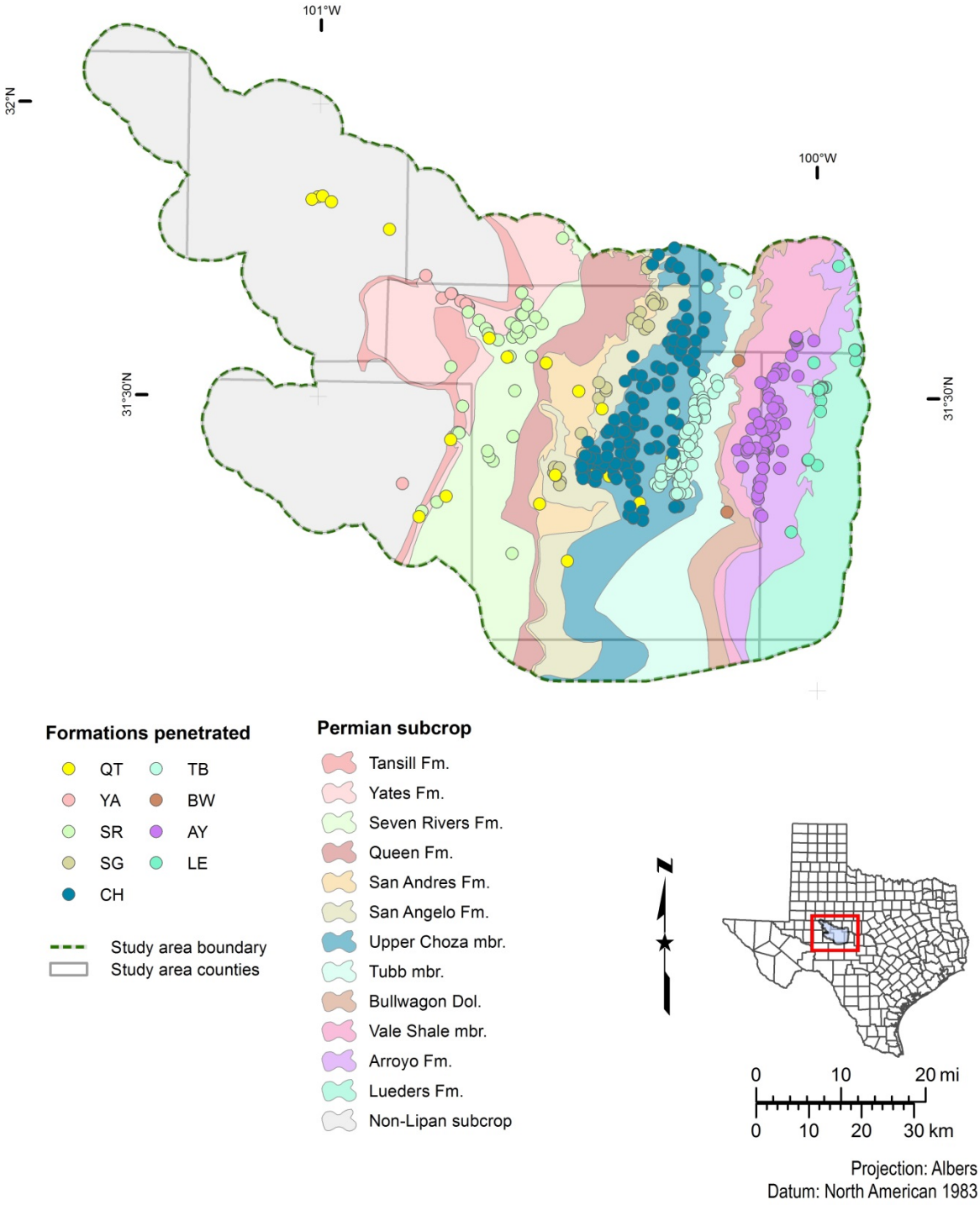

Figure 9-1. **Location of wells with aquifer test data. Refer to Table 9-1 for a summary of properties recorded. Designated formations penetrated may also include an overlying Quaternary and Neogene sediments interval. Shaded areas indicate where Permian formations either outcrop or subcrop below overlying Quaternary and Neogene sediments or Cretaceous formations. Wells with aquifer test data completed in the Trinity or Dockum groups are not shown. Cross-reference for formation labels and names are shown in Table 7.4-1. Dol = Dolomite, Fm. = Formation, mbr. = member.**

Table 9-1. Hydraulic properties of formations in the Lipan Aquifer study area. Wells penetrating the Trinity and Dockum groups or wells that may produce water from multiple Permian units are excluded.

Geological unit	Property	Sample count	Min	Max	Mean	Median
Quaternary and Neogene sediments	Well yield	24	2	750	157	35
	Drawdown	4	3	20	10	8.5
	Specific capacity	4	0.86	15	5	2.17
Yates Formation	Well yield	9	9	395	126	100
	Drawdown	3	10	15	11.7	10
	Specific capacity	3	6	26.3	13.1	7
Seven Rivers Formation	Well yield	40	2	500	54.5	16
	Drawdown	5	6	165	61	48
	Specific capacity	5	0.02	4.21	2.01	1.25
San Angelo Formation	Well yield	26	2	150	20.1	14.5
	Drawdown	2	2	12	7	7
	Specific capacity	2	1.17	15	8.1	8.1
Upper Choza member	Well yield	128	1	720	89	30
	Drawdown	11	2	60	20.4	11.5
	Specific capacity	11	0.05	75	8	0.71
Tubb member	Well yield	77	10	1,000	299	230
	Drawdown	7	2	30	12.1	8
	Specific capacity	7	16.7	475	140.2	106.3
Bullwagon Dolomite	Well yield	2	20	100	60	60
	Drawdown	N/A	N/A	N/A	N/A	
	Specific capacity	N/A	N/A	N/A	N/A	
Arroyo Formation	Well yield	65	1	1,200	148	120
	Drawdown	1	70	70	70	70
	Specific capacity	1	2.14	2.14	2.14	2.14
Lueders Formation	Well yield	25	2	400	139	120
	Drawdown	1	33	33	33	33
	Specific capacity	1	0.06	0.06	0.06	0.06

Notes: Units for well yield (gallons per minute), drawdown (feet), specific capacity (gallons per minute per foot).
N/A = not available, Min = minimum, Max = maximum.

10. Water quality data

We obtained water quality data from the TWDB Groundwater Database and published reports (Richter and others, 1990; LBG-Guyton Associates, 2008). These samples are taken from the raw water source prior to treatment. Results from Safe Drinking Water Act compliance for public water supply systems for this study were not used. These samples are taken from the distribution system after treatment and disinfection and do not provide an accurate assessment of native water quality in the aquifer. Raw water quality results exceeding Safe Drinking Water Act maximum contaminant levels (TCEQ, 2015) indicate pretreatment is required and do not imply that public water systems are providing water exceeding health limits.

We combined all water quality data collected for the study into one master water quality dataset consisting of select dissolved minerals and radionuclides. The master water quality table contains 1,003 water quality samples from 1,001 wells. Additional water quality data (for example, metals) is present in the TWDB Groundwater Database. We assigned an updated aquifer assignment for each well based on the aquifer determination task described in Section 10. This allowed us to produce maps of several important parameters that met specific well completion criteria. Wells penetrating the Trinity and Dockum groups and those in which we could not determine what geological formations the samples were taken from were excluded from mapping.

10.1 Parameters of concern for desalination

Depending on the use, brackish groundwater needs to be treated (desalinated). Without treatment, brackish water can cause scaling and corrosion problems in water wells and treatment equipment and cannot be used for municipal and industrial purposes. Groundwater containing total dissolved solids at concentrations greater than 3,000 milligrams per liter is not suitable for irrigation without dilution or desalination and, although considered satisfactory for most poultry and livestock watering, can cause health problems at increasingly higher concentrations (Warner, 2001).

The Texas Commission on Environmental Quality has established a secondary standard of 1,000 milligrams per liter of total dissolved solids for public water supply systems (TCEQ, 2015). Secondary standards are non-enforceable guidelines that may cause cosmetic or aesthetic effects in drinking water (EPA, 2016). The U.S. Environmental Protection Agency (EPA) established secondary standards for 15 contaminants (U.S. EPA, 2017). The federal secondary standard for total dissolved solids is 500 milligrams per liter. The state secondary standard has a higher concentration of total dissolved solids compared to the federal because waters in the state tend to be more saline.

Some general physical and chemical parameters of concern to desalination facilities that use reverse osmosis, the predominant desalination technology in Texas, are listed in Table 10.1-1. While the TWDB Groundwater Database contains sample results for most of these parameters, the amount of information available from a well can vary greatly. For example, the TWDB does not maintain information on silt density index from groundwater samples. If the silt density index is high, pre-treatment of the feedwater is required to avoid scaling the membranes in a reverse osmosis treatment system.

Table 10.1-1. General parameters of concern for desalination.

Physical parameters	Chemical parameters			
	Cations		Anions	Other
Conductivity	Al^{+3}	K^{+1}	Cl^{-1}	Alkalinity
pH	As^{+3}	Mg^{+2}	CO_3^{-2}	Boron
Silt density index	As^{+5}	Mn^{+2}	F^{-1}	Dissolved oxygen
Temperature	Ba^{+2}	Na^{+1}	HCO_3^{-1}	H_2S
Turbidity	Ca^{+2}	NH_4^{+1}	NO_2^{-1}	Hardness
	Cu^{+2}	Ni^{+2}	NO_3^{-1}	Pesticides
	Fe^{+2}	Sr^{+2}	OH^{-1}	Radionuclides
	Fe^{+3}	Zn^{+2}	SO_4^{-2}	Silica
				Total dissolved solids

Note: The integers with a positive or negative sign indicate the valence of the ion.

Groundwater quality in an aquifer can vary greatly due to factors such as mineral composition of aquifer materials, recharge rates, spatial distribution, chemical composition of recharge waters, and historical changes with time, geochemical processes, natural and man-made discharge rates and spatial distribution, residence time, and groundwater flow velocity.

Mapping groundwater quality data also depends on the number and spatial distribution of samples, types of samples collected, and the dates the samples were collected. A series of maps (Figure 10.2-1 through Figure 10.2-8) for the study area were created to show the distribution of select parameters of concern in desalination as well as radionuclides. The lack of significant numbers of samples in any one recent sampling year meant that we had to extract data from a multi-year period. While these maps display the spatial distribution of chemical parameters, they do not necessarily show current water quality conditions. Users interested in a specific region are encouraged to use the most current available database, GIS datasets, and GIS software to construct site-specific maps to meet project needs.

10.2 Dissolved minerals and radionuclides

Total dissolved solids concentration is a measure of the mineral content in water and is an important parameter for designing a reverse osmosis plant. *Salinity* is the term used to describe the concentration of dissolved, inorganic salts in groundwater. The unit of measurement for total dissolved solids concentration is milligrams per liter. In the study area, 972 wells containing 974 water quality samples of total dissolved solids are available. Wells drawing water from the Trinity and Dockum groups and those in which we could not determine the sampled interval were excluded. Our objective was to ensure the water quality data is exclusively from the Lipan Aquifer. This reduced the well control to 337 wells containing 339 water quality samples (Figure 10.2-1).

The total dissolved solids concentrations ranged from 194 to 65,800 milligrams per liter. The three highest measurements came from an exploratory well that sampled considerably deeper (approximately 600 to 900 feet below ground surface) than is typical of water wells in the study

area (LBG-Guyton Associates, 2008). Disregarding these samples, the maximum total dissolved solids recorded was 7,020 milligrams per liter. In the study area, 257 of the 339 samples (76 percent) exceeded the Safe Drinking Water Limit secondary maximum contaminant level for total dissolved minerals of 1,000 milligrams per liter (TCEQ, 2015).

For dissolved arsenic, 64 wells containing 64 water quality samples are available in the study area (Figure 10.2-2). Arsenic concentrations ranged from 0.001 to 0.010 milligrams per liter in the study area. None of the water quality samples exceeded the Safe Drinking Water Act maximum contaminant level for arsenic of 0.010 milligrams per liter (TCEQ, 2015).

There are no boron samples available in the study area There is no maximum contaminant level for boron in public drinking water (TCEQ, 2015). Boron is listed on the Environmental Protection Agency Contaminant Candidate List 2 developed in 2005. In natural environments, boron exists as boric acid (H_3BO_3), a weak acid that does not dissociate readily (Hem, 1985).

For chloride, 297 wells containing 298 water quality samples are available in the study area (Figure 10.2-3). Chloride concentrations ranged from 5 to 41,000 milligrams per liter. Disregarding the samples from the deep exploratory well, the highest concentration was 3,380 milligrams per liter. The Safe Drinking Water Act secondary maximum contaminant level for chloride is 300 milligrams per liter, of which 199 of the 298 samples (67 percent) exceeded this level (TCEQ, 2015).

Seven wells containing seven water quality samples analyzed for total iron concentration are available in the study area (Figure 10.2-4). Iron concentrations ranged from 0.02 to 0.41 milligrams per liter. One of the seven samples (14 percent) exceeded the Safe Drinking Water Act secondary maximum contaminant level for iron of 0.3 milligrams per liter (TCEQ, 2015). Iron in groundwater can become oxidized and will precipitate when it reaches ground surface. To avoid fouling reverse osmosis membranes, water with elevated levels of iron must be pre-treated.

Only three wells containing five water quality samples analyzed for silica are available in the study area (Table 10.2-1). Silica concentrations ranged from 11.6 to 24.0 milligrams per liter. There is no maximum contaminant level for silica in public drinking water (TCEQ, 2015). However, silica is an important desalination parameter because at elevated concentrations it can scale reverse osmosis membranes. The term *silica* is widely used to refer to dissolved silicon in natural water, but the actual form is hydrated and should be represented as H_4SiO_4 (Hem, 1985). The tetrahedron (SiO_4^{-4}) is the building block of most igneous and metamorphic rocks and is present in some form in most soils and groundwater.

Table 10.2-1. Sampled concentrations of silica. Depth in feet below ground surface.

State well number	BRACS well identification number	Sampling depth (feet)	Concentration (milligrams per liter)
	51449	615-645	18.3
	51449	675-705	12.1
	51499	903-933	11.6
4318804		112	24.0
4322404		175	14.0

For sulfate, 297 wells containing 298 water quality samples are available in the study area (Figure 10.2-5). Sulfate concentrations ranged from 4.0 to 3,120 milligrams per liter. The Safe Drinking Water Act secondary maximum contaminant level for sulfate is 300 milligrams per liter, of which 128 of the 298 samples (43 percent) exceeded this level (TCEQ, 2015). Sulfate in shallow groundwater can be attributable to weathering of minerals such as iron pyrite and gypsum or from anthropogenic sources such as oil field brines. It is not uncommon for bacteria to cause natural reduction in sulfate concentrations in shallow groundwater (Hem, 1985). Sulfate in groundwater can cause scaling and fouling of reverse osmosis membranes, requiring the source water to be pre-treated.

For dissolved barium, 104 wells containing 104 water quality samples are available in the study area (Figure 10.2-6). Barium concentrations ranged from 0.01 to 0.32 milligrams per liter. None of the samples exceeded the Safe Drinking Water Act secondary maximum contaminant level for barium of 2 milligrams per liter (TCEQ, 2015). Barium concentrations in groundwater are generally constrained by the presence of sulfate, which readily combines with barium to form barium sulfate (Hem, 1985). Barium in groundwater can cause scaling and fouling of reverse osmosis membranes.

The presence of radionuclides in groundwater is also important when selecting screen zone(s) for a well. Elevated naturally occurring radioactive material in the concentrate will impact the method of waste disposal and, thus, cost. Future test wells should always be logged with a gamma ray tool; elevated radionuclides in formation materials can be discovered using these logs.

In the study area, 29 wells containing 29 water quality samples analyzed for dissolved alpha radiation are available (Figure 10.2-7). The Safe Drinking Water Limit maximum contaminant level for dissolved alpha radiation is 15 picoCuries per liter, of which 2 of the 29 samples (7 percent) exceeded this level (TCEQ, 2015).

For dissolved natural uranium, 26 wells containing 26 water quality samples are available in the study area (Figure 10.2-8). No samples exceeded the Safe Drinking Water Limit maximum contaminant level for uranium of 30 micrograms per liter (TCEQ, 2015).

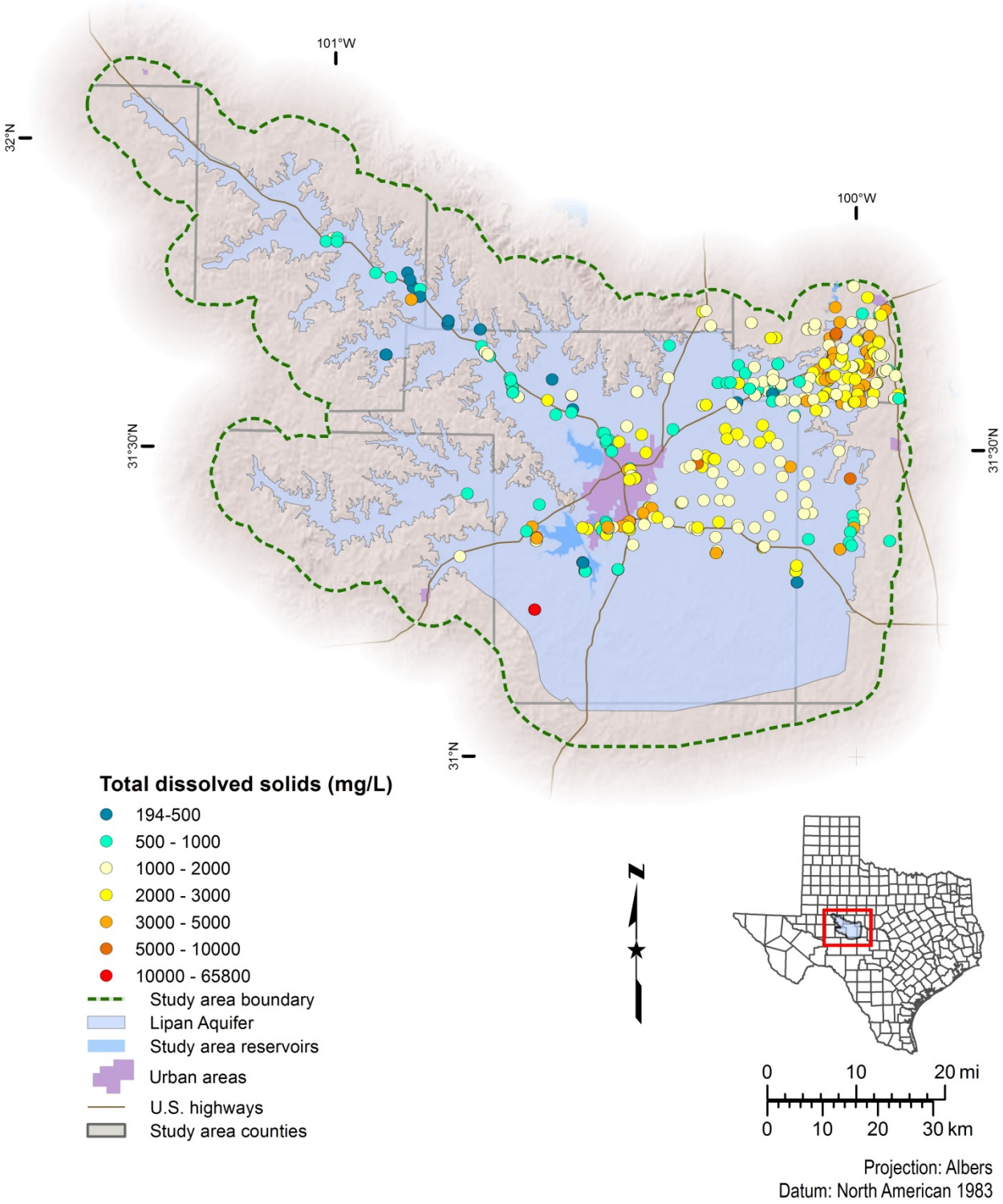

Figure 10.2-1. Distribution of wells sampled for total dissolved solids. One sample with a concentration measuring higher than 10,000 milligrams per liter was from a deep exploratory well not used for water supply (LBG-Guyton Associates, 2008). mg/L = milligrams per liter.

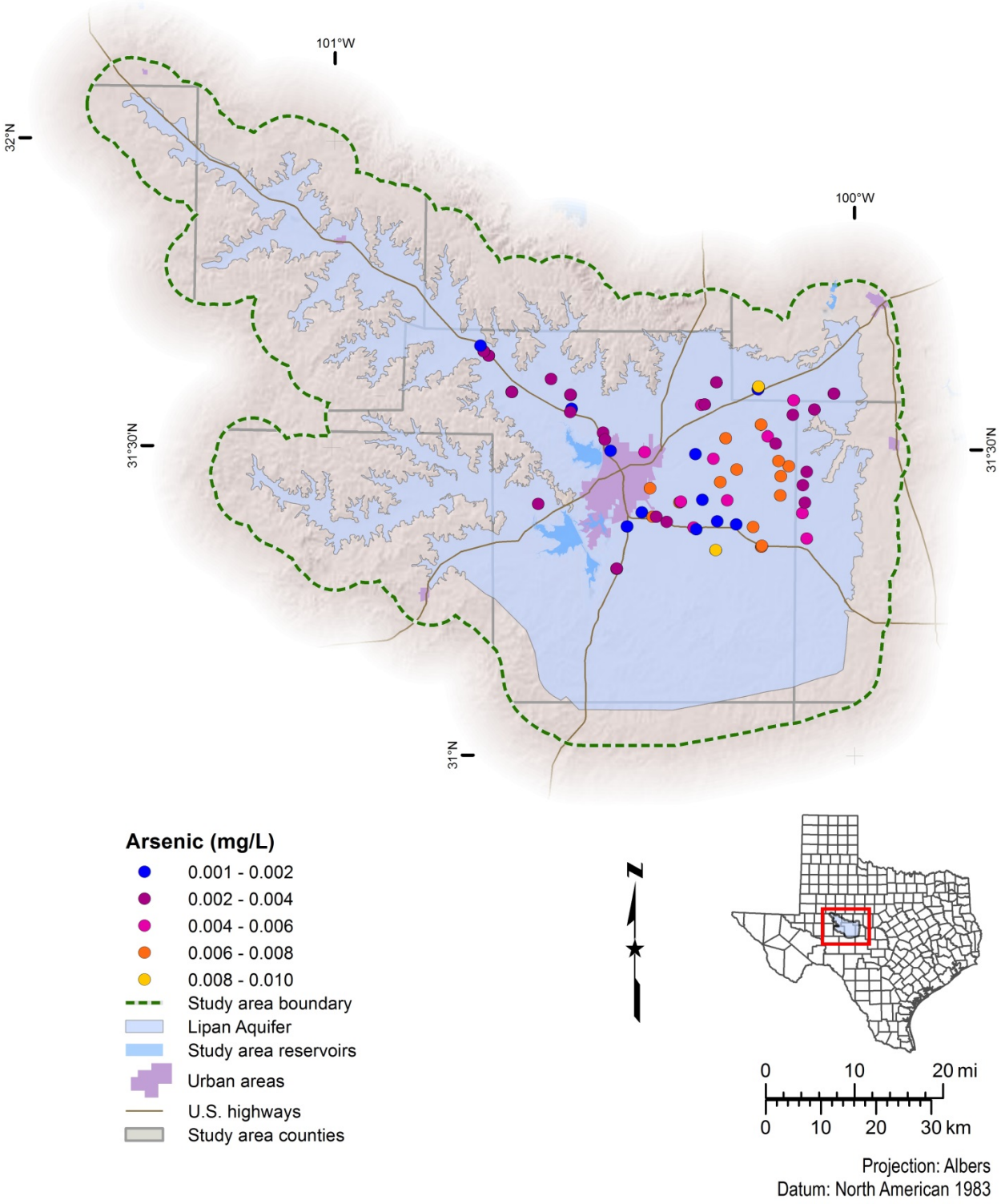

Figure 10.2-2. Distribution of wells sampled for dissolved arsenic. mg/L = milligrams per liter.

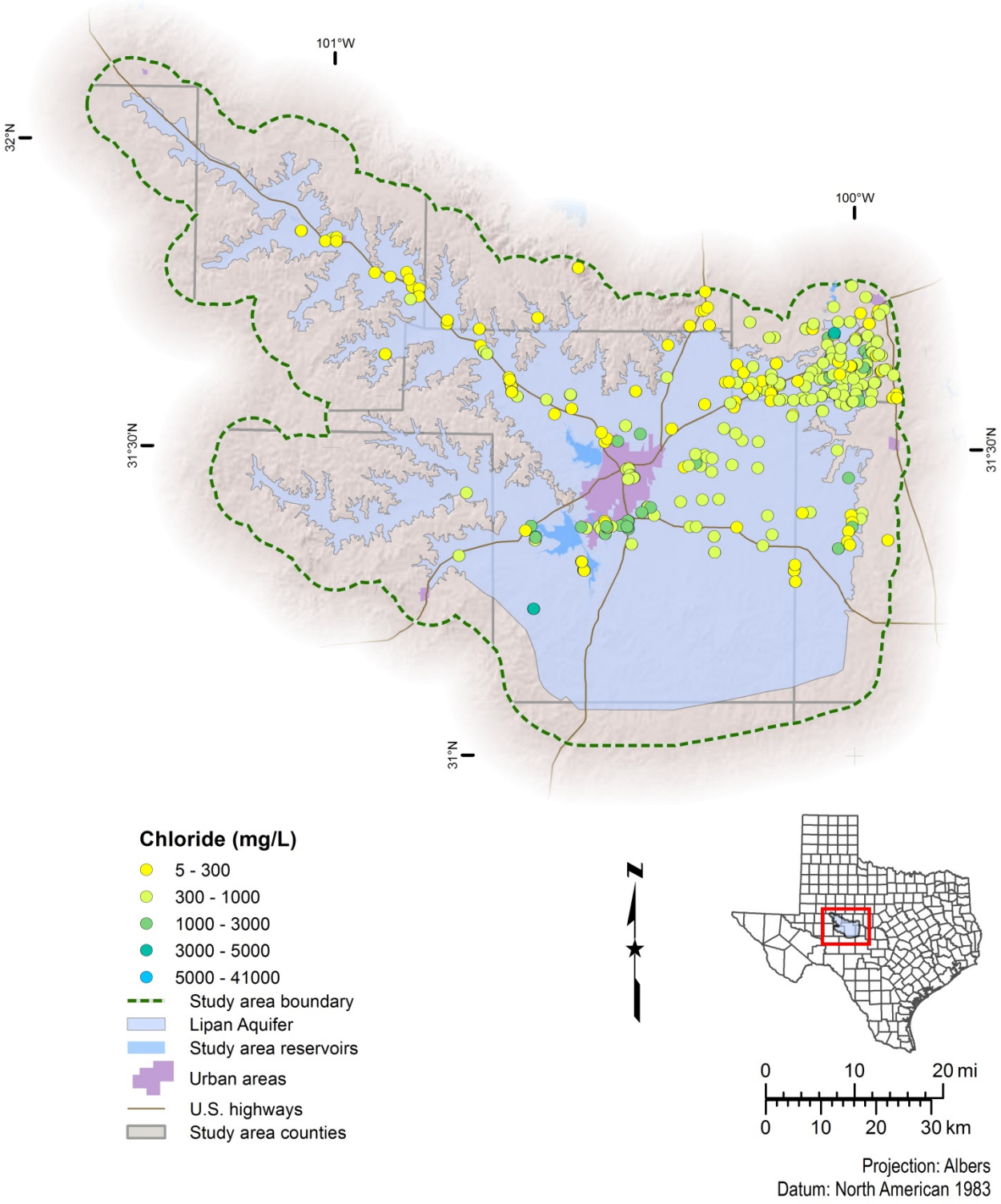

Figure 10.2-3. Distribution of wells sampled for chloride. mg/L = milligrams per liter.

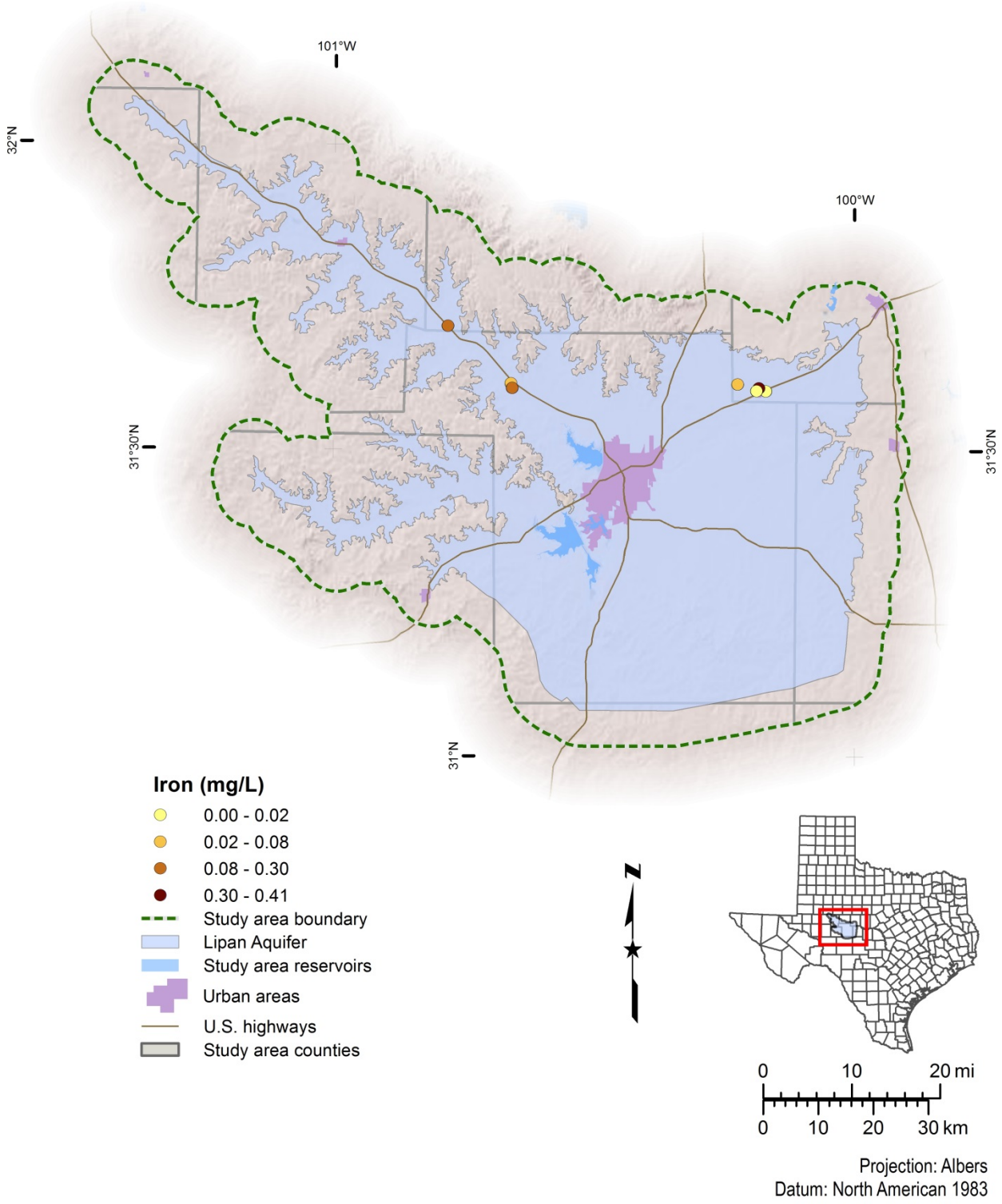

Figure 10.2-4. Distribution of wells sampled for iron. mg/L = milligrams per liter.

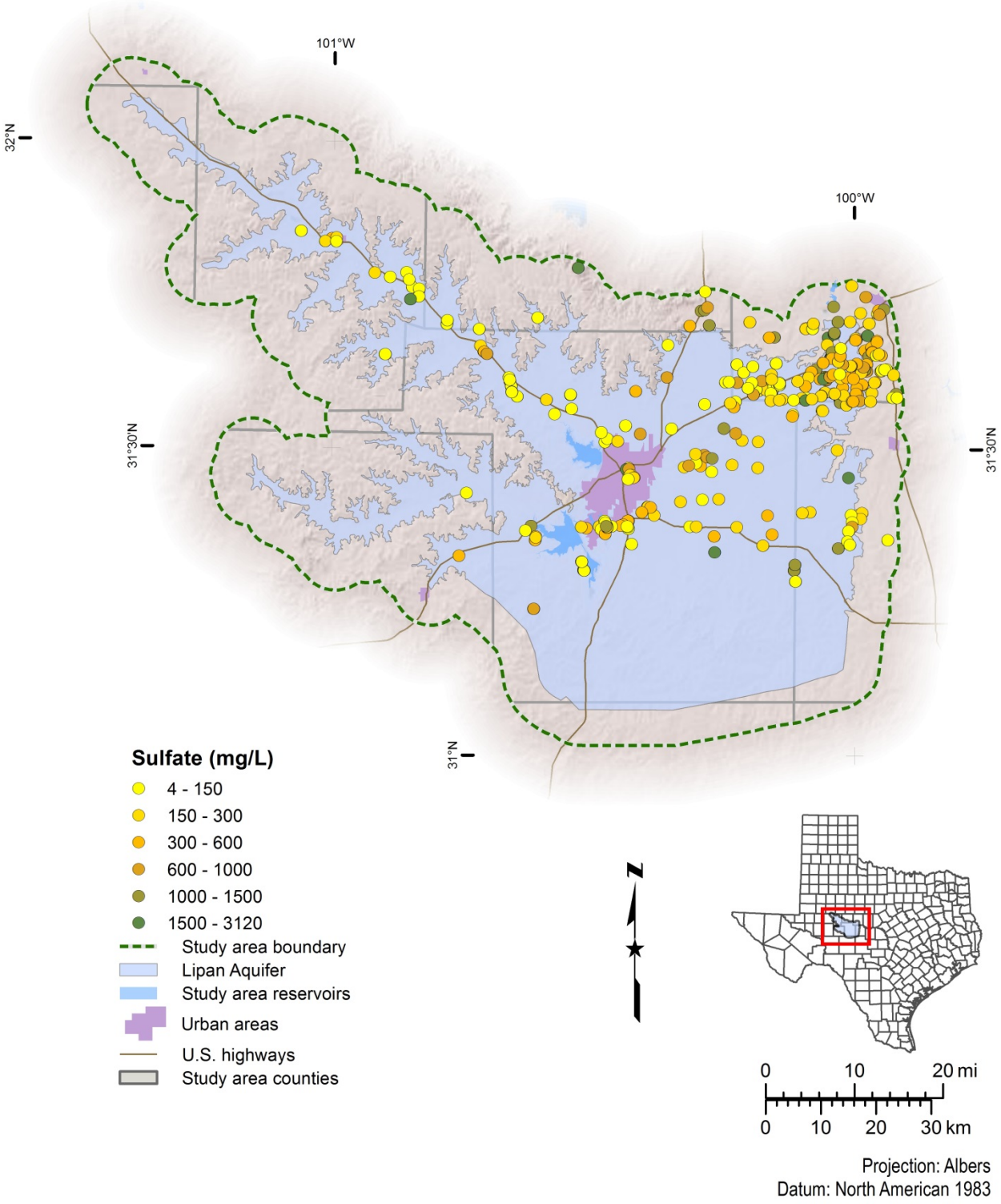

Figure 10.2-5. Distribution of wells sampled for sulfate. mg/L = milligrams per liter.

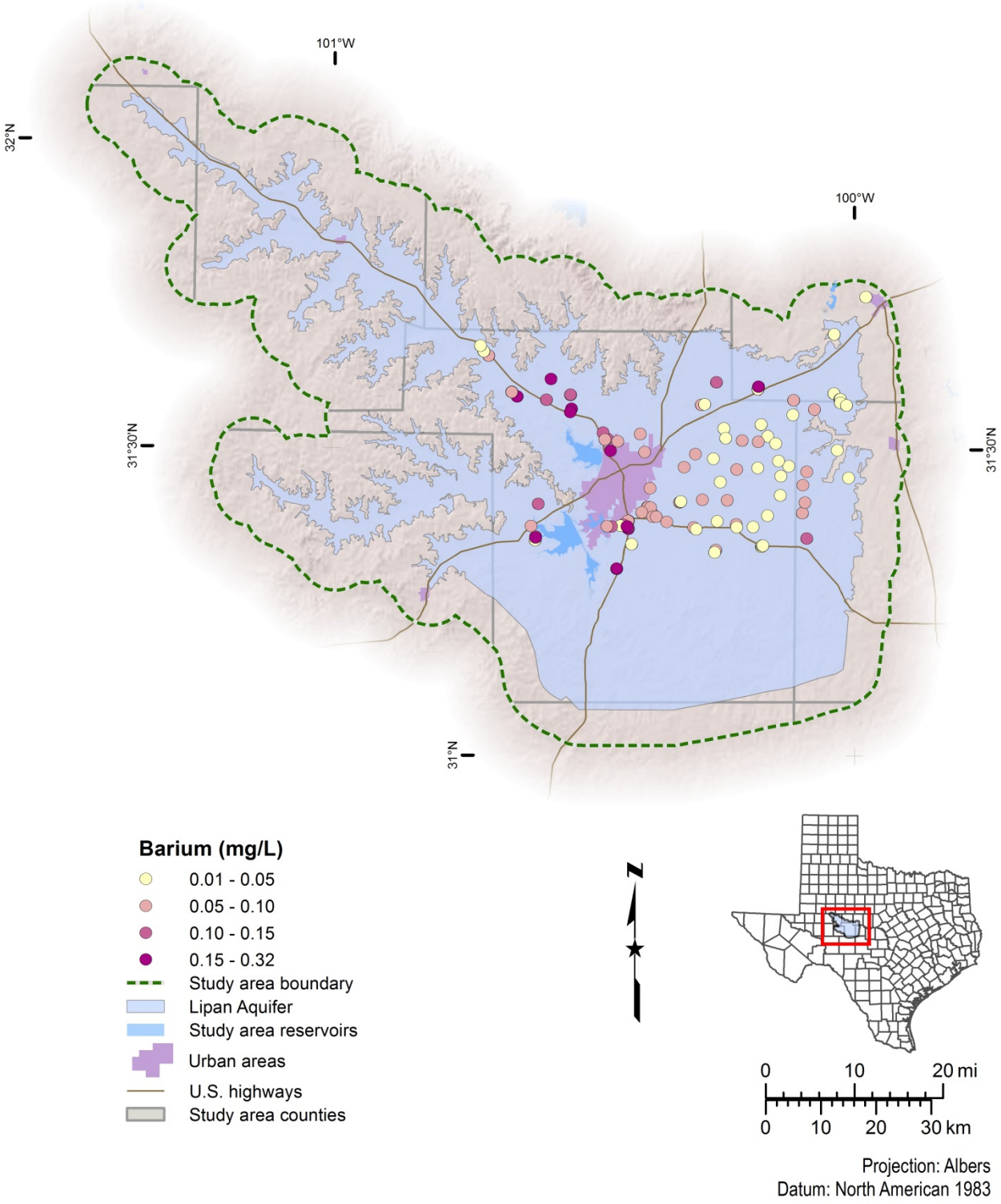

Figure 10.2-6. Distribution of wells sampled for dissolved barium. mg/L = milligrams per liter.

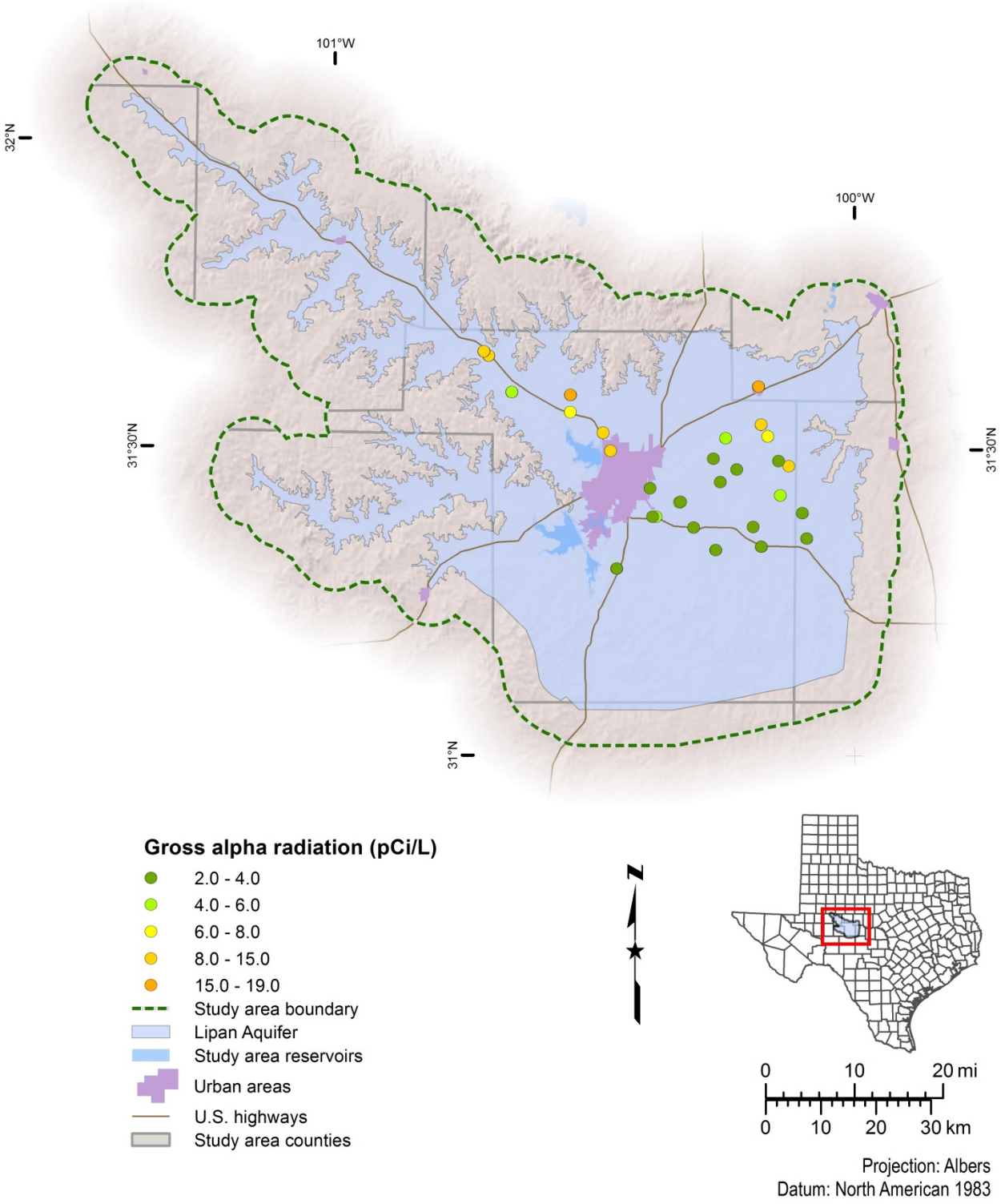

Figure 10.2-7. Distribution of wells sampled for gross alpha radiation. pCi/L = picoCuries per liter.

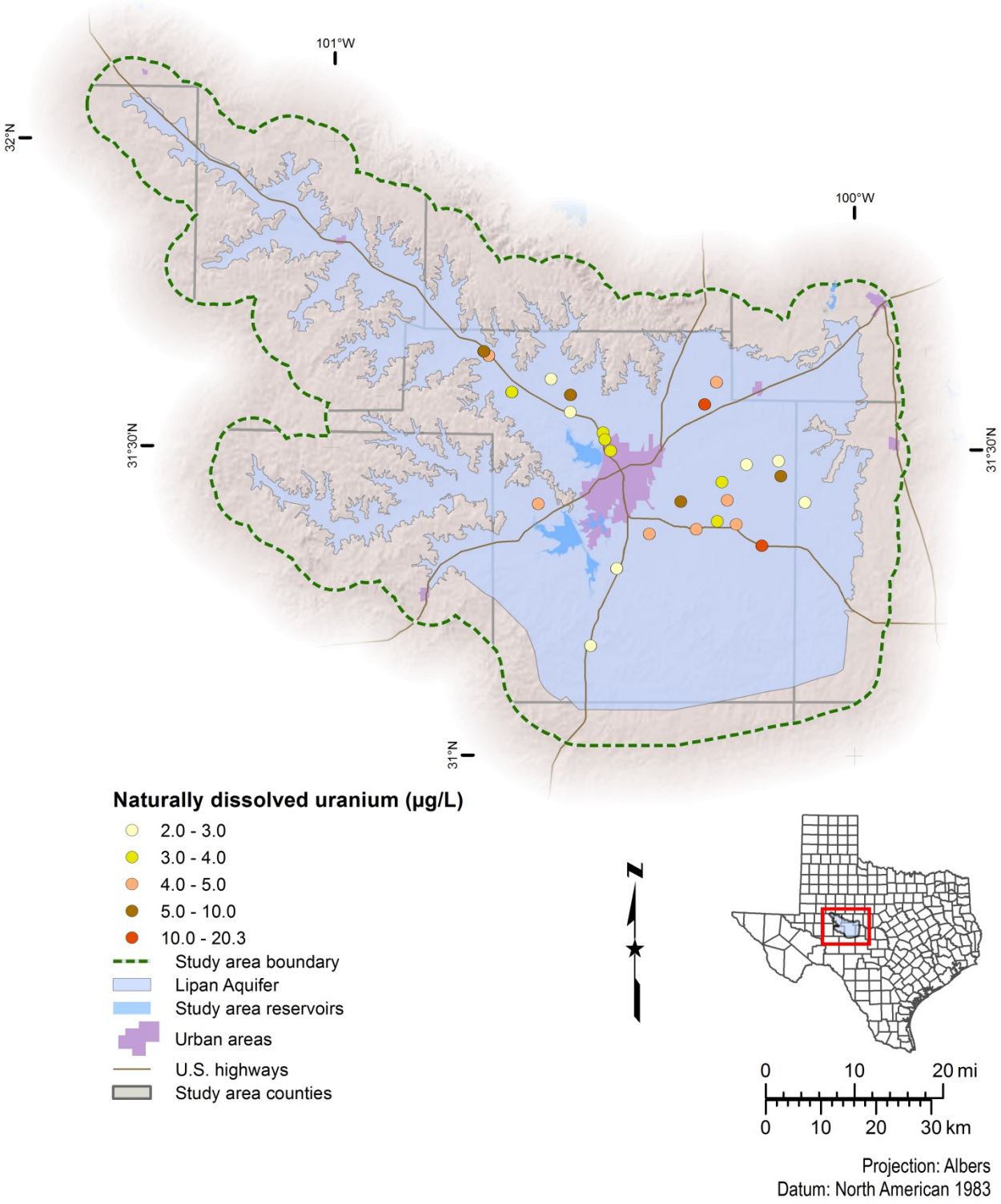

Figure 10.2-8. Distribution of wells sampled for uranium. µg/L = micrograms per liter.

10.3 Sources of dissolved minerals

Salinity within the Lipan Aquifer is the result of both natural and anthropogenic causes. Natural sources of salinity include the dissolution of Permian evaporites (primarily halite, anhydrite, and gypsum) and evaporative concentration of water. Anthropogenic sources include (1) improper irrigation methods; (2) past disposal practices of oil and gas produced water; (3) spills and leaks from oil fields; (4) abandoned water, oil, and gas wells; (5) irrigation return-flow; and (6) well pumping allowing recharge from higher salinity water.

Dutton and others (1989) discuss in detail the regional-scale migration of subsurface brines through the Permian formations and their natural mixing with locally recharged meteoric water. Comparing chemical characterizations of deep subsurface brines to waters sampled in shallow water wells, they found that it is highly probable that natural subsurface brines are upwelling and mixing with meteoric recharge. The concentration of these brines is influenced by cross-formational flow from the underlying Permian formations, the rate at which groundwater is removed from the shallow aquifer units, and the recharge rate.

Richter and Kreitler (1987) provide a detailed description of the anthropogenic sources of contamination that have occurred or could occur in the study area. They conclude that, based upon the geochemical analysis of saline waters, agricultural salinization and deep-basin brines are the primary sources for saline water in the study area.

10.4 Cretaceous/Permian formations interaction

This study is not focused on the Cretaceous formations that overlie the Permian formations we have identified as constituting the majority of the Lipan Aquifer. However, we did investigate where there are cases of interaction between the two formations. The first case is when wells penetrate the Cretaceous formations and are completed in underlying Permian formations. The second case is when there may be mixing of water from the Seven Rivers Formation with that of the overlying Cretaceous formations. Most wells completed in the Lipan Aquifer (where Cretaceous formations do not exist) are completed in either Permian formations or a combination of Permian formations and Quaternary and Neogene sediments. As an example, 323 of 339 available wells (95 percent) meet this criteria and have water quality data.

We found 3 of 137 wells (2 percent) with water quality samples from wells completed in the study area overlain by Cretaceous formations that significantly penetrated Permian formations (Table 10.4-1). These well locations are symbolized as circles in Figure 10.4-1.

Table 10.4-1. Wells drilled into Cretaceous and Permian formations. Contact interval is defined as the length the well is within the formation; it does not indicate if the well is open during this interval. Static water level and well depth is in feet below ground surface.

State well number	Total dissolved solids (milligrams per liter)	Static water level (feet)	Total well depth (feet)	Cretaceous formation thickness (feet)	Permian contact interval (feet)	Permian formation contacted
4241501	2,848	171	225	59	166	Lueders
4327406	384	24	280	60	104	Seven Rivers
4360608	2,004	180	450	389	61	Grayburg

Salinity levels in samples from wells completed in Cretaceous formations in the area typically range from 200 to 400 milligrams per liter of total dissolved solids. Water samples from two wells (state well numbers 4241501 and 4360608) had significantly higher salinity concentrations, 2,000 to 2,800 milligrams per liter of total dissolved solids. The first well had a considerable interval in contact with the Lueders Formation and the second contacted the Grayburg Formation. We do not have well construction data for these wells, so what interval(s) the wells were open is undetermined. Based on the predicted salinity levels below the top of the Permian formations presented in Section 14.2, elevated salinities such as these could be expected at these depths.

We evaluated one well (state well number 437406) with a significant Permian formation penetration that did not exhibit elevated salinity levels. The construction of the well is open hole and we calculate that 104 feet of the well is completed in the Seven Rivers Formation. It may be that (1) the shallow static water level resulting from the well's location at the base of a moderate slope and close proximity to a stream limits flow from the Seven Rivers Formation into the well at this site, (2) the native groundwater of the Seven Rivers Formation has been displaced by recharge from the Cretaceous aquifer, or (3) the Seven Rivers Formation does not have significant water-producing capability.

There is also a cluster of four wells that (1) exhibit high salinity, (2) partially penetrate the Cretaceous aquifer, and (3) are vertically separated from the underlying Permian formations (Table 10.4-2). These well locations are symbolized as squares in Figure 10.4-1.

Table 10.4-2. Wells drilled into Cretaceous with high salinity. Static water level is in feet below ground surface. Contact interval is defined as the interval the well is within the formation; it does not indicate if the well is open during this interval. Well depth is in feet below ground surface.

State well number	Total dissolved solids (milligrams per liter)	Static water level (feet)	Total well depth (feet)	Cretaceous formation thickness (feet)	Vertical separation from well bottom to Seven Rivers Formation top (feet)
4344701	1,988	70-77	80	152	72
4352202	1,249	106	150	266	116
4359303	1,579	390	450	568	118
4360101	2,346	206-213	270	399	129

The vertical separation from the bottom of the wells to the top of the underlying Seven Rivers Formation ranges from approximately 72 feet to 129 feet. The higher salinity may be an indicator of hydrologic communication between the Cretaceous formations and underlying Seven Rivers Formation. This may be due to localized geological structural or hydraulic conditions. Other wells sampled in the area with similar vertical separation do not exhibit this condition. Additional data and analysis would be required to further explain the behavior. However, drillers and potential users of groundwater in the area should be aware of this situation.

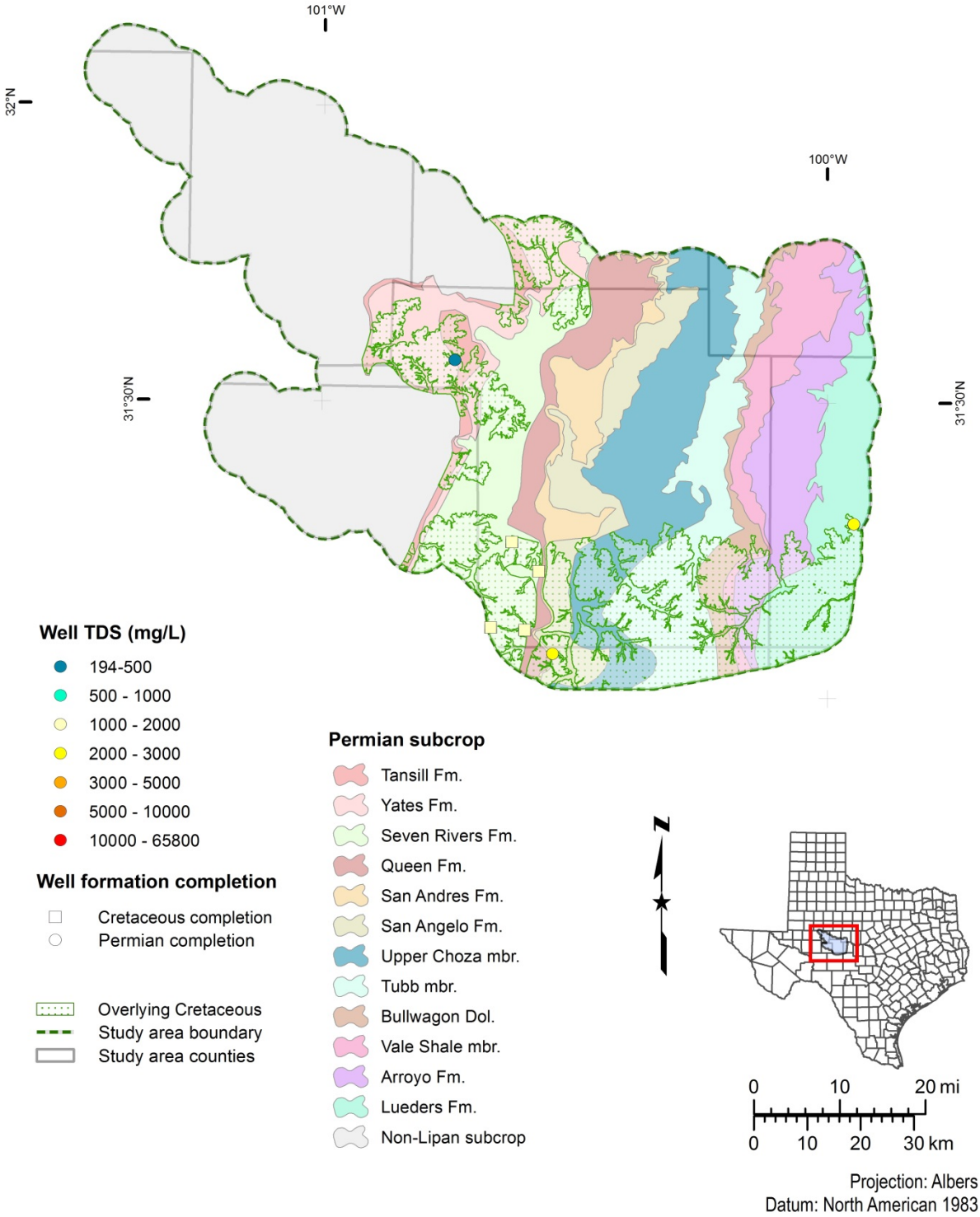

Figure 10.4-1. Areas of potential Cretaceous/Permian interaction within the Lipan Aquifer study. Shaded areas indicate where Permian formations either outcrop or subcrop below overlying Quaternary and Neogene sediments or Cretaceous formations. The Grayburg Formation subcrops below the Queen Formation and is not shown. The stippled green area indicates Cretaceous formations overlying Lipan Permian formations. Dol. = dolomite, Fm. = formation, mbr. = member, mg/L = milligrams per liter, TDS = total dissolved solids.

11. Salinity calculations from geophysical well logs

Geophysical well logs were used extensively during the course of this study for stratigraphic interpretation and to calculate interpreted total dissolved solids concentration of groundwater at different depths. In this section we will provide some basic information on the nature and capabilities of geophysical well logs and the methods used in this study to calculate total dissolved solids concentration from various curves recorded on the well logs.

11.1 Geophysical well log tools

Geophysical well logs are produced from tools that are lowered into a well bore with a wireline and retrieved back to the ground surface at a specific rate. Combinations of different tools can be assembled in standard "packages" to measure various formation, fluid, borehole, casing, and cement properties. The geophysical well log tools are selected based on several factors including (1) anticipated geology, (2) information required from logging, (3) cased or uncased bore holes, and (4) the composition of the well bore fluid (air or drilling mud). The tools have progressively improved since they were first applied to oil field investigations in the 1930s. The geophysical well logs collected for this study were produced between 1940 and the present.

Oil wells are generally logged after a section of surface casing is installed in order to stabilize the wellbore and to protect shallow groundwater aquifers. The length of the surface casing installed in oil wells within the study area varies from a few hundred to over one thousand feet below the ground surface. The amount of information that can be collected from the ground surface to the bottom of the surface casing is limited. With the exception of the gamma ray and neutron tools, the section of the wellbore containing surface casing cannot be logged. Older wells generally had a shallower bottom depth of surface casing, making these logs important for near-surface interpretations.

Resistivity tools

The resistivity of a formation can be measured with geophysical logging tools that pass electricity into the formation and record voltages between measuring electrodes. The resistivity of dry rock is usually extremely high (with the exception of metallic ores), so the only way that electricity can pass through a formation is if the rock is saturated by groundwater containing dissolved minerals. The groundwater is contained either in the pores between mineral grains or adsorbed in interstitial clay. Tools with deep depths of investigation are needed to minimize the influence of borehole fluid, mud filter cake, and the groundwater invasion zone.

A normal resistivity log usually consists of multiple tools used to measure the resistivity of the geological formation and groundwater surrounding the borehole at different depths of investigation. The spacing between the electrodes is directly proportional to the depth of investigation, with larger spacing offering deeper depth of investigation. Resistivity measurements are affected by the borehole, drilling fluid, mud filter cake, borehole fluid invasion zone, lithology of the formation being investigated, lithology of surrounding formations, and formation groundwater. Resistivity tool measurements are usually presented on the right track of a geophysical well log in units of ohm-meter. A conductivity track may also be present and is calculated from the inverse of the resistivity measurement.

The induction log is a deep investigation tool used to measure the resistivity of the geological formation and groundwater surrounding the borehole. This type of log uses focusing coils to direct the electricity into the formation and minimize the influence of the borehole, drilling fluid, surrounding formations, mud filter cake, and the invaded zone (Schlumberger, 1987). Induction tool measurements are usually presented on the right track of a geophysical well log in units of ohm-meter.

Spontaneous potential tool

The spontaneous potential log is a record of the direct current reading between a fixed electrode at the ground surface and a movable electrode (spontaneous potential tool) in the well bore. The tool must be run in an open borehole with a conductive drilling mud. Spontaneous potential is measured in millivolts. The electrochemical factors that create the spontaneous potential response are based on the salinity difference between the borehole mud filtrate and the groundwater within permeable beds (Asquith, 1982). A negative deflection of the spontaneous potential response occurs when the mud filtrate is more resistive than groundwater. A positive deflection occurs when mud filtrate is less resistive than groundwater. The spontaneous potential response of shale is relatively constant and is referred to as the shale baseline. When the mud filtrate resistivity is the same as groundwater resistivity, there is no deflection of the spontaneous potential response from the shale baseline. The permeable bed boundaries are detected at the point of inflection of spontaneous potential response.

Spontaneous potential deflection is affected by the type of cation species (positive ions such as calcium, magnesium, potassium, or sodium) present in water. Oilfield analysis equations assume that the groundwater is dominated by sodium and chloride ions. Divalent cations (with a plus two charge, such as calcium and magnesium) in groundwater with lower salinity have a larger impact on spontaneous potential deflection than sodium (Alger, 1966). The spontaneous potential response is affected by bed thickness; thin beds do not allow a full spontaneous potential response and must be corrected (Asquith, 1982; Estepp, 1998; Schlumberger, 1972). If a sand unit is less than 10 feet thick, the response curve tends to have a pointed shape and requires a correction. We did not use beds thinner than 10 feet to avoid this problem.

The spontaneous potential response is also affected by bed resistivity, borehole invasion of drilling fluid, hydrocarbons, and shale content. Methods to correct borehole invasion of drilling fluid are found in log analysis manuals (for example, Schlumberger, 1985). Shale content reduces the spontaneous potential response. Spontaneous potential tools run in freshwater wells commonly use native mud so that prior to logging the borehole fluid is essentially groundwater. In this situation, the resistivity of groundwater and borehole fluid is almost equal and the spontaneous potential tool is not capable of estimating total dissolved solids concentration (Keys, 1990).

Other factors that may cause significant measurement variations with spontaneous potential tools are (1) improper grounding of the reference electrode at the surface, (2) the presence of electrically charged pipes, (3) current rectifiers, (4) magnetization of some mobile part of the winch, and (5) variations of the free water table in the vadose zone (Torres-Verdin, 2015; Schlumberger, 1972).

Gamma ray tools

Gamma ray logs normally reflect the clay content in sedimentary formations (Schlumberger, 1972). Minerals such as illite and mica contain the radioactive potassium-40 isotope that produces gamma rays in beds containing clay or shale. Gamma ray tools encountering naturally occurring uranium or thorium will record the zone as a much higher measurement than the shale baseline response.

Advantages of using a gamma ray log include (1) it is commonly used on logging runs, (2) it can be recorded in cased holes, (3) it is generally started near ground surface, (4) it can be used to recognize many of the boundaries of geological units, (5) curve patterns can facilitate the interpretation of depositional environments, and (6) it can be used to determine clay-free zones for log analysis.

Concerns when using a gamma ray log include (1) attenuation of the overall log signature in cased and cemented boreholes, (2) masking of the more subtle changes in log response with transition from uncemented to cemented formations, (3) inability to evaluate borehole washouts because of the absence of caliper logs prior to casing the well, (4) lack of tool calibration or complete casing records on the log header, which precludes accurate interpretation, (5) older gamma ray logs may have different units of measure compared with the modern standard of American Petroleum Institute unit, (7) comparison of measurements between tools with different units is problematic, and (8) inability to differentiate clay-free sand, carbonate, and gravel.

11.2 Salinity calculations

It was necessary to use geophysical well logs to calculate the total dissolved solids concentration of deeper groundwater present within the study area because we lacked a significant number of measured water samples. We used 745 wells from the study area with total dissolved solids measurements from water samples. Of these, 566 were sampled from either the Trinity Group or the Dockum Group, which are not part of this study. Of the remaining 179 wells with water samples, only one well (BRACS well identification number 51449) sampled from a depth below 300 feet (LGB-Guyton, 2008). The remainder had an average sample depth of 98 feet below the ground surface. There were 61 water samples with measured total dissolved solids that could be associated with a single Permian formation.

Estepp (1998) provided six methods for interpreting total dissolved solids concentration in a geological formation using geophysical well logs. Each of the methods has advantages and disadvantages with respect to the type of logging tool, input parameters, formations being assessed, and expected range of groundwater salinity. Calculating groundwater salinity concentration is a complicated process because of the complexity of the geological environment and because the majority of the existing geophysical well logs were developed for petroleum exploration and production where the groundwater is dominated by high sodium and chloride concentrations.

The equations from Estepp (1998) were standardized with similar parameter names and written in Visual Basic for Applications® as a class object within the BRACS Database for automated calculation. We entered parameters into a series of data entry forms linked to tables. The type of method is selected, the calculations are performed, and output is written to tables using

Microsoft® Access®. The database tables contain the raw, intermediate, and interpreted values for each parameter for each equation so values can be retrieved for later analysis. For example, one could re-calculate the interpreted total dissolved solids value by selecting the record, entering a new parameter value such as porosity, and running the code.

The Spontaneous Potential Method and Alger-Harrison Method were selected because their input parameters can be directly read from standard resistivity geophysical well logs that are readily available throughout the project area. Additionally, the calculations do not require porosity data, which was not available for the relatively shallow intervals evaluated. Nuclear logs that are used to interpret porosity were available for study area wells; however, these wells were logged over intervals that are deeper than the Lueders Formation, the deepest geological formation in this study.

Well log analysis calibration to water quality samples was not possible because the depth of the water samples averaged 98 feet which is shallower than initial recording depth of geophysical well logs in the study area. The few deeper water samples were many miles away from any wells that had geophysical logs recorded for the sampled formation at a similar depth.

The conversion between a groundwater resistivity value and total dissolved solids requires determination of the ct conversion factor. The ct conversion factor relates conductivity, the inverse of resistivity, to total dissolved solids. The ct conversion factor is determined by crossplotting specific conductance with total dissolved solids from groundwater sample measurements. It is required to utilize well water samples collected from study area geological formations. We crossplotted 95 water samples that were in the TWDB Groundwater Database taken from study area wells that were sampled exclusively from Permian formations (Figure 11.2-1). We determined a ct conversion factor of 0.57 by fitting a trendline to the data and determining the slope (Estepp, 1998).

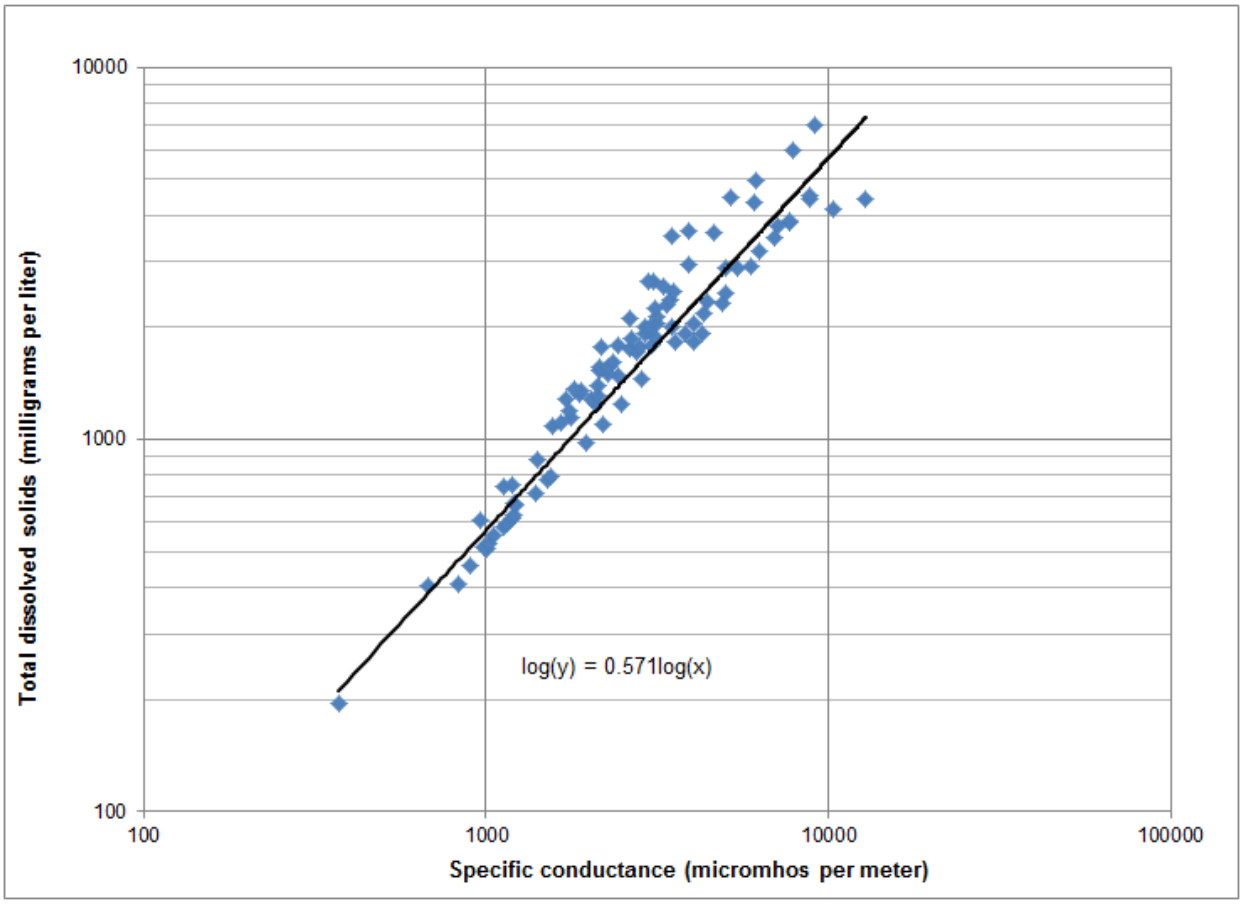

Figure 11.2-1. Crossplot of total dissolved solids concentration versus specific conductance. Plot of 95 water samples from the Permian formations in the study area.

We did not evaluate geophysical well logs with drilling mud that included additives such as "soda" and "caustic" or brine-based mud to avoid inaccurate interpretations in our salinity analysis. Interpretation of logs that were produced over such a long time span and presumably with varying tool designs and accuracies presents challenges. Obviously, some of the older logs simply could not be used in all aspects of the study. The digital image quality of some logs also presented challenges.

11.3 The Spontaneous Potential Method

The Spontaneous Potential Method provides a relatively simple way to calculate total dissolved solids concentrations in permeable water-bearing strata. The method is effective where groundwater salinities may range from 100 to 100,000 milligrams per liter of total dissolved solids. In strata of sufficient thickness where the spontaneous potential curve achieves full deflection, the calculated water resistivity will be a maximum for that strata and result in a minimum value for the interpreted total dissolved solids concentration (Estepp, 1998).

Care must be taken when using the Spontaneous Potential Method to measure the spontaneous potential curve deflection where the strata are sufficiently thick and permeable so that the measurement records the maximum possible curve development. The presence of shale within the strata will suppress the development of the spontaneous potential curve. Hydrocarbons

present within the pore space will also suppress the spontaneous potential curve. Suppression of the spontaneous potential curve will result in calculated water resistivity values being too high and corresponding interpreted total dissolved solids too low (Estepp, 1998).

We made 742 calculations for interpreted total dissolved solids using the Spontaneous Potential Method. The results were inconsistent, and we determined that the measured spontaneous potential values did not represent the true maximum deflection necessary to accurately calculate the formation water resistivity. The Permian formations in the study area are largely composed of dolomitic limestone interbedded with siltstone and shale, which suppressed the spontaneous potential response. Upon further literature review, we determined that there is no experimental or theoretical support for using the Spontaneous Potential Method in well-lithified carbonate rocks that make up the majority of the Permian formations in the study area (Schlumberger, 1972). This method was discarded, and none of these calculations were used to determine the salinity zones in the study area.

The Spontaneous Potential Method requires several input parameters in order to calculate an interpreted total dissolved solids concentration (Table 11.3-1). The parameters are described in detail in the following sections. If a parameter could not be measured, we made a reasonable assumption based on the geology of the formation being investigated.

Table 11.3-1. Input parameters for the Spontaneous Potential Method.

Parameter	Symbol	Units
Depth total	D_t	Feet
Depth formation	D_f	Feet
Temperature surface	T_s	Degrees Fahrenheit
Temperature bottom hole	T_{bh}	Degrees Fahrenheit
Resistivity of the mud filtrate	R_{mf}	Ohm-meter
Temperature of the mud filtrate	R_{mf_temp}	Degrees Fahrenheit
Spontaneous potential deflection	SP	Millivolts
CT conversion factor	Ct	(dimensionless)

Depth total

The total depth of the well is required to calculate the formation temperature at the depth of investigation. If a well was logged during multiple runs, each run represents a different depth range; the total depth of the logging run applicable to the depth of investigation must be used.

Depth formation

The depth of the formation being investigated is required to calculate the formation temperature. The depth of the middle of a given sand unit is obtained from the geophysical well log and recorded in the BRACS Database table. The depth is not corrected for kelly bushing height (kelly bushing depth corrections are made prior to GIS analysis of well points when mapping the three dimensional limits of the salinity zones).

Temperature surface
Surface temperature is required to calculate the formation temperature at the depth of investigation. Forrest and others (2005) state that mean annual surface temperature data is used for geothermal gradient calculations. Temperature records from 1951 to 1980 compiled by Larkin and Bomar (1983) indicate mean annual surface temperature in the study area ranged from 65 to 66 degrees Fahrenheit. Interpreted total dissolved solids calculations in this study used a surface temperature value of 65 degrees Fahrenheit.

Temperature bottom hole
Bottom hole temperature is required to calculate the formation temperature at the depth of investigation. Bottom hole temperature is found on the geophysical well log header. If a well was logged during multiple runs, with each run representing a different depth range, the bottom hole temperature of the logging run applicable to the depth of investigation must be used. Bottom hole temperatures are valid if the temperature was recorded after the drilling fluids in the bottom of the hole have equilibrated with the deepest formation (Forrest and others, 2005). Since there is no way to know if this situation has occurred, one must assume the bottom hole temperature is correct.

If the bottom hole temperature is missing from the log header, a bottom hole temperature can be calculated using the well site surface temperature and well depth (or depth of logging run) with a geothermal gradient calculated from the log of a nearby well with complete information. Calculated bottom hole temperatures are noted in the database table with supporting information.

Resistivity of the mud filtrate
Resistivity of the mud filtrate is recorded on the log header by the mud engineer. The resistivity of the mud filtrate is corrected to formation temperature (Estepp, 1998). If the resistivity of mud filtrate is not recorded on the log header, there are circumstances when the resistivity of the mud can be converted to a mud filtrate resistivity based on the drilling mud weight and mud type (Estepp, 1998; Schlumberger, 1985). Geophysical well logs where these conditions cannot be met are not used for log analysis.

Temperature of the mud filtrate
Temperature of the mud filtrate is recorded on the log header by the mud engineer. The temperature can be a surface or bottom hole value.

Spontaneous potential deflection
The spontaneous potential value is read from the geophysical well log in units of millivolts; it does not matter if the response is positive or negative. The spontaneous potential is determined after establishing the shale and sand baselines. The spontaneous potential response of shale is relatively constant and the shale baseline is determined by drawing a line connecting the maximum deflection of the shale beds. A sand baseline is determined using the same method, but connecting the maximum deflection of the sand beds.

The spontaneous potential value should be taken from a thick, shale-free, hydrocarbon-free sand bed. Thinner sand beds where the spontaneous potential response is not complete will need to have a spontaneous potential correction performed.

ct conversion factor

The ct conversion factor represents total dissolved solids concentration divided by specific conductance and is determined empirically from water quality samples. The ct conversion factor has a range of .55 to .75 for waters of ordinary composition up to total dissolved solids concentration of a few thousand milligrams per liter (Hem, 1985). Based upon the crossplot of total dissolved solids concentration versus specific conductance (Figure 11.2-1) the study ct conversion factor of 0.57 was used.

Spontaneous Potential Method procedure

The Spontaneous Potential Method was used for interpreted total dissolved solids calculations using the BRACS Database data entry form (formulas derived from Estepp, 1998). The calculations using the input parameters and formulas are run in Visual Basic for Applications tied to a command button on the data entry form. Note that this process could be performed with other software, provided the formulas are coded in the proper sequence. The key steps include the following:

1) Determine the input parameters and enter these values into the BRACS Database data entry forms.
2) Determine the formation being evaluated and enter this value into the data entry form.
3) Run the Spontaneous Method code to determine the interpreted total dissolved solids concentration for this depth and formation.
4) Repeat for each formation of interest on the geophysical well log.

Spontaneous Potential Method formulas

1. Determine the temperature of the formation being investigated.

$$T_f = (G_g \cdot D_f) + T_s$$

T_f	=	Temperature formation (units: degrees Fahrenheit)
D_f	=	Depth formation (units: feet)
G_g	=	Geothermal gradient (units: degrees Fahrenheit per foot)
T_s	=	Temperature surface (units: degrees Fahrenheit)

$$G_g = (T_{bh} - T_s) / D_t$$

G_g	=	Geothermal gradient (units: degrees Fahrenheit per foot)
T_{bh}	=	Temperature bottom hole (units: degrees Fahrenheit)
T_s	=	Temperature surface (units: degrees Fahrenheit)
D_t	=	Depth total (units: feet)

2. Correct resistivity of the mud filtrate to temperature at formation depth.

$$\mathbf{R_{mf\_Tf} = R_{mf} \cdot (R_{mf\_temp}/T_f)}$$

$\mathbf{R_{mf}}$	=	Resistivity mud filtrate (units: ohm-meter)
$\mathbf{R_{mf\_Tf}}$	=	Resistivity mud filtrate at temperature formation (units: ohm-meter)
$\mathbf{R_{mf\_temp}}$	=	Resistivity mud filtrate temperature (units: degrees Fahrenheit)
$\mathbf{T_f}$	=	Temperature formation (units: degrees Fahrenheit)

3. Correct resistivity of the mud filtrate for mud type.

$$\mathbf{R_{mf\_Tf} = R_{mf\_cor} * (R_{mf} * (R_{mf\_temp} / T_f))}$$

If $\mathbf{R_{mf}}$ >= 5 then: $\mathbf{R_{mf\_cor} = 1.75}$

Otherwise: $\mathbf{R_{mf\_cor} = 1}$

$\mathbf{R_{mf}}$	=	Resistivity mud filtrate (units: ohm-meter)
$\mathbf{R_{mf\_Tf}}$	=	Resistivity mud filtrate at formation temperature (units: ohm-meter)
$\mathbf{R_{mf\_temp}}$	=	Resistivity mud filtrate temperature (units: degrees Fahrenheit)
$\mathbf{T_f}$	=	Temperature formation (units: degrees Fahrenheit)

4. Calculate the temperature dependent constant **(**K).

$$\mathbf{K = 61 + (0.133 \cdot T_f)}$$

K	=	Temperature dependent constant (units: dimensionless)
$\mathbf{T_f}$	=	Temperature formation (units: degrees Fahrenheit)

5. Determine spontaneous potential value from geophysical log (Figure 11.3-1).

a) Select shale-free, hydrocarbon-free, thick bed on the spontaneous potential track
b) Define the shale baseline on the spontaneous potential track
c) Determine SP value. Record value as +/- in units of millivolts
d) If bed is thin, use spontaneous potential correction chart (Asquith, 1982, p. 34).
e) If borehole invasion is present, use spontaneous potential correction charts (Schlumberger, 1985, Chart SP3)

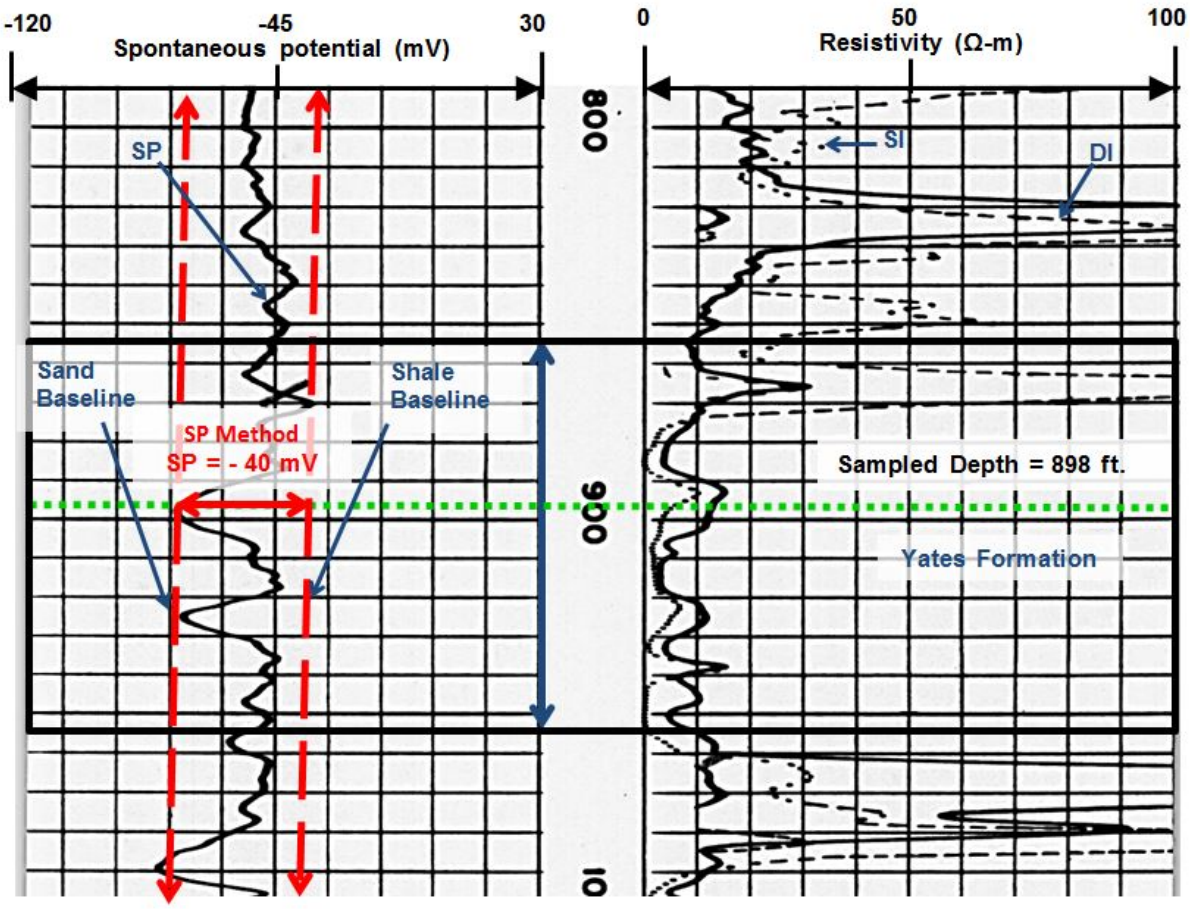

Figure 11.3-1. Example of the Spontaneous Potential Method applied to the Yates Formation (BRACS well identification number 35809). The spontaneous potential tool is shown in the left track, depth (in feet below ground surface) is shown in the middle track, and the shallow and deep induction tools are shown in the right track. DI = deep induction, mV = millivolts, SI = short induction, SP = spontaneous potential.

6. Calculate the resistivity of water equivalent (R_{we}).

$$R_{we} = 10^{[(SP + K \cdot (\text{Log } R_{mf\_tf}))/K]}$$

K	=	Temperature dependent constant (units: dimensionless)
SP	=	Spontaneous potential (units: millivolts)
$\mathbf{R_{we}}$	=	Resistivity water equivalent (units: ohm-meter)
$\mathbf{R_{mf\_Tf}}$	=	Resistivity of the mud filtrate at temperature formation (units: ohm-meter)

7. Calculate resistivity of water from resistivity of water equivalent based on groundwater type correction factor ($R_{we}\_R_w\_cor$).

$$\mathbf{R_w = R_{we}\_R_w\_cor \cdot R_{we}}$$

$\mathbf{R_{we}}$	=	Resistivity water equivalent (units: ohm-meter)
$\mathbf{R_{we}\_R_w\_cor}$	=	Groundwater type correction factor (units: dimensionless)
$\mathbf{R_w}$	=	Resistivity of water (units: ohm-meter)

Note: The following values can be used for water types:

- $\mathbf{R_{we}\_R_w\_cor}$ = 1.33 for average sodium bicarbonate (Estepp, 2010).
- $\mathbf{R_{we}\_R_w\_cor}$ = 1.75 for high sodium bicarbonate (Alger, 1966).
- $\mathbf{R_{we}\_R_w\_cor}$ = 1.1 for average sodium sulfate (Estepp, 2010).
- $\mathbf{R_{we}\_R_w\_cor}$ = 1.0 for sodium chloride solutions (Estepp, 2010).

For this study, $\mathbf{R_{we}\_R_w\_cor}$ = 1, therefore $\mathbf{R_w = R_{we}}$.

8. Convert resistivity of water at temperature formation to 75 °F (R_{w75})

$$\mathbf{R_{w75} = R_w \cdot (T_f / 75)}$$

$\mathbf{T_f}$	=	Temperature formation (units: degrees Fahrenheit)
$\mathbf{R_w}$	=	Resistivity of water (units: ohm-meter)
$\mathbf{R_{w75}}$	=	Resistivity of water at 75 °F (units: ohm-meter)

9. Convert resistivity of water at 75 °F to conductivity of water at 75 °F (C_w).

$$\mathbf{C_w = 10{,}000 / R_{w75}}$$

$\mathbf{C_w}$	=	Conductivity of water at 75 °F (units: microsiemens per centimeter)
$\mathbf{R_{w75}}$	=	Resistivity of water at 75 °F (units: ohm-meter)

Note: Conductivity is the reciprocal of resistivity. The value of 10,000 is used to convert the units appropriately.

10. Calculate total dissolved solids (TDS) using the specific conductance – TDS conversion factor (ct).

$$\mathbf{TDS = ct \cdot C_w}$$

TDS	=	Interpreted total dissolved solids (units: milligrams per liter)
ct	=	ct conversion factor (units: dimensionless)
$\mathbf{C_w}$	=	Conductivity water at 75°F (units: microsiemens per centimeter)

11.4 The Alger-Harrison Method

The Alger-Harrison Method is commonly used for determining the formation water resistivity by using the ratio of the shallow and deep resistivity curves (Estepp, 1998). The method takes advantage of the Archie equation for water saturation by setting the ratio of the resistivity of the formation water to the measured deep resistivity equal to the ratio of the resistivity of the mud filtrate to the measured shallow resistivity. This relationship has been demonstrated experimentally (Schlumberger, 1972) for a thick clean formation with an even distribution of porosity.

The Alger-Harrison Method uses measured resistivity data exclusively as a way to interpret salinity from geophysical well logs. Because resistivity curves are commonly included in geophysical well logs we were able to calculate 771 total dissolved solids concentration values. We used these calculated total dissolved solids values along with those measured from water samples to determine the salinity zones in the study area.

Shallow and deep resistivity curves may be influenced by drilling mud filtrate invasion in the formation of interest. Therefore, geophysical well logs that had invasion issues or had problems with resistivity curves were omitted. We also determined that the correction of resistivity measurements to account for mud filtrate invasion was unnecessary for this project. Industry-prepared mud filtrate invasion correction charts are exclusive to their respective electric logging tools, so every log would need a different correction chart to correct resistivity values. We observed that the maximum variance possible for a calculated salinity value when using a constant for the mud filtrate value was a 15 percent change from the final calculated salinity value and the variance in calculated salinity values decreases as salinity increases. The resistivity readings made for the Lipan Aquifer study were corrected to formation temperature using the guidelines set by Estepp (1998).

The Alger-Harrison Method requires several input parameters in order to calculate an interpreted total dissolved solids concentration (Table 11.4-1). The Alger-Harrison Method parameters are described in detail in the following sections. If a parameter could not be measured, we made a reasonable assumption based on the geology of the formation being investigated.

Table 11.4-1. Input parameters for the Alger-Harrison Method.

Parameter	Symbol	Units
Depth total	D_t	Feet
Depth formation	D_f	Feet
Temperature surface	T_s	Degrees Fahrenheit
Temperature bottom hole	T_{bh}	Degrees Fahrenheit
Resistivity of the mud filtrate	R_{mf}	Ohm-meter
Temperature of the mud filtrate	R_{mf_temp}	Degrees Fahrenheit
Shallow resistivity	R_{xo}	Ohm-meter
Deep resistivity	R_o	Ohm-meter
ct conversion factor	ct	(dimensionless)

Depth total
The total depth of the well is required to calculate the formation temperature at the depth of investigation. If a well was logged during multiple runs, each run represents a different depth range; the total depth of the logging run applicable to the depth of investigation must be used.

Depth formation
The depth of the formation being investigated is required to calculate the formation temperature. The depth of the middle of a given sand unit is obtained from the geophysical well log and recorded in the BRACS Database table. The depth is not corrected for kelly bushing height (kelly bushing depth corrections are made prior to GIS analysis of well points when mapping the three dimensional limits of the salinity zones).

Temperature surface
Surface temperature is required to calculate the formation temperature at the depth of investigation. Forrest and others (2005) state that mean annual surface temperature data is used for geothermal gradient calculations. Temperature records from 1951-1980 compiled by Larkin and Bomar (1983) indicate mean annual surface temperature in the study area ranged from 65 to 66 degrees Fahrenheit. Interpreted total dissolved solids calculations in this study used a surface temperature value of 65 degrees Fahrenheit.

Temperature bottom hole
Bottom hole temperature is required to calculate the formation temperature at the depth of investigation. Bottom hole temperature is found on the geophysical well log header. If a well was logged during multiple runs, with each run representing a different depth range, the bottom hole temperature of the logging run applicable to the depth of investigation must be used. Bottom hole temperatures are valid if the temperature was recorded after the drilling fluids in the bottom of the hole have equilibrated with the deepest formation (Forrest and others, 2005). Since there is no way to know if this situation has occurred, one must assume the bottom hole temperature is correct.

If the bottom hole temperature is missing from the log header, a bottom hole temperature can be calculated using the well site surface temperature and well depth (or depth of logging run) with a

geothermal gradient calculated from the log of a nearby well with complete information. Calculated bottom hole temperatures are noted in the database table with supporting information.

Resistivity of the mud filtrate
Resistivity of the mud filtrate is computed and recorded on the log header by the mud engineer. The resistivity of the mud filtrate is corrected to formation temperature (Estepp, 1998). If the resistivity of mud filtrate is not recorded on the log header, there are circumstances when the resistivity of the mud can be converted to a mud filtrate resistivity based on the drilling mud weight and mud type (Estepp, 1998; Schlumberger, 1985). Geophysical well logs where these conditions cannot be met are not used for log analysis.

Temperature of the mud filtrate
Temperature of the mud filtrate is recorded on the log header by the mud engineer. The temperature can be a surface or bottom hole value.

Shallow resistivity
The shallow resistivity curve is the measurement of resistivity of the geological formation adjacent to the borehole where formation fluids may be displaced or invaded by the drilling mud filtrate (Schlumberger, 1972).

Deep resistivity
The deep resistivity curve is the measurement of resistivity at some distance into the geological formation, the distance dependent on the type of logging tool. Deep resistivity measurements represent the response of the geological formation and formation water if the drilling mud filtrate has not penetrated equal to or deeper than the logging tool response depth.

ct conversion factor
The ct conversion factor represents total dissolved solids concentration divided by specific conductance and is determined empirically from water quality samples. The ct conversion factor has a range of 0.55 to 0.75 for waters of ordinary composition up to total dissolved solids concentration of a few thousand milligrams per liter (Hem, 1985). Based upon the crossplot of total dissolved solids concentration versus specific conductance (Figure 11.2-1) the study ct conversion factor of 0.57 was used.

Alger-Harrison Method procedure

The Alger-Harrison Method was used for interpreted total dissolved solids calculations using the BRACS Database data entry form (formulas derived from Estepp, 1998). The calculations using the input parameters and formulas are run in Visual Basic for Applications tied to a command button on the data entry form. Note that this process could be performed with other software, provided the formulas are coded in the proper sequence. The key steps include the following:

1) Determine the input parameters and enter these values into the BRACS Database data entry forms.
2) Determine the formation being evaluated and enter this value into the data entry form.

3) Run the Alger-Harrison Method code to determine the interpreted total dissolved solids concentration for this depth and formation.
4) Repeat for each formation of interest on the geophysical well log.

Alger-Harrison Method formulas

1. Determine the temperature of the formation being investigated.

$$\mathbf{T_f = (G_g \cdot D_f) + T_s}$$

$\mathbf{T_f}$	=	Temperature formation (units: degrees Fahrenheit)
$\mathbf{D_f}$	=	Depth formation (units: feet)
$\mathbf{G_g}$	=	Geothermal gradient (units: degrees Fahrenheit/foot)
$\mathbf{T_s}$	=	Temperature surface (units: degrees Fahrenheit)

$$\mathbf{G_g = (T_{bh} - T_s) / D_t}$$

$\mathbf{G_g}$	=	Geothermal gradient (units: degrees Fahrenheit/foot)
$\mathbf{T_{bh}}$	=	Temperature bottom hole (units: degrees Fahrenheit)
$\mathbf{T_s}$	=	Temperature surface (units: degrees Fahrenheit)
$\mathbf{D_t}$	=	Depth total (units: feet)

2. Correct Resistivity of the mud filtrate to formation temperature.

$$\mathbf{R_{mf\_Tf} = R_{mf} \cdot (R_{mf\_temp}/T_f)}$$

$\mathbf{R_{mf}}$	=	Resistivity mud filtrate (units: ohm-meter)
$\mathbf{R_{mf\_Tf}}$	=	Resistivity mud filtrate at formation temperature (units: ohm-meter)
$\mathbf{Rmf\_temp}$	=	Resistivity mud filtrate temperature (units: degrees Fahrenheit)
$\mathbf{T_f}$	=	Temperature formation (units: degrees Fahrenheit)

3. Correct Resistivity of the mud filtrate for mud type.

$$\mathbf{R_{mf\_Tf} = R_{mf\_cor} * (R_{mf} * (R_{mf\_temp} / T_f))}$$

If $\mathbf{R_{mf}}$ >= 5, then $\mathbf{R_{mf\_cor} = 1.75}$

Otherwise $\mathbf{R_{mf\_cor} = 1}$

$\mathbf{R_{mf}}$	=	Resistivity mud filtrate (units: ohm-meter)
$\mathbf{R_{mf\_Tf}}$	=	Resistivity mud filtrate at formation temperature (units: ohm-meter)
$\mathbf{R_{mf\_temp}}$	=	Resistivity mud filtrate temperature (units: degrees Fahrenheit)
$\mathbf{T_f}$	=	Temperature formation (units: degrees Fahrenheit)

4. Determine shallow (Rxo) and deep (Ro) resistivity values from geophysical log (Figure 11.4-1).

a) Select shale-free bed on resistivity track
b) Determine Rxo and Ro values. Record values with units of ohm-meter (ohm-m)

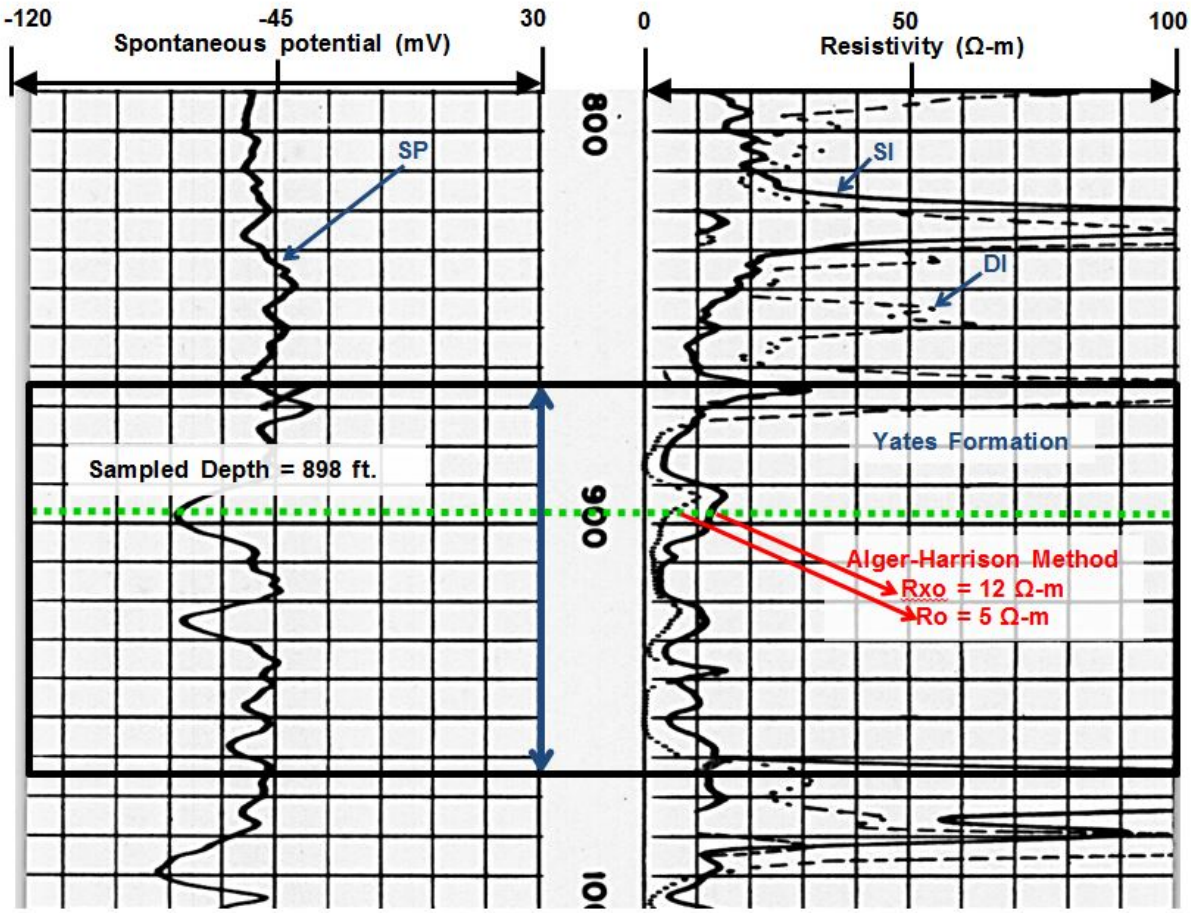

Figure 11.4-1. Example of the Alger-Harrison Method applied to the Yates Formation (BRACS well identification number 35809). The spontaneous potential tool is shown in the left track, depth (in feet below ground surface) is shown in the middle track, and the shallow and deep induction tools are shown in the right track. DI = deep induction, mV = millivolts, Ro = resistivity of the deep zone, Rxo = resistivity of the shallow zone, SI = short induction, SP = spontaneous potential, Ω-m = Ohm-meter.

5. Calculate resistivity of water equivalent (R_{we}).
There are several invasion zone correction formulas that could be used based on the type of geophysical logs used. The following formula shows no correction:

$$\mathbf{R_{we} = R_{mf\_Tf} / (R_{xo}/R_o)}$$

$\mathbf{R_{we}}$	=	Resistivity water equivalent (units: ohms-meter)
$\mathbf{R_{mf\_Tf}}$	=	Resistivity mud filtrate at temperature formation (units: ohms-meter)
$\mathbf{R_{xo}}$	=	Resistivity invaded zone (units: ohms-meter)
$\mathbf{R_o}$	=	Resistivity un-invaded zone (units: ohms-meter)

These formulas show possible invasion zone corrections (Estepp, 2010):

Dual induction log, shallow focused log:

$$\mathbf{R_{xo} / R_o = (1.45 * (R_{xo}/R_o)) - .45}$$

Dual induction log, laterlog 8:

$$\mathbf{R_{xo} / R_o = (1.85 * (R_{xo}/R_o)) - .85}$$

Lateral Log:

$$\mathbf{R_{xo} / R_o = R_{xo} / ((1.67 * R_o) – (.67 * R_{xo}))}$$

16 and 64 inch normal resitivity:

$$\mathbf{R_{xo} / R_o = (R_{16})^2 / (R_{64})^2}$$

(where $\mathbf{R_{16} = R_{xo}}$ and $\mathbf{R_{64} = R_o}$)

Hilchie (1978) provides a 16 and 64 inch normal correction factor for older logs:

$$\mathbf{R_t = (R_{64})^2 / R_{16}}$$

You can average multiple high points from R_{16} and R_{64} curves of a sand resistivity to get one value for the sand (Estepp, 1998).

6. Calculate resistivity of water from resistivity of water equivalent based on groundwater type correction factor (R_{we_cor}).

$$\mathbf{R_w = R_{we\_cor} \cdot R_{we}}$$

$\mathbf{R_{we}}$	=	Resistivity water equivalent (units: ohm-meter)
$\mathbf{R_{we\_cor}}$	=	Groundwater type correction factor (units: dimensionless)
$\mathbf{R_w}$	=	Resistivity of water (units: ohm-meter)

Note: The following **Rwe_cor** values can be used for water types:

- $\mathbf{R_{we\_cor}}$ = 1.33, for average sodium bicarbonate (Estepp, 2010).
- $\mathbf{R_{we\_cor}}$ = 1.75, for high sodium bicarbonate (Alger, 1966).
- $\mathbf{R_{we\_cor}}$ = 1.1, for average sodium sulfate (Estepp, 2010).
- $\mathbf{R_{we\_cor}}$ = 1.0, for sodium chloride solutions (Estepp, 2010).

For this study, $\mathbf{R_{we\_cor}}$ = 1, therefore $\mathbf{R_w = R_{we}}$.

7. Convert resistivity of water at temperature formation to 75 °F (R_{w75}).

$$\mathbf{R_{w75} = R_w \cdot (T_f / 75)}$$

$\mathbf{T_f}$	=	Temperature formation (units: degrees Fahrenheit)
$\mathbf{R_w}$	=	Resistivity of water (units: ohm-meter)
$\mathbf{R_{w75}}$	=	Resistivity of water at 75 °F (units: ohm-meter)

8. Convert resistivity of water at 75 °F to conductivity of water at 75 °F.

$$\mathbf{C_w = 10000 / R_{w75}}$$

$\mathbf{C_w}$	=	Conductivity of water at 75 °F (units: microsiemens per centimeter)
$\mathbf{R_{w75}}$	=	Resistivity of water at 75 °F (units: ohm-meter)

Note: Conductivity is reciprocal to resistivity. The value of 10,000 is used for unit conversion.

9. Calculate total dissolved solids (TDS) using the specific conductance – TDS conversion factor (ct).

$$\mathbf{TDS = ct \cdot C_w}$$

TDS	=	Interpreted total dissolved solids (units: milligrams per liter)
ct	=	ct conversion factor (units: dimensionless)
$\mathbf{C_w}$	=	Conductivity of water at 75°F (units: microsiemens per centimeter)

12. Salinity zone determination

The geologic history of the area records periods of shallow marine deposition during the Permian followed by a long period of exposure and erosion prior to deposition of Upper Triassic Dockum Group strata. This process was repeated after Dockum Group deposition and prior to the transgression of the Cretaceous seas and deposition of the Trinity Group. As a result, we believe that the Permian formations developed a relatively thick weathered zone. This weathered zone may provide an area of increased permeability and porosity depending upon the original lithology of the Permian formations. We also believe that the weathered zone is where mixing can occur between high salinity brine that discharges from Permian formations and downward percolating fresh meteoric water, a process described in detail by Richter and others (1990).

Because of the significant lithologic differences between the Permian formations in the study area, we decided to study the distribution of total dissolved solids concentration with depth for each potential water-bearing geological formation. We combined the 771 total dissolved solids concentrations calculated with the Alger-Harrison Method from geophysical well logs with 5,702 measurements derived from groundwater samples stored in either the TWDB Groundwater Database or the TWDB BRACS Database resulting in a total of 6,473 measurements. Ultimately, only 918 of these measurements were uniquely associated with the Permian water-bearing formations in the study area and could be used in this analysis.

The water quality data was subdivided by geological formation in order to identify possible variations attributable to stratigraphy. We compared water well quality samples with interpreted total dissolved solids concentration in the same geological formation and where only the Quaternary and Neogene sediments overlaid the geological formation of interest. Every interpreted total dissolved solids concentration calculated from geophysical well logs was assigned to a specific formation when they were initially determined. We further limited our analysis to nine stratigraphic units of Permian age that are known to be composed of rock types that have aquifer characteristics amenable to groundwater storage and flow. We have highlighted the geological formations considered most likely to be capable of acting as significant aquifers in the stratigraphic column (Figure 7.2-1). The Cretaceous and Triassic formations are aquifers in the area but will be considered separately in future TWDB studies.

12.1 Salinity versus depth analysis

Our initial approach was to cross-plot the sampled and calculated total dissolved solids concentration values versus depth below ground surface. However, the resulting plots for the nine Permian formations did not clearly define where groundwater vertically transitions between defined groundwater salinity zones within the study area. We therefore decided to “bin” the combined measured water sample and calculated Alger-Harrison Method total dissolved solids data by determining the average total dissolved solids concentration for each Permian formation using the sample depth below the top of the Permian formations. The resulting average bin values for the total dissolved solids concentration were plotted at the center depth value for each bin range for the sample depth below the top of the Permian formations. The ten bin depth intervals are: (1) 0 to 99, (2) 100 to 199, (3) 200 to 299, (4) 300 to 399, (5) 400 to 499, (6) 500 to 599, (7) 600 to 699, (8) 700 to 799, (9) 800 to 899, and (10) 900 to 999 feet.

Plots of the trend lines of the binned salinity data generally show that from 0 to 500 feet below the top of the Permian formations there is a general correlation that shows greater total dissolved solids concentration with increasing depth. Below that depth, the trend lines have no discernable slope and track each other with only slight variations between 20,000 and 30,000 milligrams per liter of total dissolved solids. We believe that this indicates that Alger-Harrison Method can be used to calculate approximate formation fluid resistivities in the weathered portions of the Permian formations. However, in the unweathered portions of the Permian formations the Alger-Harrison Method will calculate resistivities that are too high leading to lower than expected total dissolved solids concentrations. This is because of the lithified nature of the calcareous strata and the shaly interbeds that result in a complex arrangement of porosity and permeability within the Permian formations.

The TWDB defines salinity in terms of total dissolved solids concentration (Winslow and Kister, 1956). Groundwater salinity categories are fresh (0 to 999 milligrams per liter), slightly saline (1,000 to 2,999 milligrams per liter), moderately saline (3,000 to 9,999 milligrams per liter), very saline (10,000 to 34,999 milligrams per liter), and brine (greater than 35,000 milligrams per liter. We define brackish groundwater as slightly to moderately saline water (1,000 to 9,999 milligrams per liter of total dissolved solids). These terms will be used as we discuss the salinity versus depth plots for each of the Permian aquifers in the sections below.

12.1.1 Yates Formation salinity

We plotted total dissolved solids concentration versus depth below the top of the Permian formations for the Yates Formation without binning (Figure 12.1.1-1) and with binning (Figure 12.1.1-2). Each plot shows the total dissolved solids concentration lines that separate the defined salinity zones. The water quality samples for the Yates Formation came from three wells and all reported more than 1,000 milligrams per liter of total dissolved solids. Calculated total dissolved solids concentrations that were determined to be significantly impacted by the lithologic characteristics of the unweathered portions of the Permian formation are highlighted in red and were not used in the binning process.

The trend of the depth below top of Permian formation line in Figure 12.1.1-2 shows salinity rapidly increasing with depth in the first 250 feet below the top of the Permian formations before the trend begins to flatten. This indicates that the impact of meteoric recharge diminishes with depth.

We determined that for water produced exclusively from the Yates Formation (1) no fresh water should be expected, (2) slightly saline groundwater will be expected from 0 to 110 feet below the Permian top, (3) moderately saline groundwater will be expected from 110 to 215 feet below the Permian top, and (4) very saline groundwater will be expected at depths greater than 215 feet below the Permian top (Figure 12.1.1-2).

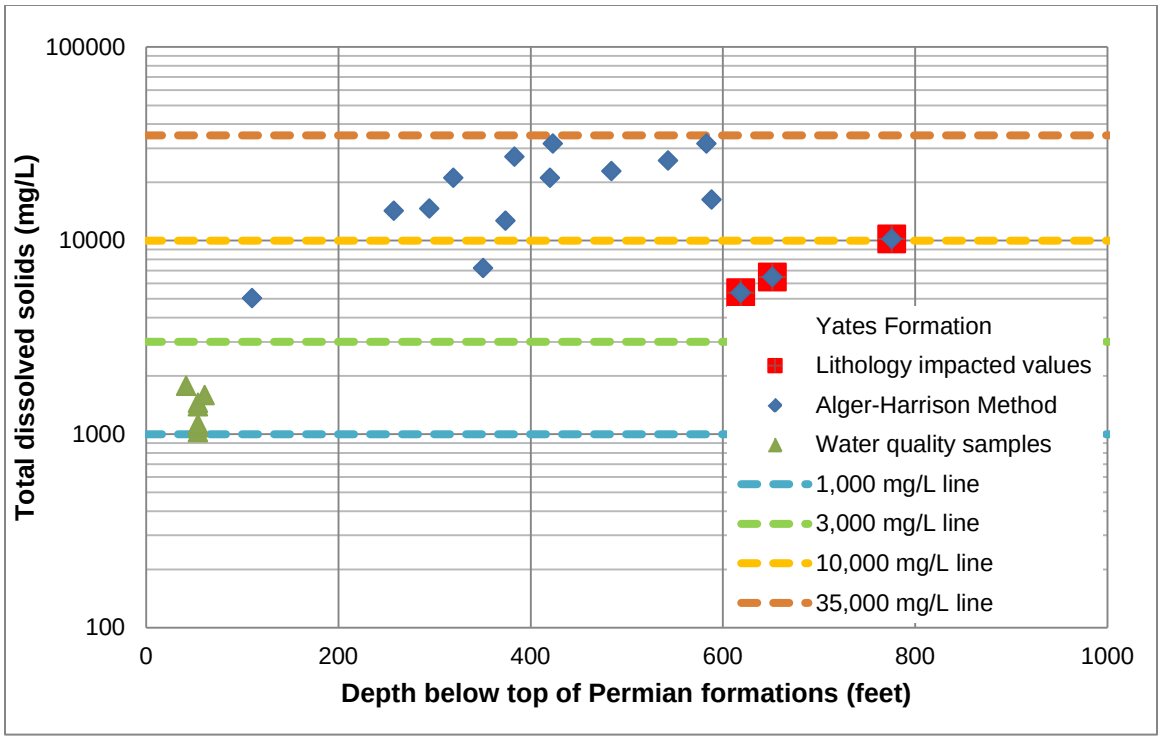

Figure 12.1.1-1. Yates Formation salinity plot. Depth is feet below top of Permian formations. mg/L = milligrams per liter.

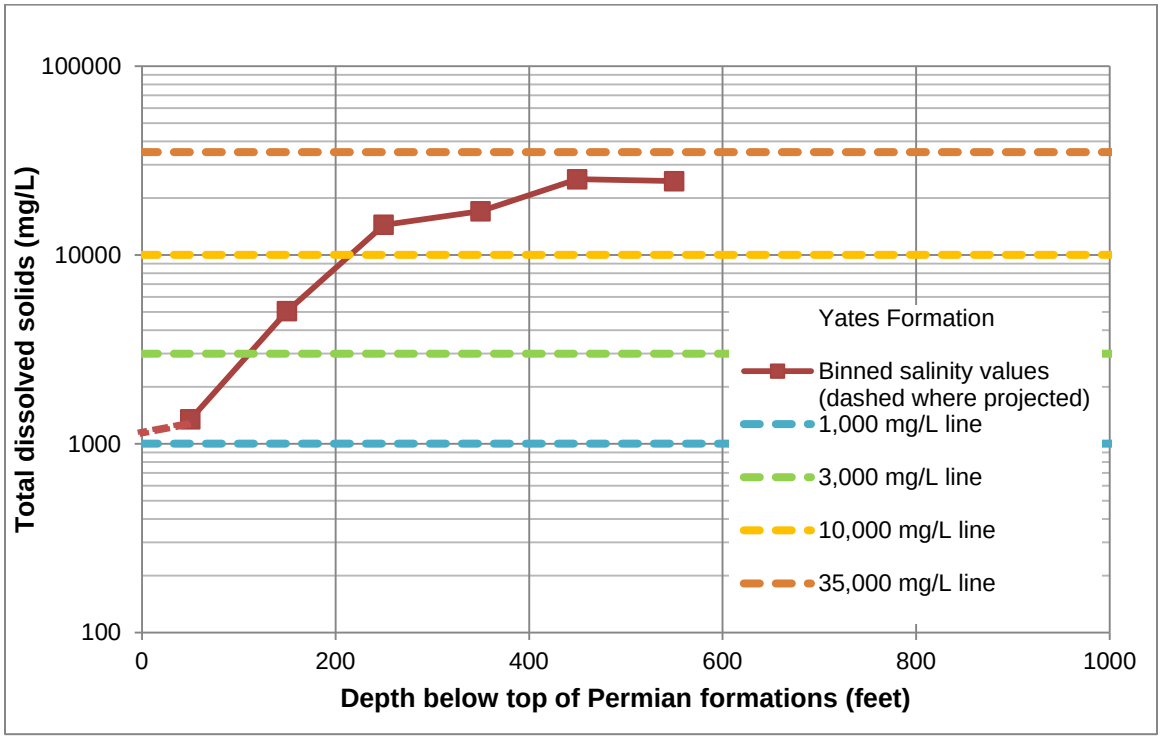

Figure 12.1.1-2. Yates Formation binned salinity plot. mg/L = milligrams per liter.

12.1.2 Seven Rivers Formation salinity

We plotted total dissolved solids concentration versus depth below the top of the Permian formations for the Seven Rivers Formation without binning (Figure 12.1.2-1) and with binning (Figure 12.1.2-2). Each plot shows the total dissolved solids concentration lines that separate the defined salinity zones. The water quality samples for the Seven Rivers Formation came from 13 wells with seven reporting less than 1,000 milligrams per liter of total dissolved solids. All of the water quality samples reporting fresh water are from wells completed in both the Seven Rivers Formation and the Quaternary and Neogene sediments. Calculated total dissolved solids concentrations that were determined to be significantly impacted by the lithologic characteristics of the unweathered portions of the Permian formations are highlighted in red and were not used in the binning process.

The trend of the depth below top of Permian formations line in Figure 12.1.2-2 shows salinity rapidly increasing with depth in the first 200 feet below the top of the Permian formations before the trend begins to flatten. This indicates that the impact of meteoric recharge diminishes rapidly with depth.

We determined that for water produced exclusively from the Seven Rivers Formation (1) no fresh water should be expected, (2) slightly saline groundwater will be expected from 0 to 60 feet below the Permian top, (3) moderately saline groundwater will be expected from 60 to 315 feet below the Permian top, and (4) very saline groundwater will be expected at depths greater than 315 feet below the Permian top (Figure 12.1.2-2).

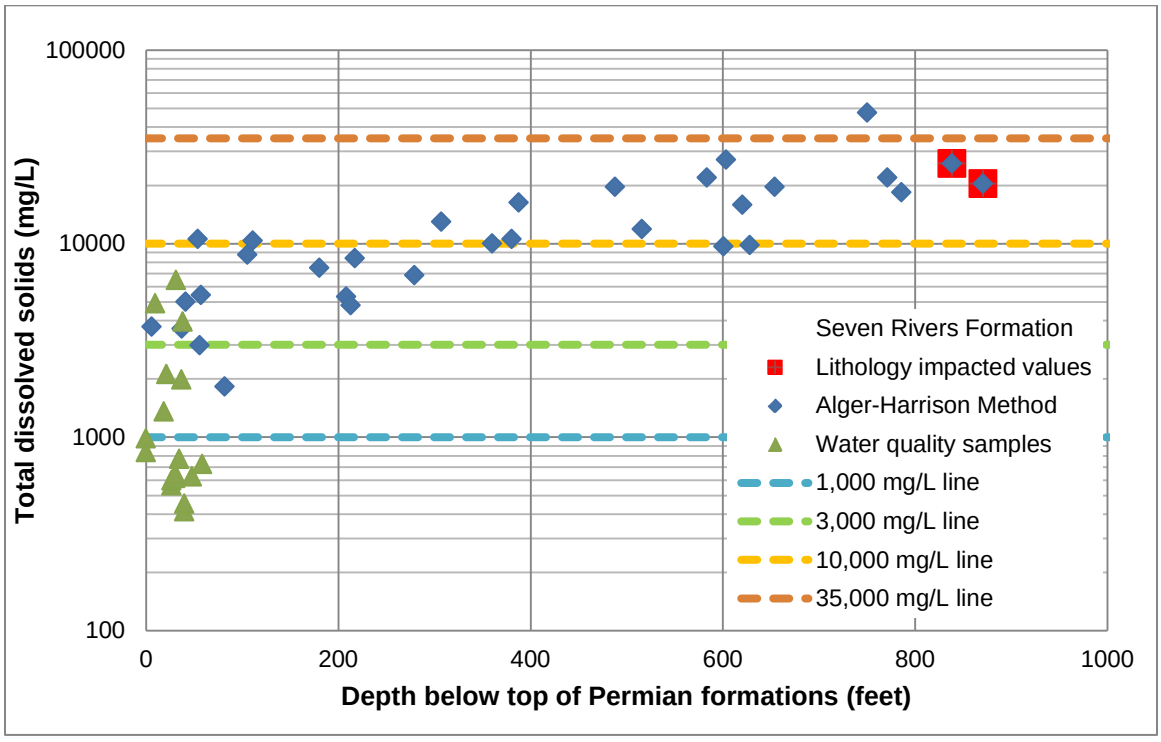

Figure 12.1.2-1. Seven Rivers Formation salinity plot. Depth is feet below top of Permian formations. mg/L = milligrams per liter.

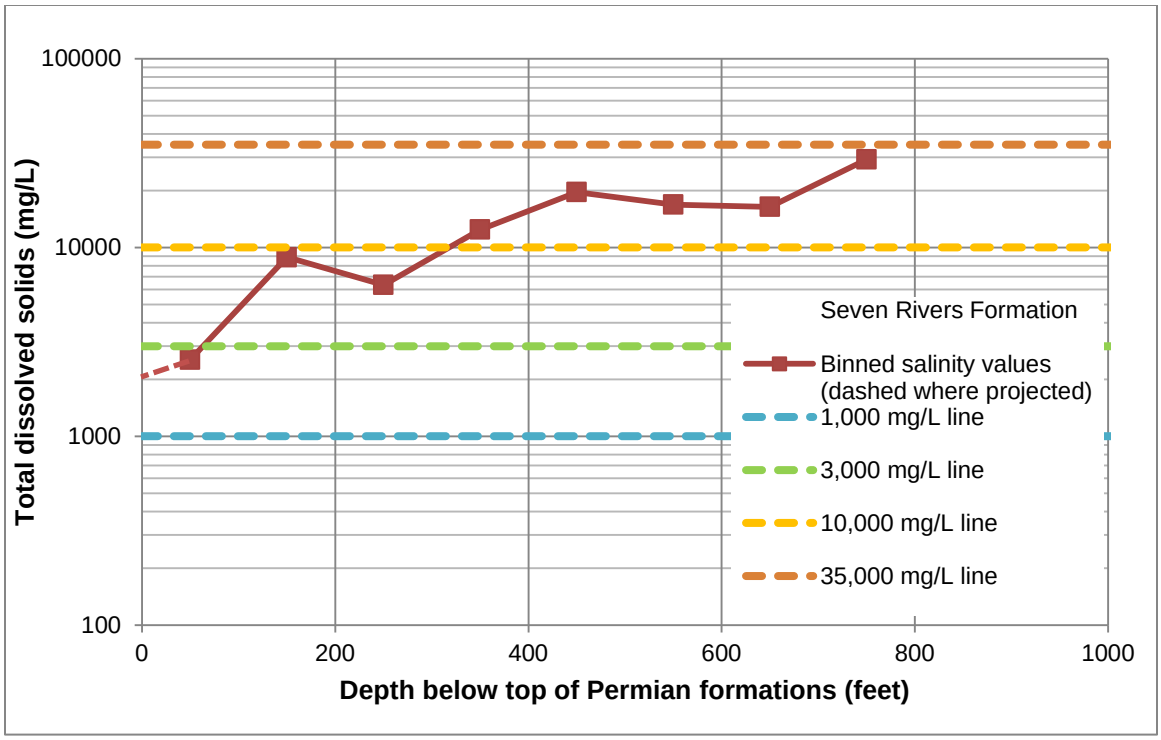

Figure 12.1.2-2. Seven Rivers Formation binned salinity plot. mg/L = milligrams per liter.

12.1.3 Queen Formation salinity

We plotted total dissolved solids concentration versus depth below top of Permian formations for the Queen Formation without binning (Figure 12.1.3-1) and with binning (Figure 12.1.3-2). Each plot shows the total dissolved solids concentration lines that separate the defined salinity zones. There were no water quality samples from this geological formation. Calculated total dissolved solids concentrations that were determined to be significantly impacted by the lithologic characteristics of the unweathered portions of the Permian formations are highlighted in red and were not used in the binning process.

The trend of the depth below top of Permian formations line in Figure 12.1.3-2 shows moderate to high salinity beginning at less than 100 feet below the top of the Permian formations with only a gradual increasing with depth trend. This indicates that the impact of meteoric recharge extends less than 100 feet into the Queen Formation.

We determined that for water produced exclusively from the Queen Formation (1) no fresh water should be expected, (2) no slightly saline groundwater should be expected, (3) moderately saline groundwater will be expected from 0 to 390 feet below the Permian top, and (4) very saline groundwater will be expected at depths greater than 390 feet below the Permian top (Figure 12.1.3-2).

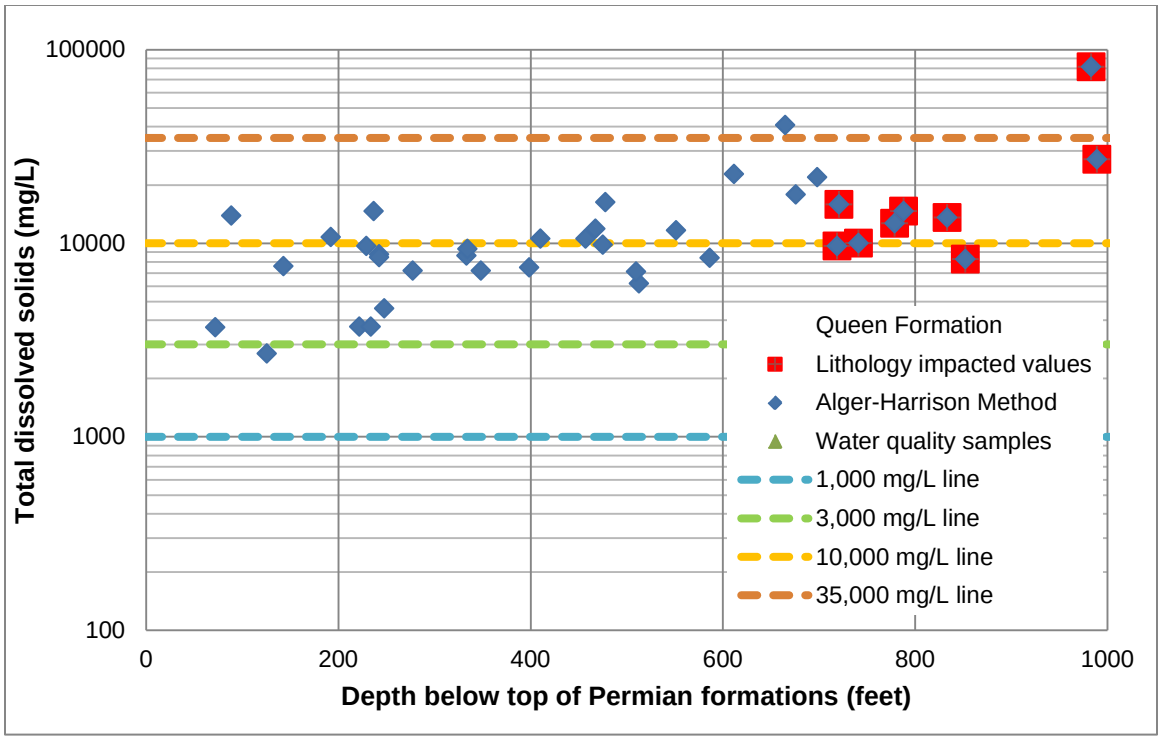

Figure 12.1.3-1. Queen Formation salinity plot. Depth is feet below top of Permian formations. mg/L = milligrams per liter.

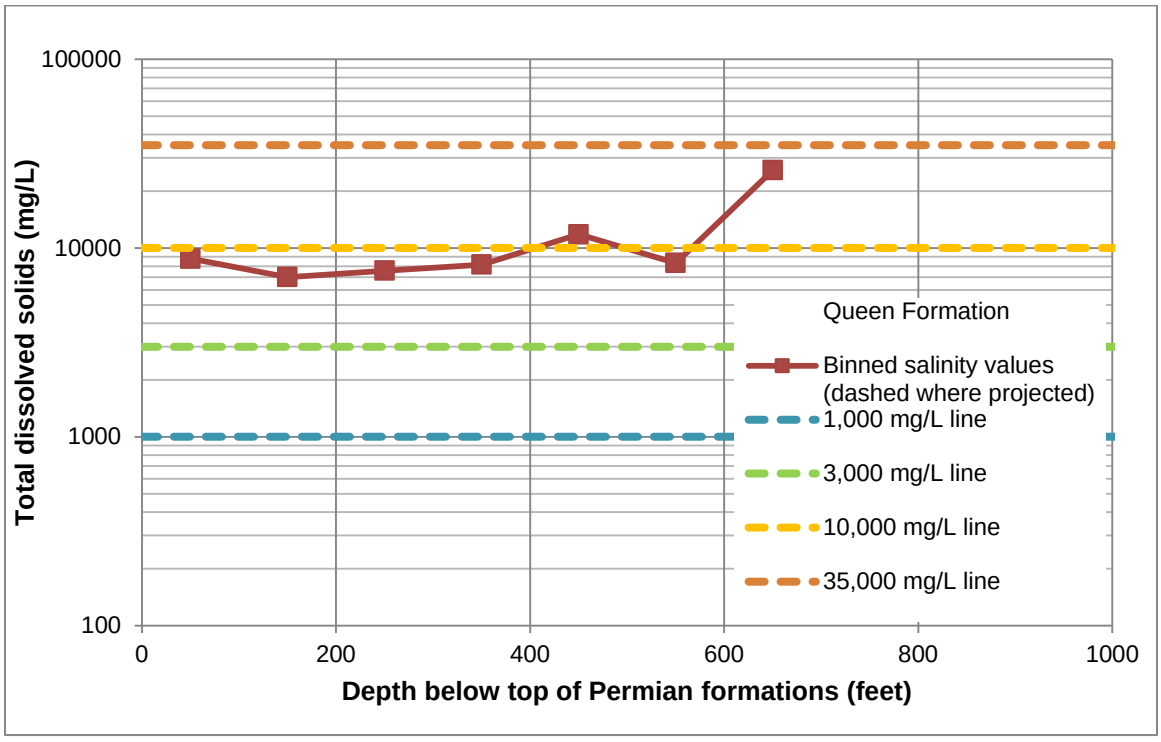

Figure 12.1.3-2. Queen Formation binned salinity plot. mg/L = milligrams per liter.

12.1.4 San Angelo Formation salinity

We plotted total dissolved solids concentration versus depth below the top of Permian formations for the San Angelo Formation without binning (Figure 12.1.4-1) and with binning (Figure 12.1.4-2). Each plot shows the total dissolved solids concentration lines that separate the defined salinity zones. The water quality samples for the San Angelo Formation came from seven wells. One of the wells reported a water quality sample with fresh water that was completed in both the San Angelo Formation and the Quaternary and Neogene sediments. Calculated total dissolved solids concentrations that were determined to be significantly impacted by the lithologic characteristics of the unweathered portions of the Permian formations are highlighted in red and were not used in the binning process.

The trend of the depth below top of Permian formations line in Figure 12.1.4-1 shows salinity rapidly increasing with depth in the first 500 feet below the top of the Permian formations before the trend begins to flatten. This indicates that the impact of meteoric recharge diminishes with depth.

We determined that for water produced exclusively from the San Angelo Formation (1) no fresh water should be expected, (2) slightly saline groundwater will be expected from 0 to 205 feet below the Permian top, (3) moderately saline groundwater will be expected from 205 to 445 feet below the Permian top, and (4) very saline groundwater will be expected at depths greater than 445 feet below the Permian top (Figure 12.1.4-2).

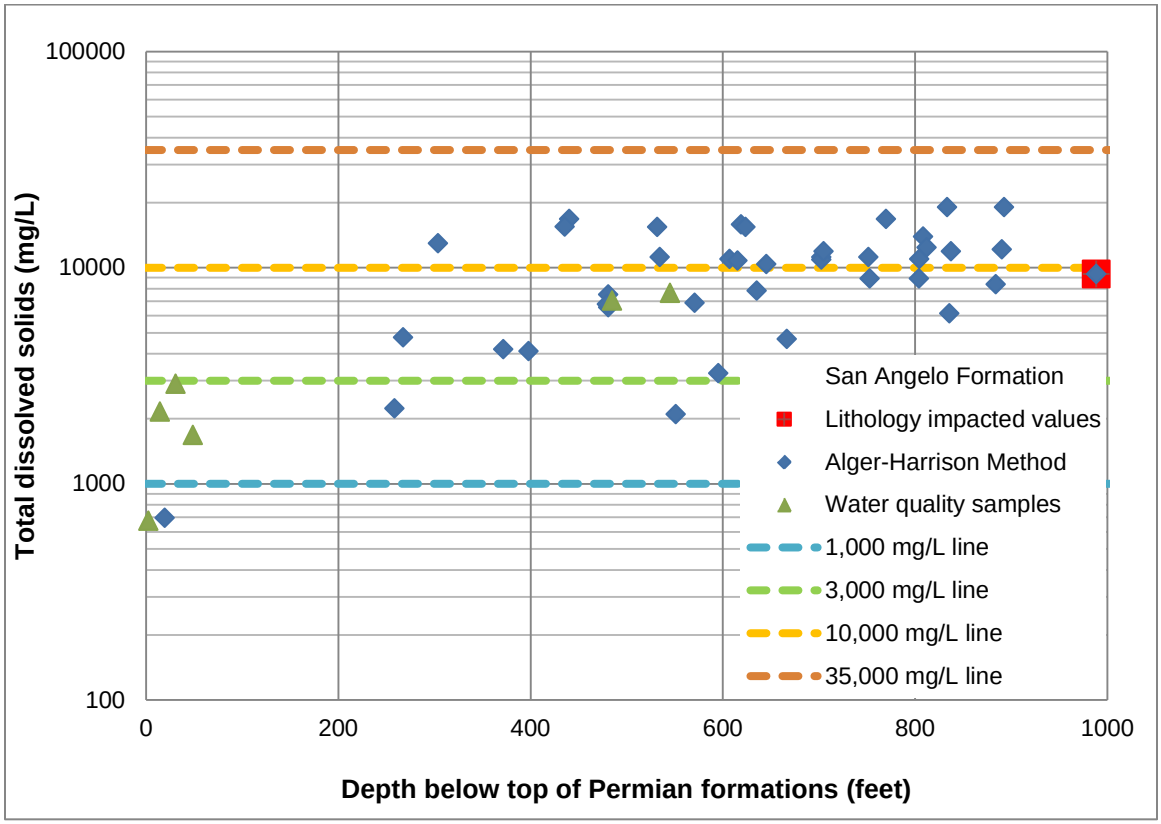

Figure 12.1.4-1. Yates Formation salinity plot. Depth is feet below top of Permian formations. mg/L = milligrams per liter.

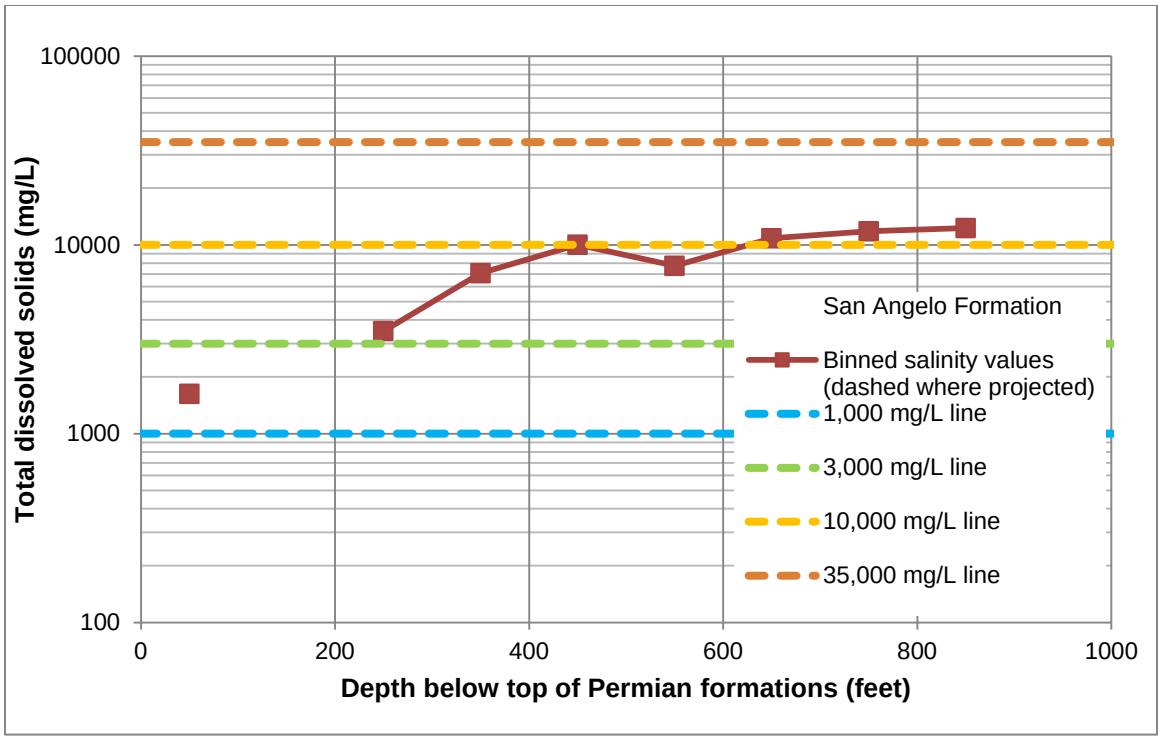

Figure 12.1.4-2. San Angelo Formation binned salinity plot. mg/L = milligrams per liter.

12.1.5 Upper Choza member salinity

We plotted total dissolved solids concentration versus depth below the top of Permian formations for the Upper Choza member without binning (Figure 12.1.5-1) and with binning (Figure 12.1.5-2). Each plot shows the total dissolved solids concentration lines that separate the defined salinity zones. The water quality samples for the Upper Choza member came from 42 wells with 8 reporting less than 1,000 milligrams per liter of total dissolved solids. The eight water quality samples reporting fresh water are from wells completed in both the Upper Choza member and the Quaternary and Neogene sediments. Calculated total dissolved solids concentrations that were determined to be significantly impacted by the lithologic characteristics of the unweathered portions of the Permian formations are highlighted in red and were not used in the binning process.

The trend of the depth below the top of Permian formations line in Figure 12.1.5-2 shows salinity rapidly increasing with depth in the first 400 feet below the top of the Permian formations before the trend begins to flatten. This indicates that the impact of meteoric recharge diminishes with depth. The water sample at 773 feet below the top of the Permian formations is the only measured water sample in the study area that provides an indication of the depth to the top of brine groundwater which would be at approximately 675 feet below the top of the Permian formations in the Upper Choza member.

We determined that for water produced exclusively from the Upper Choza member (1) no fresh water should be expected, (2) slightly saline groundwater will be expected from 0 to 185 feet below the Permian top, (3) moderately saline groundwater will be expected from 185 to 385 feet

below the Permian top, and (4) very saline groundwater will be expected at depths greater than 385 feet below the Permian top (Figure 12.1.5-2).

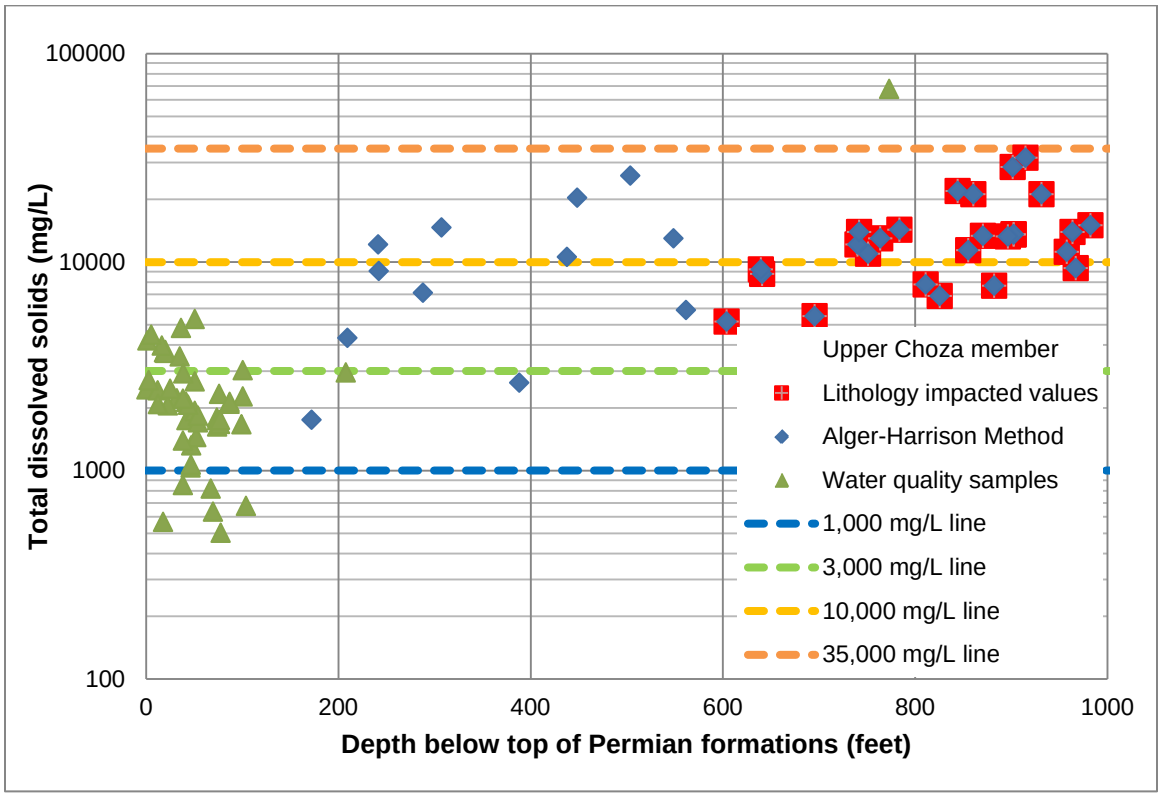

Figure 12.1.5-1. Upper Choza member salinity plot. Depth is feet below top of Permian formations. mg/L = milligrams per liter.

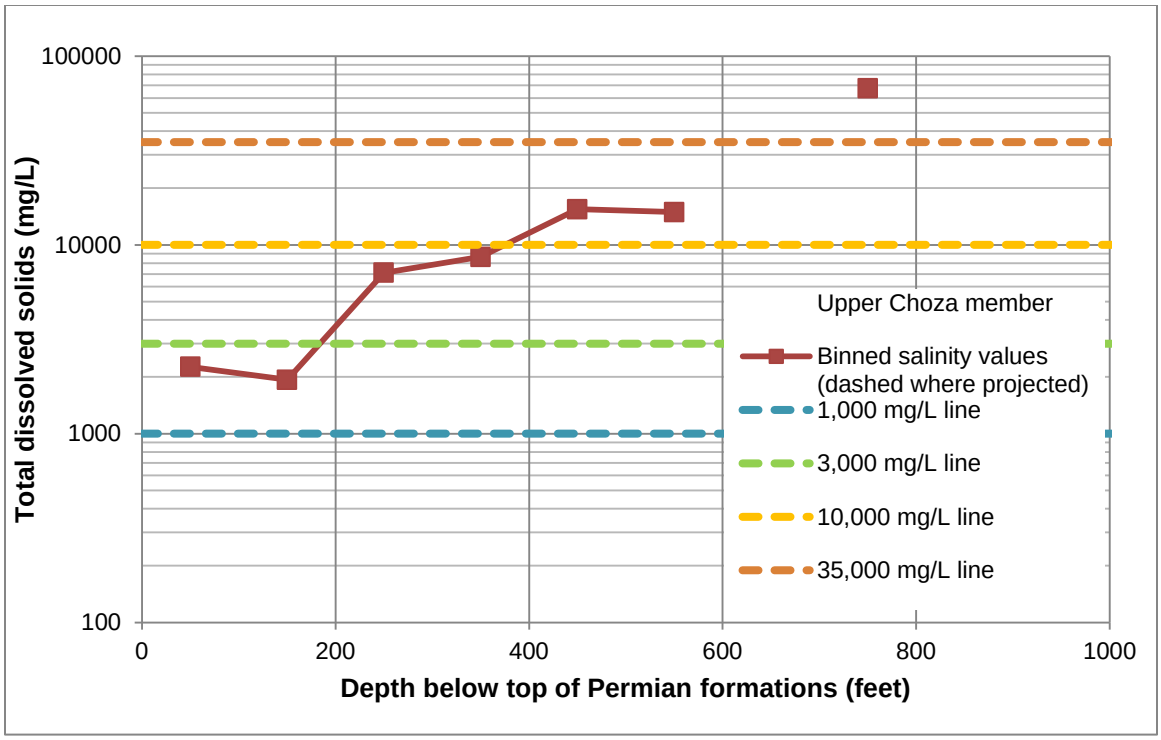

Figure 12.1.5-2. Upper Choza member binned salinity plot. mg/L = milligrams per liter.

12.1.6 Tubb member salinity

We plotted total dissolved solids concentration versus depth below the top of Permian formations for the Tubb member without binning (Figure 12.1.6-1) and with binning (Figure 12.1.6-2). Each plot shows the total dissolved solids concentration lines that separate the defined salinity zones. The water quality samples for the Tubb member came from 11 wells with all reporting more than 1,000 milligrams per liter of total dissolved solids. Calculated total dissolved solids concentrations that were determined to be significantly impacted by the lithologic characteristics of the unweathered portions of the Permian formations are highlighted in red and were not used in the binning process.

The trend of the depth below the top of Permian formations line in Figure 12.1.6-2 shows salinity rapidly increasing with depth in the first 300 feet below the top of the Permian formations before the trend begins to flatten. This indicates that the impact of meteoric recharge diminishes with depth.

We determined that within the Tubb member (1) no fresh water should be expected, (2) slightly saline groundwater will be expected from 0 to 150 feet below the Permian top, (3) moderately saline groundwater will be expected from 150 to 425 feet below the Permian top, and (4) very saline groundwater will be expected at depths greater than 425 feet below the Permian top (Figure 12.1.6-2).

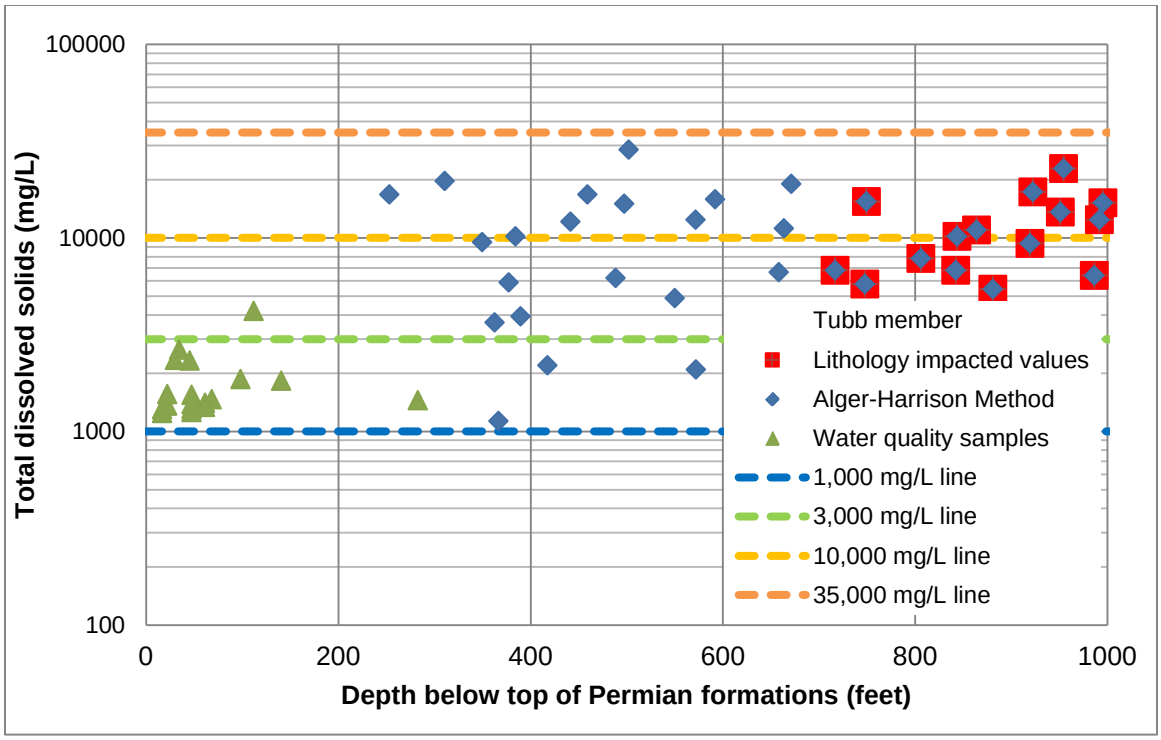

Figure 12.1.6-1. Tubb member salinity plot. Depth is feet below top of Permian formations. mg/L = milligrams per liter.

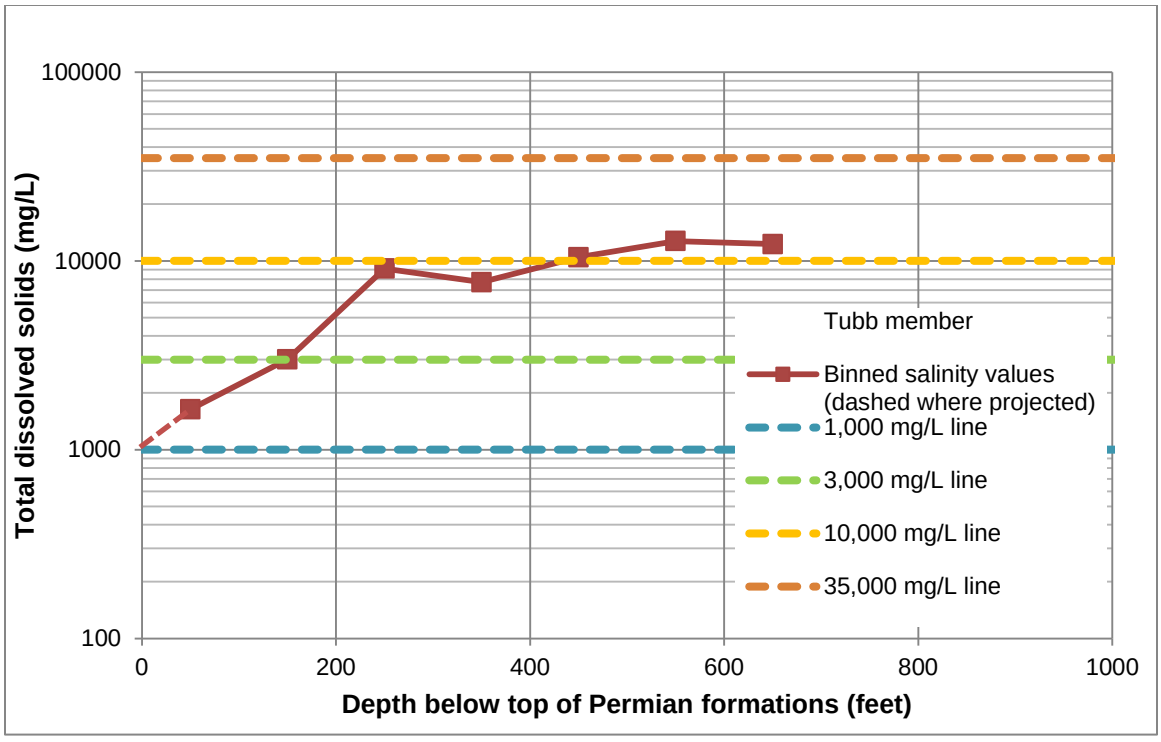

Figure 12.1.6-2. Tubb member binned salinity plot. mg/L = milligrams per liter.

12.1.7 Bullwagon Dolomite salinity

We plotted total dissolved solids concentration versus depth below the top of Permian formations for the Bullwagon Dolomite without binning (Figure 12.1.7-1) and with binning (Figure 12.1.7-2). Each plot shows the total dissolved solids concentration lines that separate the defined salinity zones. The water quality samples for the Bullwagon Dolomite came from four wells with two reporting less than 1,000 milligrams per liter of total dissolved solids. One of the water quality samples reporting fresh water is from a well completed in both the Bullwagon Dolomite and the Quaternary and Neogene sediments. The second well (state well number 43-31-203) that reported less than 1,000 milligrams per liter of total dissolved solids has been sampled 12 times between 1948 and 1982 and since 1971 all samples have recorded total dissolved solids concentrations greater than 1,000 milligrams per liter. Calculated total dissolved solids concentrations that were determined to be significantly impacted by the lithologic characteristics of the unweathered portions of the Permian formations are highlighted in red and were not used in the binning process.

The trend of the depth below the top of Permian formations line in Figure 12.1.7-2 shows salinity rapidly increasing with depth in the first 400 feet below the top of the Permian formations before the trend begins to flatten. This indicates that the impact of meteoric recharge diminishes with depth.

We determined that for water produced exclusively from the Bullwagon Dolomite (1) no fresh water should be expected, (2) slightly saline groundwater will be expected from 0 to 115 feet below the Permian top, (3) moderately saline groundwater will be expected from 115 to 290 feet below the Permian top, and (4) very saline groundwater will be expected at depths greater than 290 feet below the Permian top (Figure 12.1.7-2).

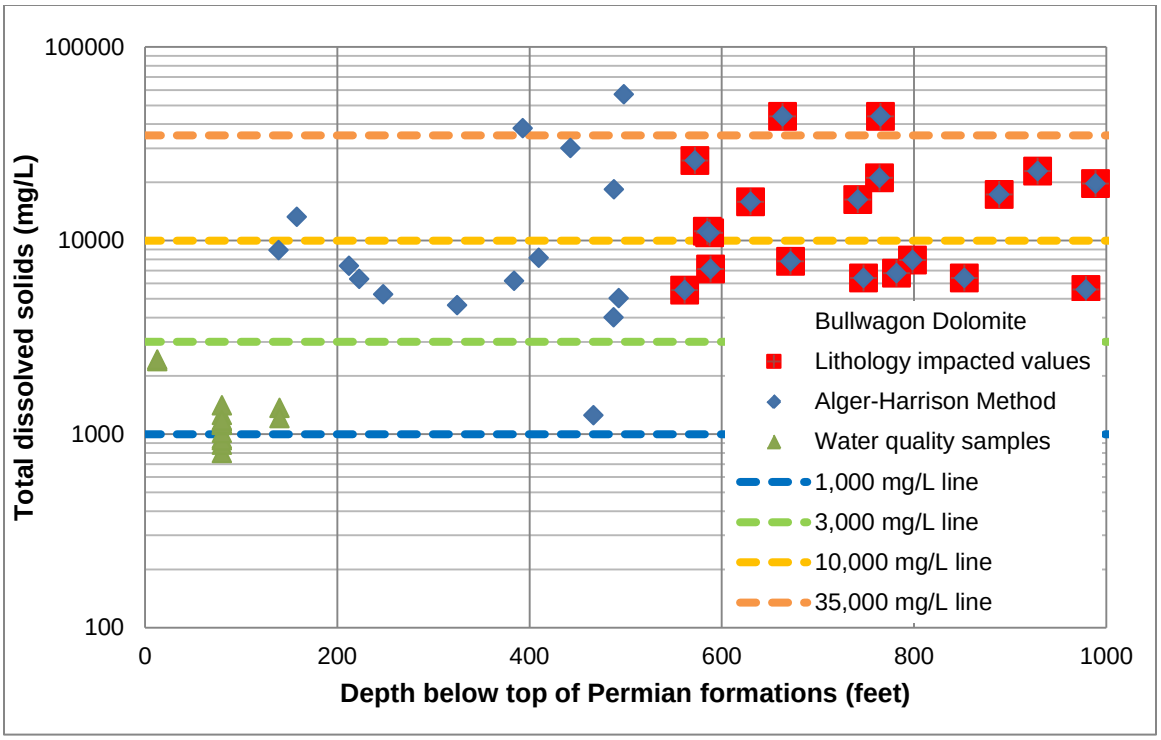

Figure 12.1.7-1. Bullwagon Dolomite salinity plot. Depth is feet below top of Permian formations. mg/L = milligrams per liter.

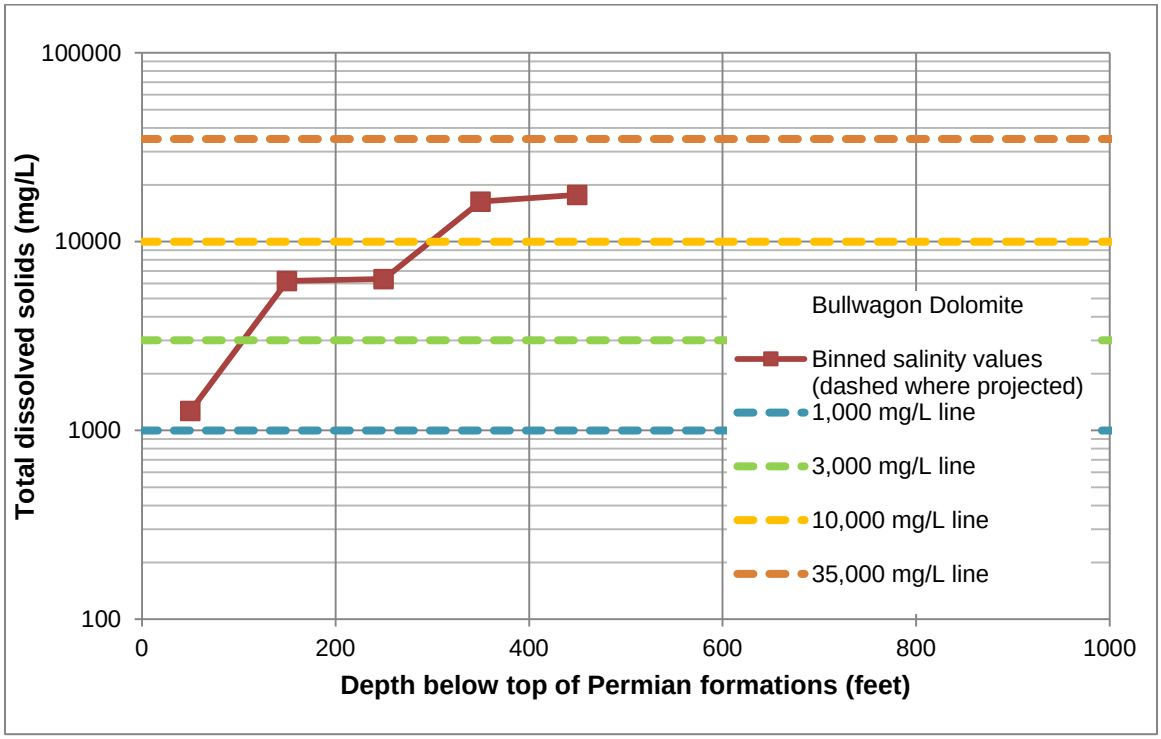

Figure 12.1.7-2. Bullwagon Dolomite binned salinity plot. mg/L = milligrams per liter.

12.1.8 Arroyo Formation salinity

We plotted total dissolved solids concentration versus depth below the top of Permian formations for the Arroyo Formation without binning (Figure 12.1.8-1) and with binning (Figure 12.1.8-2). Each plot shows the total dissolved solids concentration lines that separate the defined salinity zones. The water quality samples for the Arroyo Formation came from 11 wells with 3 reporting less than 1,000 milligrams per liter of total dissolved solids. The water quality sample reporting fresh groundwater is from a well completed in both the Arroyo Formation and the Quaternary and Neogene sediments. Calculated total dissolved solids concentrations that were determined to be significantly impacted by the lithologic characteristics of the unweathered portions of the Permian formations are highlighted in red and were not used in the binning process.

The trend of the depth below the top of Permian formations line in Figure 12.1.8-2 shows salinity rapidly increasing with depth in the first 500 feet below the top of the Permian formations before the trend begins to flatten. This indicates that the impact of meteoric recharge diminishes with depth.

We determined that for water produced exclusively from the Arroyo Formation (1) no fresh water should be expected, (2) slightly saline groundwater will be expected from 0 to 80 feet below the Permian top, (3) moderately saline groundwater will be expected from 80 to 260 feet below the Permian top, and (4) very saline groundwater will be expected at depths greater than 260 feet below the Permian top (Figure 12.1.8-2).

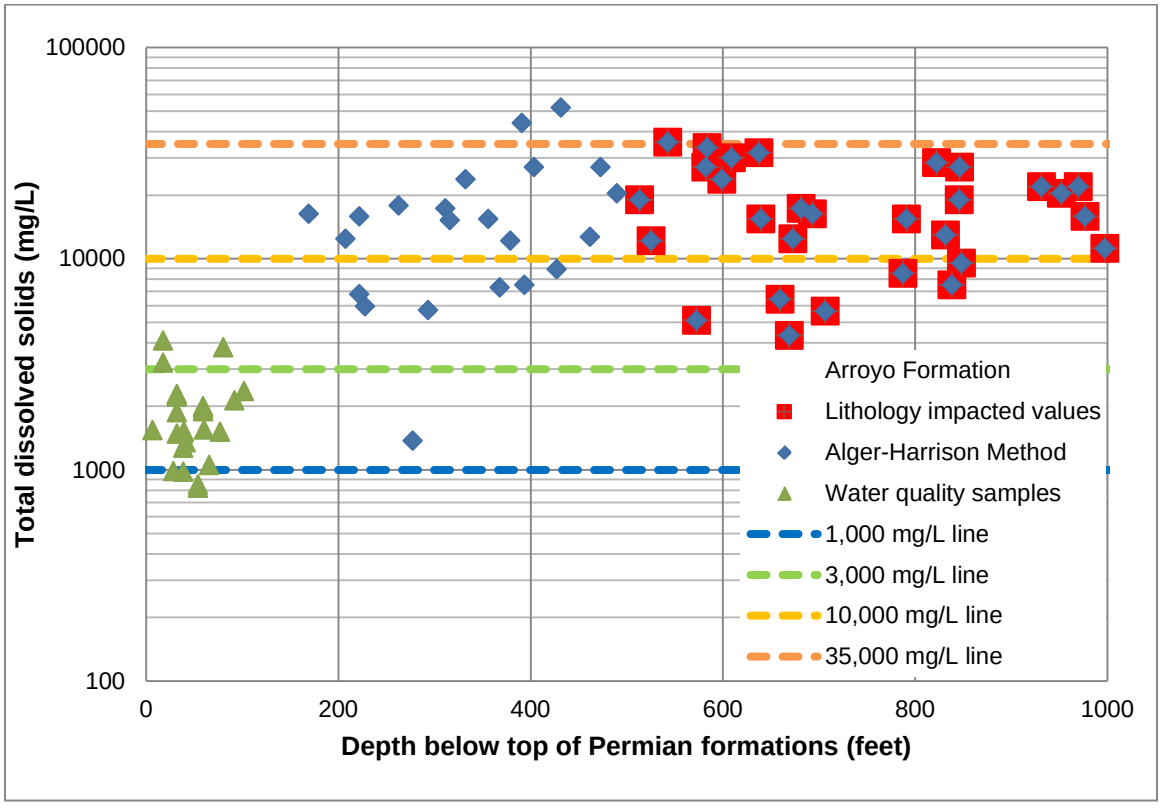

Figure 12.1.8-1. Arroyo Formation salinity plot. Depth is feet below top of Permian formations. mg/L = milligrams per liter.

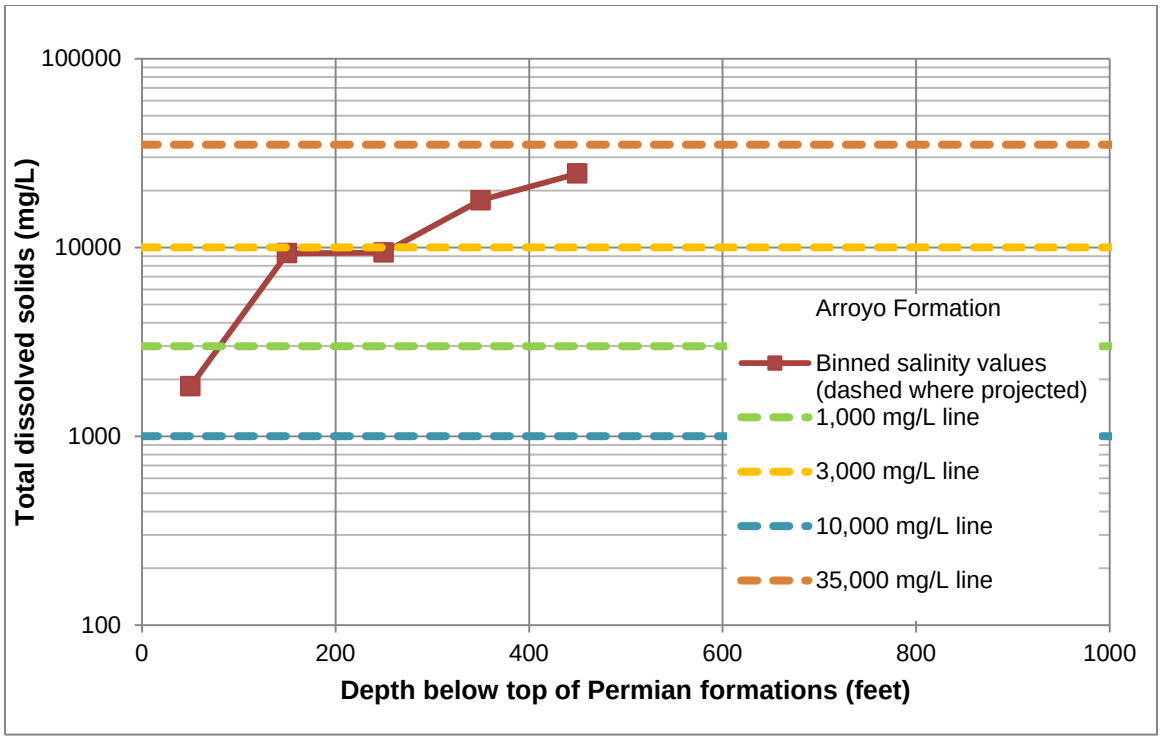

Figure 12.1.8-2. Arroyo Formation binned salinity plot. mg/L = milligrams per liter.

12.1.9 Lueders Formation salinity

We plotted total dissolved solids concentration versus depth below the top of Permian formations for the Lueders Formation without binning (Figure 12.1.9-1) and with binning (Figure 12.1.9-2). Each plot shows the total dissolved solids concentration lines that separate the defined salinity zones. The water quality samples for the Lueders Formation came from three wells and all reported more than 1,000 milligrams per liter of total dissolved solids. Calculated total dissolved solids concentrations that were determined to be significantly impacted by the lithologic characteristics of the unweathered portions of the Permian formations are highlighted in red and were not used in the binning process.

The trend of the depth below the top of Permian formations line in Figure 12.1.9-2 shows salinity rapidly increasing with depth in the first 300 feet below the top of the Permian formations before the trend begins to flatten. This indicates that the impact of meteoric recharge diminishes with depth.

We determined that within the Lueders Formation (1) no fresh water should be expected, (2) slightly saline groundwater will be expected from 0 to 40 feet below the Permian top, (3) moderately saline groundwater will be expected from 40 to 225 feet below the Permian top, and (4) very saline groundwater will be expected at depths greater than 225 feet below the Permian top (Figure 12.1.9-2).

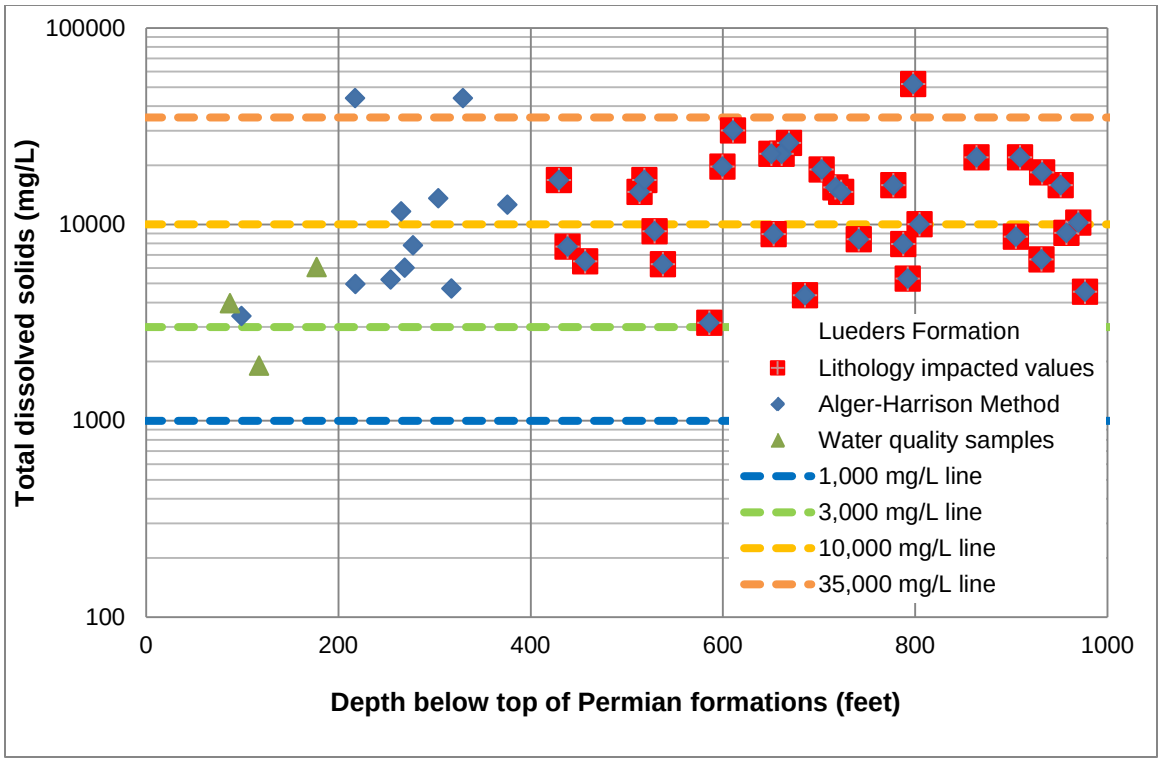

Figure 12.1.9-1. Lueders Formation salinity plot. Depth is feet below top of Permian formations. mg/L = milligrams per liter.

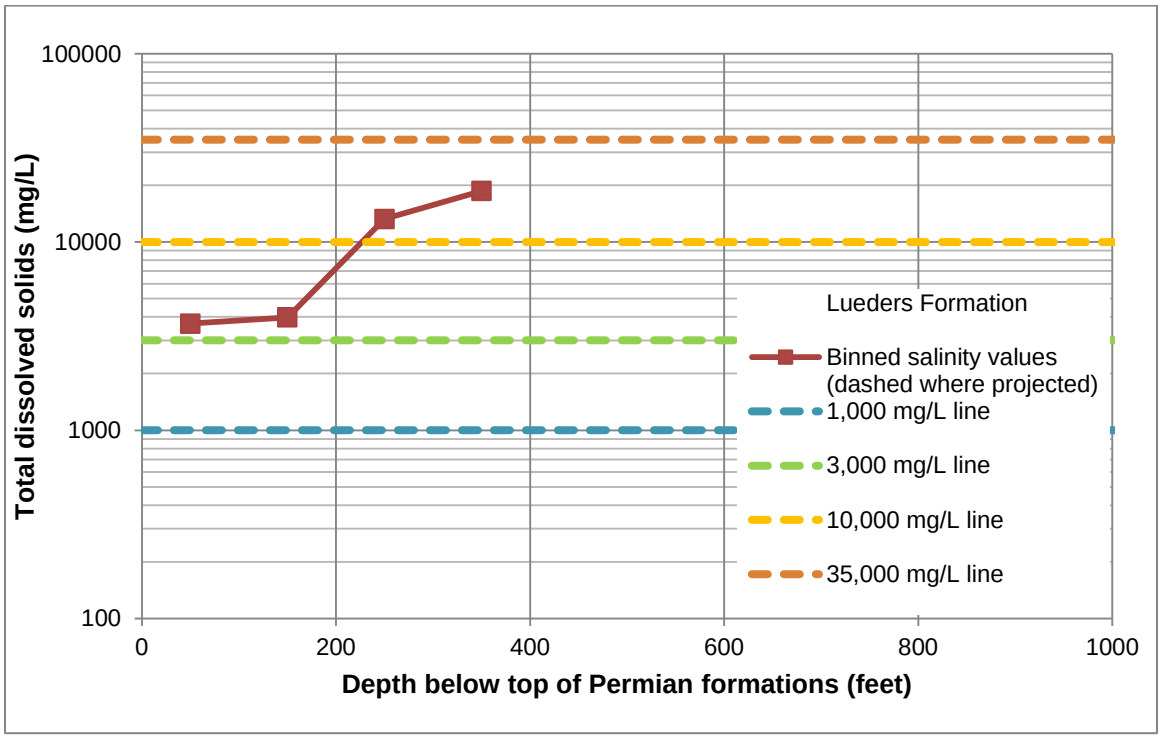

Figure 12.1.9-2. Lueders Formation binned salinity plot. mg/L = milligrams per liter.

12.2 Salinity zone surfaces

We analyzed each of the salinity versus depth plots to determine the depth that the trend lines intersect the 3,000 and the 10,000 milligrams per liter total dissolved solids concentration lines. The trend lines were projected (1) if a bin had no values and (2) to the zero depth line. A summary of the depths of the intersections between the defined salinity lines and the trend lines has been tabulated (Table 12.2-1). These results show the wide variation between the different geological formations with regards to the depths at which fresh, slightly saline, moderately saline, and very saline groundwater can be expected. We were not able to clearly define the depth at which brine would be expected in the Permian formations but generally expect a brine interface between 500 and 1,000 feet below the Permian top depending upon the geological formation.

Table 12.2-1. **Salinity versus depth curves by geological formation. mg/L = milligrams per liter.**

	Depth below top of Permian (feet)	
Geological formation	**3,000 mg/L**	**10,000 mg/L**
Yates Formation	110	215
Seven Rivers Formation	60	315
Queen Formation	0	390
San Angelo Formation	205	445
Upper Choza member	185	385
Tubb member	150	425
Bullwagon Dolomite	115	290
Arroyo Formation	80	260
Lueders Formation	40	225
Average	**105**	**328**

Based upon our understanding of the geology and groundwater salinities for the Lipan Aquifer, we prepared surfaces that define the depth below ground surface where one is likely to encounter each range of total dissolved solids. These surfaces are presented in both depth below the ground surface and in elevation above mean sea level.

Fresh groundwater (0 to 999 milligrams per liter total dissolved solids) is generally limited to the Quaternary and Neogene sediments within the study area. Fresh groundwater is also found in the surrounding Cretaceous formations but those aquifers are not part of this study.

Figure 12.2-1 and Figure 12.2-2 show the top of the slightly saline groundwater zone (1,000 to 2,999 milligrams per liter total dissolved solids) in terms of the elevation relative to mean sea level and depth below ground surface. This surface was defined by (1) the base of the Trinity Group, (2) the base of the Cretaceous and Neogene sediments, or (3) the ground surface. Slightly saline waters are likely to be encountered where the Permian formations outcrop at the ground surface.

Figure 12.2-3 and Figure 12.2-4 show the top of the moderately saline groundwater zone (3,000 to 9,999 milligrams per liter total dissolved solids) in terms of the elevation relative to mean sea level and depth below ground surface. This surface is 105 feet below the top of the slightly saline surface based on the average depth below the slightly saline surface that moderately saline groundwater is likely to be encountered.

Figure 12.2-5 and Figure 12.2-6 show the top of the very saline groundwater zone (10,000 to 34,999 milligrams per liter total dissolved solids) in terms of the elevation relative to mean sea level and depth below ground surface. This surface is 225 feet below the top of the moderately saline surface based on the average depth below the moderately saline surface that very saline groundwater is likely to be encountered.

We did not create a surface for the top of the brine groundwater zone (greater than 35,000 milligrams per liter total dissolved solids) because of the lack of sufficient data points from either water quality samples or geophysical well log calculations. LBG-Guyton Associates (2008) did obtain a water sample from the Upper Choza member at a depth of 903 feet below ground surface with total dissolved solids measured at 65,800 milligrams per liter. It will require additional groundwater sampling from known depths in wells that are deeper than conventional water wells to more accurately delineate the brine surface.

.

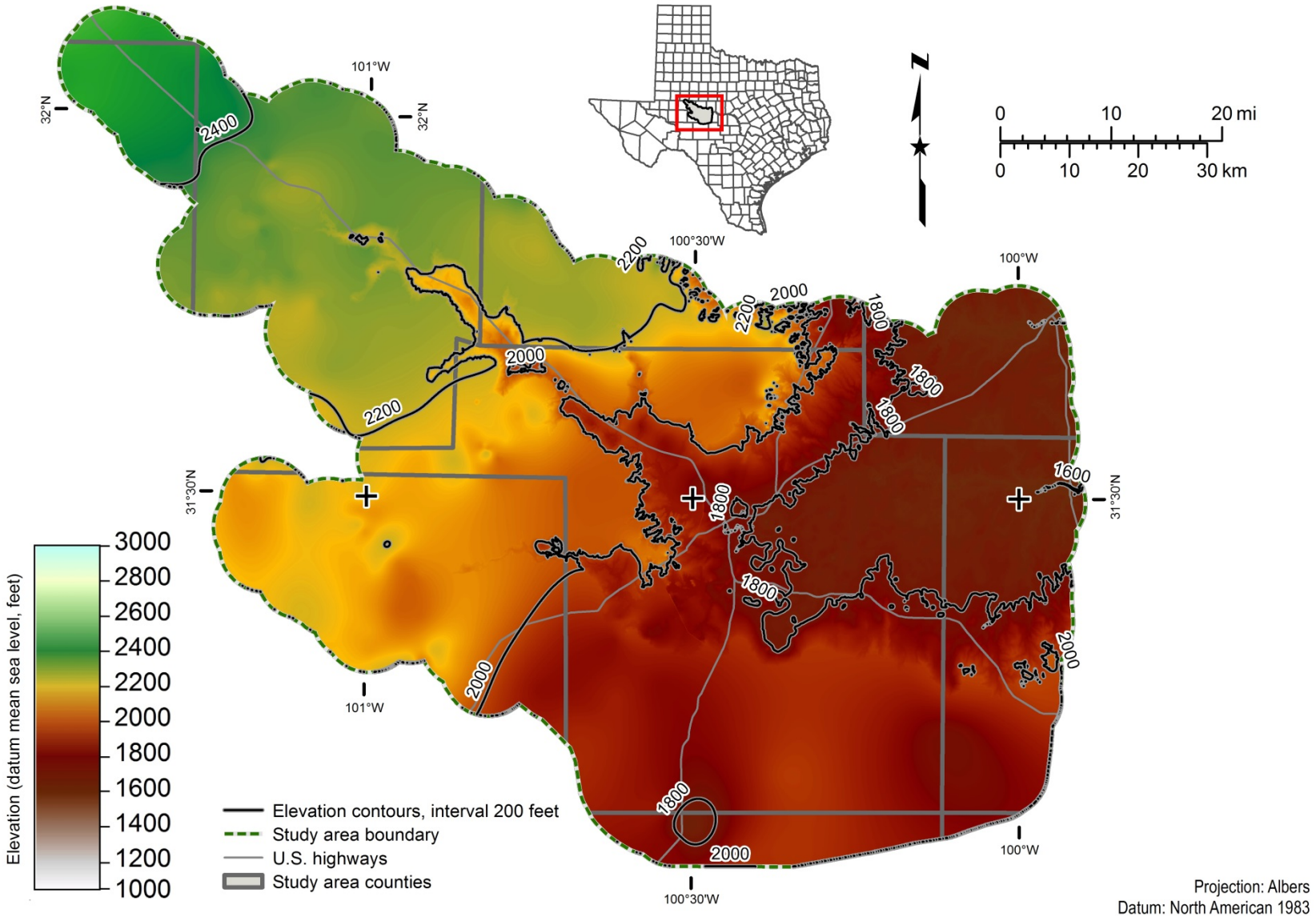

Figure 12.2-1. Top elevation of the slightly saline groundwater zone in feet above mean sea level. Slightly saline groundwater has a total dissolved solids concentration between 1,000 and 2,999 milligrams per liter.

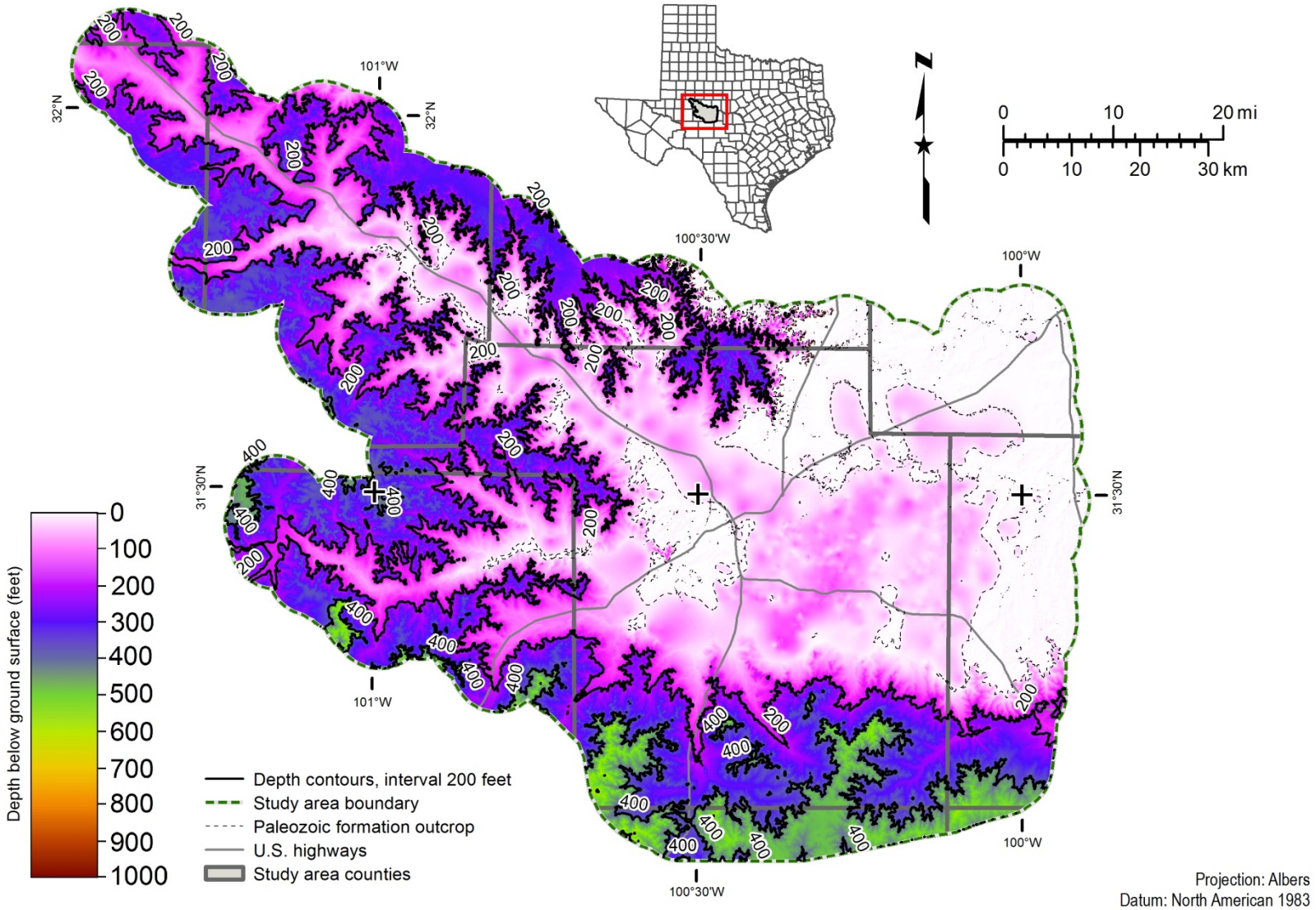

Figure 12.2-2. Depth to top of the slightly saline groundwater zone in feet below ground surface. Slightly saline groundwater has a total dissolved solids concentration between 1,000 and 2,999 milligrams per liter. Dotted line on map represents where Permian formations outcrop at or near the ground surface.

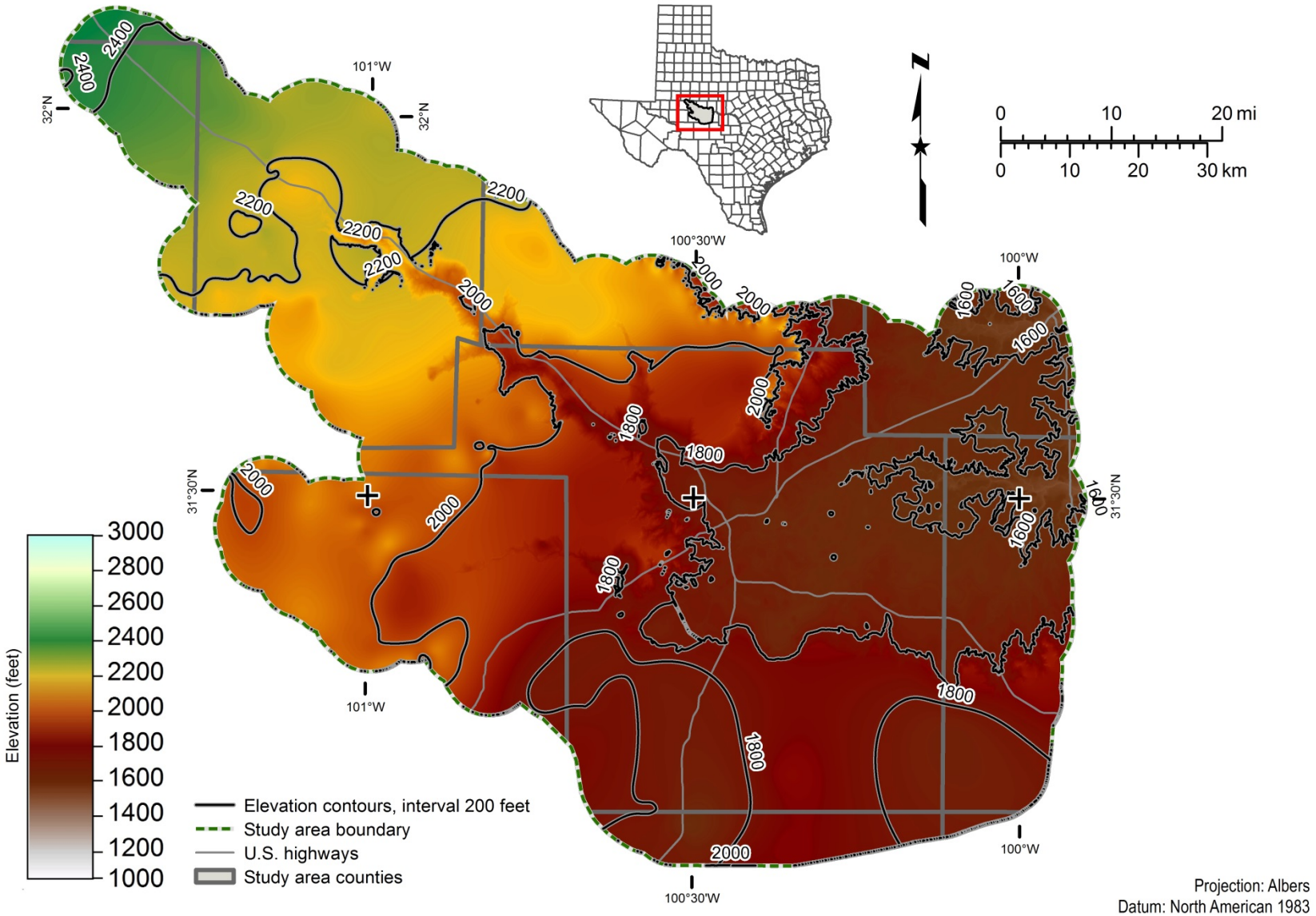

Figure 12.2-3. Top elevation of the moderately saline groundwater zone in feet above mean sea level. Moderately saline groundwater has a total dissolved solids concentration between 3,000 and 9,999 milligrams per liter.

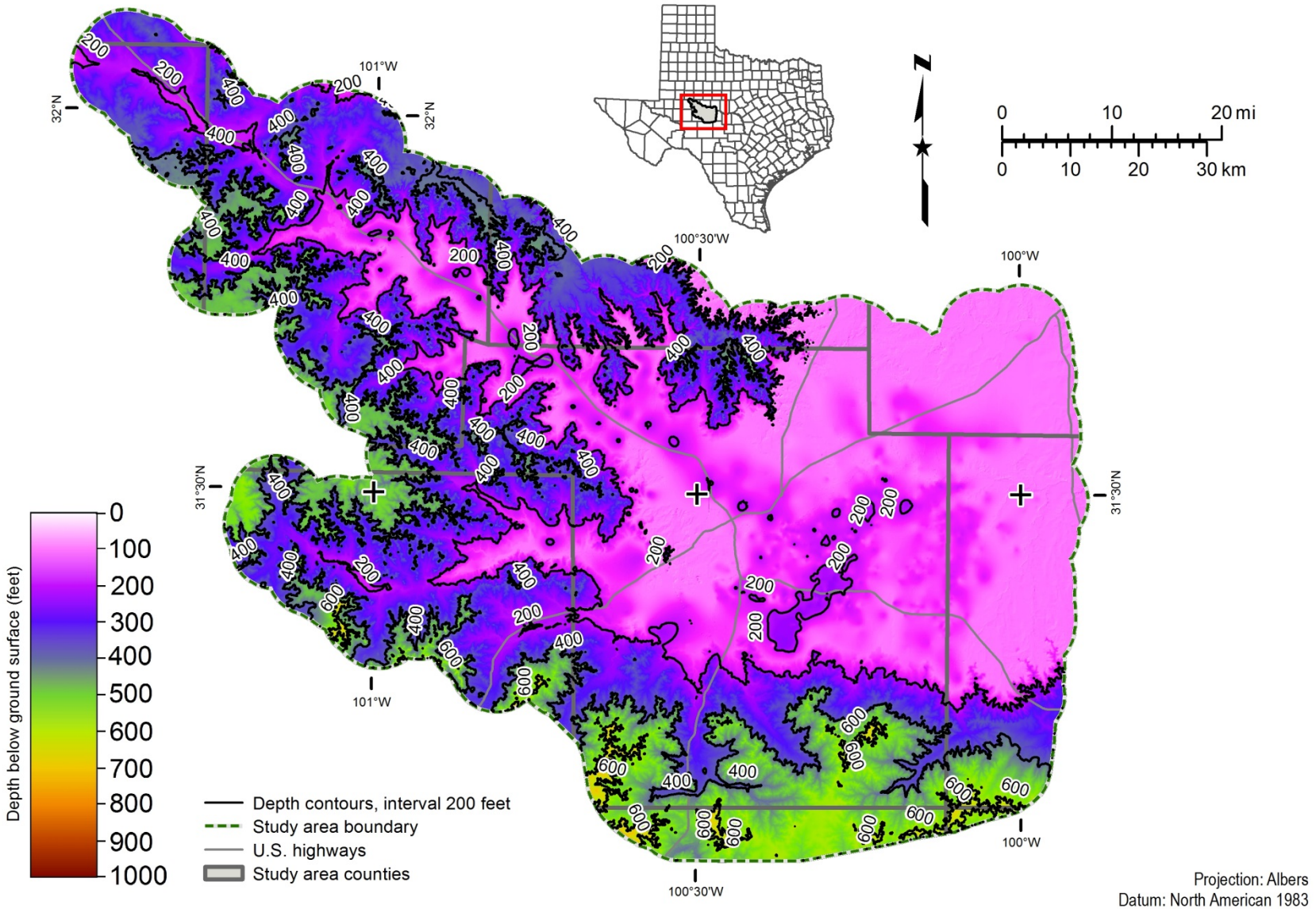

Figure 12.2-4. Depth to top of the moderately saline groundwater zone in feet below ground surface. Moderately saline groundwater has a total dissolved solids concentration between 3,000 and 9,999 milligrams per liter.

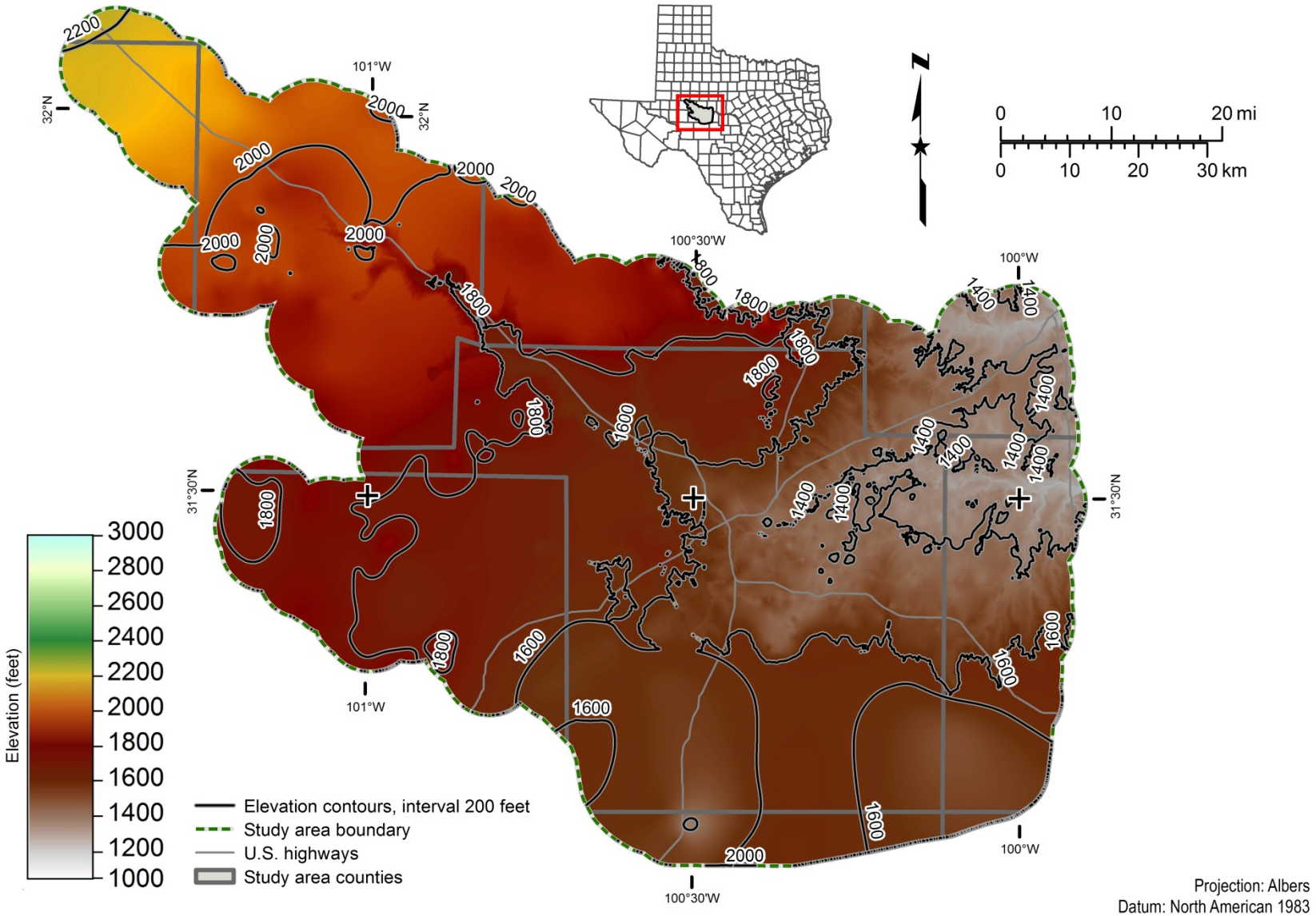

Figure 12.2-5. Top elevation of the very saline groundwater zone in feet above mean sea level. Very saline groundwater has a total dissolved solids concentration between 10,000 and 34,999 milligrams per liter.

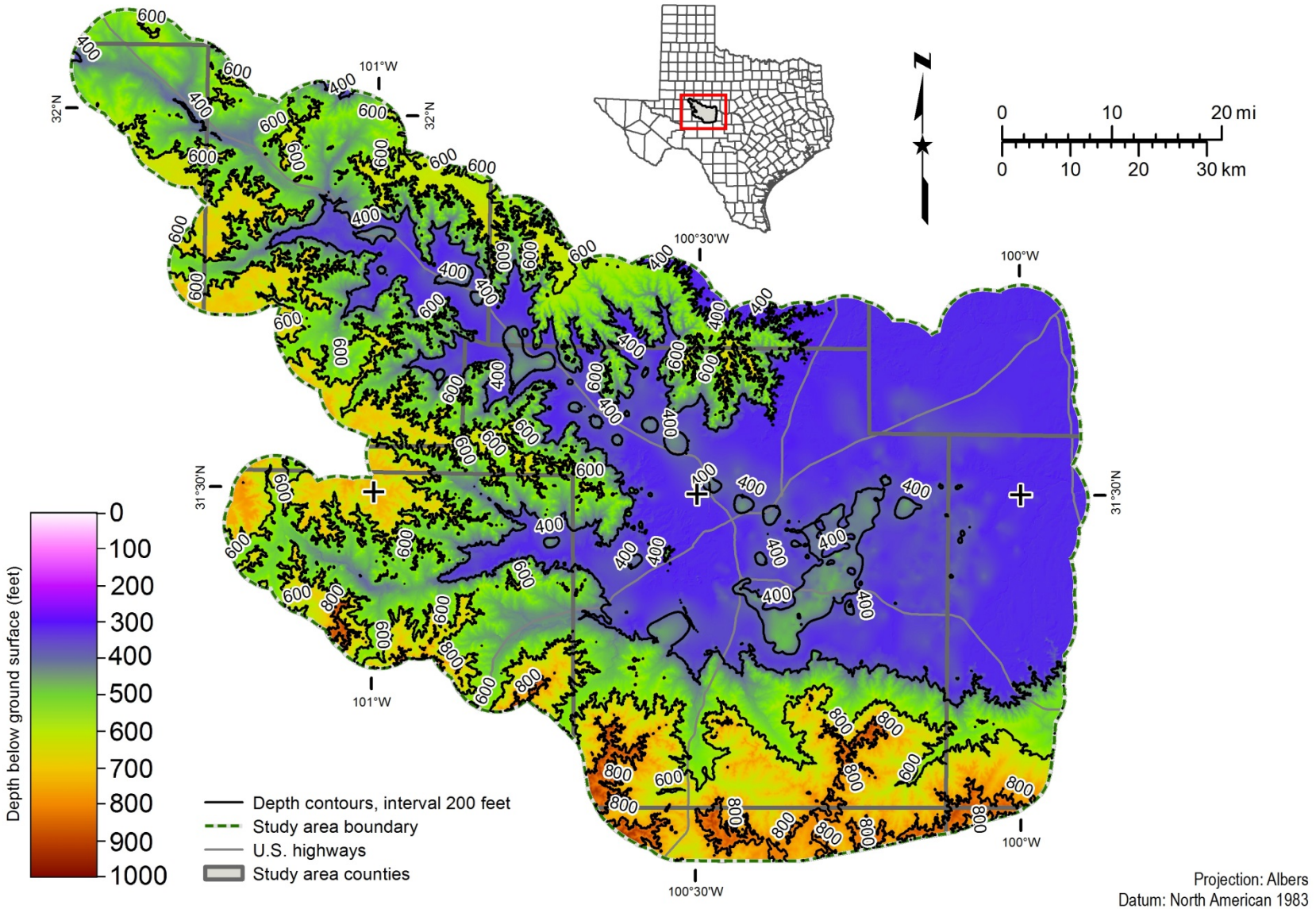

Figure 12.2-6. Depth to top of the very saline groundwater zone in feet below ground surface. Very saline groundwater has a total dissolved solids concentration between 10,000 and 34,999 milligrams per liter.

13. Groundwater volume methodology

We calculated the gross volume of rock available for each salinity zone in each of the geological formations. We further calculated the volume of rock below the static water level for each geological formation in order to identify the saturated portion.

Specific yield is the ratio of the volume of water that will drain by force of gravity from a saturated material to the total volume of that material and is used to determine the amount of groundwater within a bulk volume of the aquifer formations. We lacked sufficient data on the hydrologic properties of the geological formations in the study area to calculate values for specific yield and instead utilized the specific yield values used in previous studies (Beach and others, 2004; LBG-Guyton Associates, 2003). A specific yield value of 0.05 was assigned to the Quaternary and Neogene sediments and the slightly saline groundwater zone. A specific yield value of 0.005 was assigned to the moderately saline groundwater zone, which reflects the expected decrease in porosity and permeability for relatively unweathered Permian units. This lower specific yield value represents very localized fracture porosity and is highly variable across the study area.

13.1 Static water levels and saturated thickness

We developed a static water level grid map from water wells completed in the Lipan Aquifer. The map was created for the purpose of generating the Lipan Aquifer saturated thickness map and to estimate brackish groundwater volumes. A significant challenge in creating the static water level map was that measurements have been recorded over a period of more than 80 years in the study area. The TWDB Groundwater Database currently has 23,134 static water level measurements from 2,053 wells completed in the study area. We decided to utilize only those water level measurements taken since January 1, 2001, in wells that were not completed in the Cretaceous formations. The resulting dataset contained 167 wells and a total of 14,755 recorded water level measurements. A summary of this data (Figure 13.1-1) averages all water level measurements on a monthly basis.

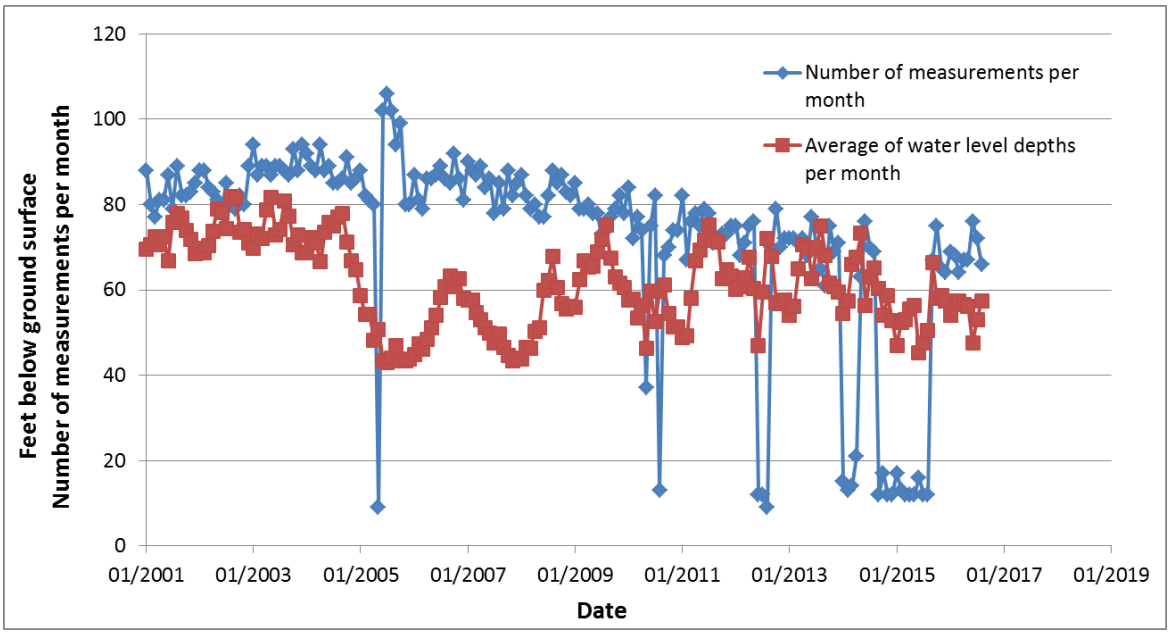

Figure 13.1-1. Static water level measurements 2001–2016.

A typical static water level map is created using data from one winter season, producing a water level surface that reflects minimum influence from seasonal irrigation pumping. Although the database contains 14,755 water level records from 167 wells, the number of winter-season water levels from wells completed in the study area is typically less than 80 measurements in any given season during the last 15 years. The wells are clustered in small areas and created significant problems for developing a study area map.

We decided to average all well measurements during the 2001 to 2016 time period to create one average static water level value per well. The final dataset contains 167 water wells completed in either the Quaternary and Neogene or Permian aquifers. The spatial distribution of the data was sufficient to create a study area static water level surface. The well points were extracted from Microsoft® Access® and imported into ArcGIS® and georeferenced. The points were interpolated using the ArcGIS® Spatial Analyst® Topo to Raster tool. The resulting grid map (Figure 13.1-2) was compared with input points to verify accuracy. Some areas have fewer data points, resulting in a rough approximation of the static water table surface. A major pumping center is clearly visible in the south-central portion of Tom Green County.

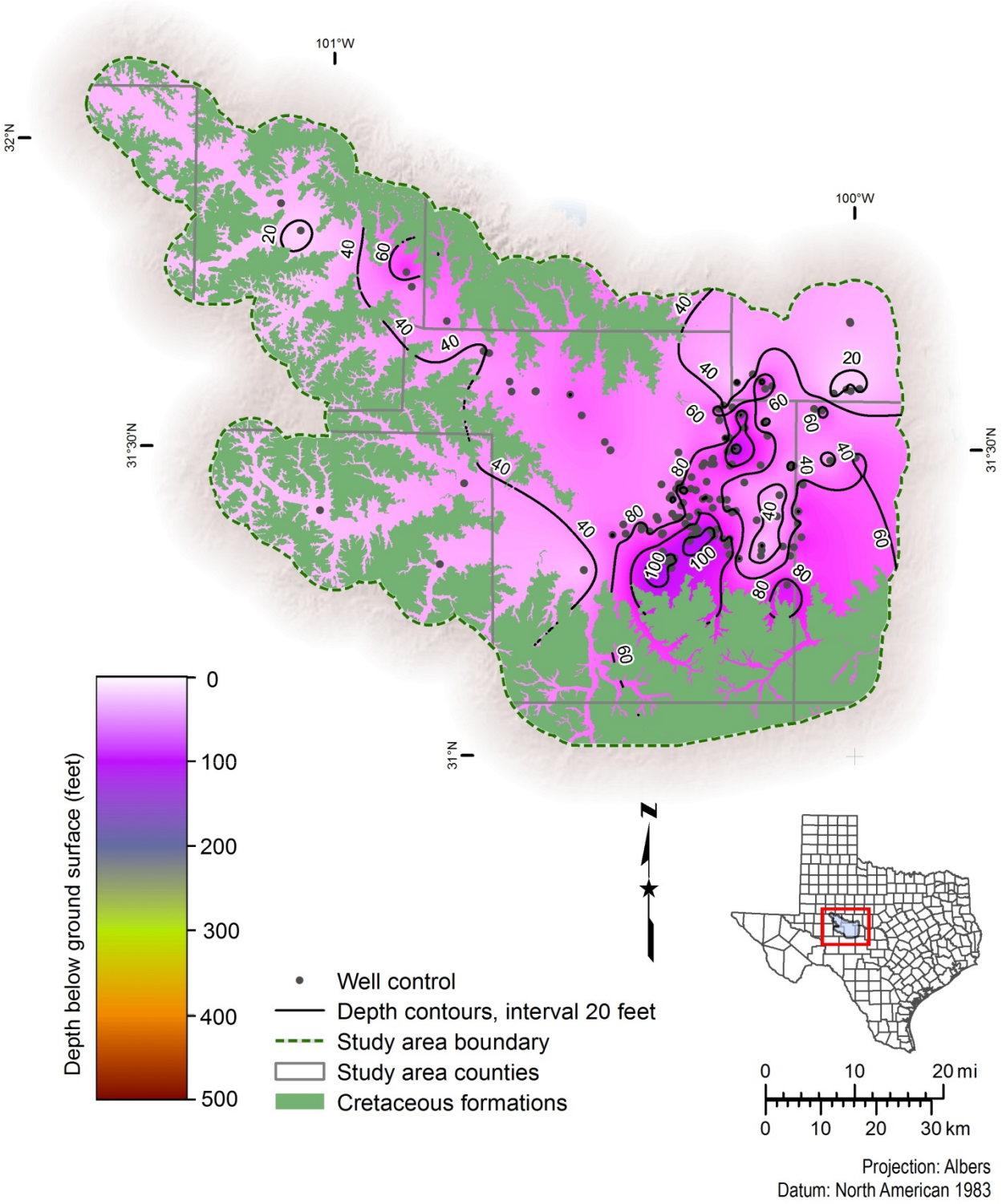

Figure 13.1-2. **Static water level surface and well control in the Lipan Aquifer study area. Green areas are where the Cretaceous formations outcrop. The dataset used for this map was created for the calculation of brackish groundwater volume. Static water level measurements compiled from records 2001 through 2016.**

13.2 Bulk volume calculation

A schematic representation of the geologic model used to calculate groundwater volumes is shown in Figure 13.2-1. The static water level surface represents the average depth to the top of the saturated zone in the study area. The fresh groundwater (0 to 999 milligrams per liter of total dissolved solids) exists principally in the Quaternary and Neogene sediments below the static water level surface. The slightly saline groundwater zone (1,000 to 2,999 milligrams per liter of total dissolved solids) exists in the saturated, highly-weathered Permian formations and is approximately 105 feet thick. The moderately saline groundwater zone (3,000 to 9,999 milligrams per liter of total dissolved solids) exists in the saturated, moderately-weathered Permian formations and is approximately 223 feet thick.

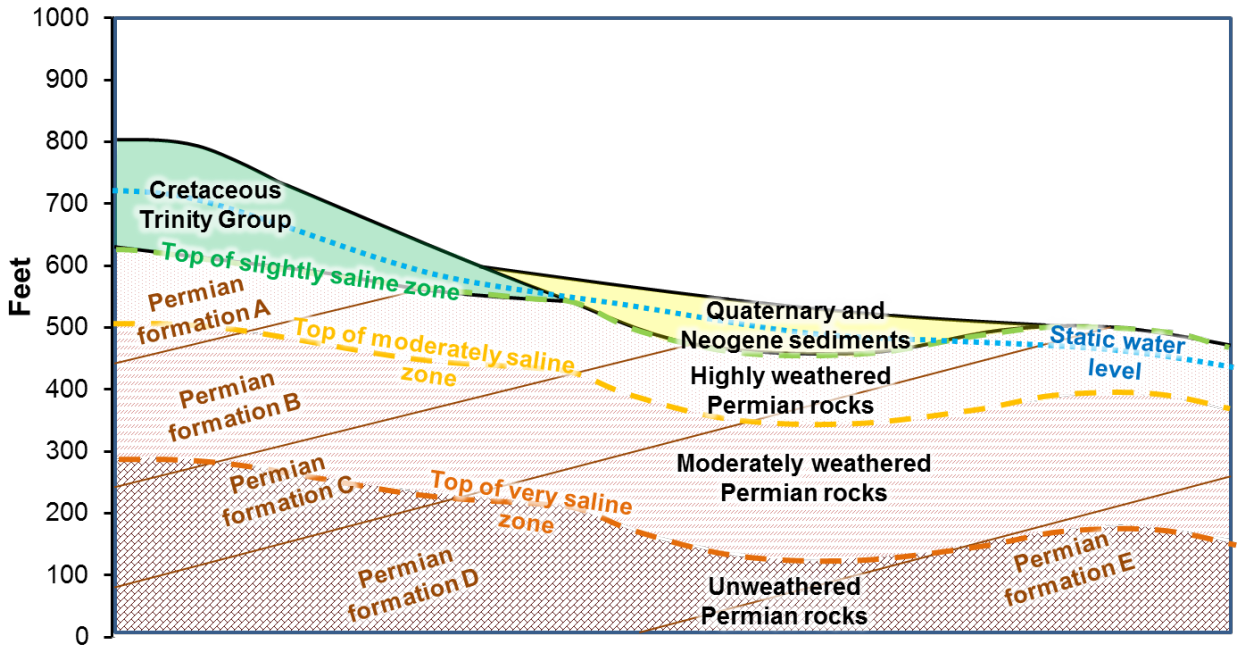

Figure 13.2-1. Schematic representation of brackish groundwater salinity zones.

We did not quantify the volume of the very saline water zone (total dissolved solids between 10,000 and 34,999 milligrams per liter) because there was a lack of sufficient data capable of clearly defining the bottom of the zone. There was only one water sample that had a total dissolved solids measurement greater than 35,000 milligrams per liter (BRACS well identification number 51449, total dissolved solids concentration of 65,800 milligrams per liter at a depth of 903 feet below ground surface).

We calculated the saturated bulk material volume for each of the 10 potential water-bearing stratigraphic intervals within the defined salinity zones in the study area using the Cut and Fill tool in ArcGIS® Spatial Analyst®. This process required up to four separate calculations for each geological formation: (1) volume of fresh zone, (2) volume of slightly saline zone, (3) volume of moderately saline zone, and (4) volume of the unsaturated zone. We imported the data table from each Cut and Fill grid file into Microsoft® Excel® and summed the volume of each individual polygon record to calculate the total volume for a geological formation. The results of these

calculations represent the total potential aquifer volume within the study area for each geological formation (Table 13.2-1).

Table 13.2-1. **Total saturated bulk material volumes calculated for each potential water-bearing geological formation for defined salinity zones.**

Geological formation	Saturated bulk material volume (million cubic feet)		
	Fresh	Slightly saline	Moderately saline
Lueders Formation	0	944,447	4,073,862
Arroyo Formation	0	449,598	1,962,219
Bullwagon Dolomite	0	208,596	440,634
Tubb member	0	527,067	1,391,130
Upper Choza member	0	427,797	1,341,568
San Angelo Formation	0	157,029	833,100
Queen Formation	0	122,300	727,997
Seven Rivers Formation	0	678,368	2,192,383
Yates Formation	0	354,141	1,026,302
Quaternary and Neogene sediments	149,591	0	0

13.3 Groundwater volume calculation

We believe that both the Quaternary and Neogene sediments and the underlying weathered Permian formations that make up the Lipan Aquifer are in hydrologic communication even where the Permian formations are covered by Cretaceous formations. This assumption is supported by Beach and others (2004), who believe that cross-formational flow occurs between the Cretaceous formations and the underlying aquifers. When combined with the understanding that the weathering of the Permian formations has developed pathways for water to move vertically, it allows us to utilize a common static water level surface throughout the Lipan Aquifer system for purposes of volume calculations.

We used specific yield values from previous studies (Beach and others, 2004; LBG-Guyton Associates, 2003) in conjunction with the volumes listed in Table 13.2-1 to calculate groundwater volumes for each salinity zone in each of the geological formations. For the fresh and slightly saline zones, a specific yield value of 0.05 was used because of the relatively high percentage of silt, clay, and carbonate cement found in these intervals. For the moderately saline zone, a specific yield value of 0.005 was used. This lower specific yield value represents very localized fracture porosity and is highly variable across the study area. The resulting groundwater volumes (Table 13.3-1) are the estimated total available groundwater volume within each salinity zone in each geological formation.

Table 13.3-1. Total available groundwater volume subdivided by salinity zones in each geological formation.

Geological formation	Available groundwater volume (acre-feet)		
	Fresh	**Slightly saline**	**Moderately saline**
Lueders Formation	0	1,084,079	467,616
Arroyo Formation	0	516,069	225,232
Bullwagon Dolomite	0	239,435	50,578
Tubb member	0	604,992	159,680
Upper Choza member	0	491,044	153,991
San Angelo Formation	0	180,245	95,627
Queen Formation	0	140,381	83,563
Seven Rivers Formation	0	778,661	251,652
Yates Formation	0	406,499	117,804
Quaternary and Neogene sediments	171,707	0	0
Total volume	**171,707**	**4,441,405**	**1,605,743**

We estimate that the total volume of fresh groundwater in the study area is 0.17 million acre-feet and is limited to the Quaternary and Neogene sediments. We estimate that the total volume of brackish groundwater (1,000 to 9,999 milligrams per liter of total dissolved solids) is 6.05 million acre-feet and is limited to the slightly to moderately weathered Permian formations at depths less than 328 feet below the top of the Permian.

Jones and others (2013) calculated the total estimated recoverable storage of groundwater in the Lipan Aquifer to be 4.2 million acre-feet. Their model is based upon a constant aquifer thickness of 400 feet below the ground surface and includes the underlying Dockum Aquifer and the overlying Edwards-Trinity Plateau Aquifer groundwater within the spatial extent of the Lipan Aquifer, so its value for comparison purposes is limited.

LBG-Guyton Associates (2003) calculated the total estimated in place volume of brackish groundwater to be 1.25 million acre-feet plus an additional 2,500 acre-feet of confined availability. They used the pre-2007 geographic extent of the Lipan Aquifer that was limited to the central portions of Tom Green County and small portions of Runnels and Concho counties (TWDB, 2007b). They also used an estimated average aquifer thickness of 75 feet, which is significantly less than the thicknesses of the brackish salinity zones determined by this study.

14. Desalination concentrate disposal

Many desalination plants in Texas discharge concentrate (concentrate from the reverse osmosis process) to a surface water body or evaporation pond in accordance with Texas Commission on Environmental Quality wastewater discharge permits. The recommended groundwater desalination projects for Concho Rural Water Supply Corporation and City of San Angelo propose evaporation ponds and injection wells for concentrate disposal, respectively (Freese and Nichols and LBG-Guyton Associates, 2015).

Class II injection wells dispose produced water, obtained from oil and gas wells, into subsurface zones where groundwater is greater than 10,000 milligrams per liter total dissolved solids (except in very specific circumstances). Railroad Commission of Texas rules further require that freshwater strata be protected from the disposal formation by impervious beds (16 TAC § 3.9). Class II injection wells can be used for disposal of nonhazardous desalination concentrate or nonhazardous drinking water treatment residuals if the following well types and conditions apply (CDM Smith, 2014):

Class II Type 1:	*Disposal injection well into a nonproductive oil and gas zone or interval. The well can be dually permitted as a Class I injection well under the Texas Commission of Environmental Quality General Permit. The well must meet all applicable construction standards of a Class I well under 30 Texas Administrative Code Section 331.62.*
Class II Type 2:	*Injection well into a productive oil and gas zone or interval. The well can be dually permitted as a Class I injection well under the Texas Commission of Environmental Quality General Permit. The well must meet all applicable construction standards of a Class I well under 30 Texas Administrative Code Section 331.62.*
Class II Type 3:	*Enhanced recovery injection well. This type of well can receive a permit amendment under the Railroad Commission of Texas.*

For future desalination plants that may be built in the study area, if disposal of desalination concentrate using a Class II injection well is considered as a potential option, a considerable amount of research must be undertaken to ensure that the well meets construction requirements, appropriate permits are obtained, and a contract with the owner of the injection well can be obtained for the lifetime of the project (Mace and others, 2006; CDM Smith, 2014).

Class II injection well data was obtained from the Underground Injection Control Database of the Railroad Commission of Texas. We mapped the location of Class II injection wells to identify sites where produced water may have been disposed within the study area. A total of 1,383 Class II injection wells were located within the study area. We prepared two maps of Class II injection wells: wells that have not been plugged (Figure 14-1), and wells that have been plugged (Figure 14-2). Well status is summarized in Table 14-1.

Users of this information should conduct a thorough investigation of a well should a Class II well be considered for concentrate disposal or if groundwater development is considered near an existing Class II well. Another option for concentrate disposal is using a Class I injection well permitted under the Texas Commission on Environmental Quality General Permit. The Class I General Permit only applies to wells disposing of nonhazardous desalination concentrate or nonhazardous drinking water treatment residuals.

Table 14-1. Class II injection wells in the Lipan Aquifer study area. Data obtained in 2012 from the Underground Injection Control Database of the Railroad Commission of Texas.

Class II well type	Plugging status	Activity status	Total well count
1	Not plugged	Active	26
1	Not plugged	Not active	9
2	Not plugged	Active	134
2	Not plugged	Not active	17
3	Not plugged	Active	600
3	Not plugged	Not active	115
1	Plugged	Active	35
1	Plugged	Not active	16
2	Plugged	Active	153
2	Plugged	Not active	11
3	Plugged	Active	222
3	Plugged	Not active	45

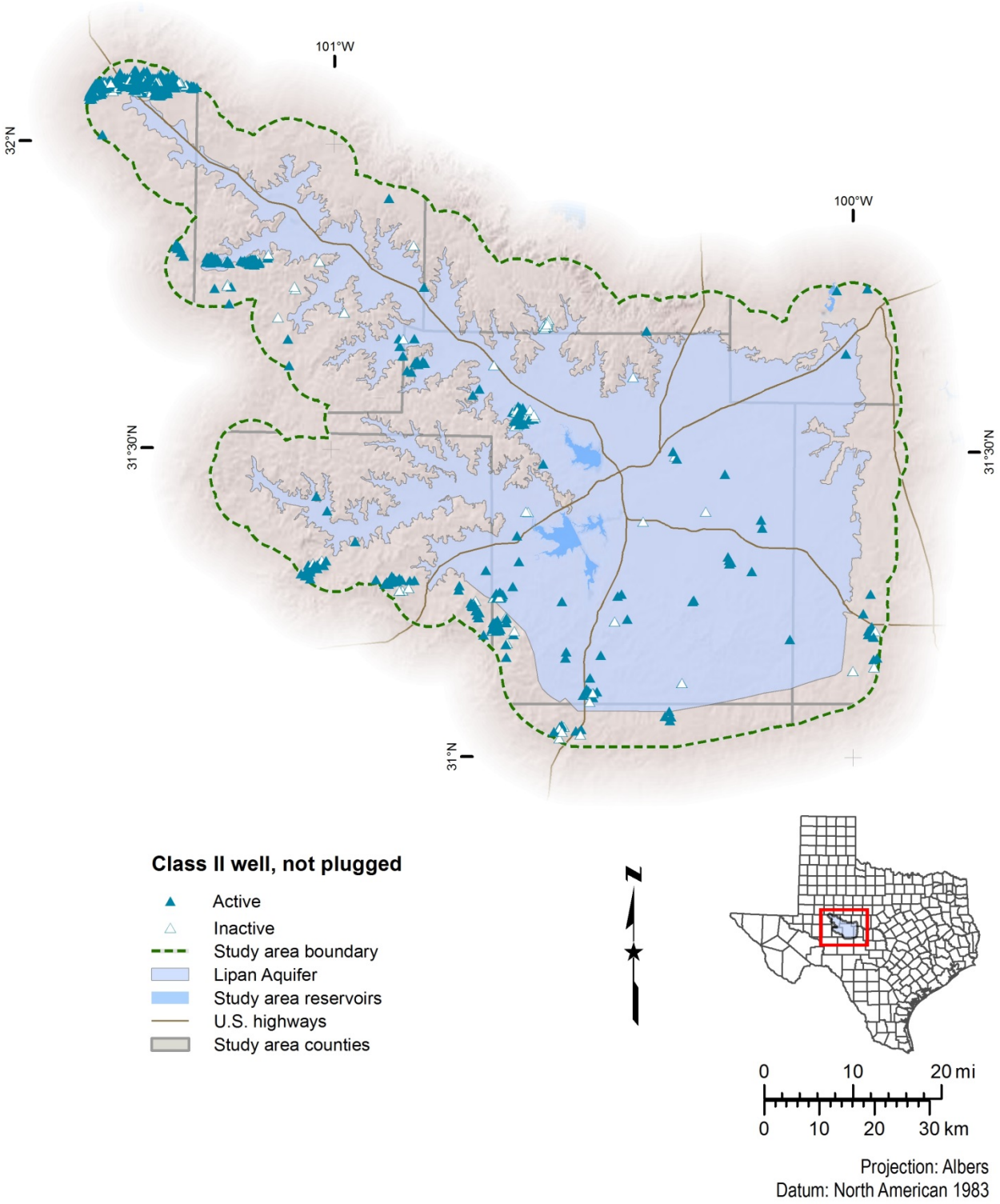

Figure 14-1. **Distribution of non-plugged Class II injection wells in the Lipan Aquifer study area. Data obtained in 2012 from the Underground Injection Control Database of the Railroad Commission of Texas.**

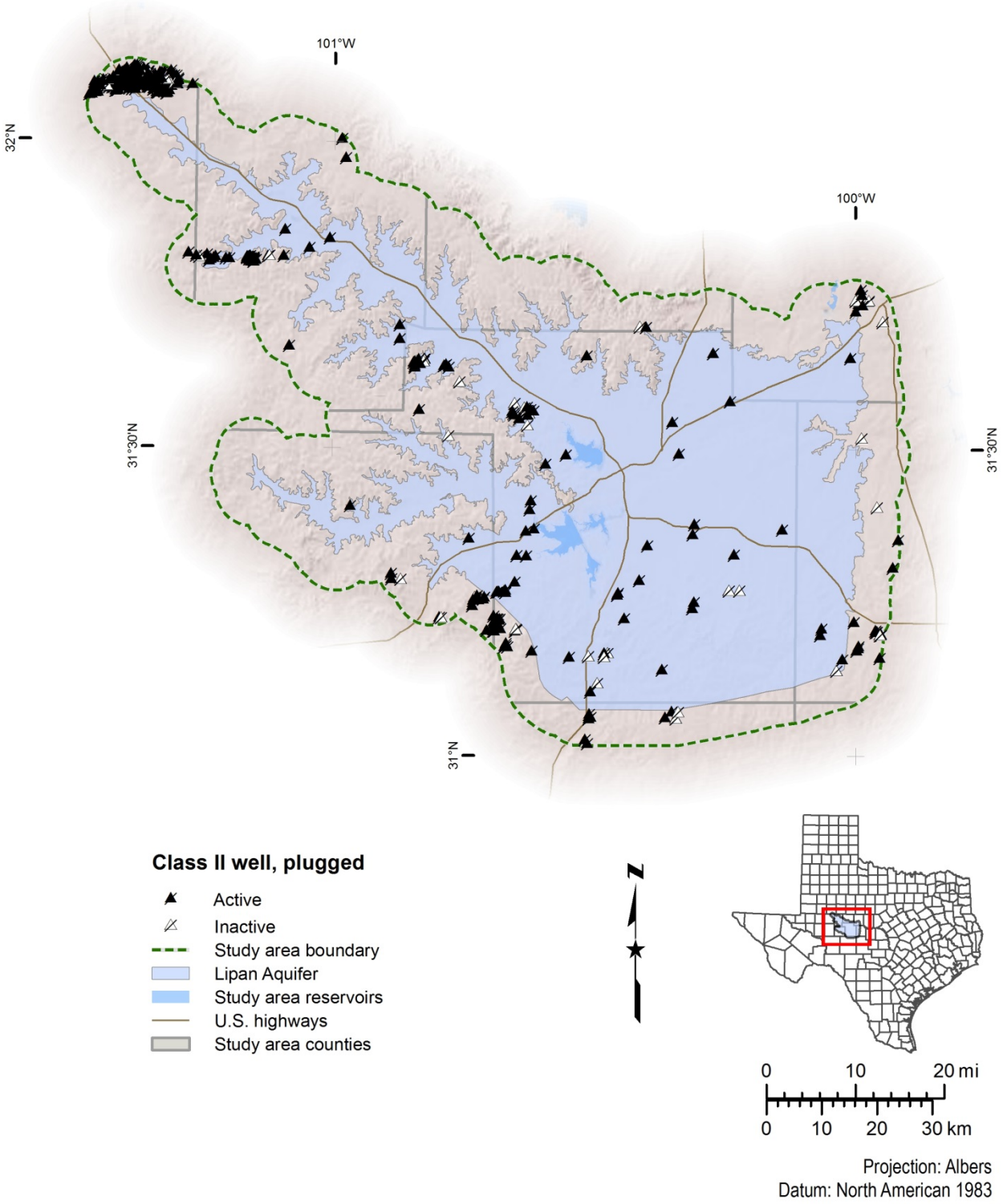

Figure 14-2. **Distribution of plugged Class II injection wells in the Lipan Aquifer study area. Data obtained in 2012 from the Underground Injection Control Database of the Railroad Commission of Texas.**

15. Brackish groundwater production zone consideration

In 2015, the 84th Texas Legislature passed House Bill 30, directing the TWDB to (1) identify and designate brackish groundwater production zones, (2) determine the volumes of groundwater that a brackish groundwater production zone can produce over 30-year and 50-year periods without causing significant impact to water availability or water quality, (3) work with groundwater conservation districts and stakeholders, and (4) make recommendations on reasonable monitoring to observe the effects of brackish groundwater production within the zone. The legislation further requires the TWDB to complete designating brackish groundwater production zones in the whole state by December 1, 2022. On October 20, 2016, the Board designated a total of eight brackish groundwater production zones in the Carrizo-Wilcox, the Gulf Coast, and the Rustler aquifers. No zones were designated in the Blaine Aquifer.

House Bill 30 requires that brackish groundwater production zones are in areas with moderate to high availability and productivity of brackish groundwater and that are separated by hydrogeologic barriers sufficient to prevent significant impacts to water availability or water quality in geologic strata that have an average total dissolved solids concentrations of 1,000 milligrams per liter or less.

House Bill 30 also excluded certain areas from designation:

- The Edwards (Balcones Fault Zone) Aquifer located within the jurisdiction of the Edwards Aquifer Authority.
- Areas within the boundaries of the Barton Springs-Edwards Aquifer Conservation District, the Harris-Galveston Subsidence District, and the Fort Bend Subsidence District.
- Aquifers, subdivisions of aquifers, or geologic strata that have an average total dissolved solids concentration of more than 1,000 milligrams per liter and serve as a significant source of water supply for municipal, domestic, or agricultural purposes.
- Geologic formations that are designated or used for wastewater injection through the use of injection or disposal wells permitted under Texas Water Code Chapter 27.

The Lipan Aquifer was evaluated based on House Bill 30 requirements and no brackish groundwater production zones are recommended for designation. There are two requirements that the Lipan Aquifer does not meet and exclude it from consideration. The first is that hydrogeologic barriers do not exist between the brackish Permian units and the overlying Quaternary and Neogene sediments where fresh water occurs. The second is that groundwater average total dissolved solids concentration is greater than 1,000 milligrams per liter and the Lipan Aquifer serves as a significant water source for municipal, domestic, and agricultural purposes. Available water quality data for total dissolved solids was evaluated from the Permian units and the overlying Quaternary and Neogene sediments. The average measured total dissolved solids concentration was approximately 1,600 milligrams per liter. Samples with a concentration above 4,000 milligrams per liter were considered outliers and excluded from this calculation.

The Texas Commission on Environmental Quality records were reviewed for Class I, III, IV, and V injection wells and determined no such wells exist in the study area. These types of wells may be used for wastewater disposal under Texas Water Code Chapter 27. The permitted Class II

injection wells from the Railroad Commission of Texas in the study area were mapped (refer to Section 14). Since brackish groundwater production zones are not being recommended for designation, no further effort was made to evaluate identified Class II wells in the study area. However, any entity that is considering groundwater development should perform a thorough investigation of any injection wells in the area.

16. Future improvements

This study relied upon records from thousands of wells drilled for both water and hydrocarbons that have been collected into public databases over the past 50 years. Yet even with this large volume of data and information, we found that there are practically no reports on the water chemistry and aquifer hydraulics of the brackish groundwater formations that make up the Lipan Aquifer. As new wells are drilled in the Lipan Aquifer area, it would be helpful to obtain water quality information using discrete interval sampling methods from deeper brackish water formations. In brackish water intervals that appear to contain significant groundwater, pumping test data would greatly enhance our knowledge of the hydraulic properties of these formations.

We also found that the existing groundwater availability model (Beach and others, 2004) is overly simplified and may not represent an accurate physical model of the Lipan Aquifer system. The model assumes a single 400-foot-thick layer that extends beneath ground surface regardless of the geology. We found in this study that groundwater quality is strongly controlled by the geological formations and that there is a definite vertical gradation of aquifer hydraulic properties. An advanced numerical groundwater availability model that incorporates the hydrostratigraphy detailed in this report would provide a more accurate predictive model.

New geophysical remote sensing techniques such as high resolution seismic tomography, electrical resistivity, and ground penetrating radar may be capable of providing detailed visualizations of the shallow Lipan Aquifer. These techniques utilize nondestructive energy sources to detect variations in rock densities and groundwater salinities within a few hundred feet of the ground surface, although data from boreholes are still required to accurately interpret and calibrate the results.

17. Conclusions

The Lipan Aquifer study area experienced severe drought conditions beginning in 2011 when annual precipitation was one-third the historical average. Storage in major surface water reservoirs decreased to 13 percent of capacity. Despite increased statewide precipitation in 2014 and 2015, area reservoirs increased to only 19 percent by 2016. In response to requests from stakeholders in the region to evaluate drought resistant water management strategies, the TWDB performed a BRACS study of the Lipan Aquifer.

We found that there are approximately 0.17 million acre-feet of fresh water (0 to 999 milligrams per liter of total dissolved solids), 4.44 million acre-feet of slightly saline water (1,000 to 2,999 milligrams per liter of total dissolved solids), and 1.61 million acre-feet of moderately saline water (3,000 to 9,999 milligrams per liter of total dissolved solids) available in the Lipan Aquifer. The total volume of brackish groundwater is 6.05 million acre-feet. Not all of the brackish groundwater can be economically or technically produced. Nevertheless, these estimates provide indications of the potential availability of this important resource.

For the study, we collected thousands of water well and geophysical well logs for geological, water chemistry, water level, and aquifer test data from a wide variety of sources to characterize groundwater in the Lipan Aquifer. We used this data to perform detailed stratigraphic mapping that was critical to our understanding of this complex hydrogeologic system.

We present in this study structural and stratigraphic models in greater detail than those previously available for the study area. The salinity zone model of the weathered Permian formations documented in this study provides a useful tool for understanding the occurrence of brackish groundwater and a guide for developing this resource in the future. A significant portion of the brackish groundwater is within weathered Permian formations overlain by Cretaceous formations. There are very few instances where wells have been completed within the Permian formations in these overlain areas, which suggests that the development of brackish groundwater in these areas may represent an untapped resource.

We have proposed a new model for the fresh water-bearing Quaternary and Neogene sediments that fill the Lipan Flat portion of the study area. Our model suggests that the basal conglomerates are probably Neogene in age and may be time equivalent to the Ogallala Formation. This fresh water-bearing conglomerate lies directly upon Permian aged formations and is capped in most places with a 20- to 50-foot thick caliche interval that may locally be a confining layer.

Because of the relatively large variation of the distribution of the total dissolved solids concentrations calculated from geophysical well logs, we found it necessary to statistically bin the results. This technique allowed us to generate charts of total dissolved solids concentration versus depth for each potentially water-bearing formation in the study. We subsequently were able to use these charts to determine at what depths the fresh, slightly saline, and moderately saline groundwater salinity zones could be expected.

This study should be a valuable guide for water providers planning on future brackish groundwater developments. The 2016 Region F Regional Water Plan predicts a need of an additional 57,832 acre-feet of new water supply annually by decade 2070 for Concho, Runnels,

and Tom Green counties. The plan includes recommended water management strategies for the City of San Angelo and the Concho Rural Water Supply Corporation for 3,900 acre-feet of desalinated brackish groundwater.

TWDB staff did not recommend designation of brackish groundwater production zones in the Lipan Aquifer because (1) of the lack of hydrogeologic barriers separating fresh and brackish groundwater and (2) brackish groundwater (with an average total dissolved solid concentration of more than 1,000 milligrams per liter) is currently serving as a significant source for municipal, domestic, or agricultural purposes.

Study deliverables include a peer-reviewed published report, Geographic Information System (GIS) map files, BRACS Database and Data Dictionary, and water well and geophysical well log files. The real value of this study is the GIS and BRACS Database information. The data can be used by stakeholders to map areas for potential groundwater development. Finally, information contained in the report is not intended to serve as a substitute for site-specific studies that are required to evaluate local aquifer characteristics and groundwater conditions for a desalination project.

18. Acknowledgments

We would like to thank Allan Lange and Michael Hoelscher of the Lipan-Kickapoo Water Conservation District for their assistance in understanding the local groundwater management and drilling practices in the study area. We thank Tom Green Precinct 3 County Commissioner Rick Bacon for his interest in and advocacy of the study. Dr. James Ward of Angelo State University provided beneficial insight into the area's geology. TWDB staff members John Meyer and Andrea Croskrey were invaluable in their assistance in the use of the BRACS Database and GIS methods, respectively. We would like to thank TWDB staff members Lauren Munguia for editing, Wendy Mason for cover art design, and Mike Parcher for publication support. Finally, this work could not have been undertaken or completed without the support and encouragement of Erika Mancha (manager of the Innovative Water Technologies Department), Kevin Kluge (director of the Conservation and Innovative Water Technologies Division), Dr. Sanjeev Kalaswad (former director of the Conservation and Innovative Water Technologies Division), and Dr. Robert E. Mace (former deputy executive administrator of the Office of Water Science and Conservation).

19. References

Alger, R.P., 1966, Interpretation of electric logs in fresh water wells in unconsolidated sediments, in Society of Professional Well Log Analysts, Tulsa, Oklahoma, 7th Annual Logging Symposium Transaction, 25 p.

Asquith, G., 1982, Basic well log analysis for geologists: American Association of Petroleum Geologists Methods in Exploration Series, 216 p.

Beach, J.A., Burton, S., and Kolarik, B., 2004, Groundwater availability model for the Lipan Aquifer in Texas: LBG-Guyton Associates, contract report to the Texas Water Development Board, variously paginated.

Beede, J.W., and Bentley, W.P., 1918, The geology of Coke County: University of Texas Bulletin No. 1850, 80 p.

Beede, J.W., and Waite, V.V., 1918, The geology of Runnels County: University of Texas Bulletin No. 1816, 64 p.

CDM Smith, 2014, Guidance manual for permitting Class I and Class II wells for the injection and disposal of desalination concentrate: CDM Smith, contract report to the Texas Water Development Board, variously paginated.

Dutton, A.R., Richter, B.C., and Kreitler, C.W., 1989, Brine discharge and salinization, Concho River watershed, West Texas: Ground Water, v. 27, no. 3, p. 375-383.

Eifler, G.K., Jr., Frye, J.C., and Leonard, A.B., 1974, Geologic Atlas of Texas, Big Spring Sheet: The University of Texas at Austin, Bureau of Economic Geology map, scale 1:250,000.

Eifler, G.K., Jr., 1976, Geologic Atlas of Texas, San Angelo Sheet: The University of Texas at Austin, Bureau of Economic Geology map, scale 1:250,000.

Estepp, J.D., 1998, Evaluation of ground-water quality using geophysical logs: Texas Natural Resource Conservation Commission, unpublished report, 516 p.

Estepp, J.D., 2010, Determining groundwater quality using geophysical logs: Texas Commission on Environmental Quality, unpublished report, 85 p.

Forrest, J., Marcucci, E., and Scott, P., 2005, Geothermal gradients and subsurface temperatures in the northern Gulf of Mexico: Gulf Coast Association of Geological Societies Transactions v. 55, p. 233-248.

Freese and Nichols, and LBG-Guyton Associates, 2006, San Angelo groundwater evaluation phase I report initial feasibility assessment: Freese and Nichols Inc., contract report to the Texas Water Development Board, variously paginated.

Freese and Nichols, and LBG-Guyton Associates, 2015, 2016 Region F water plan, volume I appendices: Freese and Nichols Inc., contract report to the Region F Water Planning Group, variously paginated.

Gradstein, F.M., Ogg, J.G., Schmitz, M.D., and Ogg, G.M., editors, 2012, The geological time scale 2012: Amsterdam, Elsevier, 2 volumes, 1144 p.

HDR, 2011, Texas water system map: The compilation of a statewide geodataset and digital maps of water service area boundaries: HDR, contract report to the Texas Water Development Board, 35 p. and digital datasets.

Hem, J.D., 1985, Study and interpretation of the chemical characteristics of natural water: U.S. Geological Survey Water-Supply Paper 2254, 263 p. and 4 plates.

Henderson, G.G., 1928, The geology of Tom Green County: University of Texas Bulletin No. 2807, 116 p.

Hilchie, D.W., 1978, Applied openhole log interpretation for geologist and engineers: Douglas W. Hilchie, Inc., Golden, Colorado, variously paginated.

Hill, J.M., 1972, Late Paleozoic sedimentation in West Texas Permian Basin: American Association of Petroleum Geologist Bulletin, v. 56, no. 12, p. 2303-2322.

Hill, R.T., and Vaughan, T.W., 1889, Papers chiefly of a theoretic nature: U.S. Geological Survey 18th Annual Report, Part 2, p. 193-321.

Jones, I.C., Bradley, R., Boghici, R., Kohlrenken, W., and Shi, J., 2013, GAM task 13-030: total estimated recoverable storage for aquifers in Groundwater Management Area 7: Texas Water Development Board unpublished report, 51 p.

Keys, W.S., 1990, Borehole geophysics applied to ground-water investigations: U.S. Geological Survey Techniques of Water Resources Investigations, Chapter E2, 150 p.

Kier, R.S., Brown, L.F., Jr., Harwood, P., and Barnes, V.E., 1976, Geologic Atlas of Texas, Brownwood Sheet: The University of Texas at Austin, Bureau of Economic Geology map, scale 1:250,000.

Larkin, T.J., and Bomar, G.W., 1983, Climatic atlas of Texas: Texas Department of Water Resources Report LP 192, 151 p.

LBG-Guyton Associates, 2003, Brackish groundwater manual for Texas regional water planning groups: LBG-Guyton Associates, contract report to the Texas Water Development Board, 188 p.

LBG-Guyton Associates, 2004, An evaluation of brackish and saline water resources in Region F: LBG-Guyton Associates, contract report prepared for the Region F Regional Water Planning Group, 65 p.

LBG-Guyton Associates, 2005, An evaluation of Triassic and Permian brackish groundwater resources in the San Angelo, Texas area: LBG-Guyton Associates, contract report to the Texas Water Development Board, 28 p.

LBG-Guyton Associates, 2008, Report on brackish source water exploration in the San Angelo, Texas area: LBG-Guyton Associates, contract report to the Texas Water Development Board, variously paginated.

Lee, J.N., 1986, Shallow ground-water conditions, Tom Green County, Texas: U.S. Geological Survey Water-Resources Investigations Report 86-4177, 88 p.

Mace, R.E., Nicot, J.P., Chowdhury, A.H., Dutton, A.R., and Kalaswad, S., 2006, Please pass the salt: using oil fields for the disposal of concentrate from desalination plants: Texas Water Development Board Report 366, 214 p.

McKalips, D., Rose, P.R., and Lozo, F.E., Jr., 1981, Geologic Atlas of Texas, Sonora Sheet: The University of Texas at Austin, Bureau of Economic Geology map, scale 1:250,000.

Mear, C.E., 1963, Stratigraphy of Permian outcrops, Coke County, Texas: American Association of Petroleum Geologists Bulletin, v. 47, no. 11, p. 1952-1962.

Meyer, J.E., 2012, Geologic characterization of and data collection in the Corpus Christi Aquifer Storage and Recovery Conservation District and surrounding counties: Texas Water Development Board Open File Report 12-01, 42 p.

Meyer, J.E., 2017, Brackish resources aquifer characterization system database data dictionary: Texas Water Development Board Open File Report 12-02, Third Edition, 195 p.

Meyer, J.E., Wise, M.R., and Kalaswad, S., 2012, Pecos Valley Aquifer, West Texas: Structure and Brackish Groundwater: Texas Water Development Board Report 382, 86 p.

Meyer, J.E., Croskrey, A.D., Wise, M.R., and Kalaswad, S., 2014, Brackish Groundwater in the Gulf Coast Aquifer, Lower Rio Grande Valley, Texas: Texas Water Development Report 383, 169 p.

Muzzullo, S.J., 1982, Stratigraphic and depositional mosaics of Lower Clear Fork and Wichita Groups (Permian), Northern Midland Basin, Texas: American Association of Petroleum Geologists Bulletin, v. 66, no. 2, p. 210-227.

Novalis, S., 1999, Access 2000 Visual Basic for applications handbook: Sybex, Inc., 845 p.

Plummer, F.B., 1932, The Pre-Paleozoic and Paleozoic systems in Texas, *in* Sellards, E.H., Adkins, W.S., and Plummer, F.B., The geology of Texas, volume I, stratigraphy: The University of Texas at Austin, Bureau of Economic Geology Bulletin 3232, p. 15-238.

Railroad Commission of Texas, 2012, Underground Injection Control Database.

Richter, B.C., Dutton, A.R., and Kreitler, C.W., 1990, Identification of sources and mechanisms of salt-water pollution affecting ground-water quality: a case study, West Texas: The University of Texas at Austin, Bureau of Economic Geology Report of Investigations 191, 43 p.

Richter, B.R., and Kreitler, C.W., 1987, Sources of ground water salinization in parts of West Texas: Ground Water Monitoring Review, v. 7, no. 4, p. 75-84.

Ruppel, S.C., and Ward, W.B., 2013, Outcrop-based characterization of the Leonardian carbonate platform in West Texas: Implications for sequence-stratigraphic styles in the Lower Permian: American Association of Petroleum Geologists Bulletin, v. 97, no. 2, p. 223-250.

Schlumberger, 1972, Log interpretation, volume 1 – principles: Schlumberger Limited, 113 p.

Schlumberger, 1985, Log interpretation charts: Schlumberger Well Services, 112 p.

Schlumberger, 1987, Log interpretation principles/applications: Schlumberger Educational Services, 198 p.

Sellards, E.H., 1932, Cenozoic systems in Texas, in Sellards, E.H., Adkins, W.S., and Plummer, F.B., The geology of Texas, volume I, stratigraphy: The University of Texas at Austin, Bureau of Economic Geology Bulletin 3232, p. 519-818.

Seni, S.J., 1980, Sand-body geometry and depositional systems, Ogallala Formation, Texas: The University of Texas, Austin, Bureau of Economic Geology Report of Investigations 105, 36 p.

Stueber, A.M., Saller, A.H., and Ishida, H., 1998, Origin, migration, and mixing of brines in the Permian Basin: Geochemical evidence from the Eastern Central Basin Platform, Texas: American Association of Petroleum Geologists Bulletin, v. 82, no. 9, p. 1652-1672.

16 TAC (Texas Administrative Code) § 3.9.

TCEQ (Texas Commission on Environmental Quality), 2015, Subchapter F: Drinking water standards governing water quality and reporting requirements for public water systems: 30 Texas Administrative Code Chapter 290, §§290.101 – 290.122.

Texas Board of Water Engineers, 1941, Tom Green County, Texas, records of well and springs, drillers' logs, water analyses, and map showing locations of well and springs: Works Projects Administration, 82 p.

Texas Department of Licensing and Regulation, 2016, Submitted Driller's Report Database.

Thoms, E., 2005, Creating and managing digital cross section within ArcGIS: U.S. Geological Survey Open-file Report 2005-1428, p. 247-251.

Torres-Verdin, C., 2015, Integrated geological-petrophysical interpretation of well logs: The University of Texas at Austin, Department of Petroleum and Geosystems Engineering, 126 p.

TWDB (Texas Water Development Board), 2007a, The geologic atlas of Texas, tnris.org/data-catalog/entry/geologic-database-of-texas/, accessed December 2016.

TWDB (Texas Water Development Board), 2007b, Water for Texas, Volume 2: Texas Water Development Board Report GP-8-1, 392 p.

TWDB (Texas Water Development Board), 2016a, BRACS Database.

TWDB (Texas Water Development Board), 2016b, Groundwater Database.

TWDB (Texas Water Development Board), 2016c, Water for Texas, 2017 state water plan: Texas Water Development Board, 133 p.

U.S. EPA, 2017, Secondary drinking water standards: guidance for nuisance chemicals, www.epa.gov/dwstandardsregulations/secondary-drinking-water-standards-guidance-nuisance-chemicals**,** accessed May 2017.

Udden, J.A., and Phillips, W.B., 1911, Report on oil, gas, and coal and water prospects near San Angelo, Tom Green County, Texas: report to the Chamber of Commerce, San Angelo, Texas, 36 p.

Warner, D.L., 2001, Technical and economic evaluations of the protection of saline ground water under the safe drinking water act and the UIC Regulations: Report submitted to the Ground Water Protection Research Foundation, 44 p.

Willis, G.W., 1954, Ground-water resources of Tom Green County, Texas: Texas Board of Water Engineers Bulletin 5411, 101 p.

Winslow, A.G., and Kister, L.R., 1956, Saline-water resources of Texas: U.S. Geological Survey Water-Supply Paper 1365, 105 p.

Wise, M.R., 2014, Queen City and Sparta aquifers, Atascosa and McMullen counties, Texas: Structure and Brackish Groundwater: Texas Water Development Board Technical Note 14-01, 67 p.

Wrather, W.E., 1917, Notes on the Texas Permian: American Association of Petroleum Geologist Bulletin, v. 1, p. 93-106.

20. Appendices

20.1 Formation surfaces

We created raster surfaces representing elevations of the geological formations in the study area using geophysical well log correlations from wells in the BRACS Database.

Using these rasters we created geological formation maps depicting the (1) depth to the top (in units of feet below ground surface), (2) elevation of the top (in units of feet, datum mean sea level, and (3) isochore lines (in units of feet) for many of the geological units located in the study area. Isochore lines are lines along which true, vertical thickness remains the same (as opposed to isopach lines that indicate the thickness of a geological unit perpendicular to the top and bottom of the unit and do not take into account post-depositional tilting). The maps are presented in this appendix in ascending stratigraphic order, from oldest to youngest. The maps showing the elevation and depth to the top of the geological units are presented together in alternating pages (Figure 20.1-1 through Figure 20.1-32) followed by a map of the ground-surface elevation (Figure 20.1-33); isochore line maps follow in a separate group (Figure 20.1-34 through Figure 20.1-50). An isochore map showing the thickness of the Lueders Formation was not created because we did not map the base of the Lueders Formation.

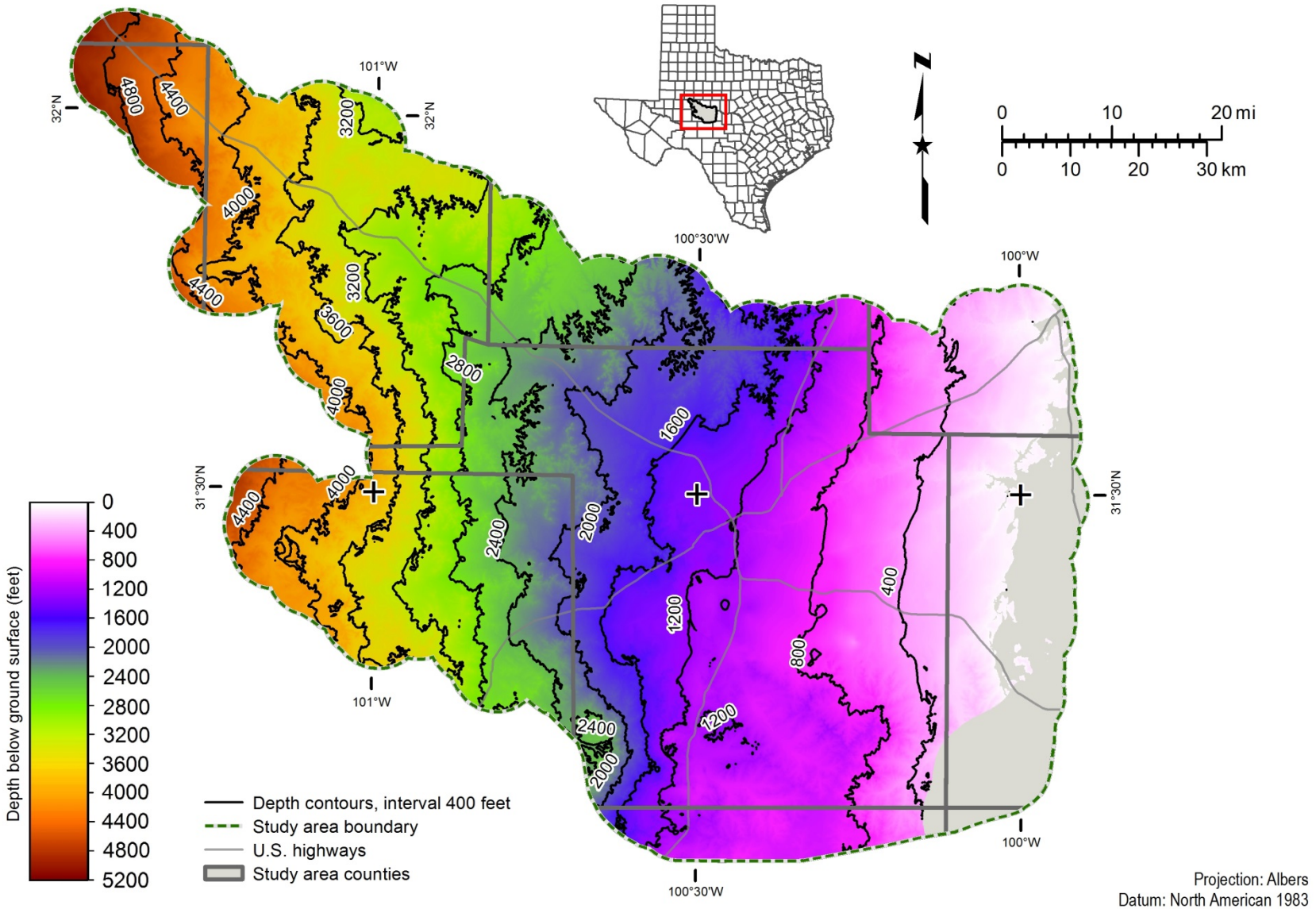

Figure 20.1-1. Lueders Formation top (depth below ground surface, feet) in the Lipan Aquifer study area. Gray area in map represents places where the top of the Lueders Formation does not occur.

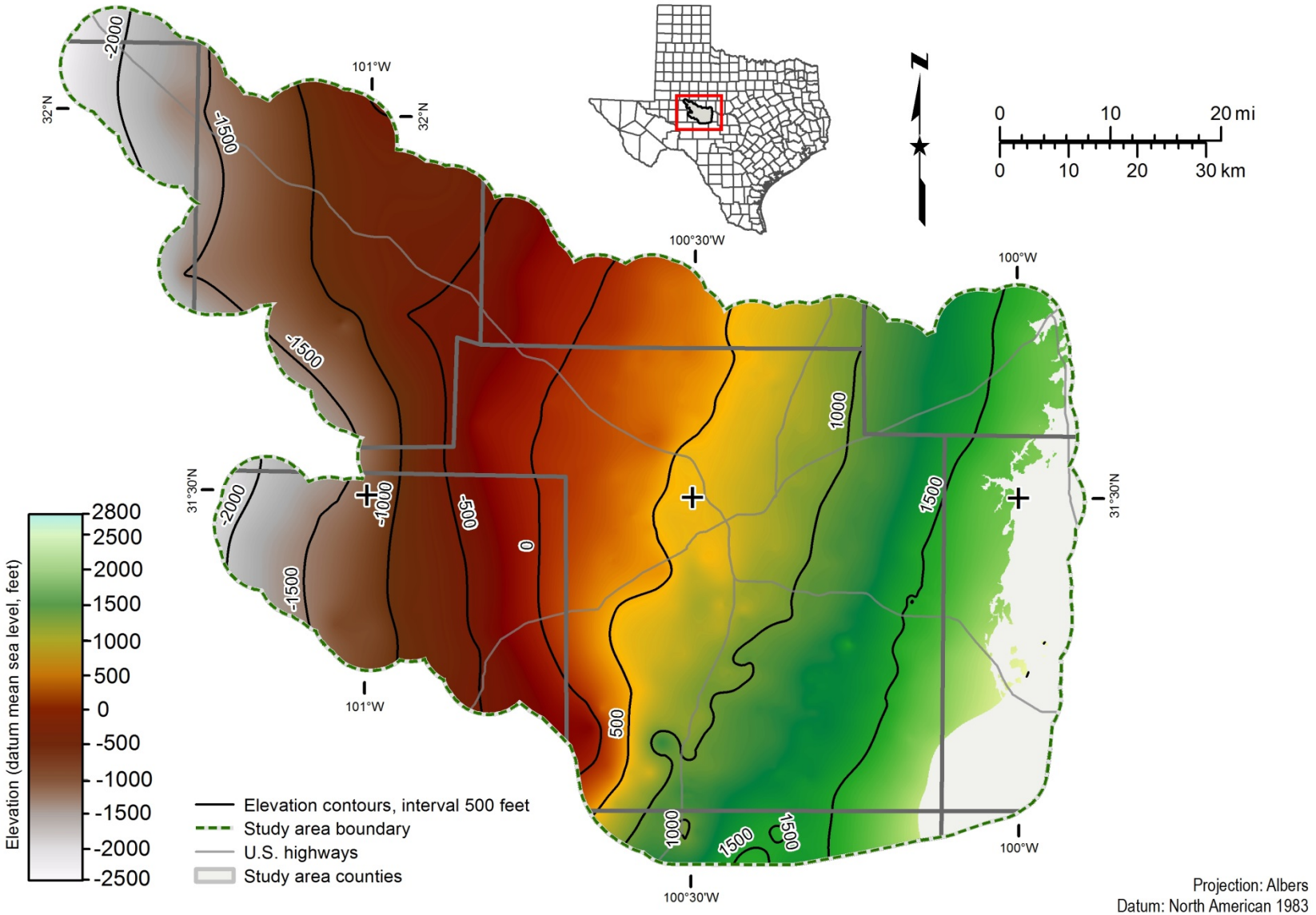

Figure 20.1-2. Lueders Formation top (elevation datum mean sea level, feet) in the Lipan Aquifer study area. Gray area in map represents places where the top of the Lueders Formation does not occur.

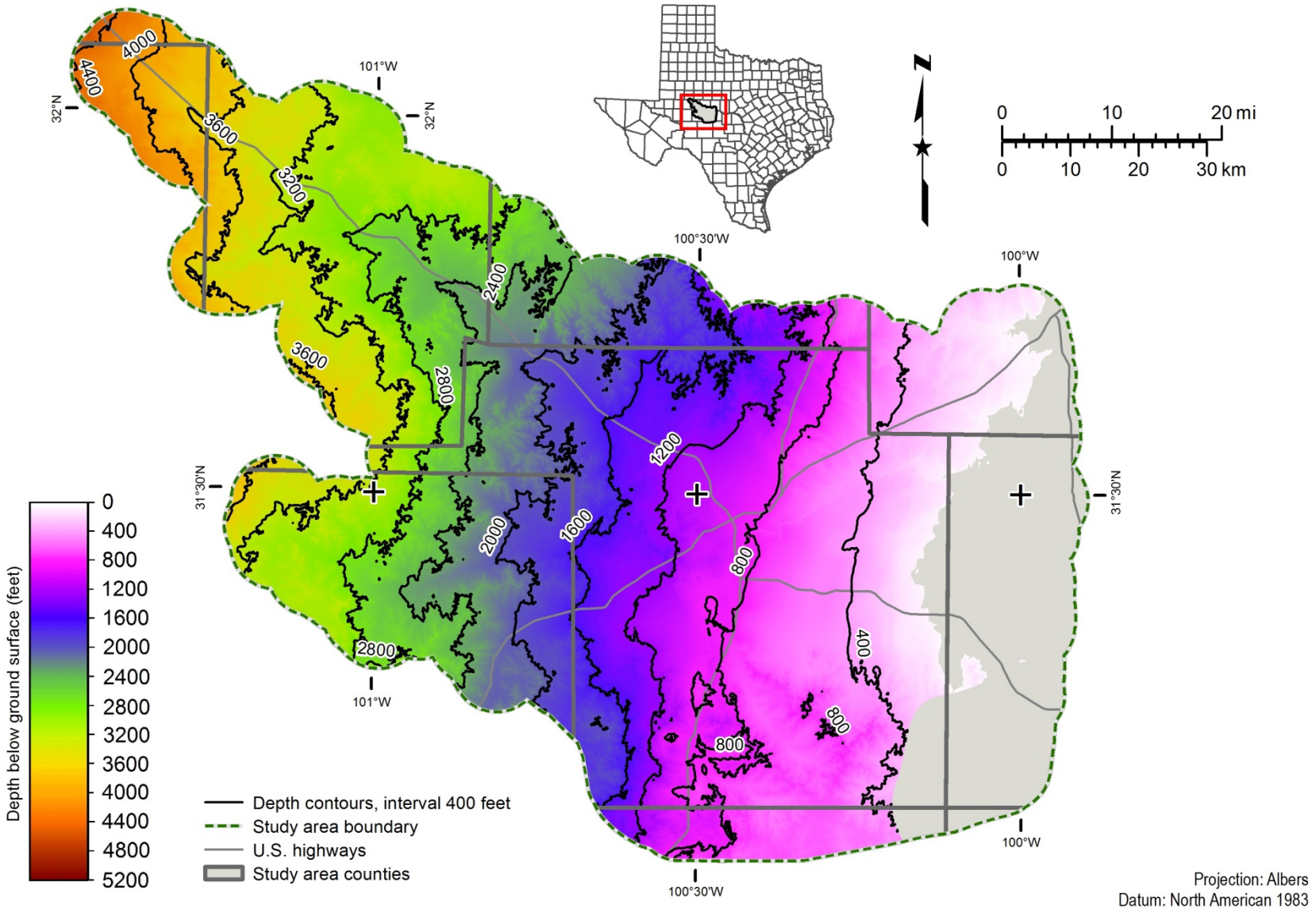

Figure 20.1-3. Arroyo Formation top (depth below ground surface, feet) in the Lipan Aquifer study area. Gray area in map represents places where the top of the Arroyo Formation does not occur.

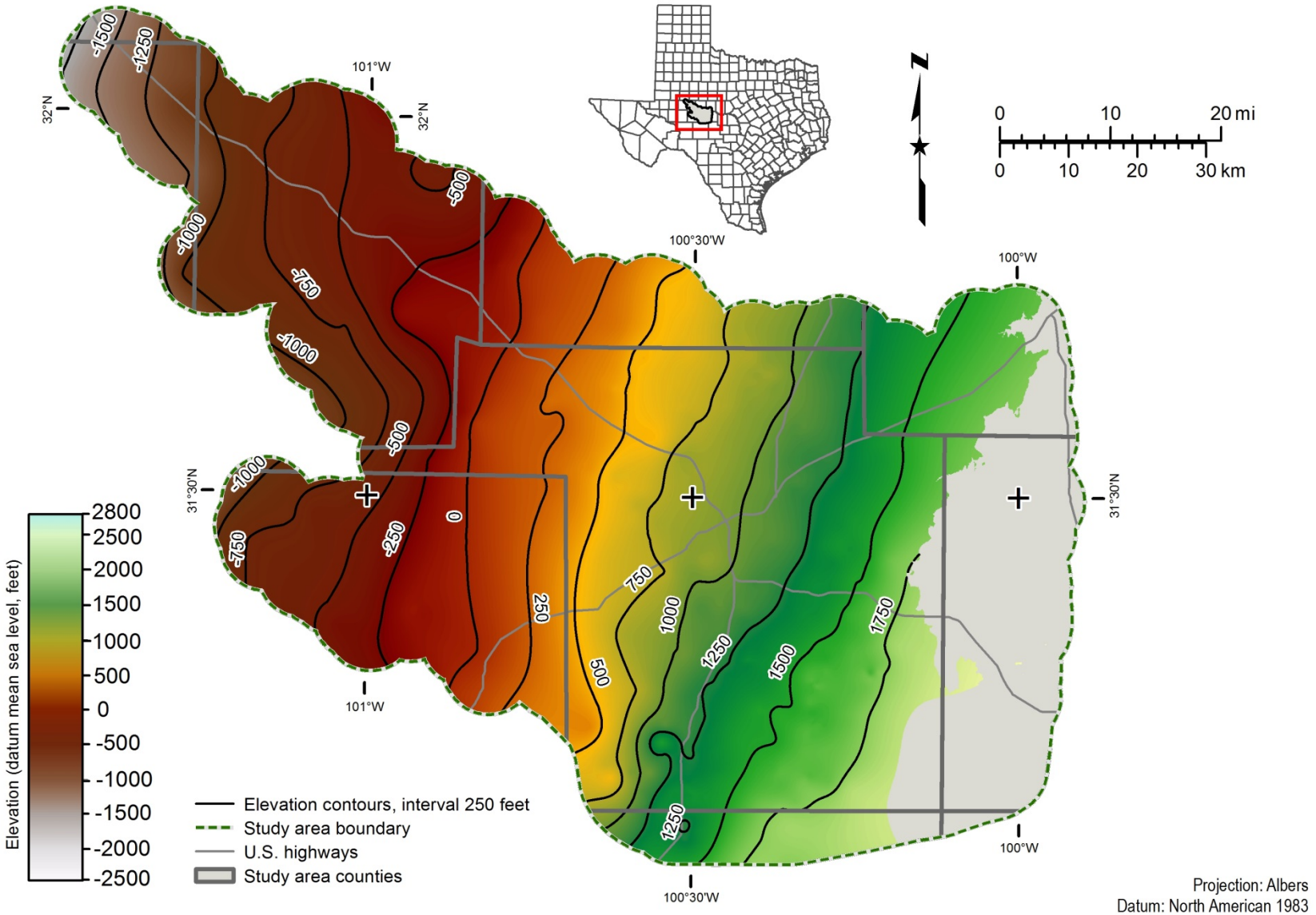

Figure 20.1-4. Arroyo Formation top (elevation datum mean sea level, feet) in the Lipan Aquifer study area. Gray area in map represents places where the top of the Arroyo Formation does not occur.

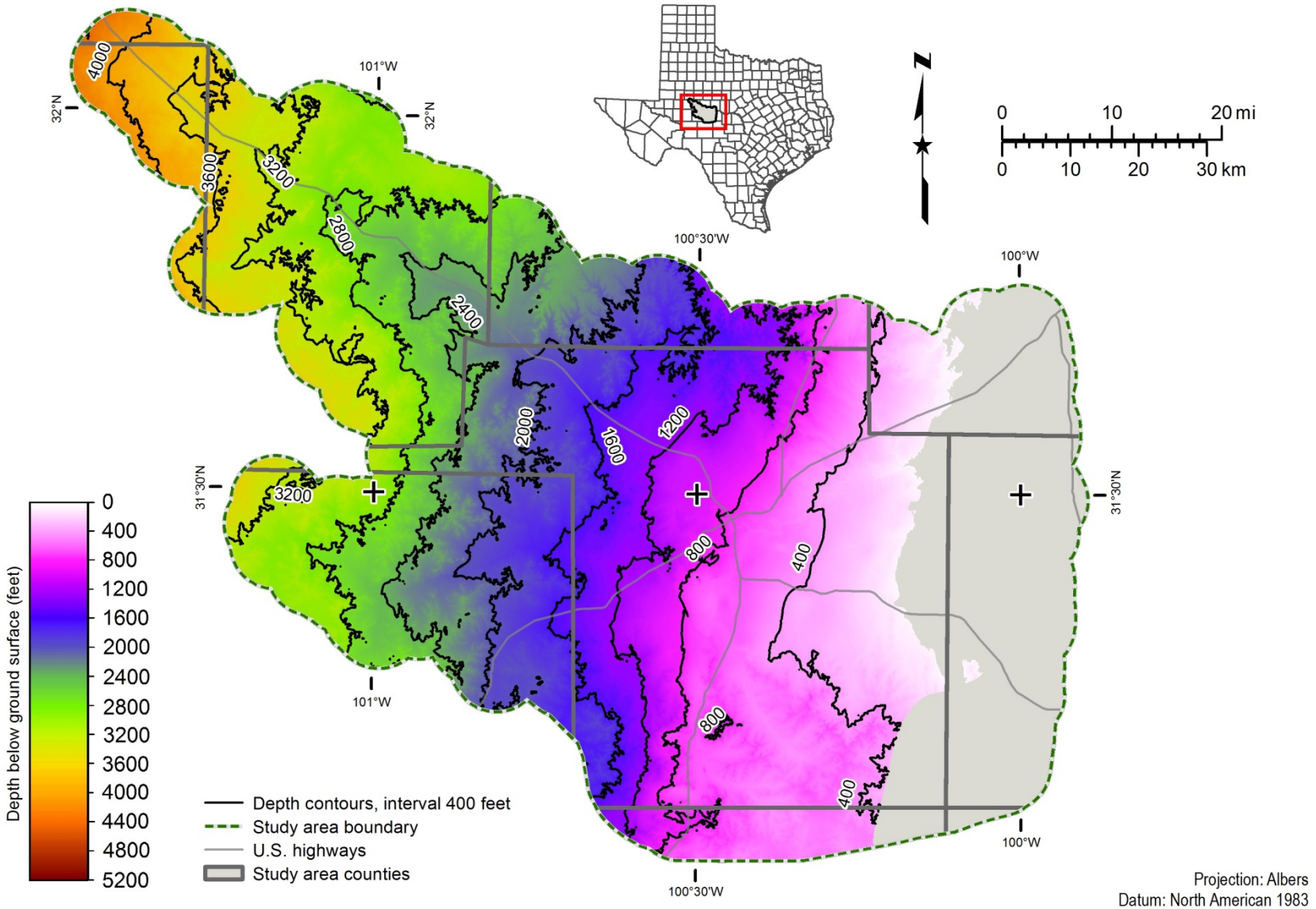

Figure 20.1-5. Vale Shale member top (depth below ground surface, feet) in the Lipan Aquifer study area. Gray area in map represents places where the top of the Vale Shale member does not occur.

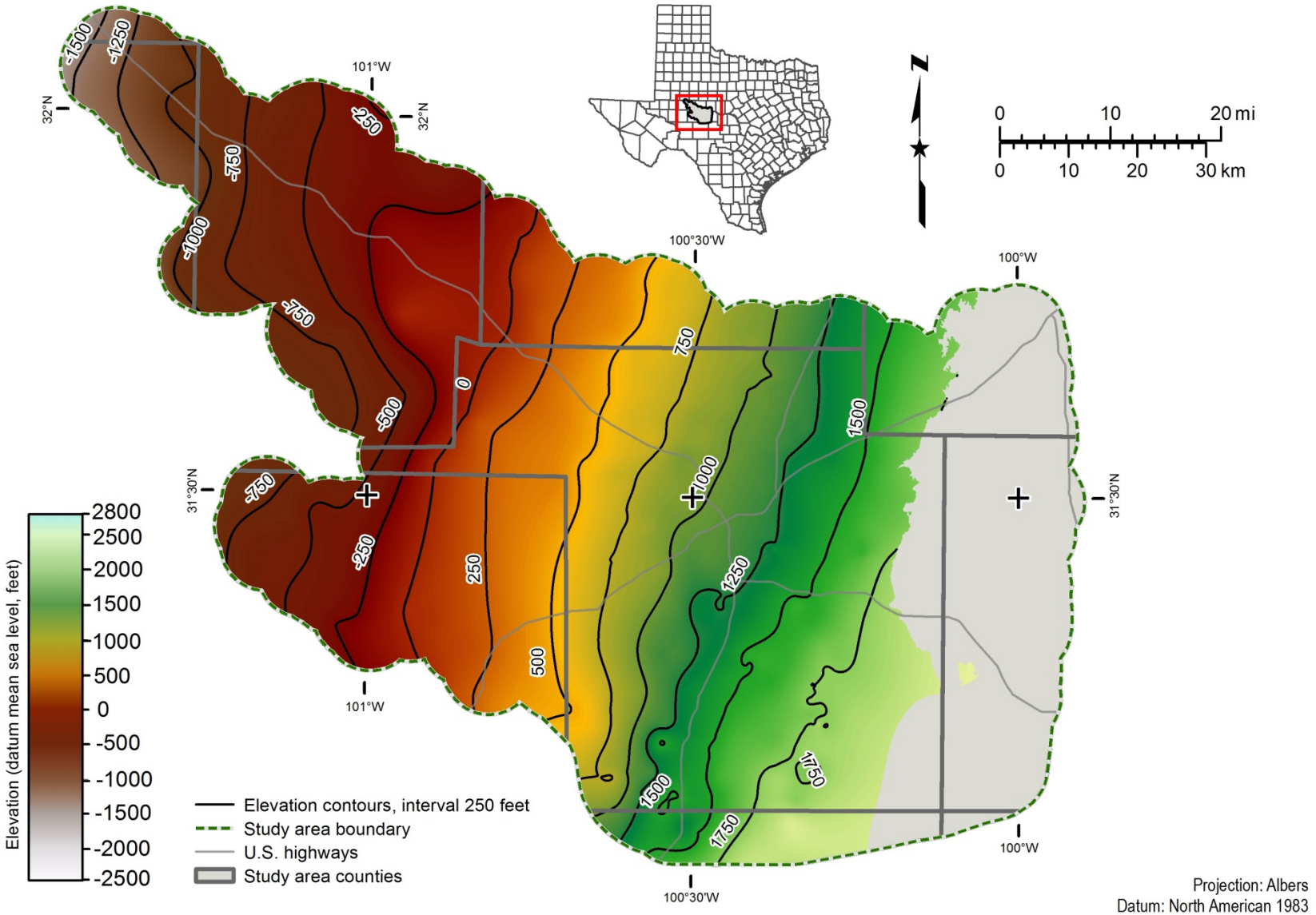

Figure 20.1-6. Vale Shale member top (elevation datum mean sea level, feet) in the Lipan Aquifer study area. Gray area in map represents places where the top of the Vale Shale member does not occur.

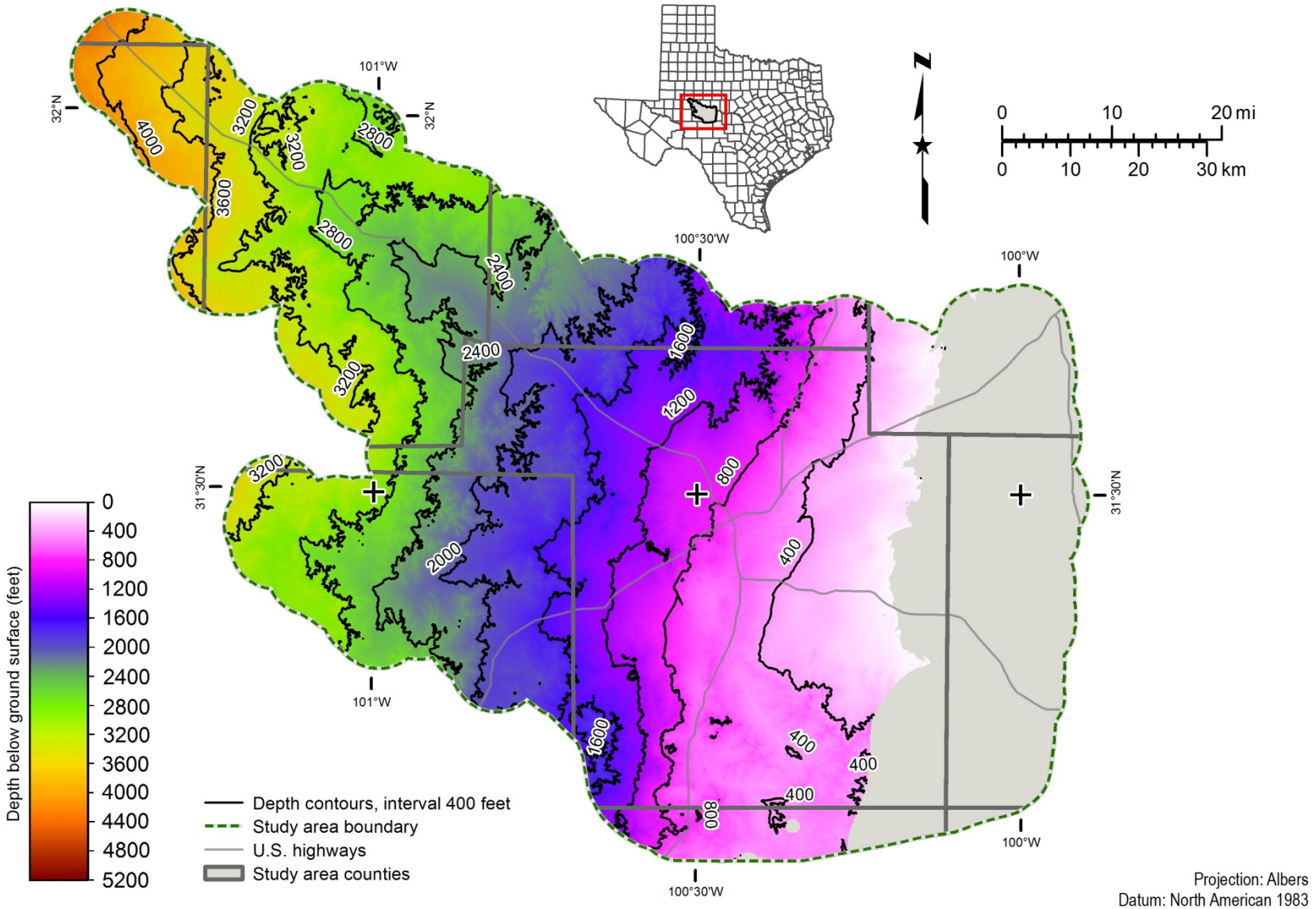

Figure 20.1-7. Bullwagon Dolomite top (depth below ground surface, feet) in the Lipan Aquifer study area. Gray area in map represents places where the top of the Bullwagon Dolomite does not occur.

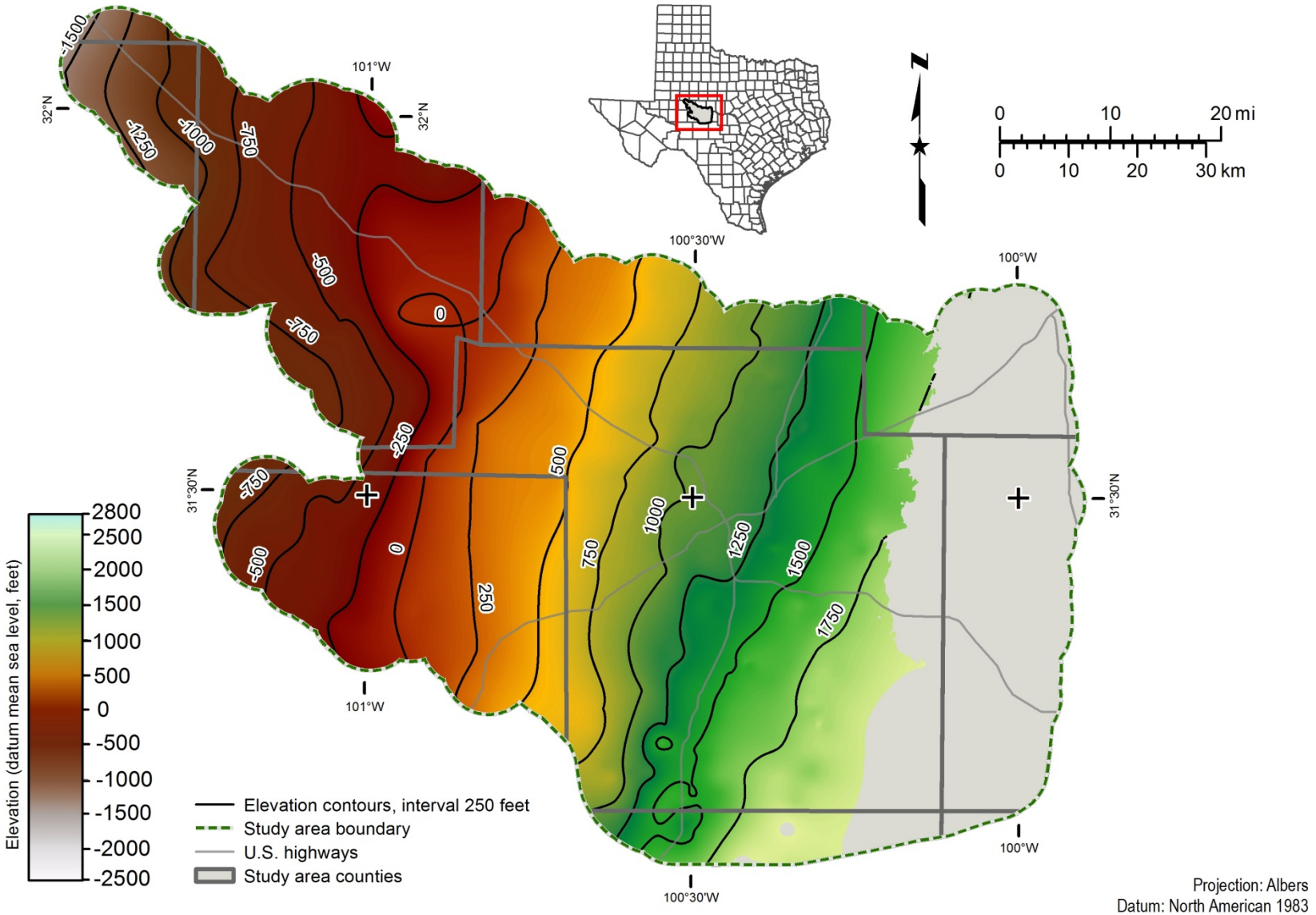

Figure 20.1-8. Bullwagon Dolomite top (elevation datum mean sea level, feet) in the Lipan Aquifer study area. Gray area in map represents places where the top of the Bullwagon Dolomite does not occur.

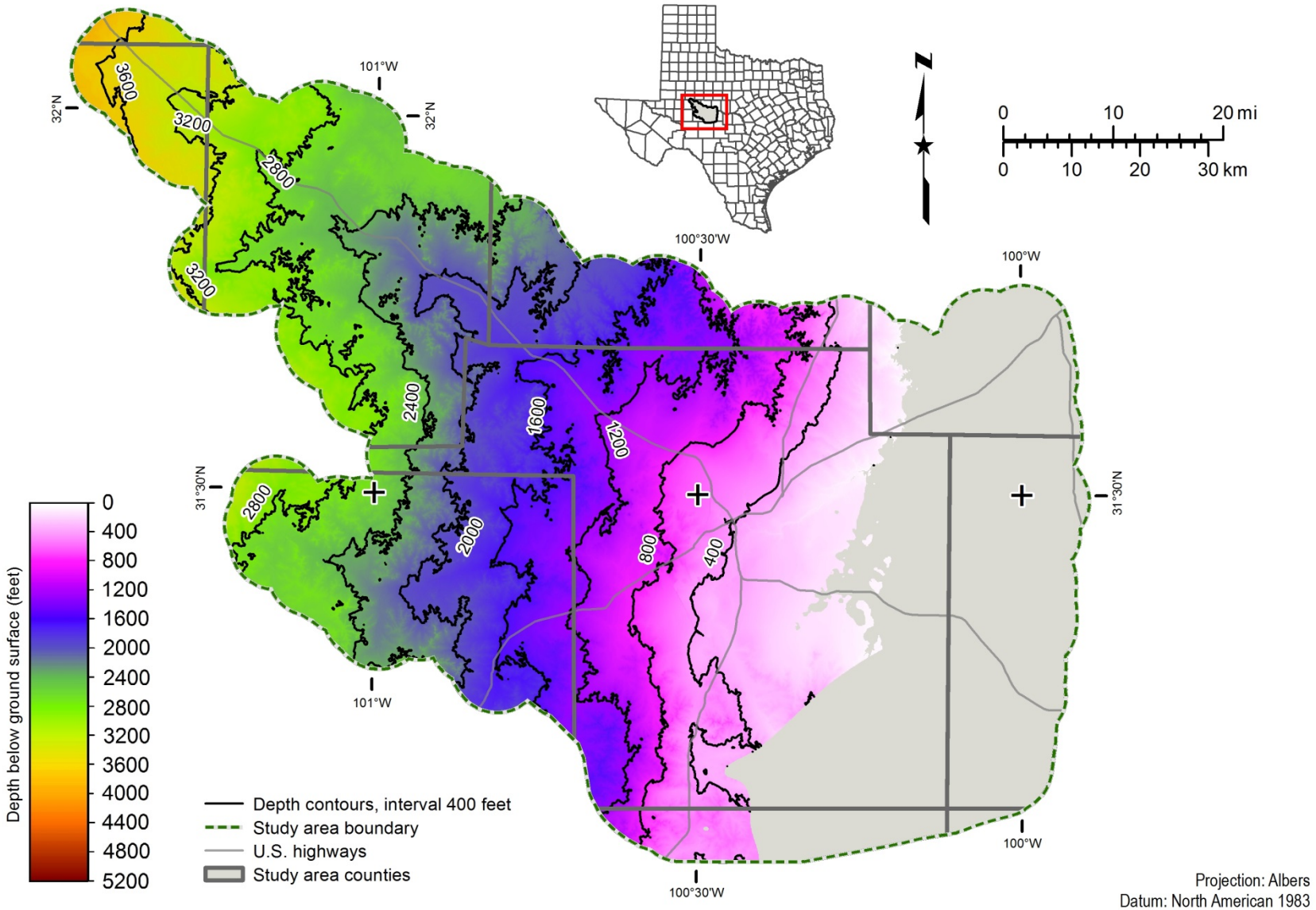

Figure 20.1-9. Tubb member top (depth below ground surface, feet) in the Lipan Aquifer study area. Gray area in map represents places where the top of the Tubb member does not occur.

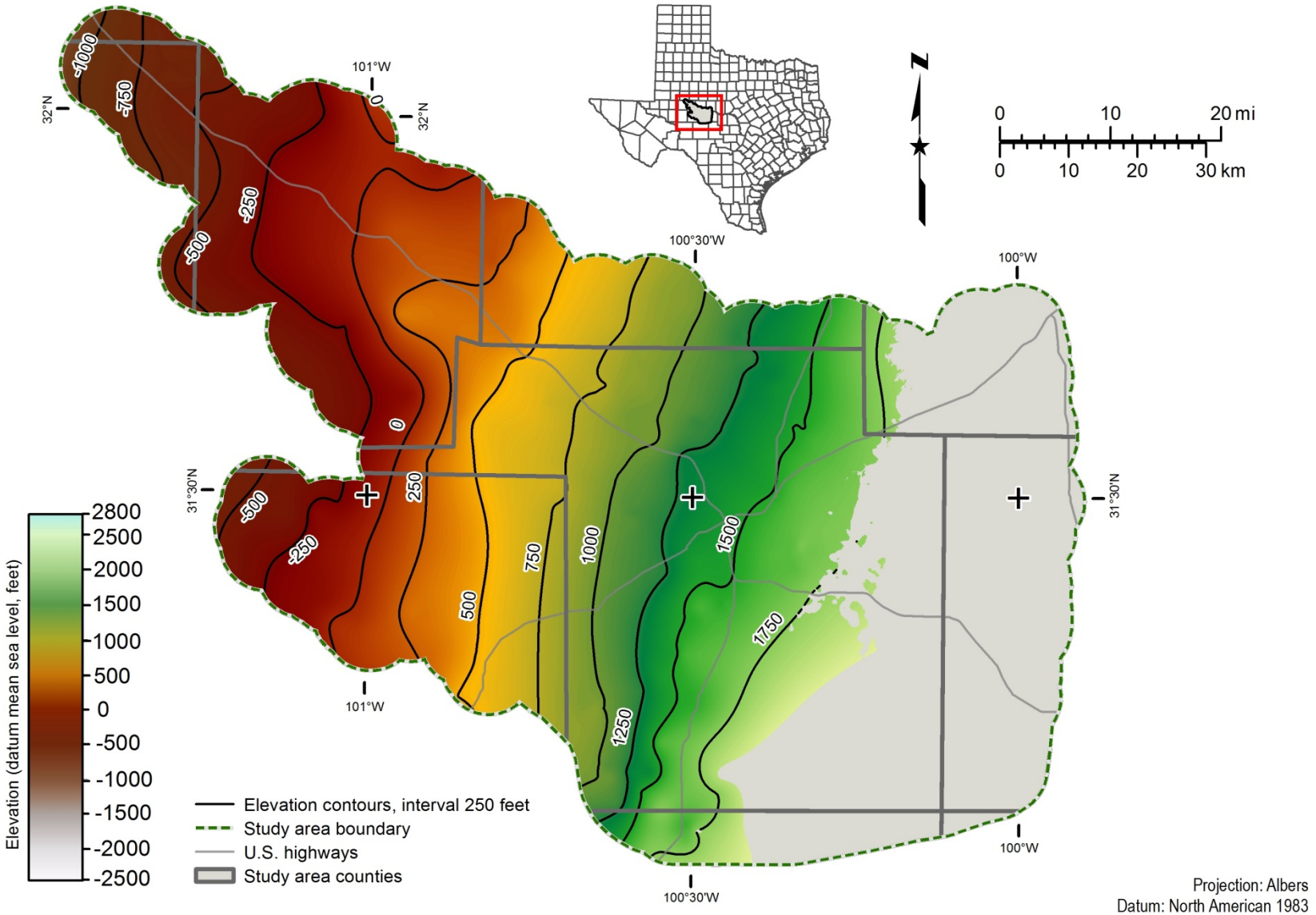

Figure 20.1-10. Tubb member top (elevation datum mean sea level, feet) in the Lipan Aquifer study area. Gray area in map represents places where the top of the Tubb member does not occur.

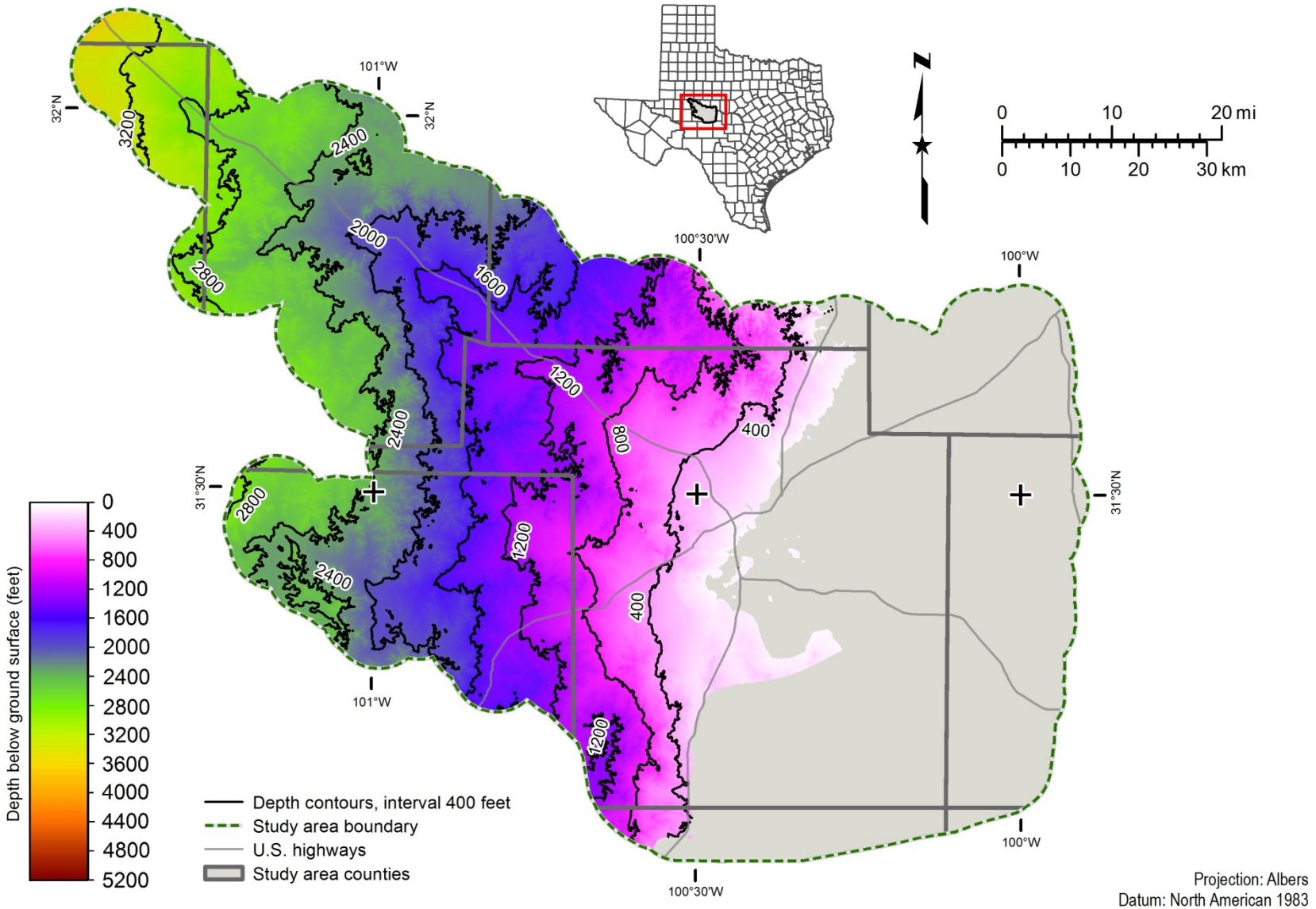

Figure 20.1-11. Upper Choza member top (depth below ground surface, feet) in the Lipan Aquifer study area. Gray area in map represents places where the top of the Upper Choza member does not occur.

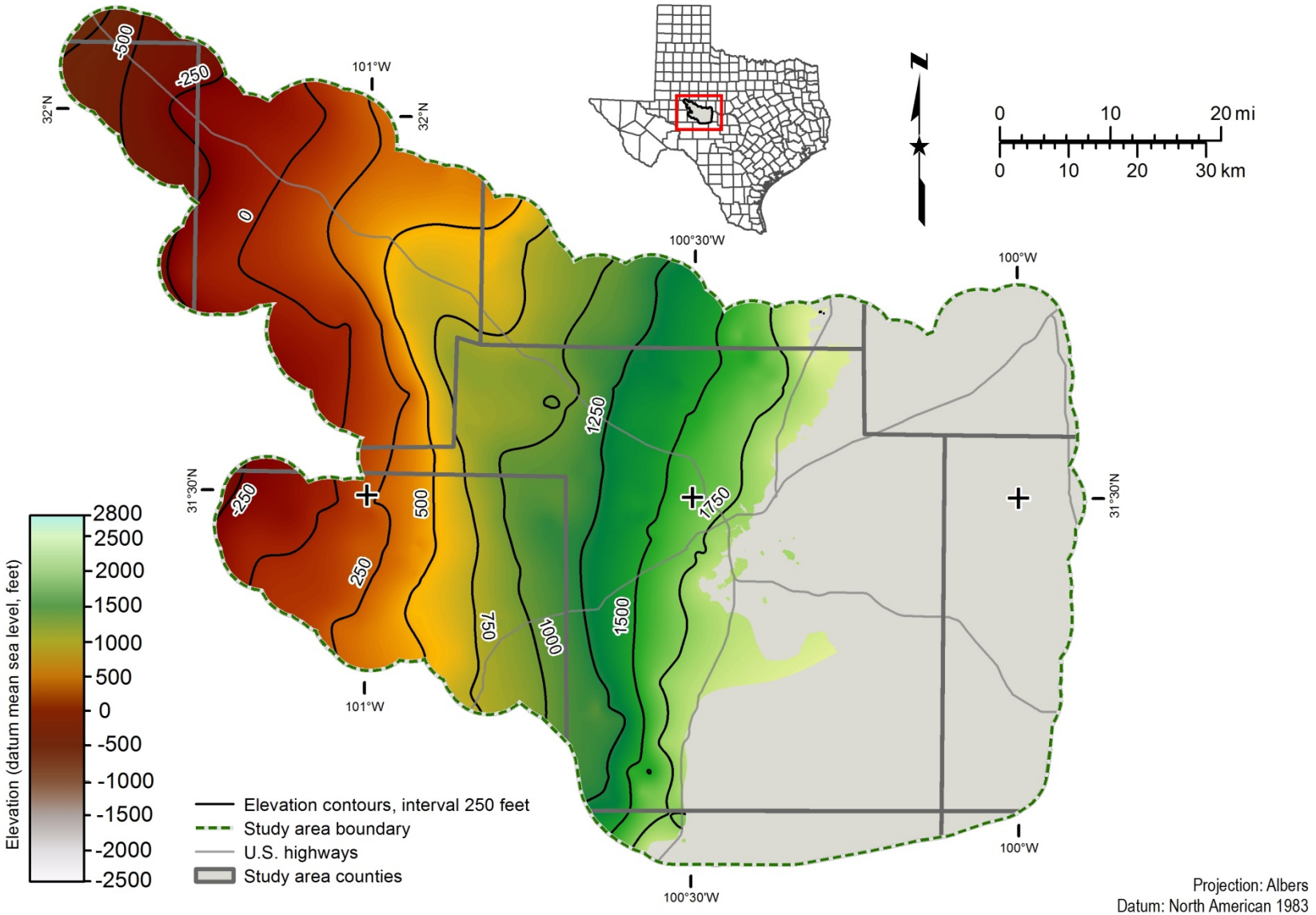

Figure 20.1-12. Upper Choza member top (elevation datum mean sea level, feet) in the Lipan Aquifer study area. Gray area in map represents places where the top of the Upper Choza member does not occur.

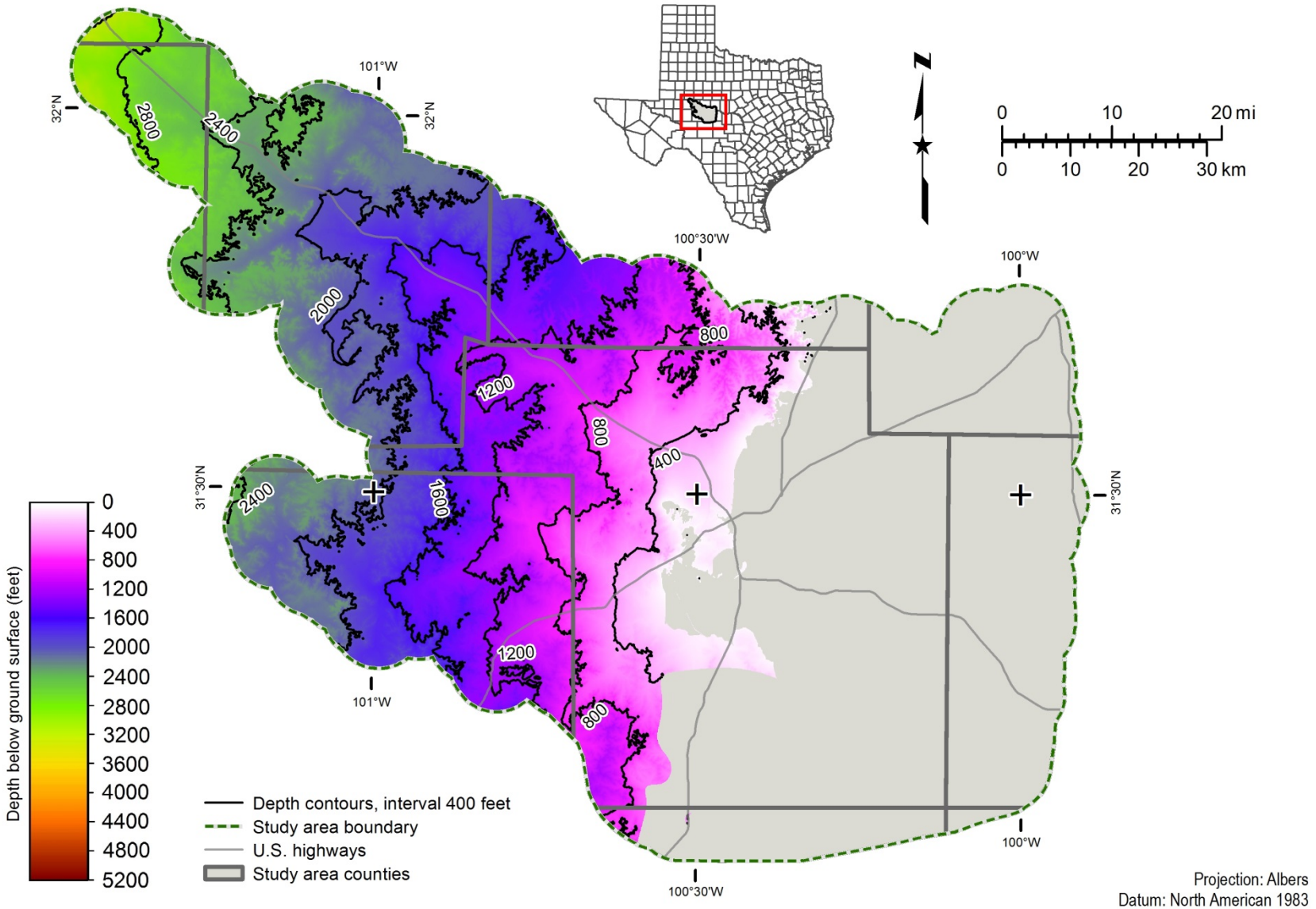

Figure 20.1-13. San Angelo Formation top (depth below ground surface, feet) in the Lipan Aquifer study area. Gray area in map represents places where the top of the San Angelo Formation does not occur.

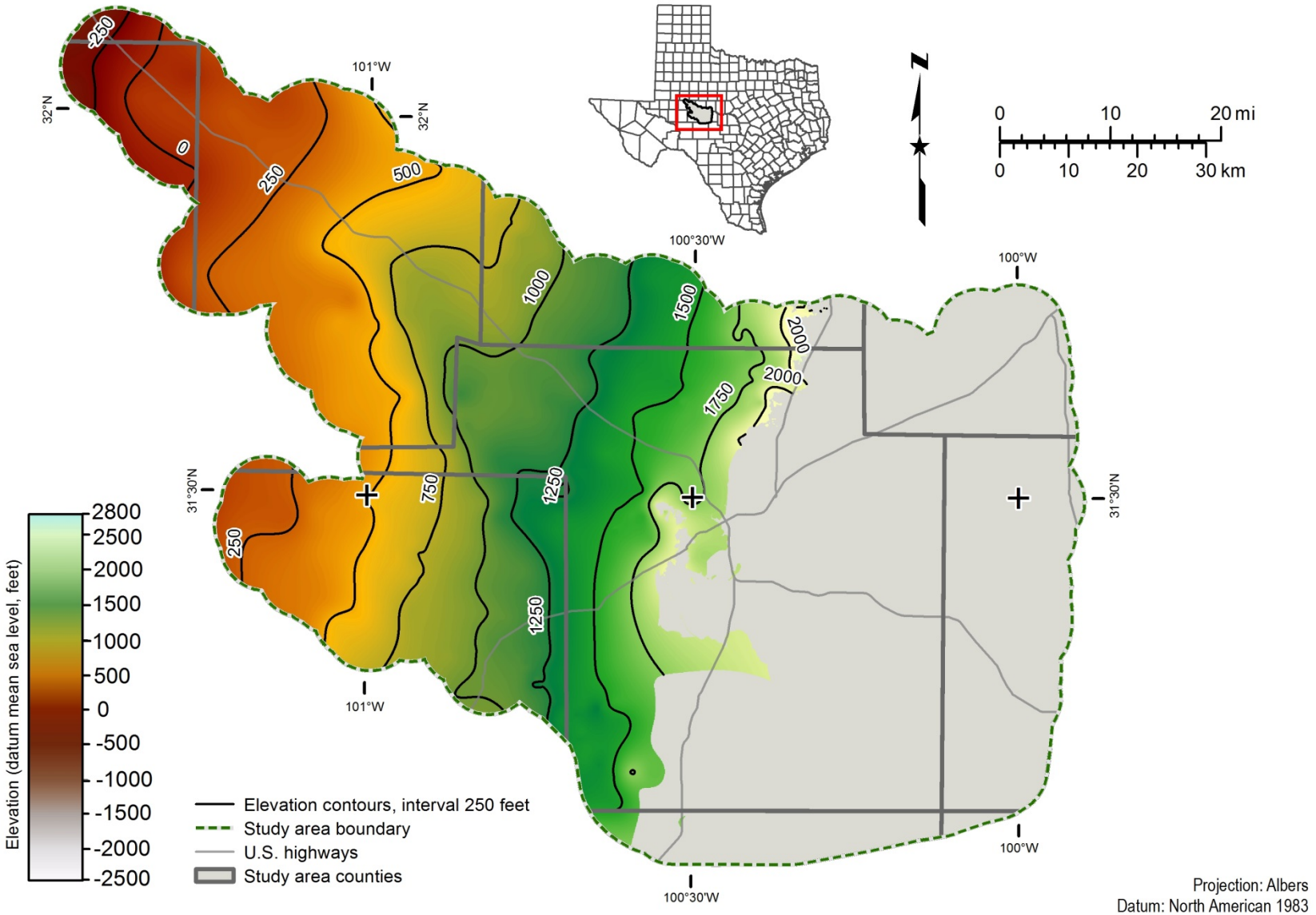

Figure 20.1-14. San Angelo Formation top (elevation datum mean sea level, feet) in the Lipan Aquifer study area. Gray area in map represents places where the top of the San Angelo Formation does not occur.

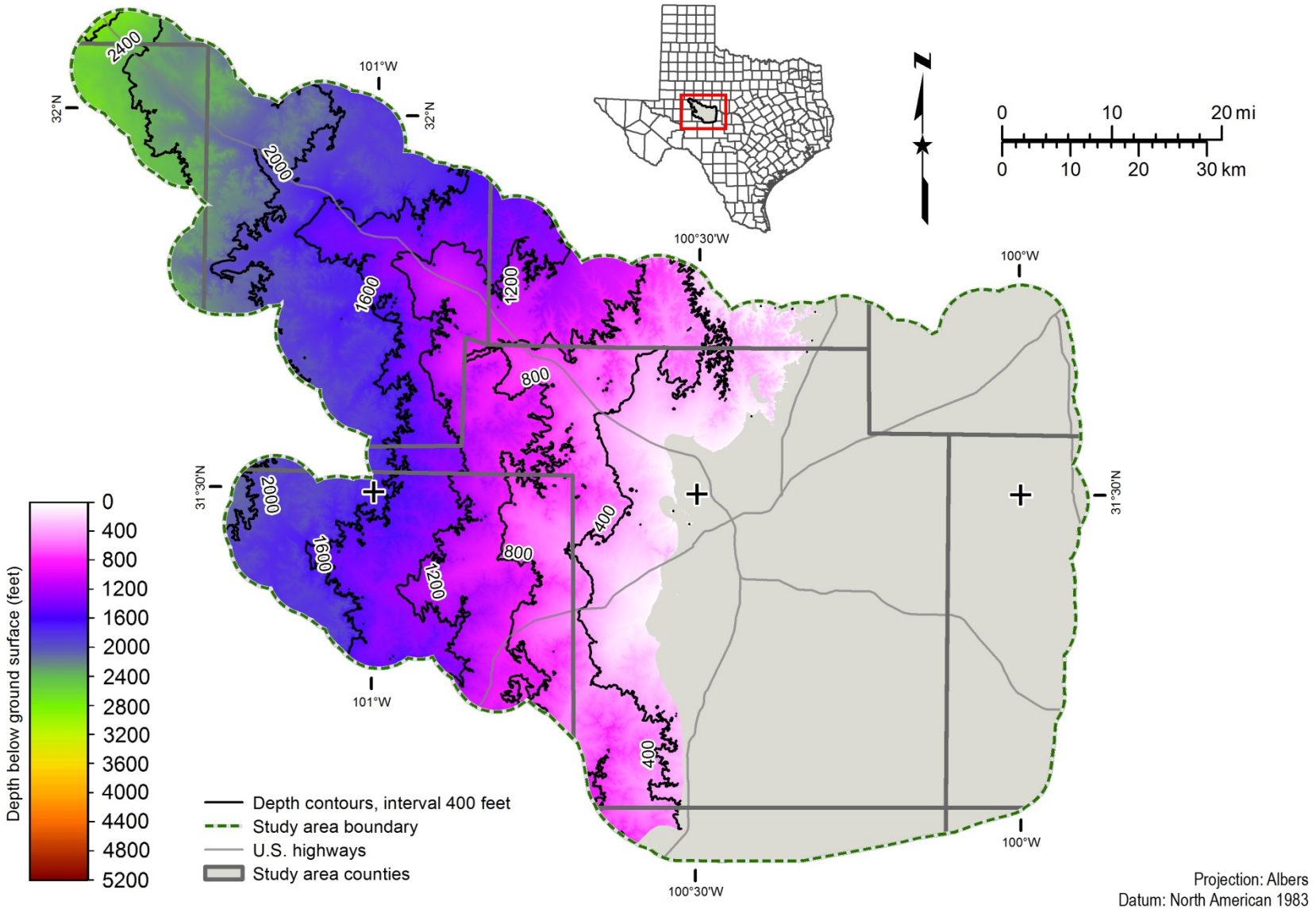

Figure 20.1-15. San Andres Formation top (depth below ground surface, feet) in the Lipan Aquifer study area. Gray area in map represents places where the top of the San Andres Formation does not occur.

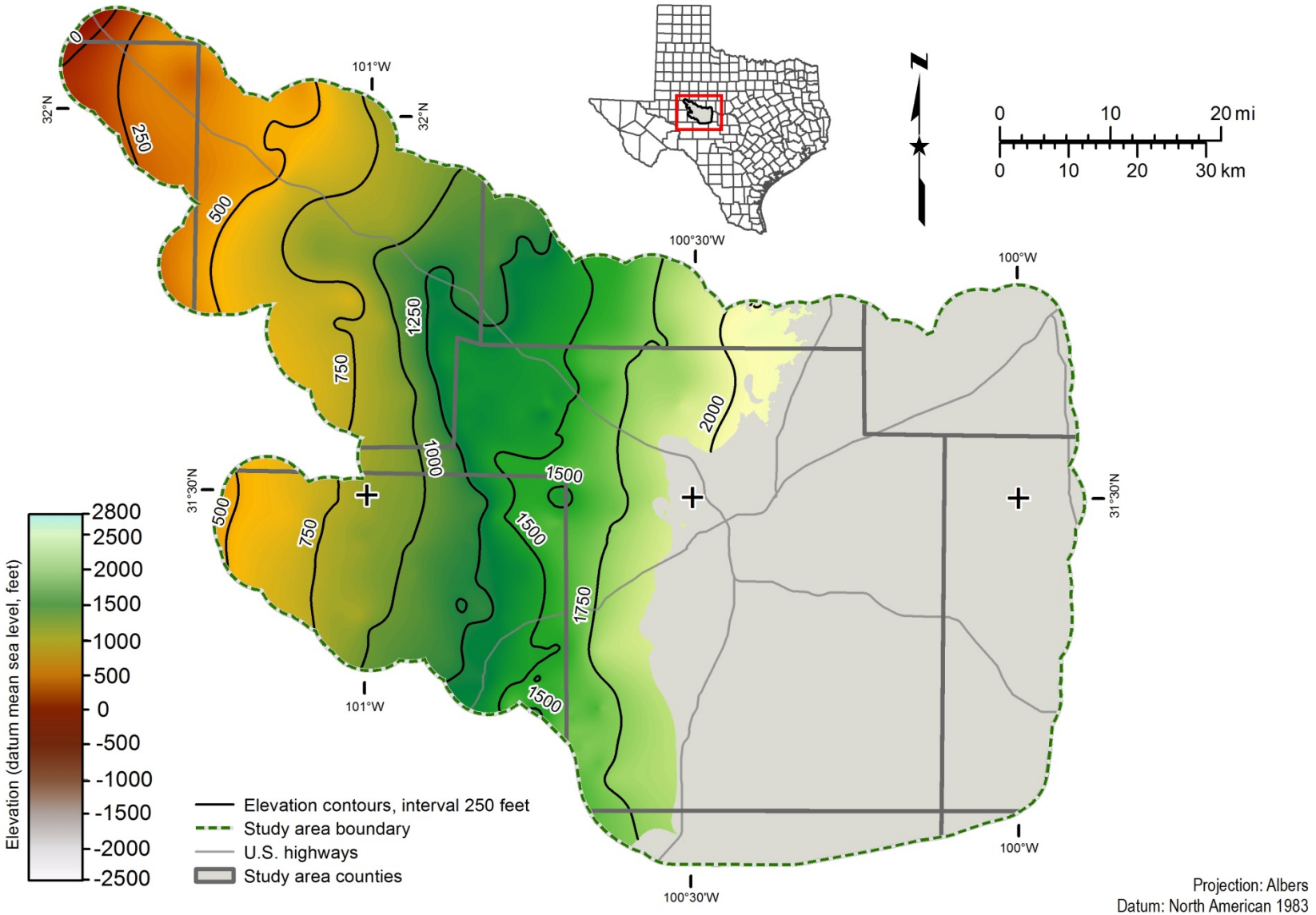

Figure 20.1-16. San Andres Formation top (elevation datum mean sea level, feet) in the Lipan Aquifer study area. Gray area in map represents places where the top of the San Andres Formation does not occur.

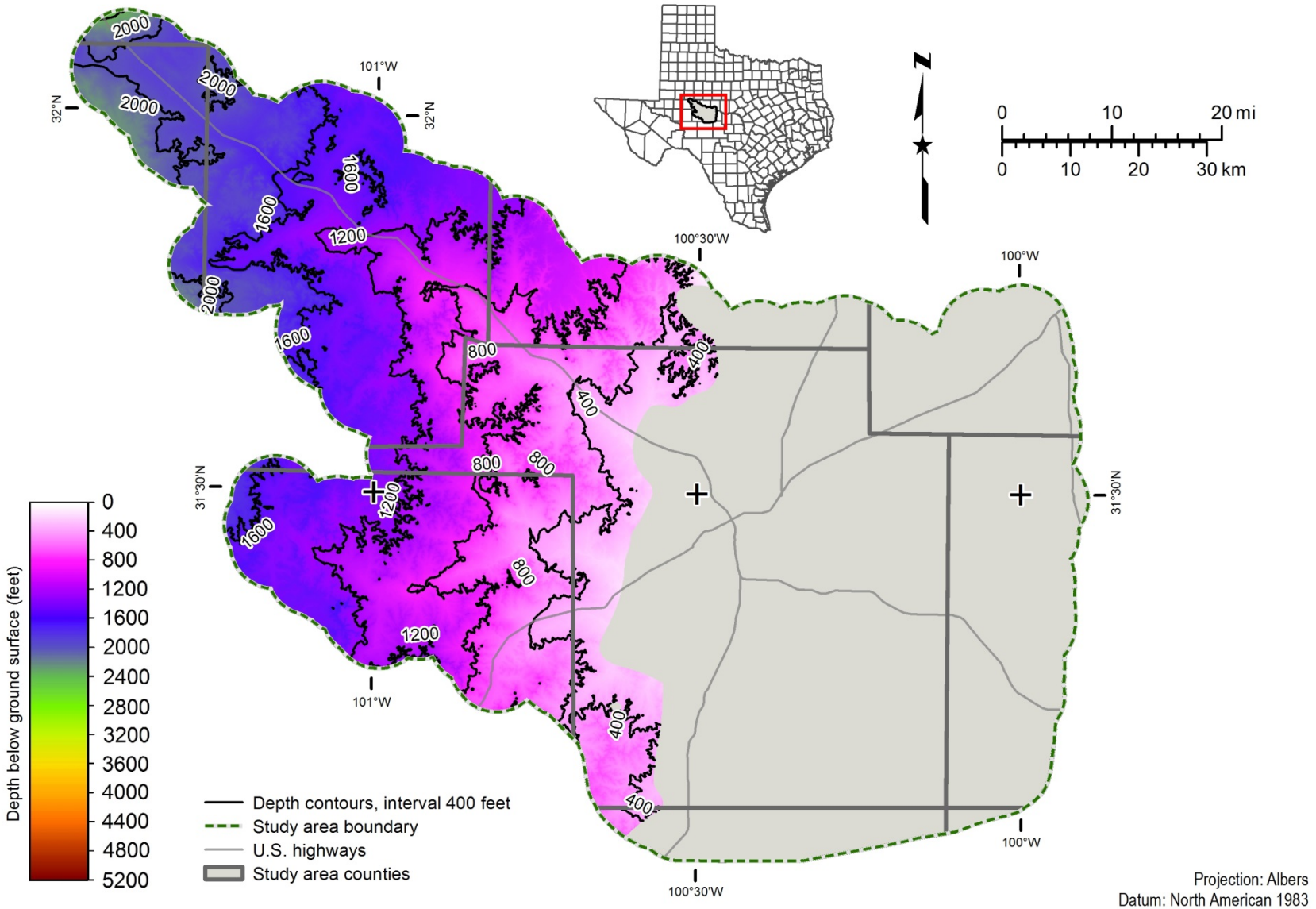

Figure 20.1-17. Grayburg Formation top (depth below ground surface, feet) in the Lipan Aquifer study area. Gray area in map represents places where the top of the Grayburg Formation does not occur.

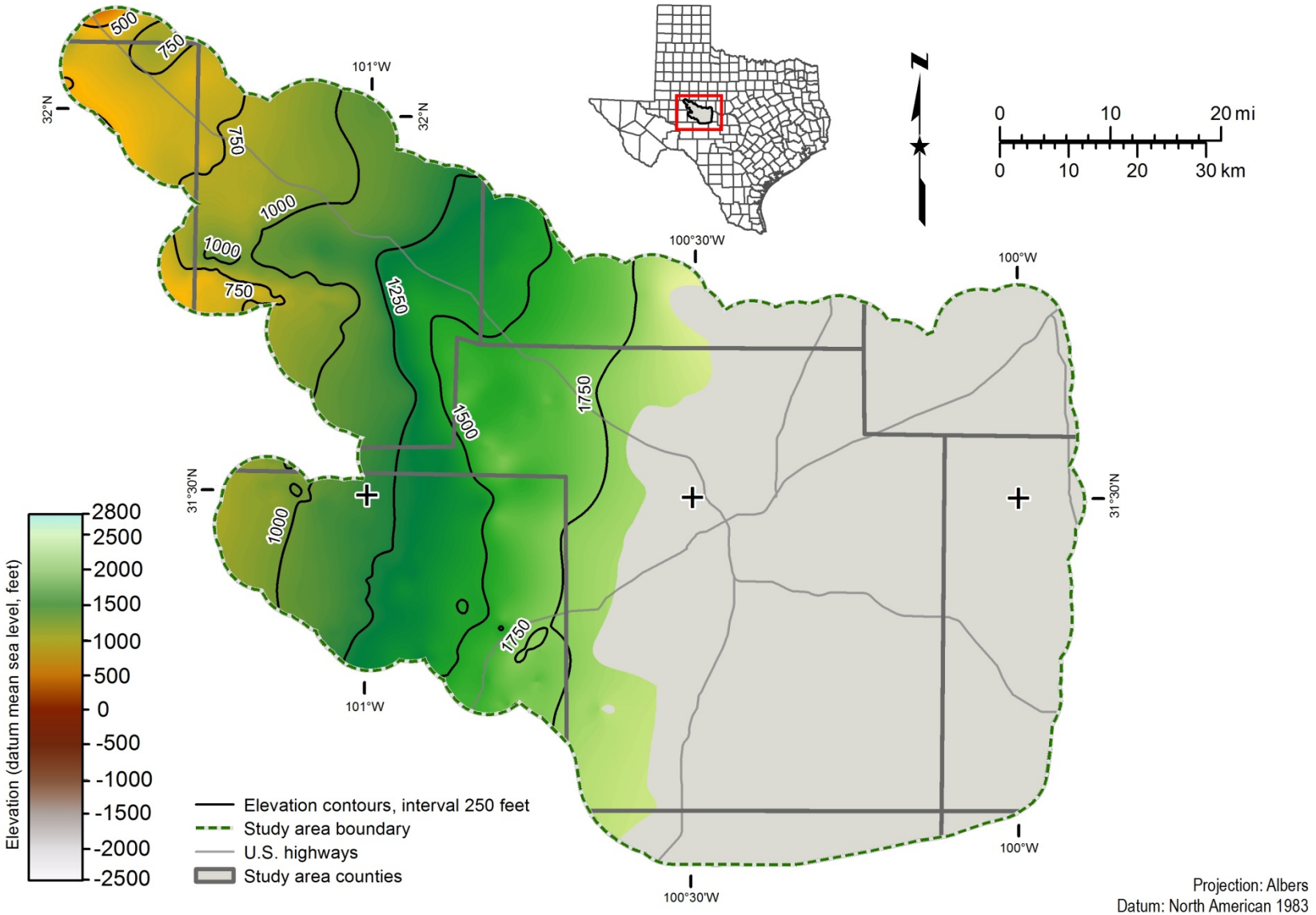

Figure 20.1-18. Grayburg Formation top (elevation datum mean sea level, feet) in the Lipan Aquifer study area. Gray area in map represents places where the top of the Grayburg Formation does not occur.

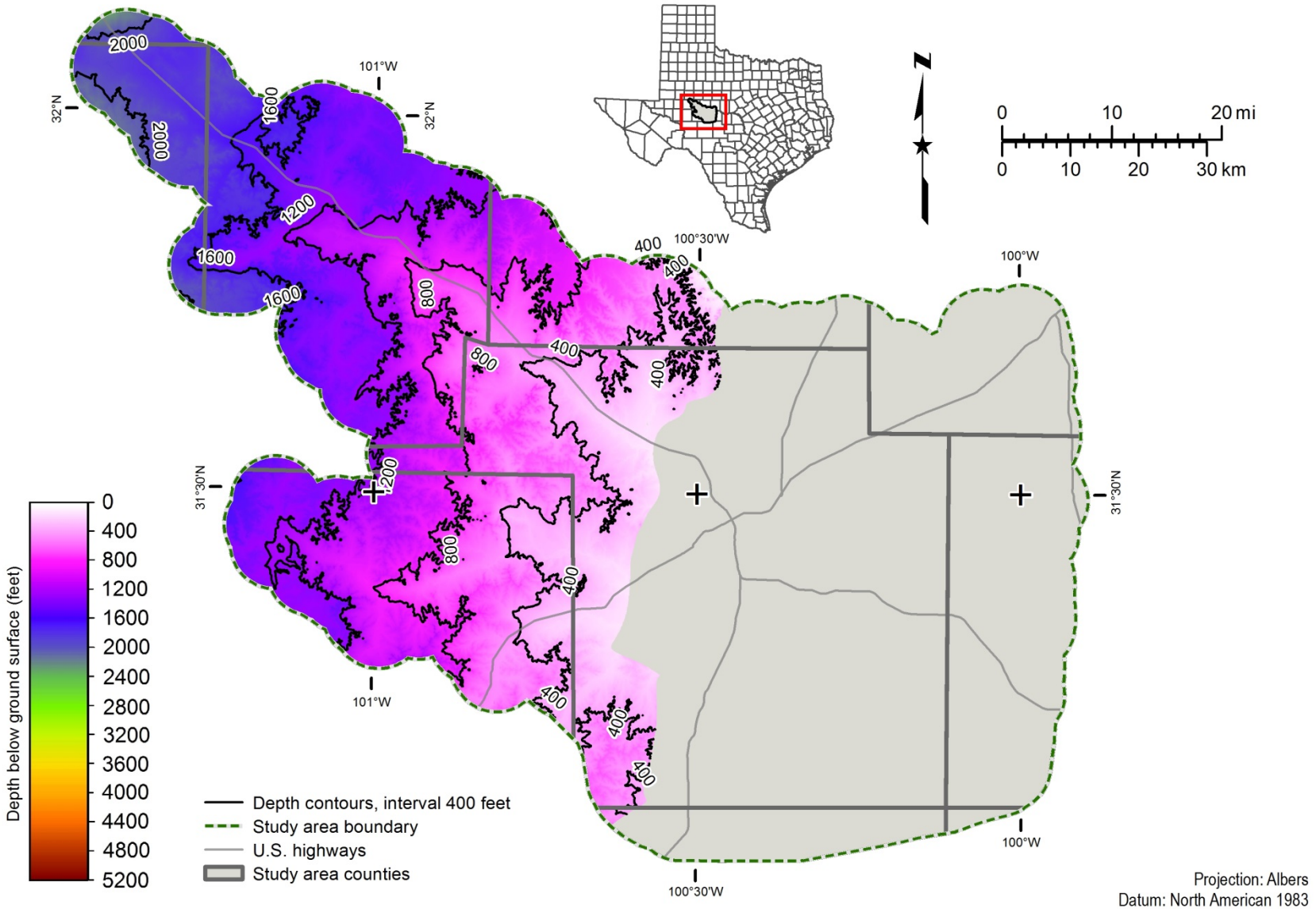

Figure 20.1-19. Queen Formation top (depth below ground surface, feet) in the Lipan Aquifer study area. Gray area in map represents places where the top of the Queen Formation does not occur.

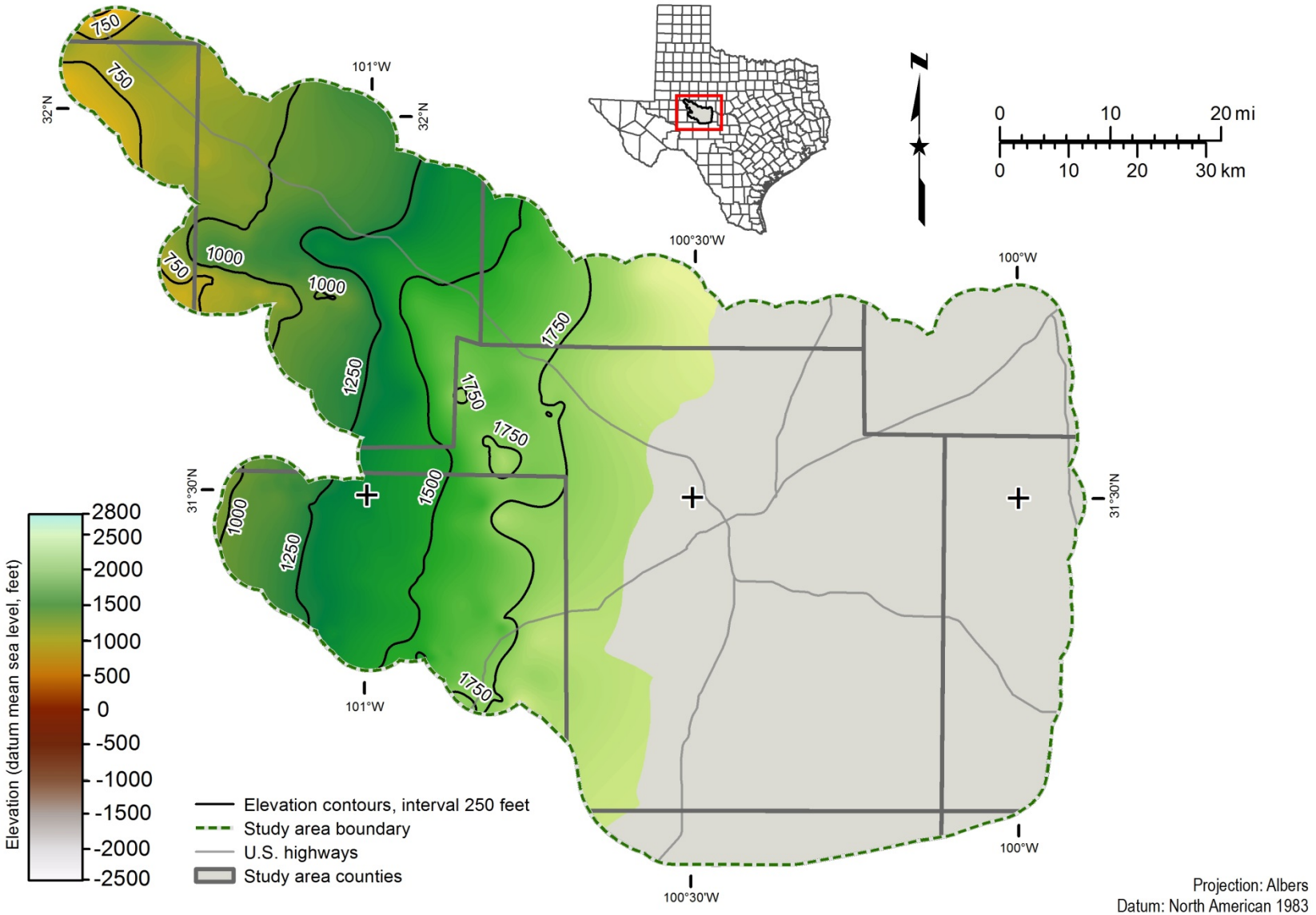

Figure 20.1-20. Queen Formation top (elevation datum mean sea level, feet) in the Lipan Aquifer study area. Gray area in map represents places where the top of the Queen Formation does not occur.

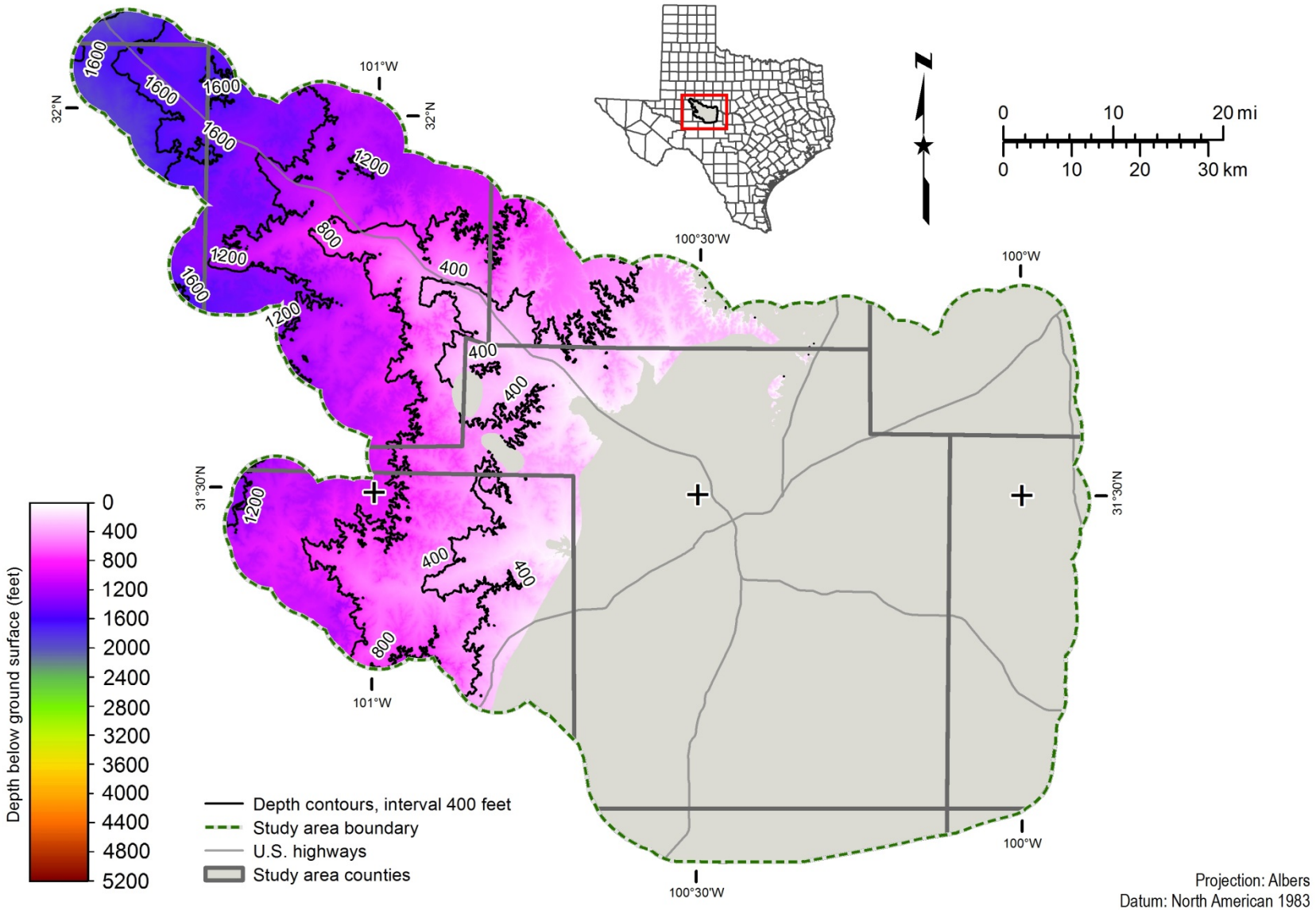

Figure 20.1-21. Seven Rivers Formation top (depth below ground surface, feet) in the Lipan Aquifer study area. Gray area in map represents places where the top of the Seven Rivers Formation does not occur.

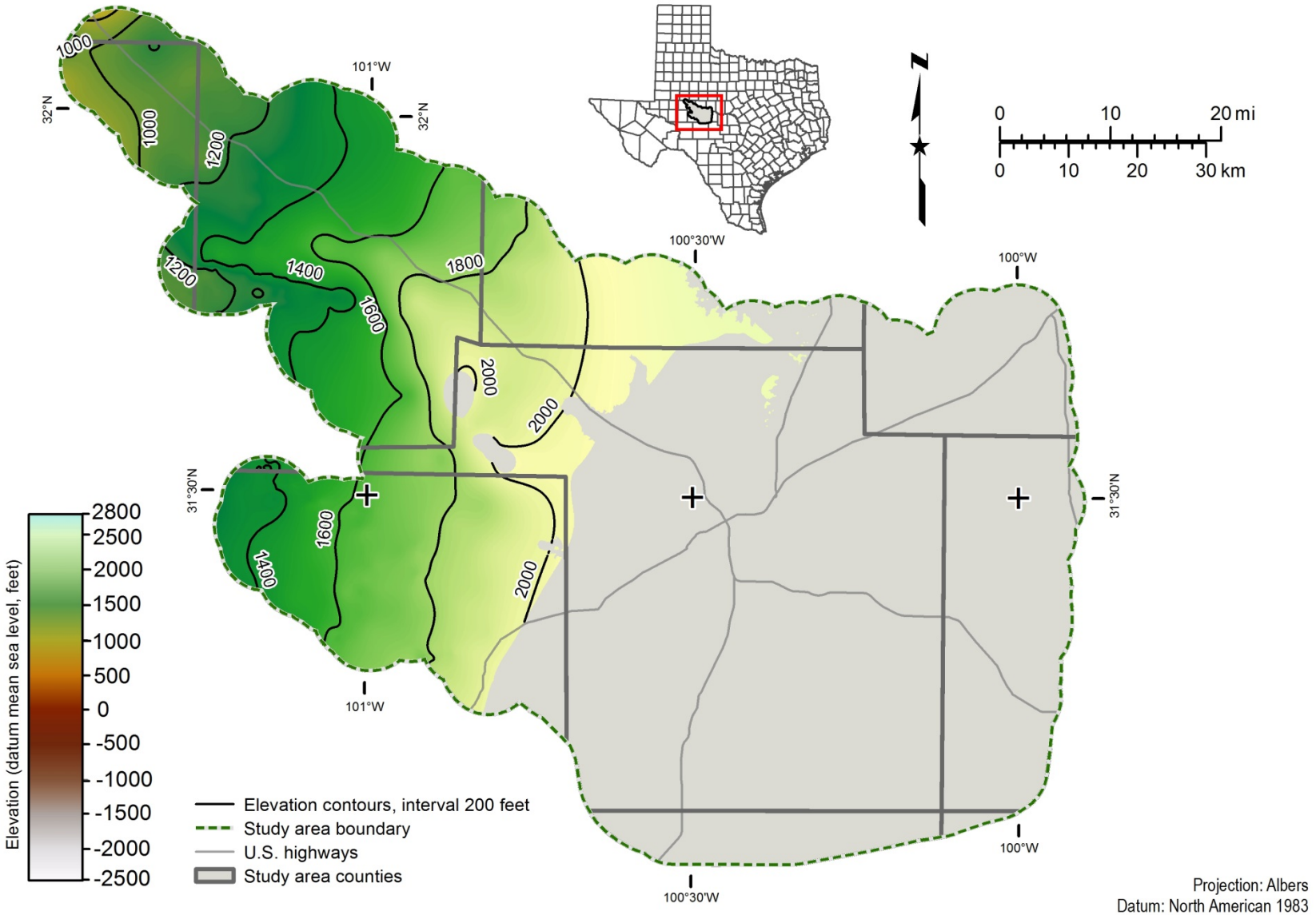

Figure 20.1-22. Seven Rivers Formation top (elevation datum mean sea level, feet) in the Lipan Aquifer study area. Gray area in map represents places where the top of the Seven Rivers Formation does not occur.

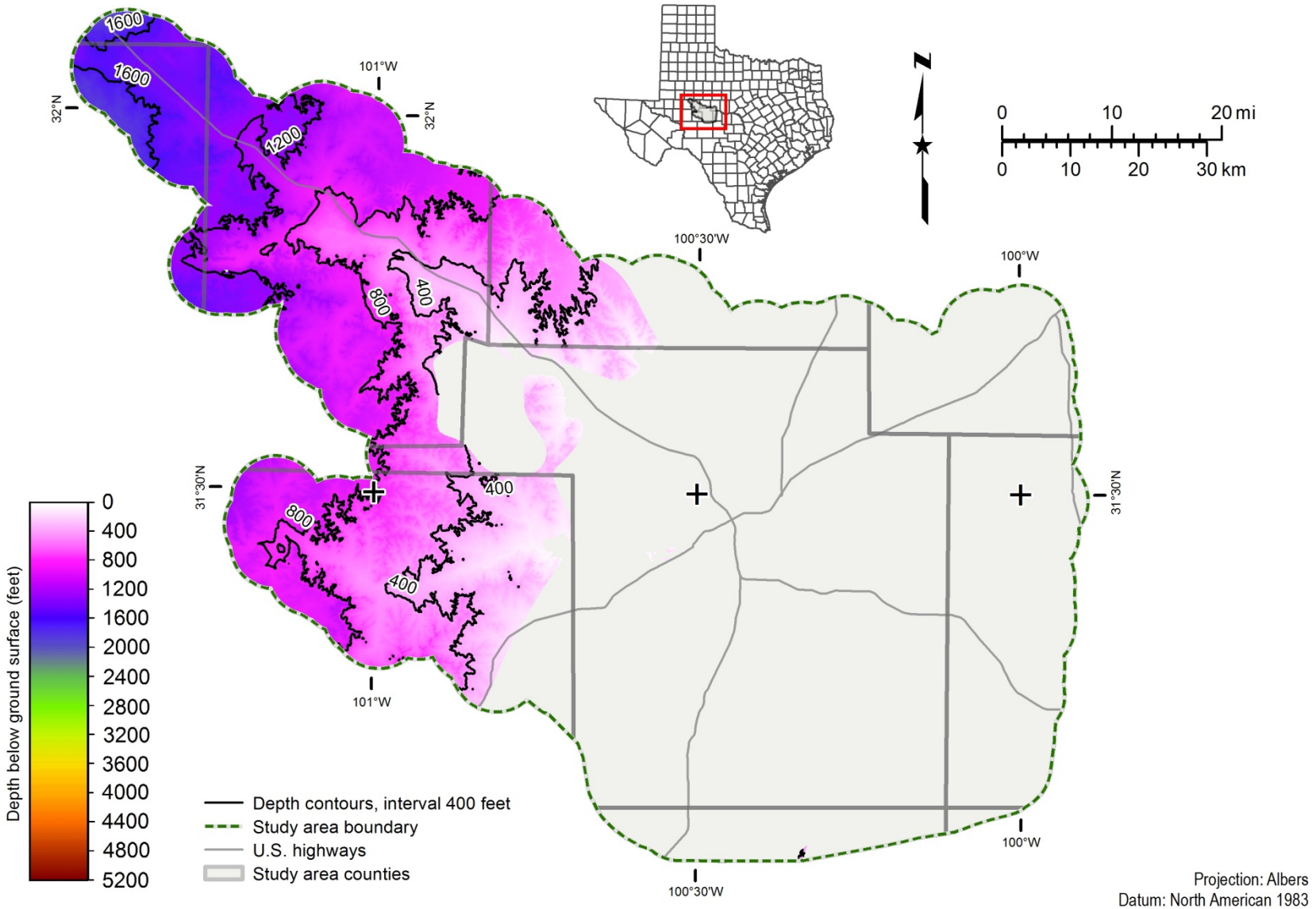

Figure 20.1-23. Yates Formation top (depth below ground surface, feet) in the Lipan Aquifer study area. Gray area in map represents places where the top of the Yates Formation does not occur.

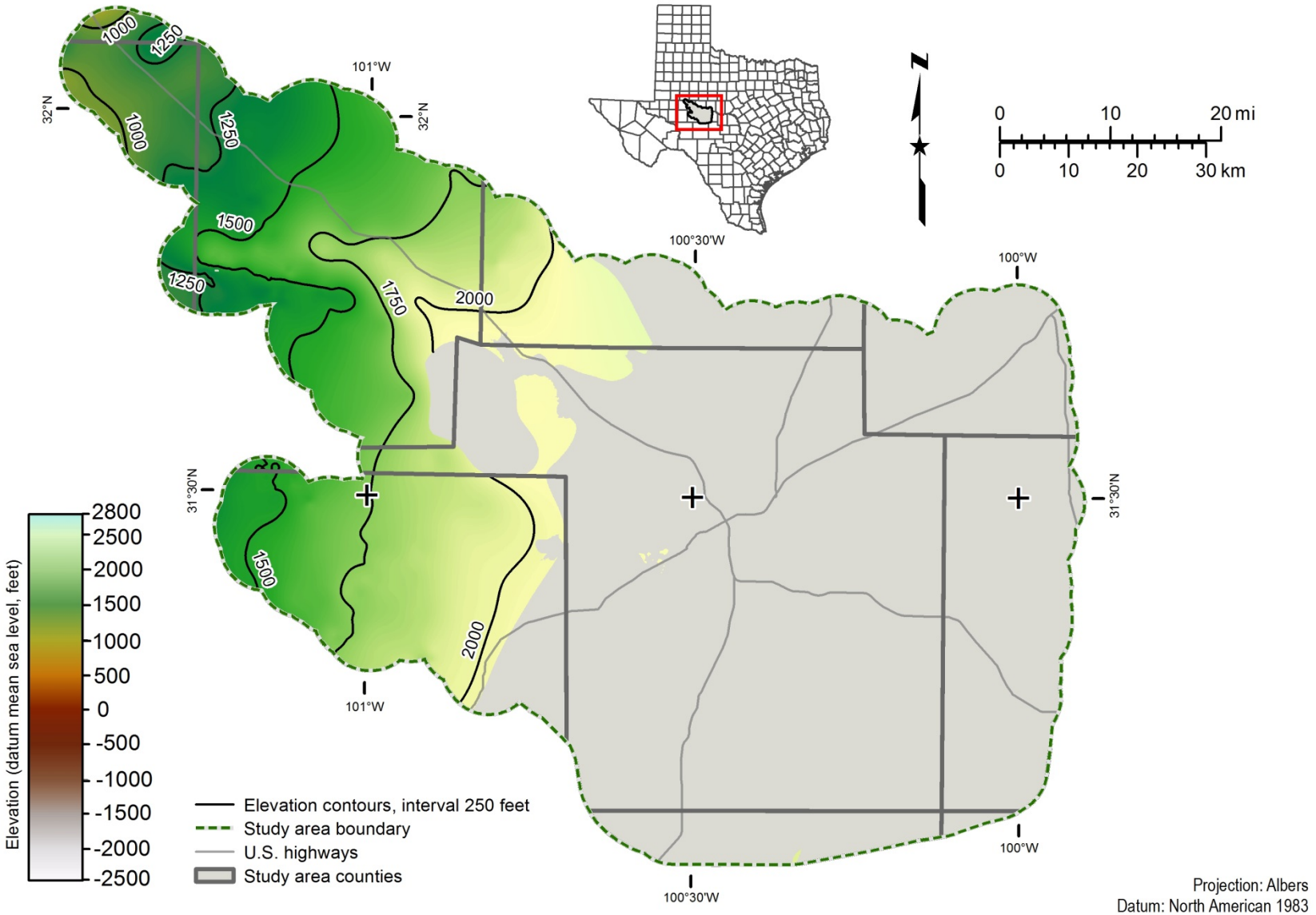

Figure 20.1-24. Yates Formation top (elevation datum mean sea level, feet) in the Lipan Aquifer study area. Gray area in map represents places where the top of the Yates Formation does not occur.

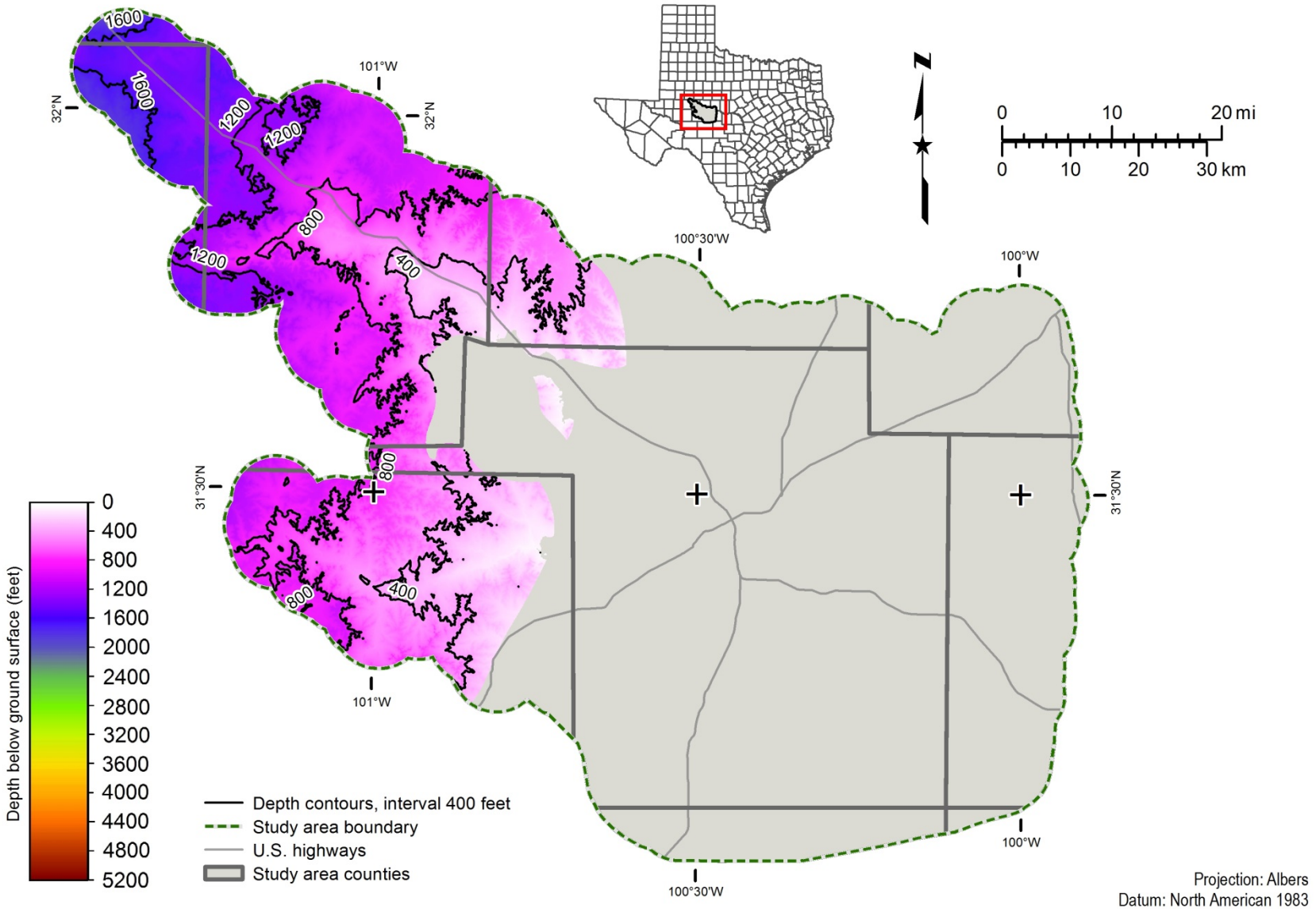

Figure 20.1-25. Tansill Formation top (depth below ground surface, feet) in the Lipan Aquifer study area. Gray area in map represents places where the top of the Tansill Formation does not occur.

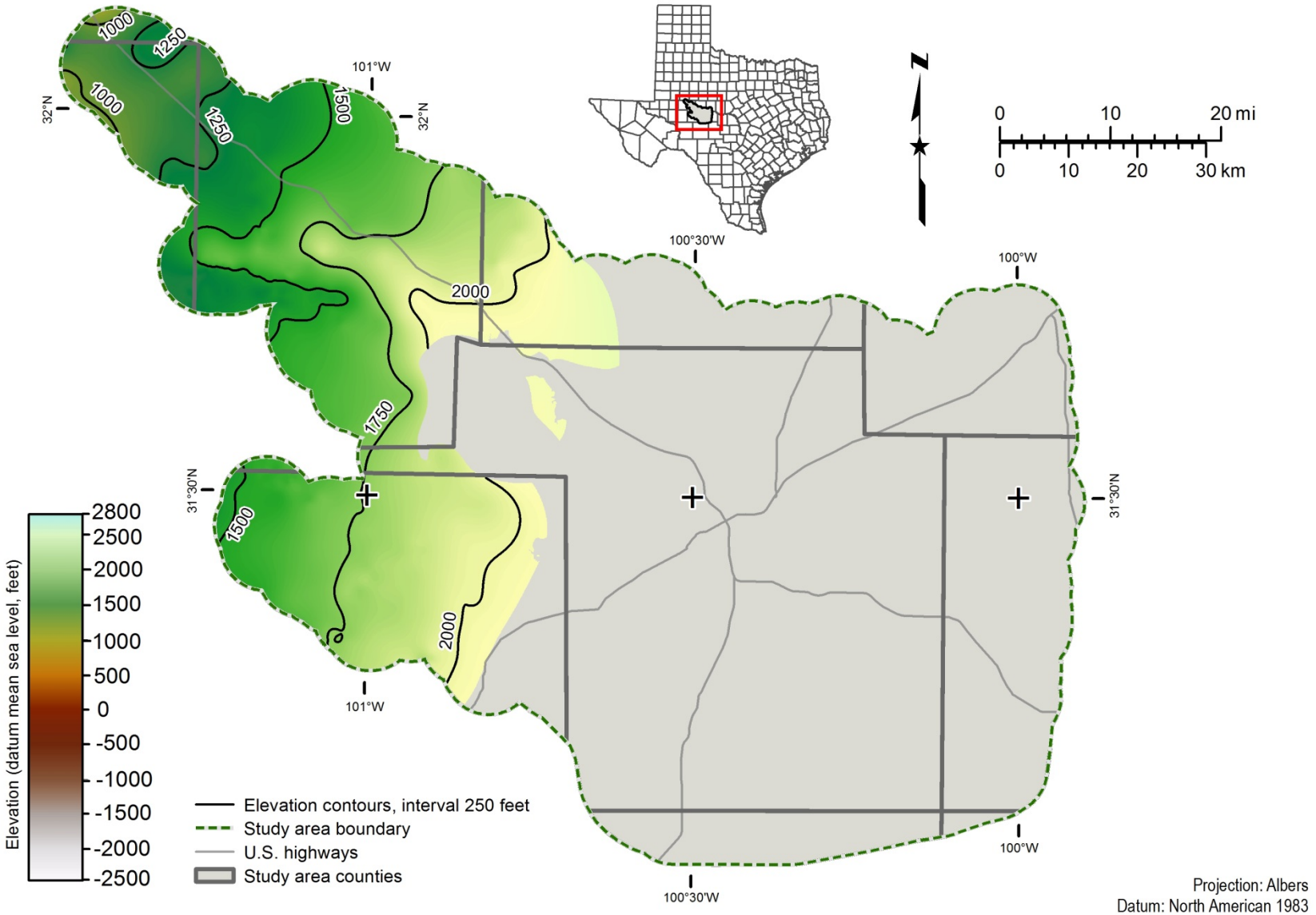

Figure 20.1-26. Tansill Formation top (elevation datum mean sea level, feet) in the Lipan Aquifer study area. Gray area in map represents places where the top of the Tansill Formation does not occur.

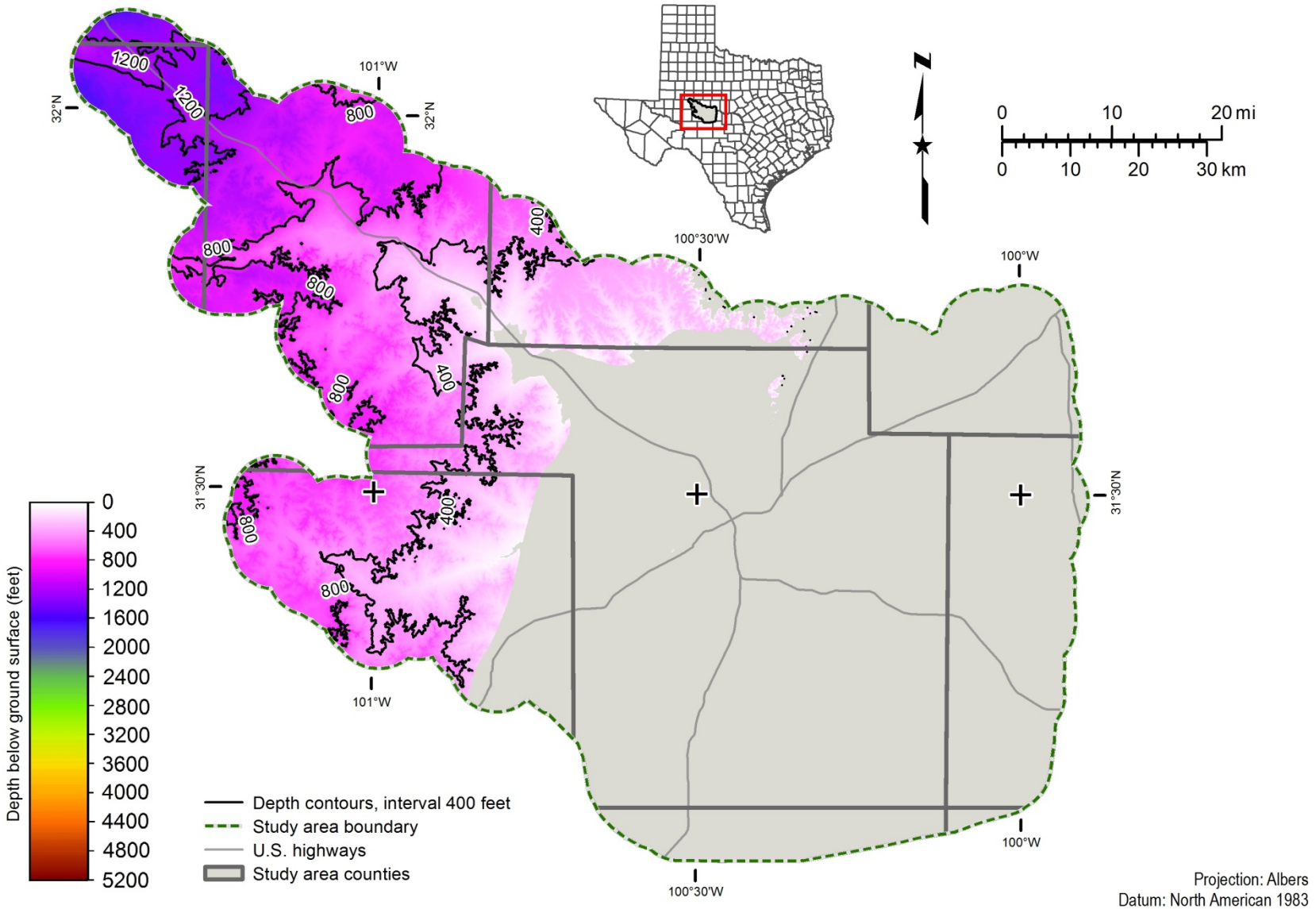

Figure 20.1-27. Rustler-Salado formations top (depth below ground surface, feet) in the Lipan Aquifer study area. Gray area in map represents places where the top of the Rustler-Salado formations does not occur.

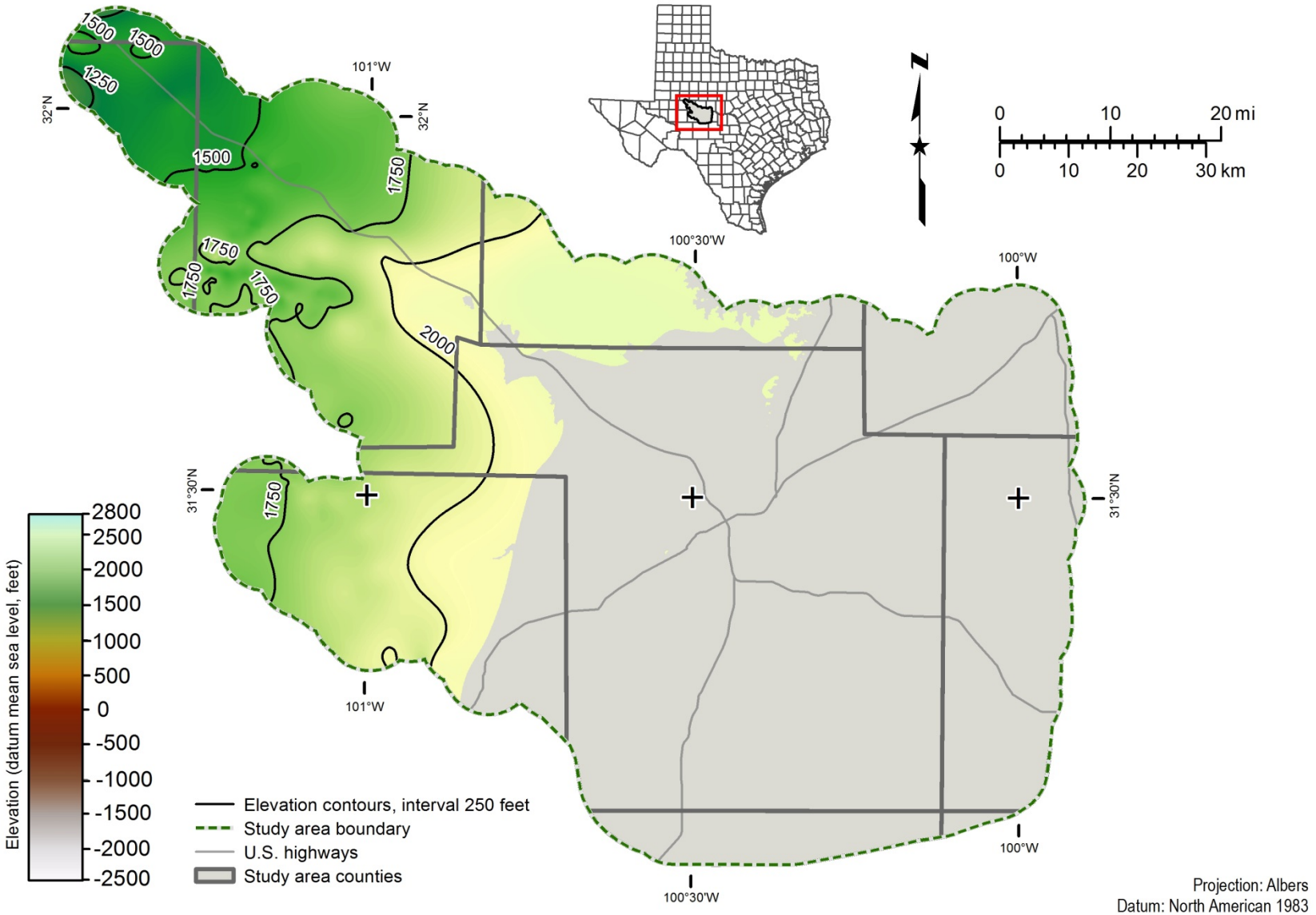

Figure 20.1-28. Rustler-Salado formations top (elevation datum mean sea level, feet) in the Lipan Aquifer study area. Gray area in map represents places where the top of the Rustler-Salado formations does not occur.

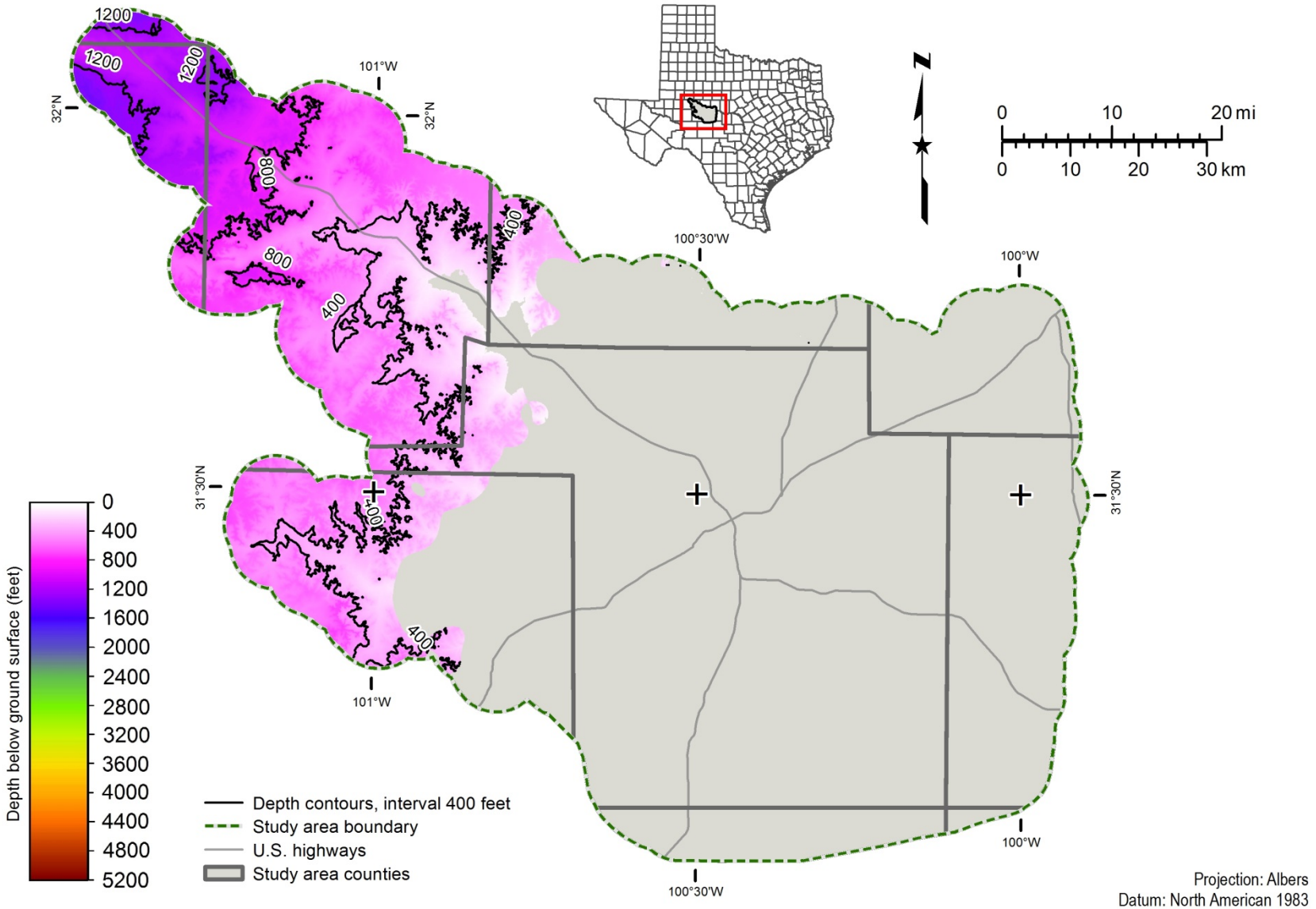

Figure 20.1-29. Dewey Lake Formation top (depth below ground surface, feet) in the Lipan Aquifer study area. Gray area in map represents places where the top of the Dewey Lake Formation does not occur.

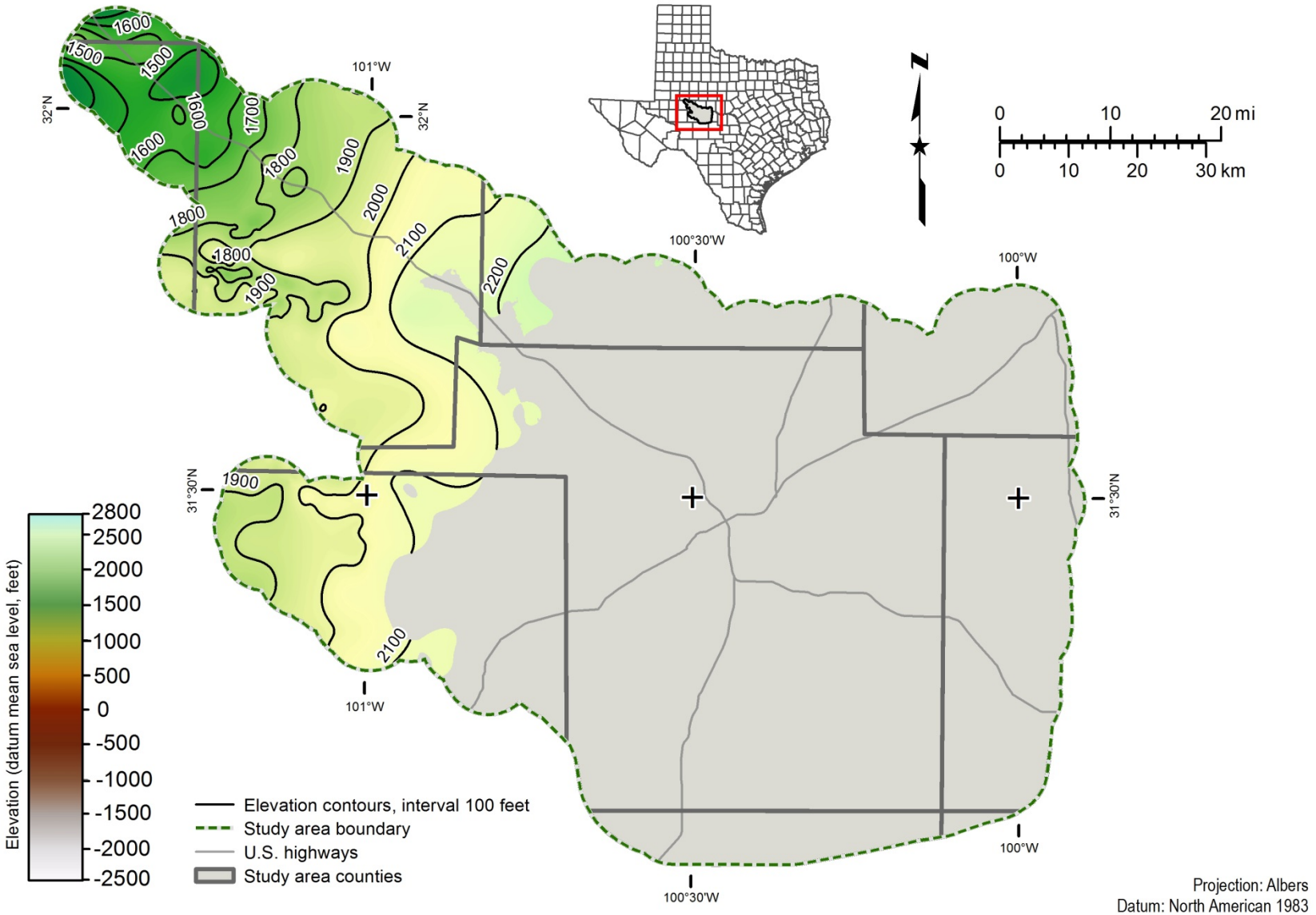

Figure 20.1-30. Dewey Lake Formation top (elevation datum mean sea level, feet) in the Lipan Aquifer study area. Gray area in map represents places where the top of the Dewey Lake Formation does not occur.

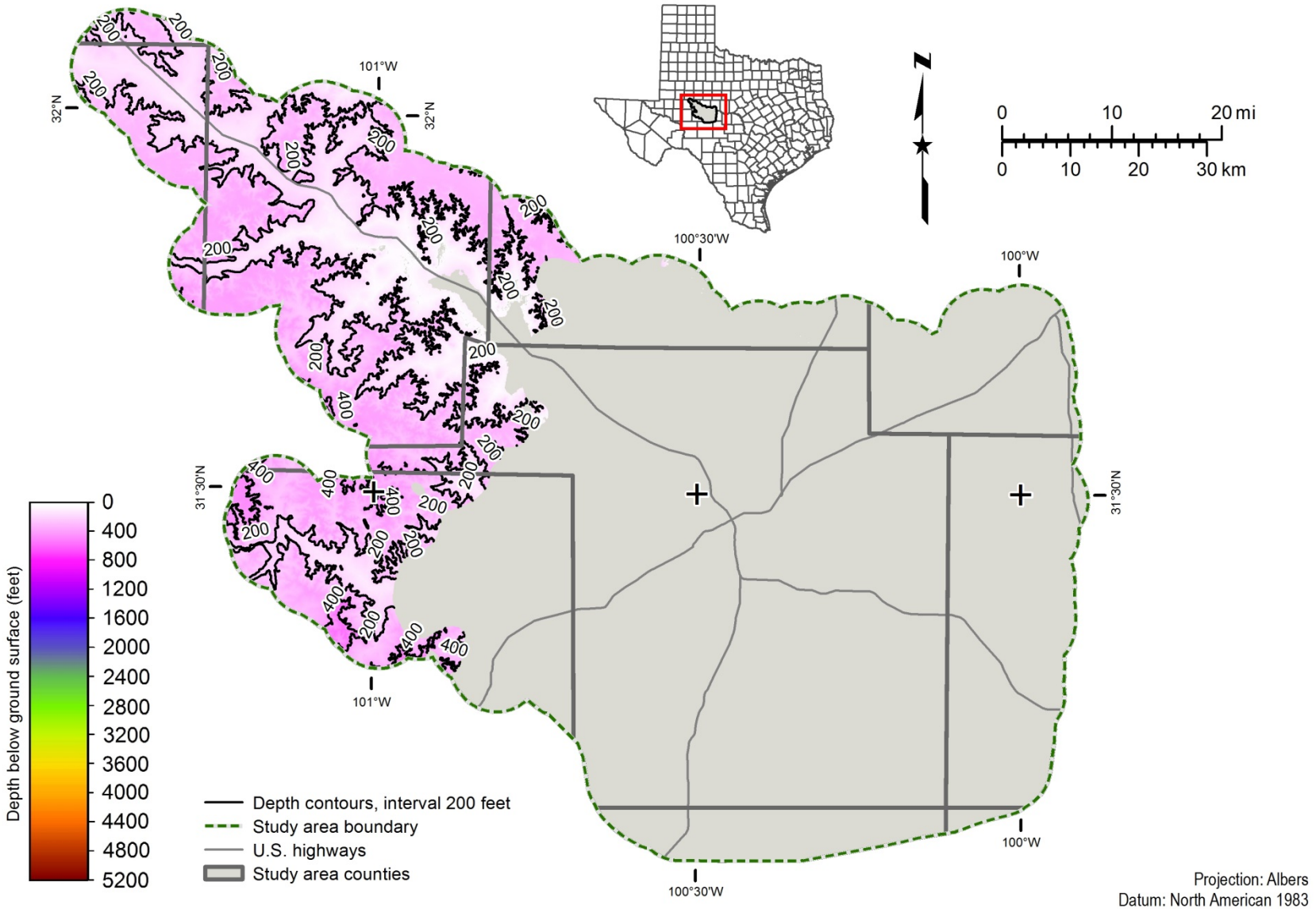

Figure 20.1-31. Dockum Group top (depth below ground surface, feet) in the Lipan Aquifer study area. Gray area in map represents places where the top of the Dockum Group does not occur. Note that the eastern subcrop extent is different than the official TWDB boundary.

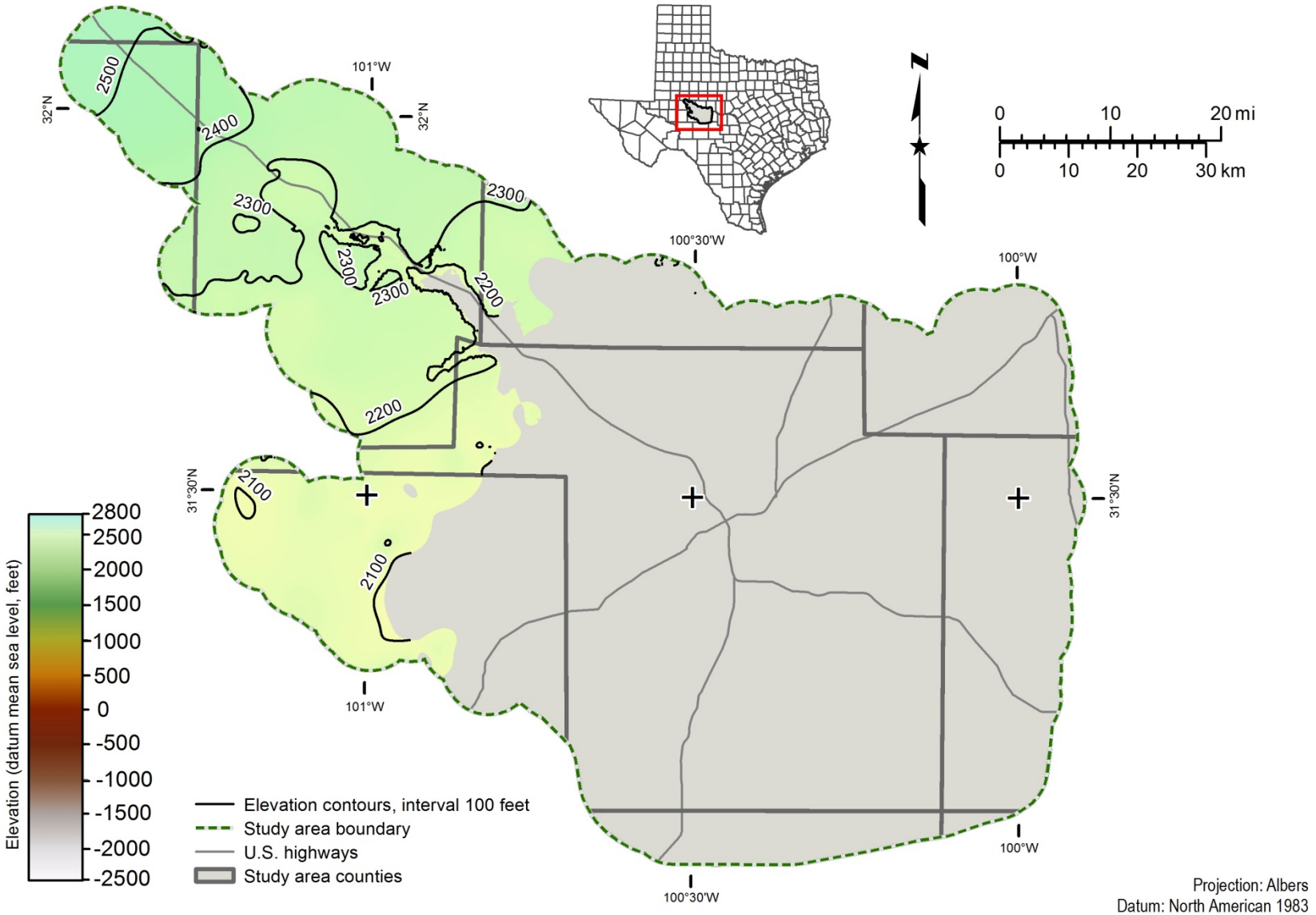

Figure 20.1-32. Dockum Group top (elevation datum mean sea level, feet) in the Lipan Aquifer study area. Gray area in map represents places where the top of the Dockum Group does not occur. Note that the eastern subcrop extent is different than the official TWDB boundary.

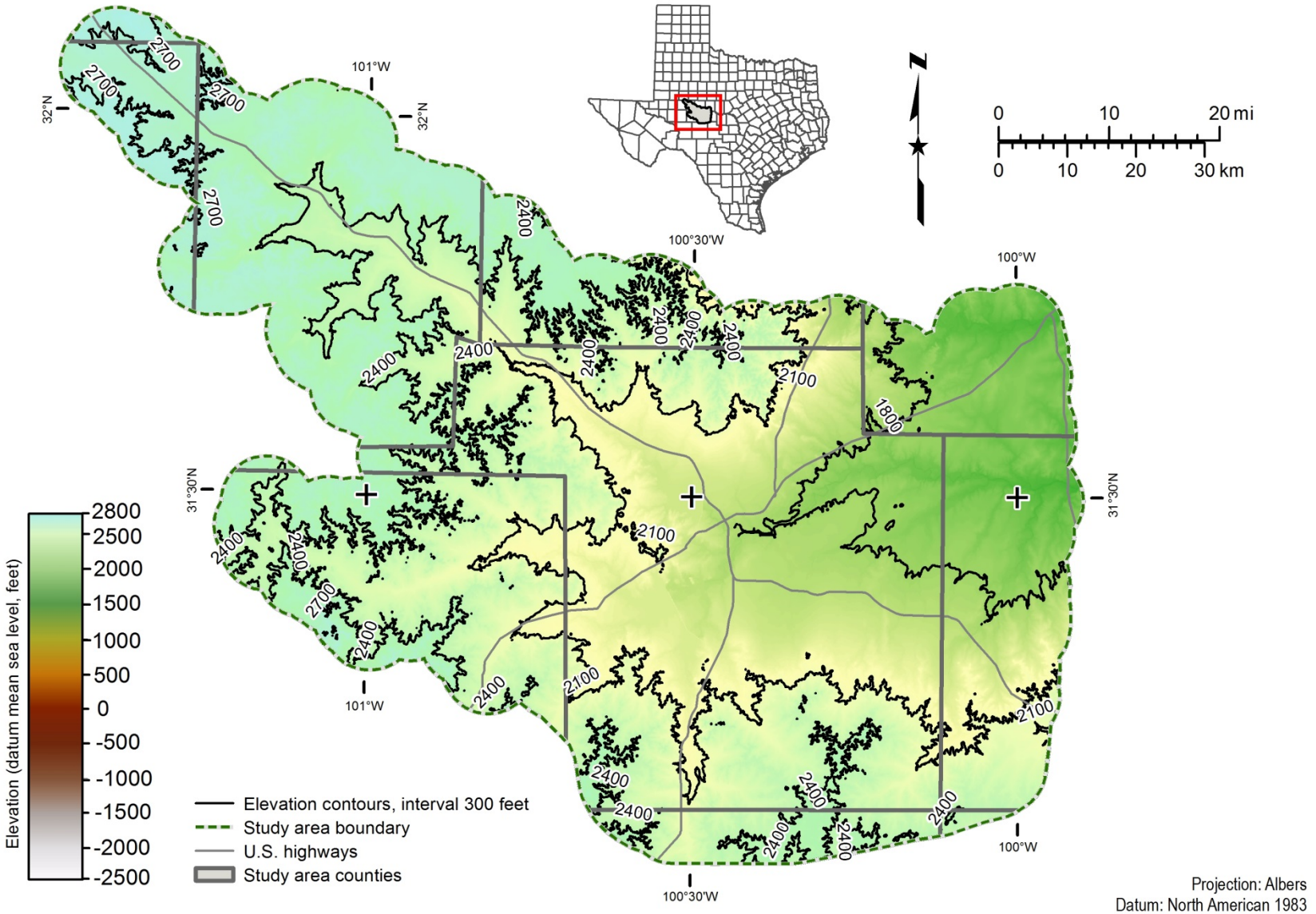

Figure 20.1-33. Ground surface (elevation datum mean sea level, feet) in the Lipan Aquifer study area.

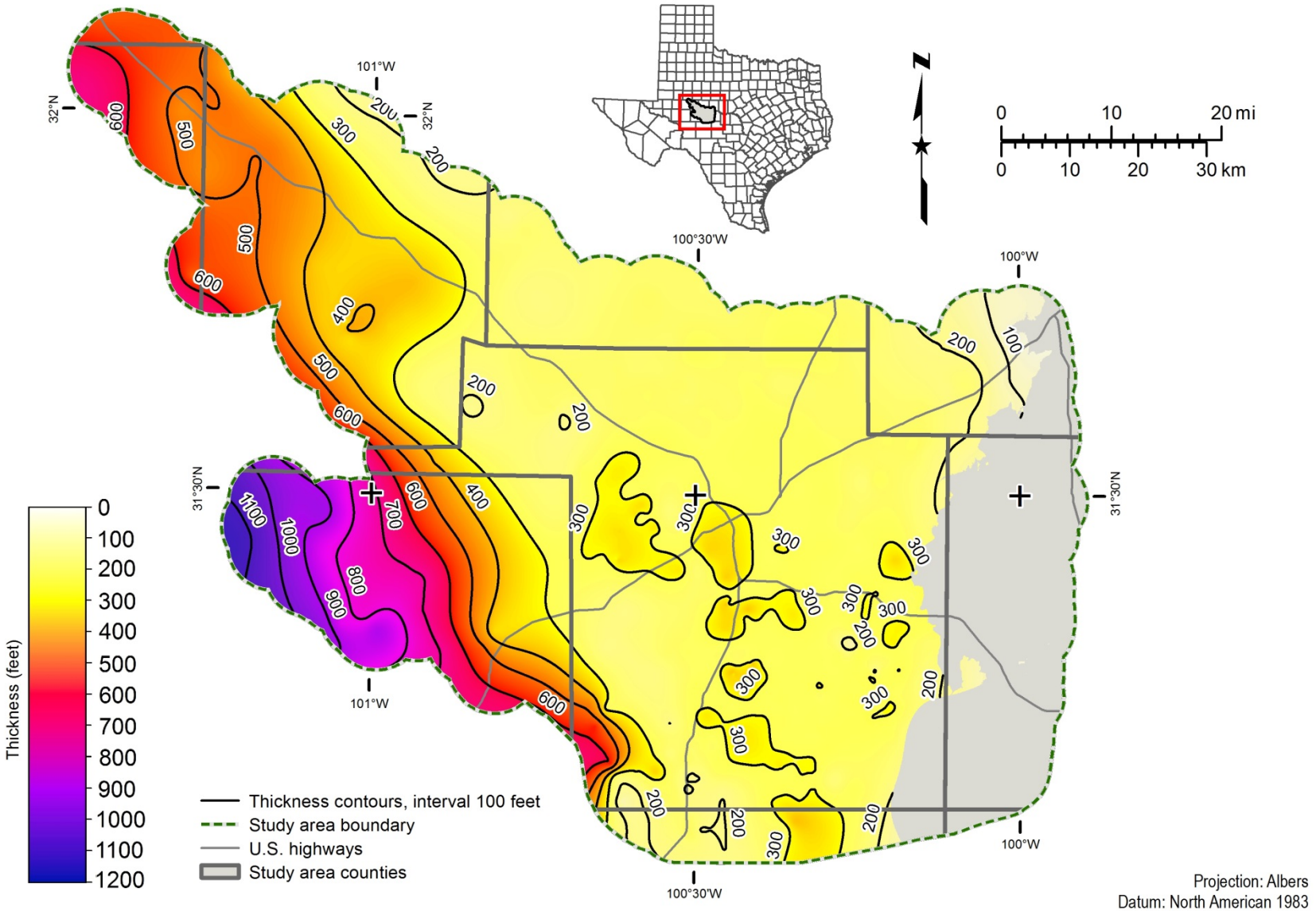

Figure 20.1-34. Isochore map of the Arroyo Formation in the Lipan Aquifer study area (thickness in feet). Gray area in map represents places where the top of the Arroyo Formation does not occur.

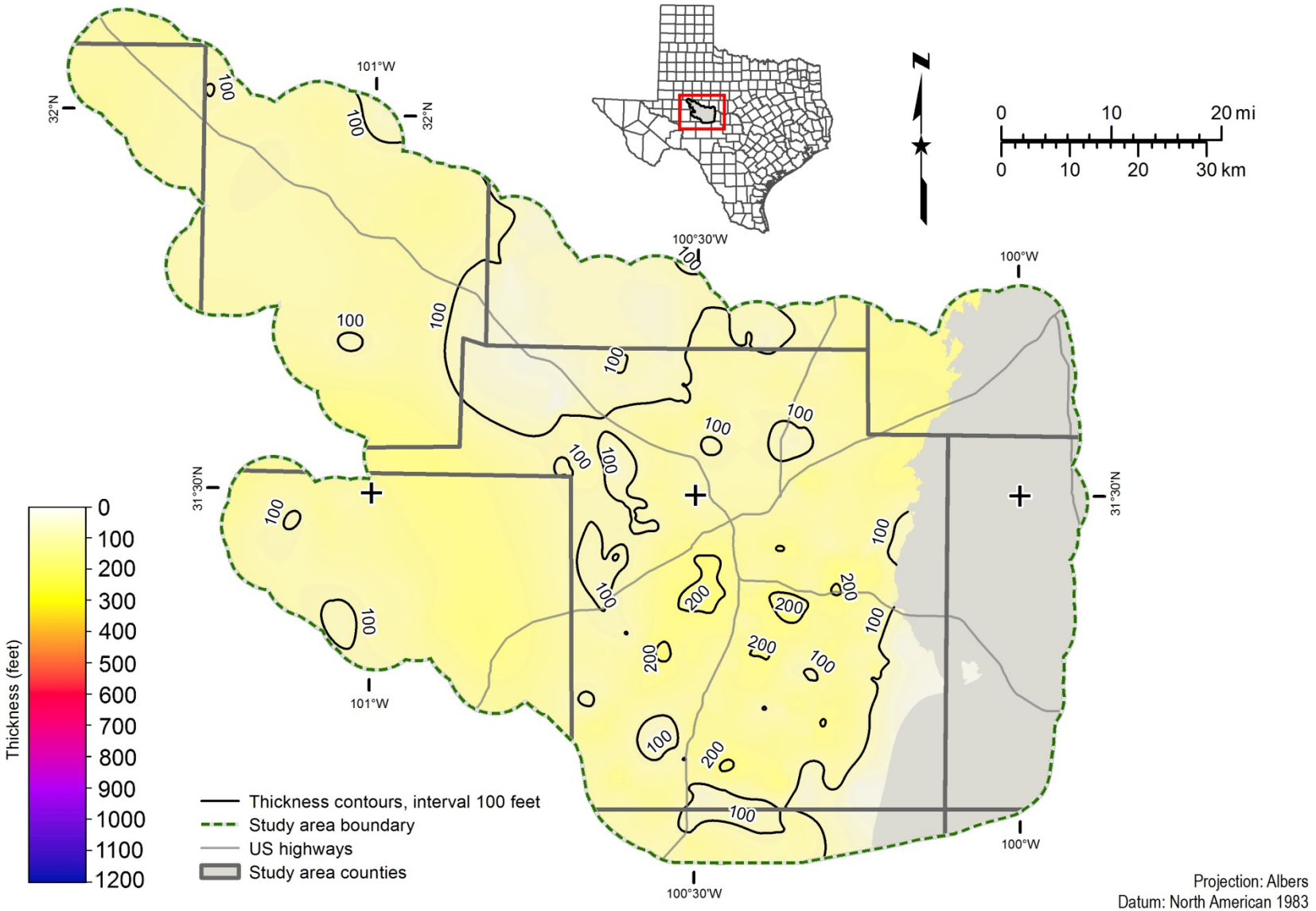

Figure 20.1-35. Isochore map of the Vale Shale member in the Lipan Aquifer study area (thickness in feet). Gray area in map represents places where the top of the Vale Shale member does not occur.

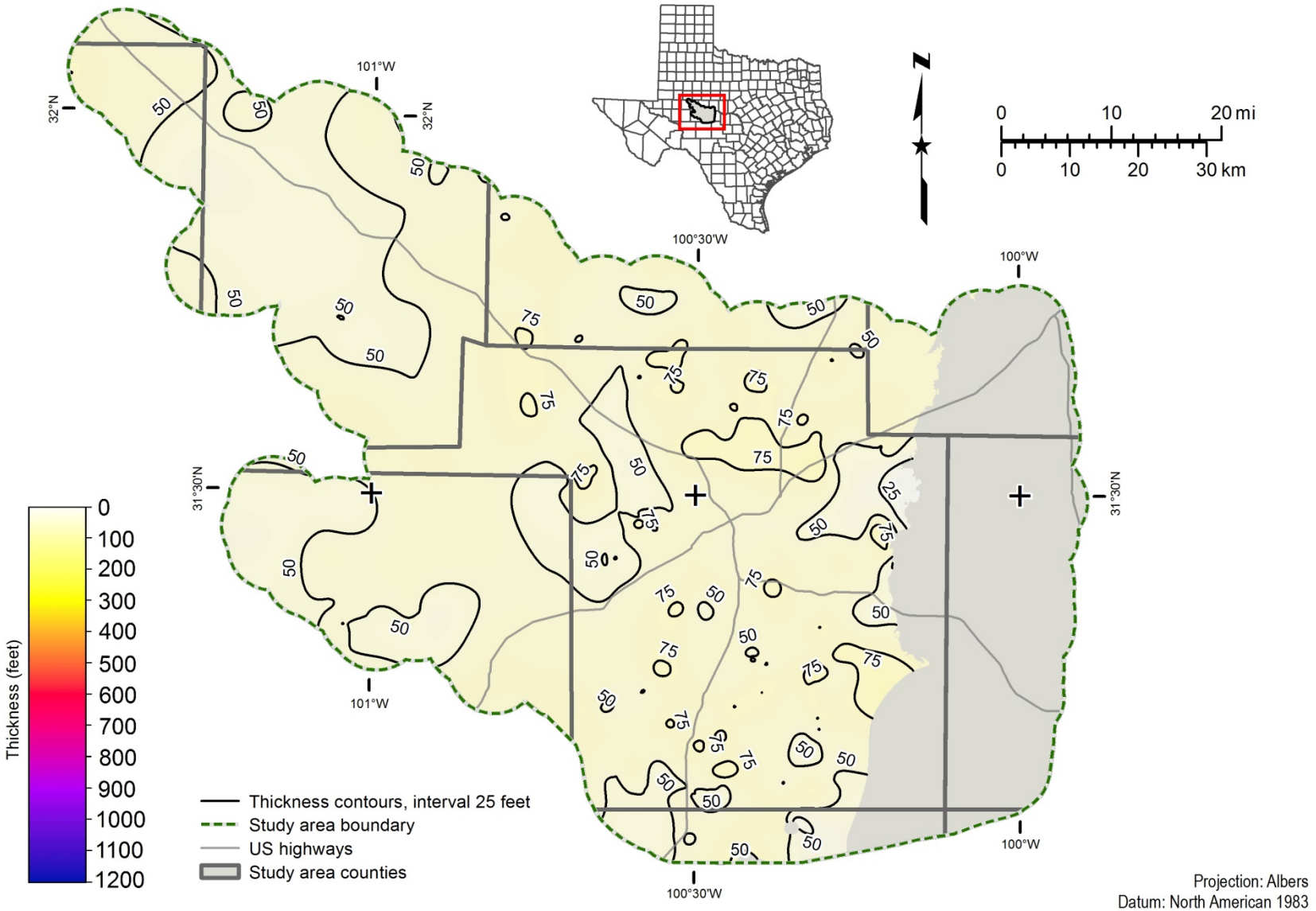

Figure 20.1-36. Isochore map of the Bullwagon Dolomite in the Lipan Aquifer study area (thickness in feet). Gray area in map represents places where the top of the Bullwagon Dolomite does not occur.

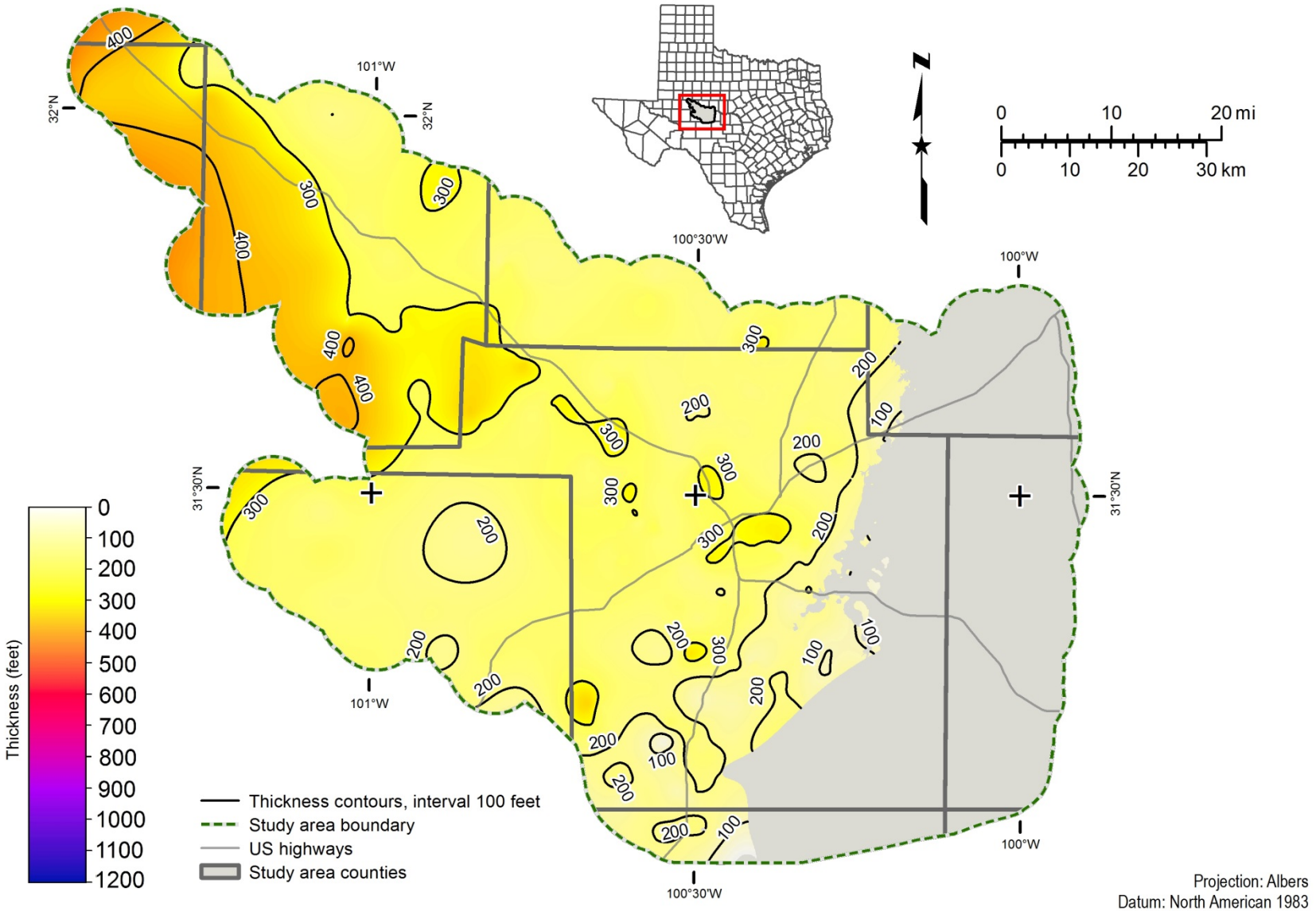

Figure 20.1-37. Isochore map of the Tubb member in the Lipan Aquifer study area (thickness in feet). Gray area in map represents places where the top of the Tubb member does not occur.

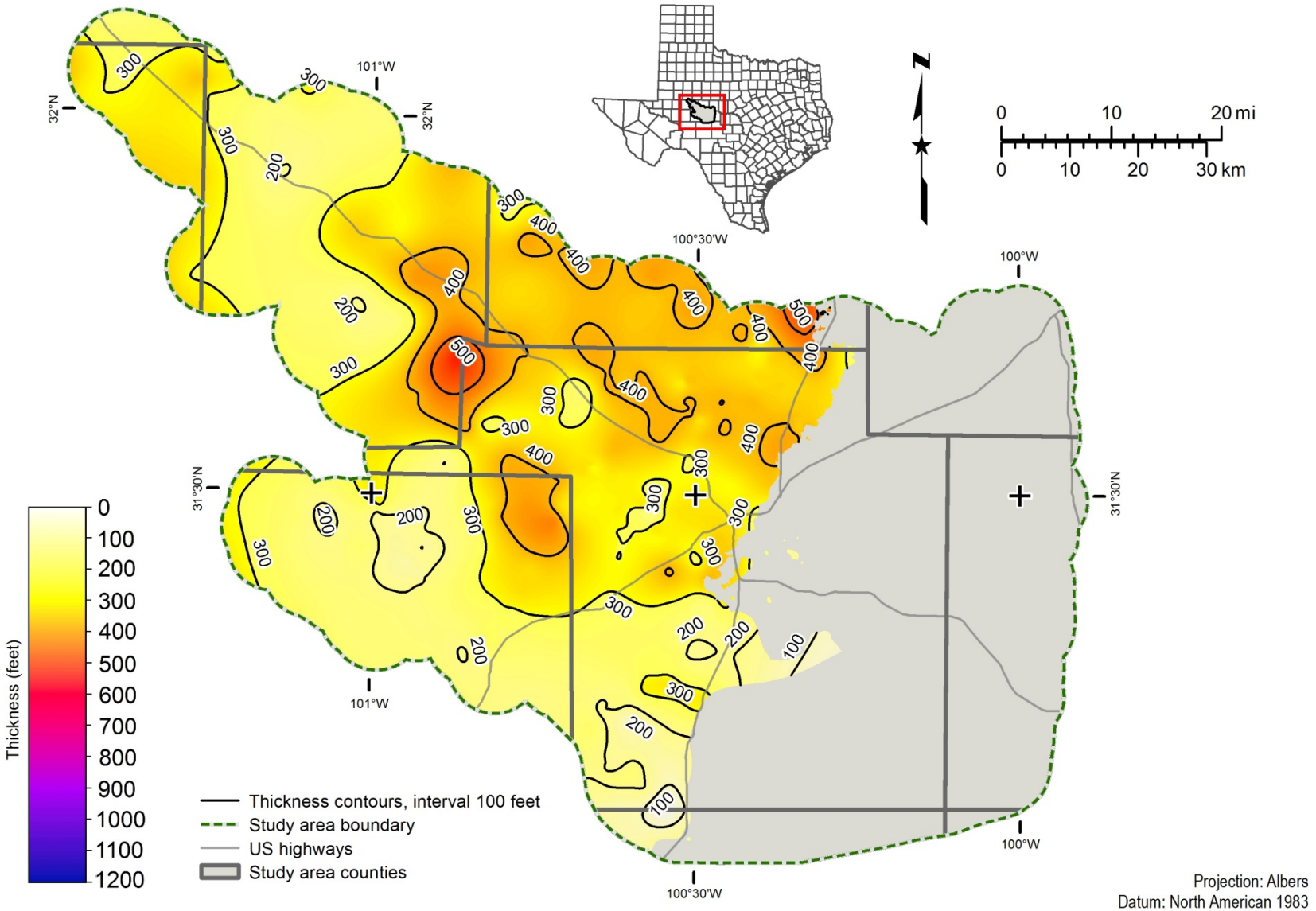

Figure 20.1-38. Isochore map of the Upper Choza member in the Lipan Aquifer study area (thickness in feet). Gray area in map represents places where the top of the Upper Choza member does not occur.

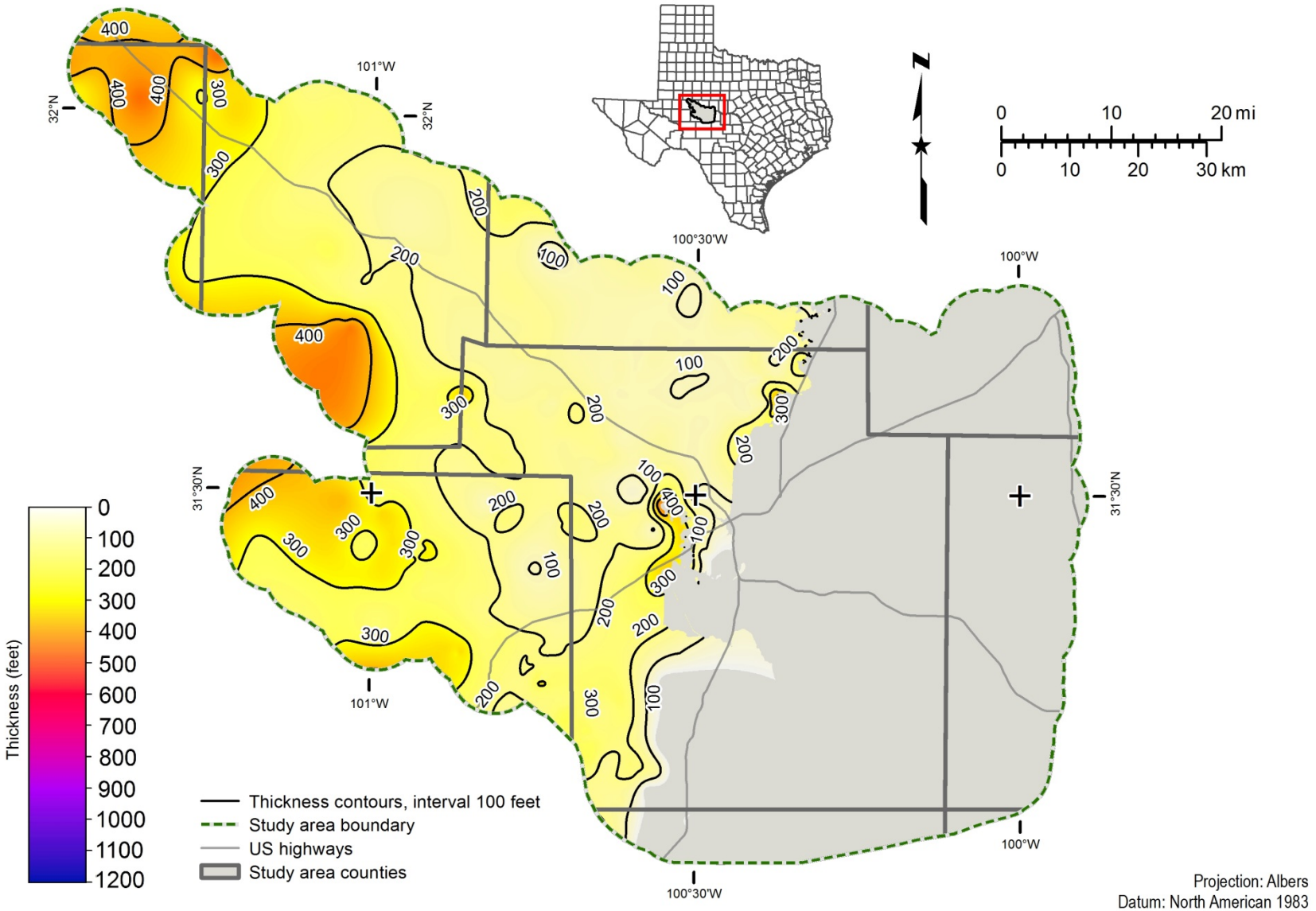

Figure 20.1-39. Isochore map of the San Angelo Formation in the Lipan Aquifer study area (thickness in feet). Gray area in map represents places where the top of the San Angelo Formation does not occur.

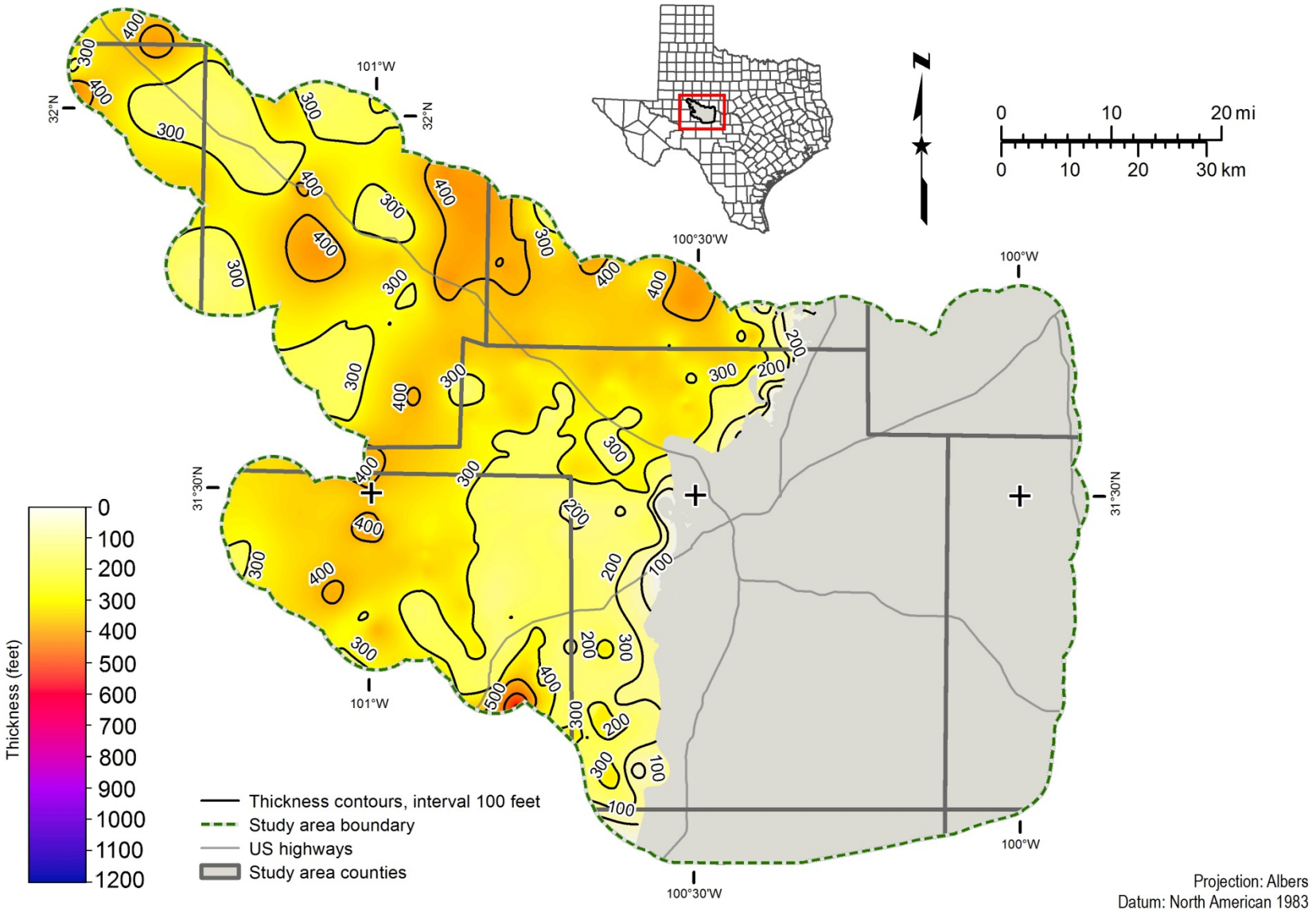

Figure 20.1-40. Isochore map of the San Andres Formation in the Lipan Aquifer study area (thickness in feet). Gray area in map represents places where the top of the San Andres Formation does not occur.

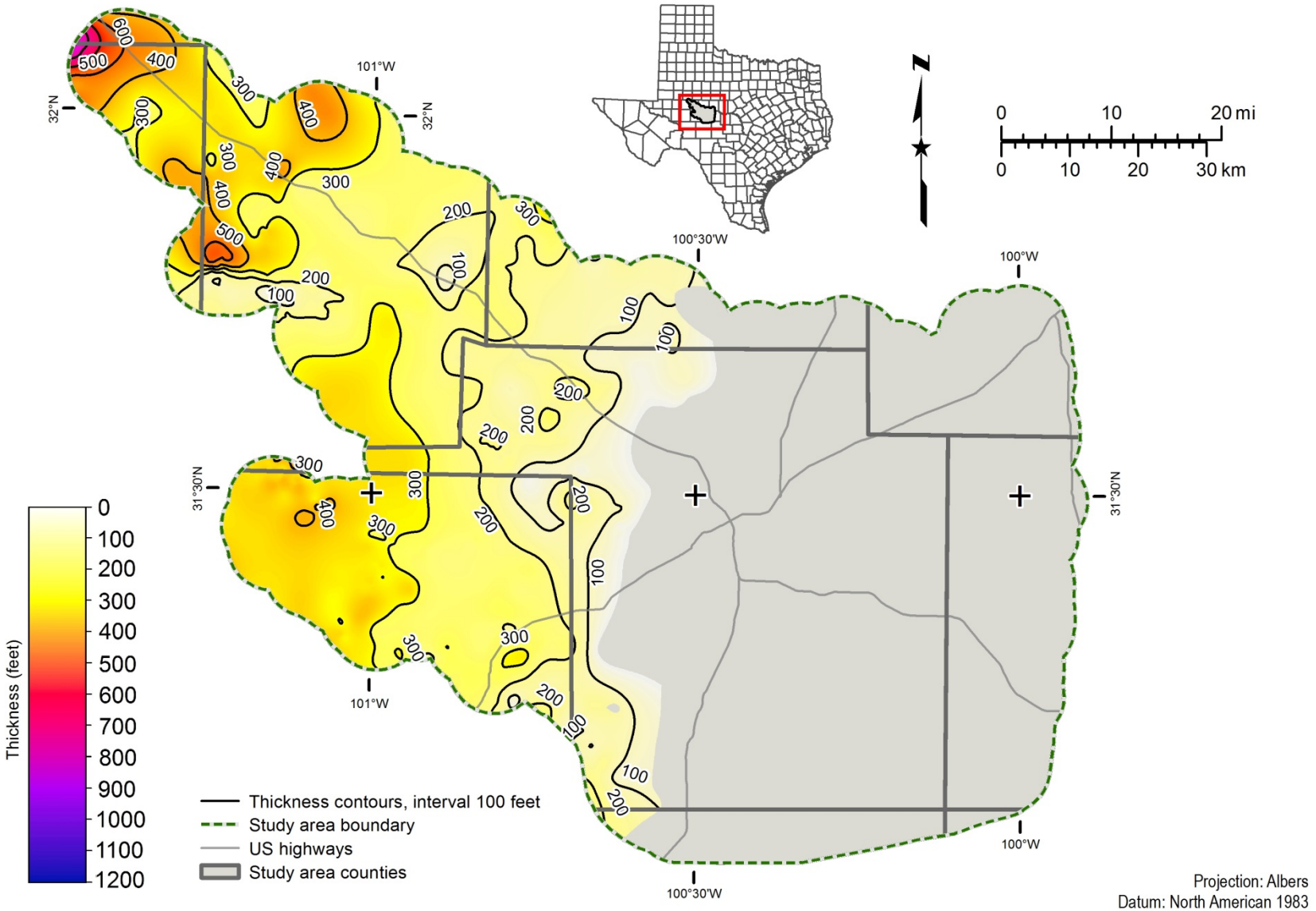

Figure 20.1-41. Isochore map of the Grayburg Formation in the Lipan Aquifer study area (thickness in feet). Gray area in map represents places where the top of the Grayburg Formation does not occur.

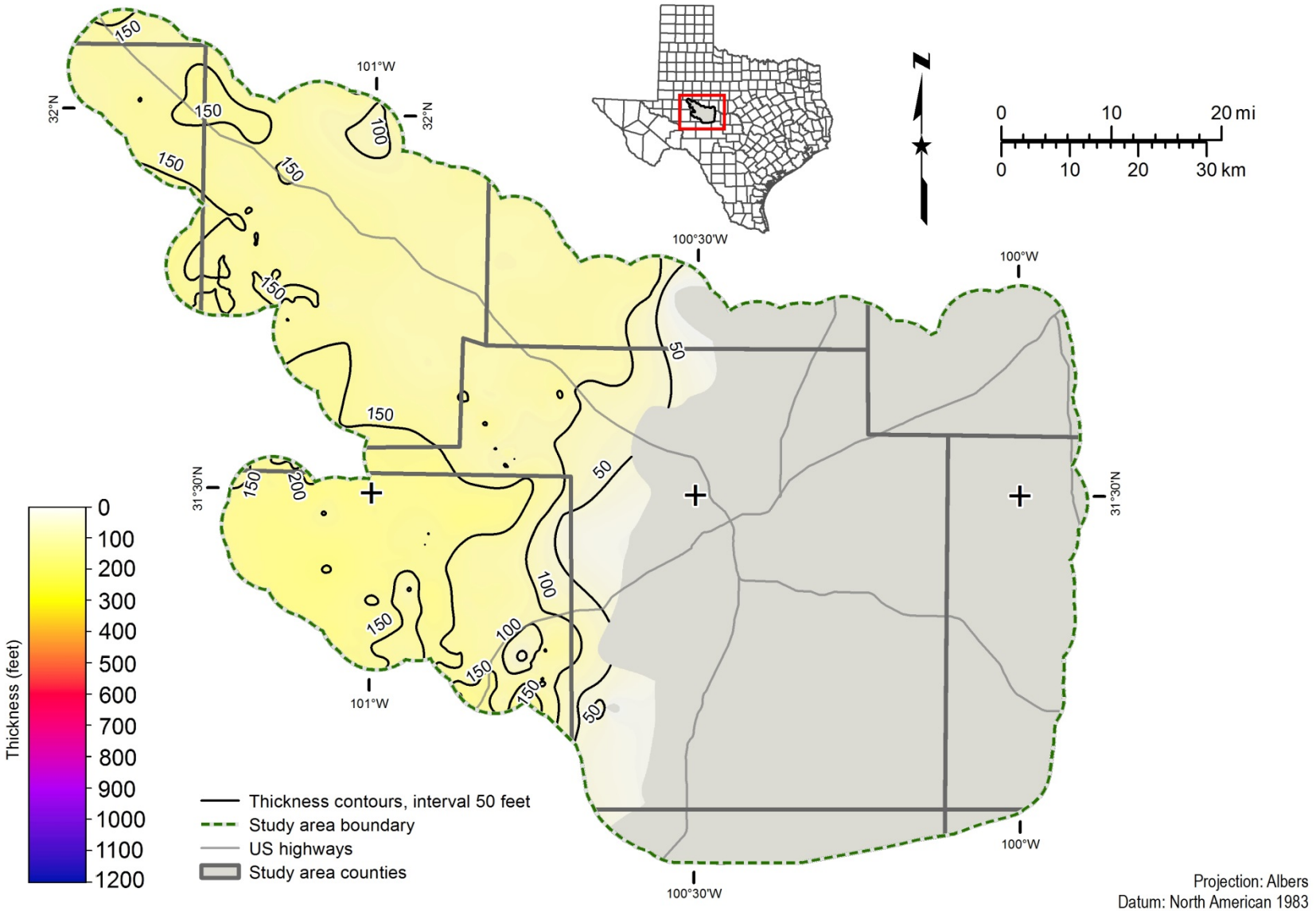

Figure 20.1-42. Isochore map of the Queen Formation in the Lipan Aquifer study area (thickness in feet). Gray area in map represents places where the top of the Queen Formation does not occur.

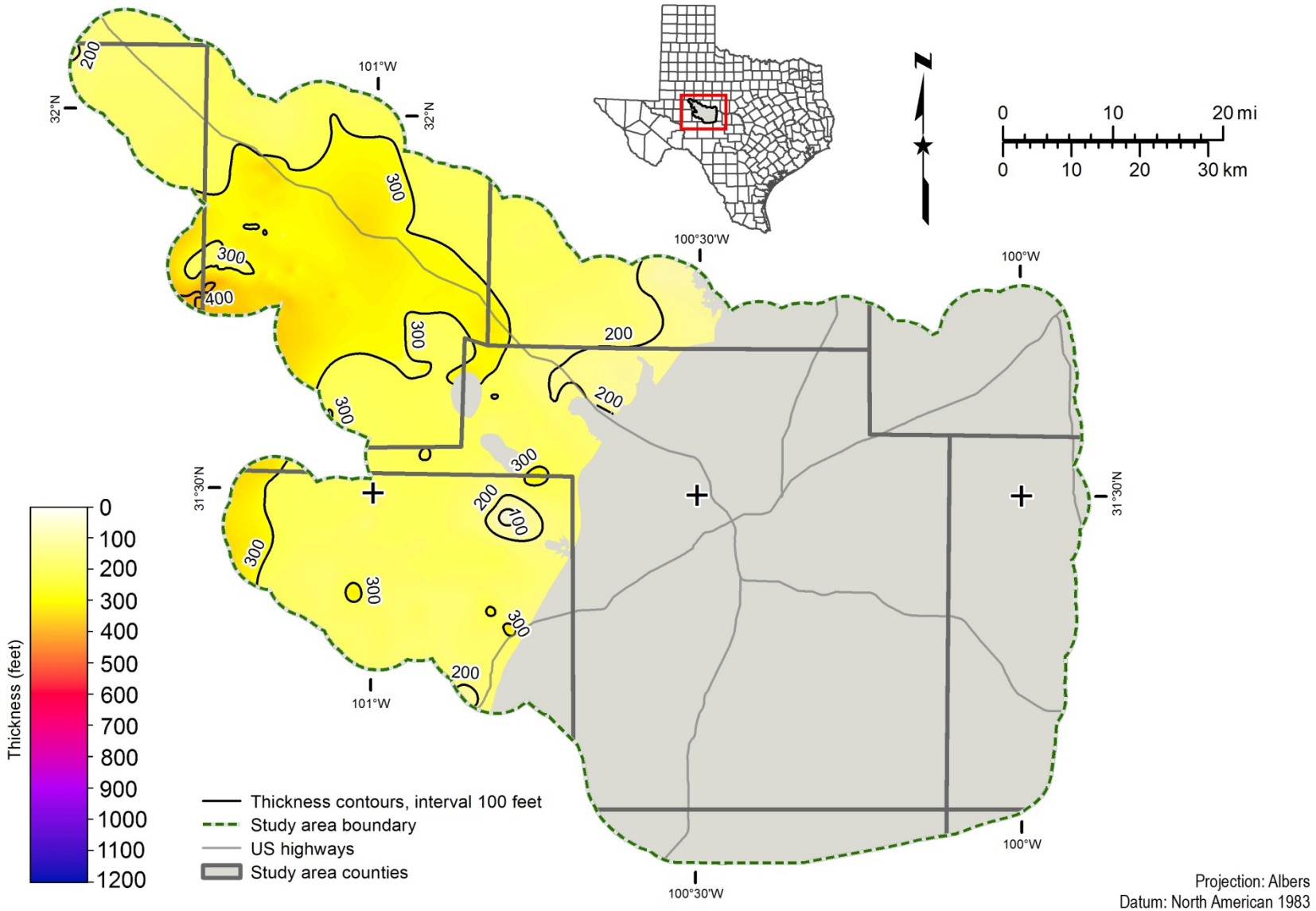

Figure 20.1-43. Isochore map of the Seven Rivers Formation in the Lipan Aquifer study area (thickness in feet). Gray area in map represents places where the top of the Seven Rivers Formation does not occur.

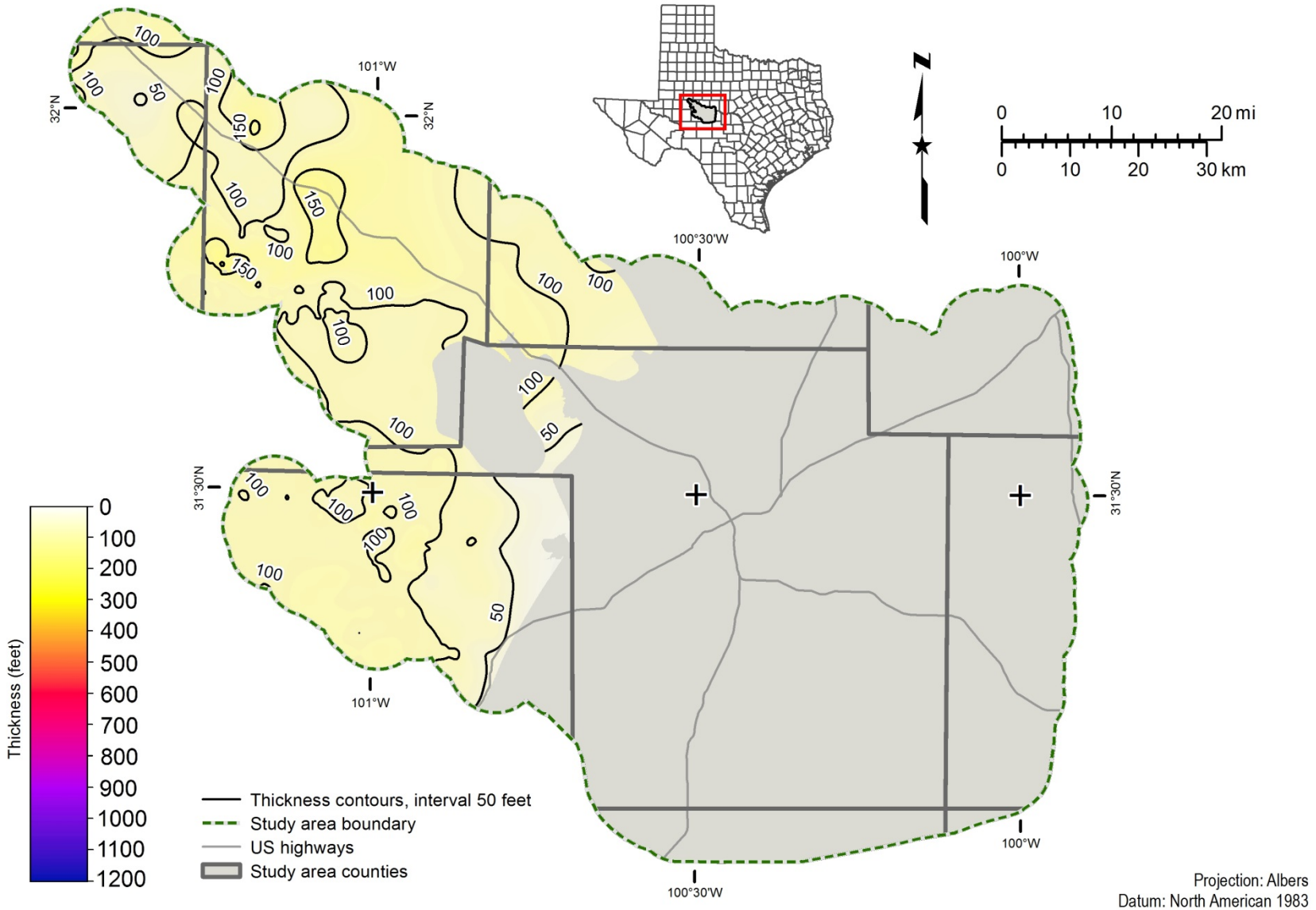

Figure 20.1-44. Isochore map of the Yates Formation in the Lipan Aquifer study area (thickness in feet). Gray area in map represents places where the top of the Yates Formation does not occur.

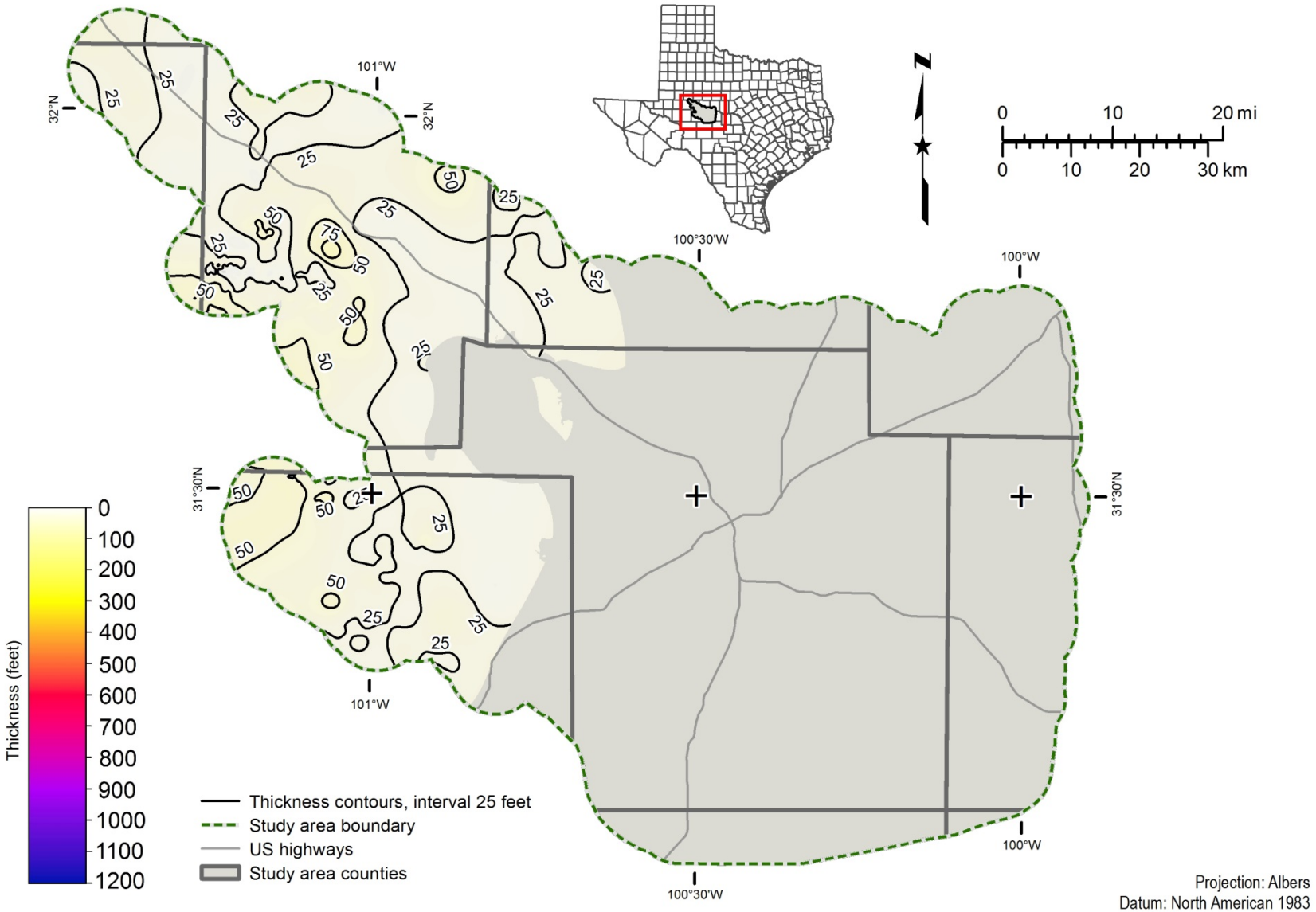

Figure 20.1-45. Isochore map of the Tansill Formation in the Lipan Aquifer study area (thickness in feet). Gray area in map represents places where the top of the Tansill Formation does not occur.

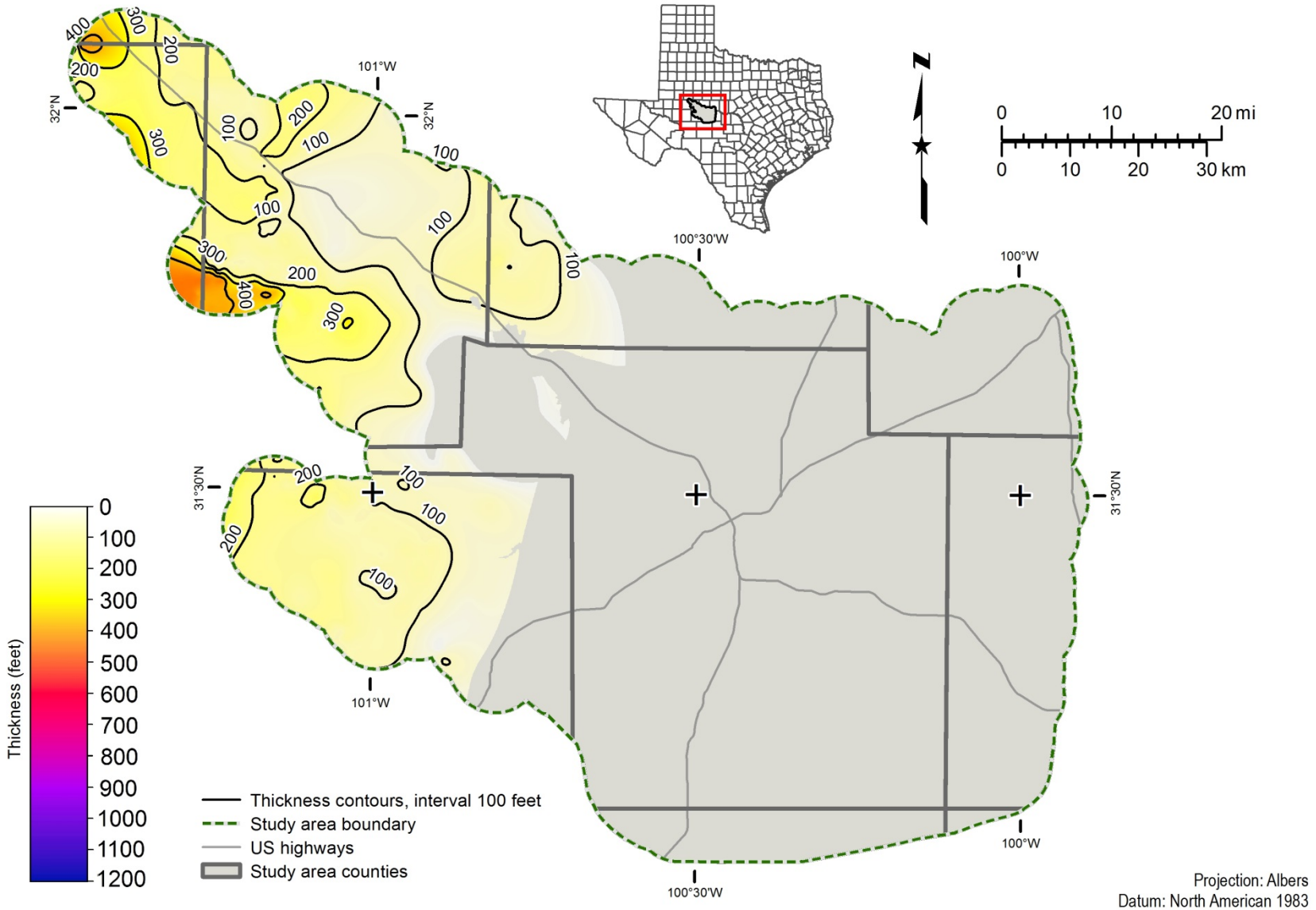

Figure 20.1-46. Isochore map of the Rustler-Salado formations in the Lipan Aquifer study area (thickness in feet). Gray area in map represents places where the top of the Rustler-Salado formations does not occur.

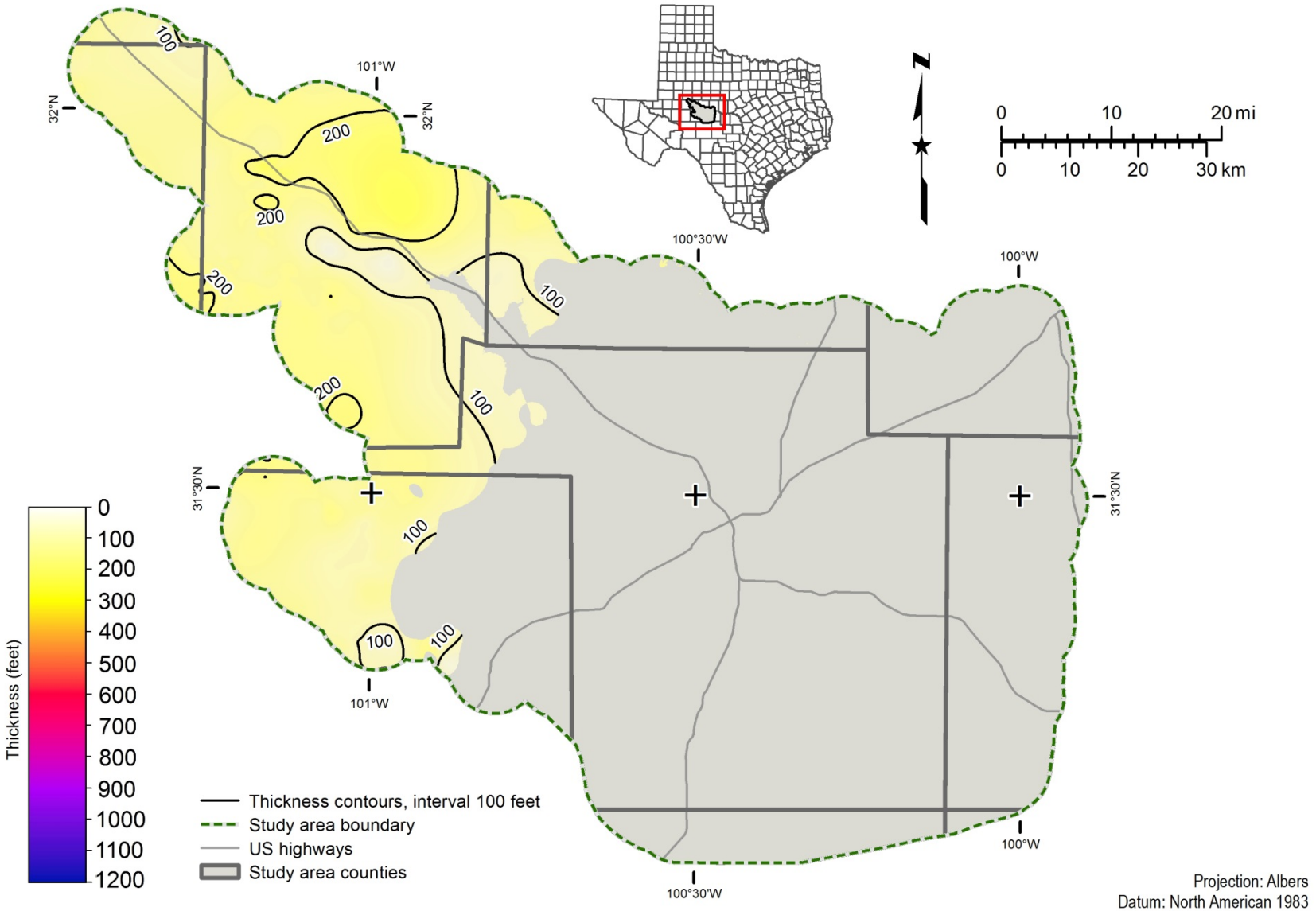

Figure 20.1-47. Isochore map of the Dewey Lake Formation in the Lipan Aquifer study area (thickness in feet). Gray area in map represents places where the top of the Dewey Lake Formation does not occur.

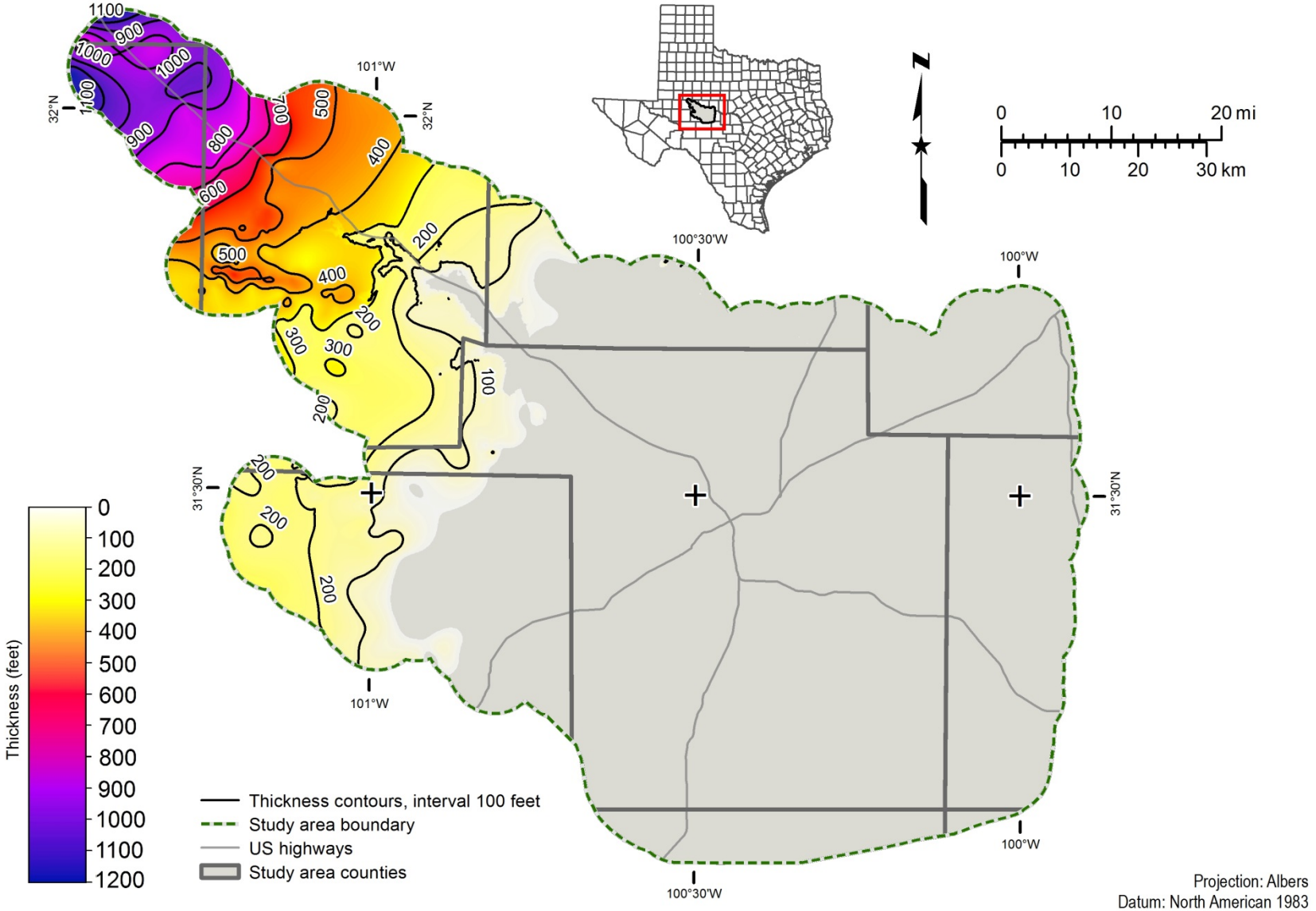

Figure 20.1-48. Isochore map of the Dockum Group in the Lipan Aquifer study area (thickness in feet). Gray area in map represents places where the top of the Dockum Group does not occur.

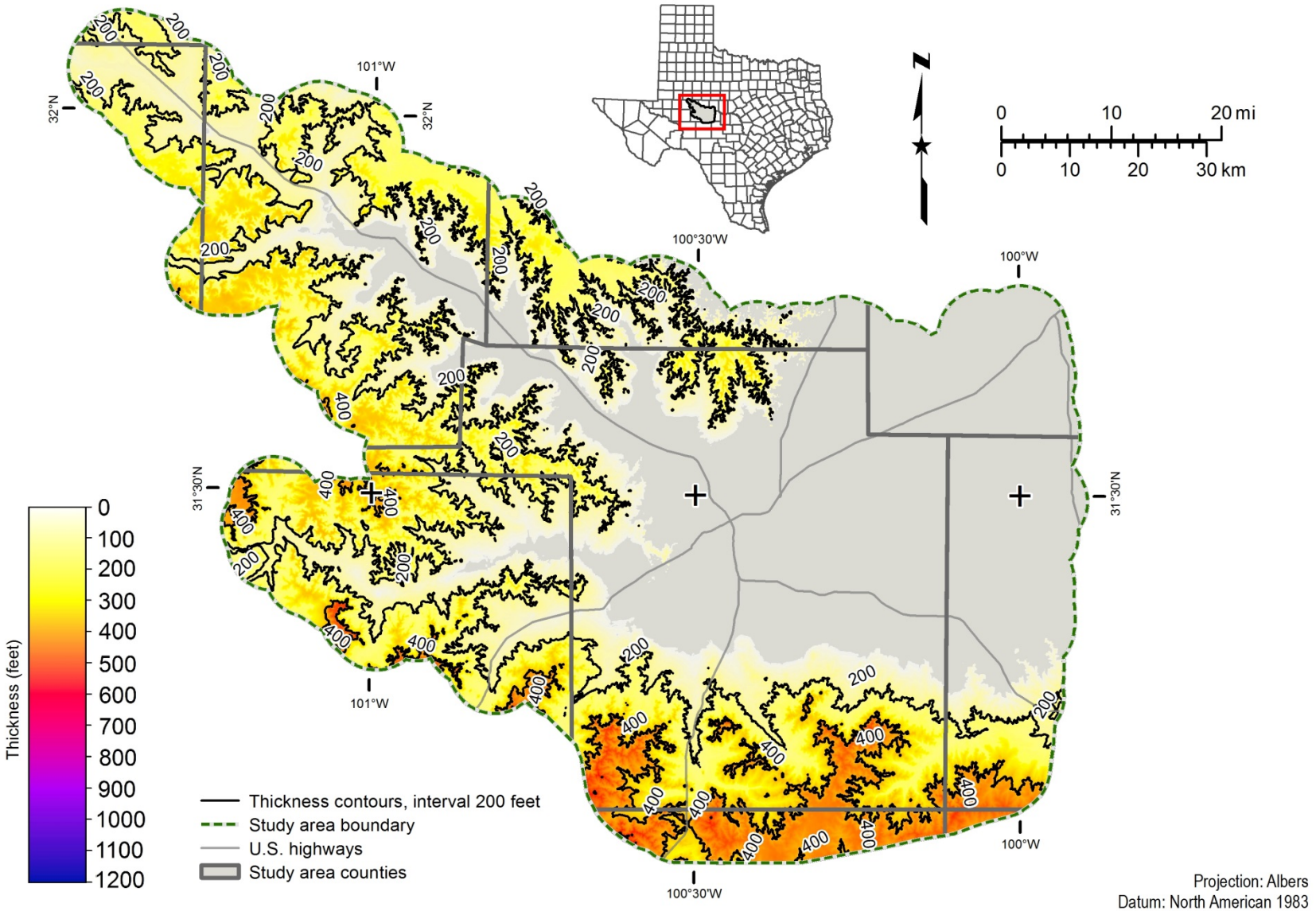

Figure 20.1-49. Isochore map of the Trinity Group in the Lipan Aquifer study area (thickness in feet). The Trinity Group occurs at the ground surface over much of the study area. Gray area in map represents places where the Trinity Group does not occur.

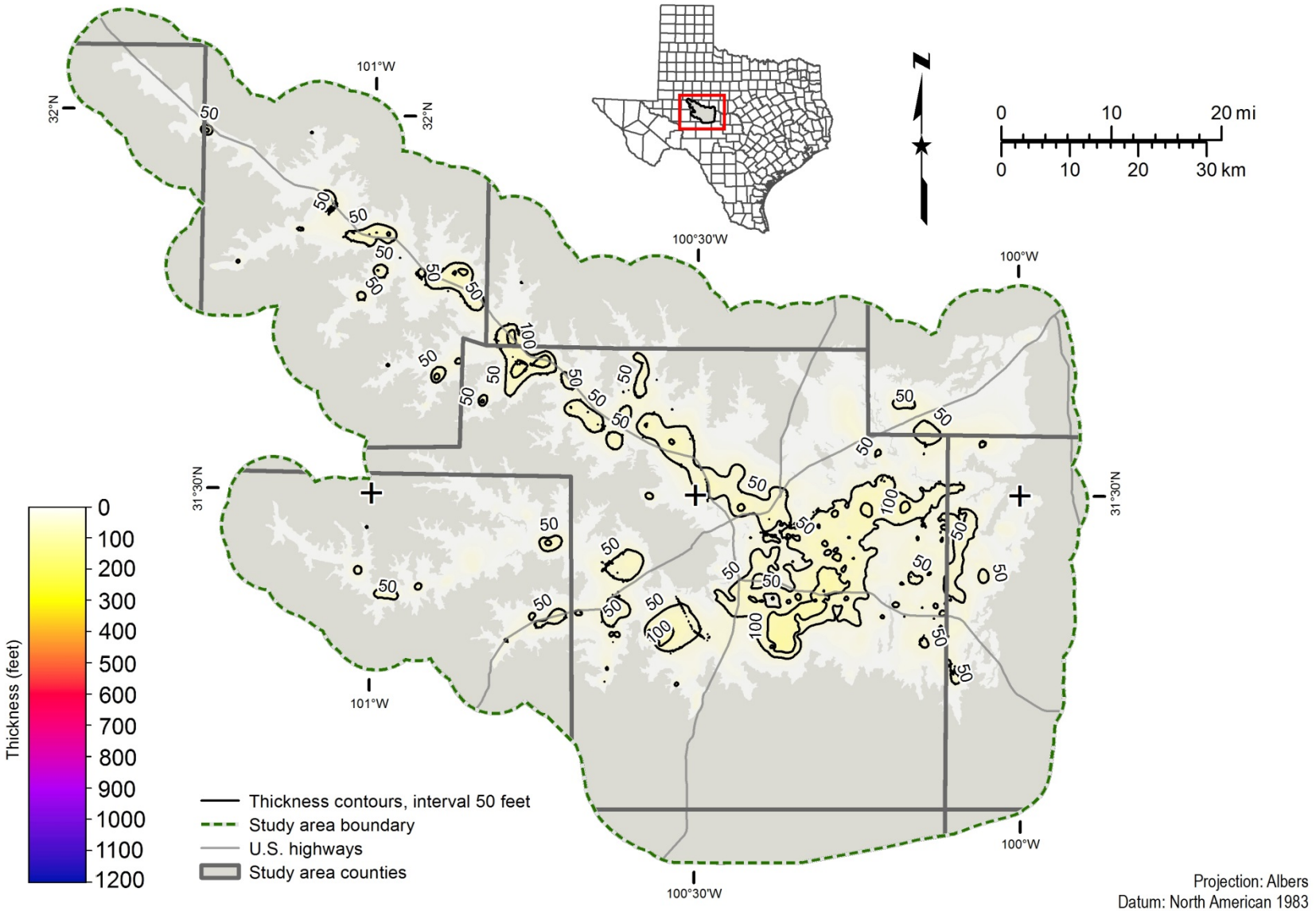

Figure 20.1-50. Isochore map of the Quaternary and Neogene sediments in the Lipan Aquifer study area (thickness in feet). Gray area in map represents places where the Quaternary and Neogene sediments do not occur.

20.2 BRACS Database

All water well and geophysical well log information and supporting databases for the Lipan Aquifer study are managed in the BRACS Database using Microsoft® Access® 2010. When spatial analysis is required, copies of information are exported into ArcGIS®. Information developed in ArcGIS® is then exported back into Microsoft® Access® and the tables are updated accordingly. Although this approach may be cumbersome, it takes advantage of the strengths of the software. The project also relied on other software for specific tasks, including Microsoft® Excel® and Schlumberger Blueview® (for geophysical well log analysis).

For the study, we assembled information from external agencies and updated these databases frequently. All of these databases are maintained in Microsoft® Access® and GIS files were developed for spatial analysis and well selection. Many of the database objects were built from scratch or were redesigned to meet project objectives. Data from external agencies or projects were available in many different data designs, so establishing a common design structure proved beneficial in leveraging information compiled by other groups.

The BRACS and supporting databases are fully relational. Data fields common to multiple datasets have been standardized in data type and name with lookup tables shared between all databases. Database object names use a self-documenting style that follows the Hungarian naming convention (Novalis, 1999). The volume of project information required us to develop comprehensive data entry and analysis procedures (coded as tools) that were embedded on forms used to display information. Visual Basic for Applications® is the programming language used in Microsoft® Access®, and all code was written at the Microsoft® ActiveX® Data Objects level with full code annotation. The code for geophysical well log resistivity analysis was specifically written with class objects to support a rapid analysis of information with the benefit of only having data appended when the user approved the results.

The BRACS Database is described in the BRACS Database and Data Dictionary (Meyer, 2017), which both are available from the TWDB website (www.twdb.texas.gov/innovativewater/bracs/database.asp). We develop custom tables for each study and incorporate these into the BRACS Database and add a study appendix describing these tables to the data dictionary after each study is completed.

20.2.1 Table relationships

The BRACS Database contains 18 primary tables of information (Figure 20.2-1), 32 lookup tables, tables designed for GIS export, and many supporting tables for analysis purposes. A brief description of each of the primary tables is provided in this section. Lookup tables provide control on data entry codes or values for specific data fields (for example, a county lookup table with all 254 county names in Texas). The tables for GIS export are copies of information obtained from one or more tables and in some cases are reformatted to meet GIS analysis needs. These tables can be custom tailored to meet study needs and will not be discussed further.

A fully relational database design has information organized into tables based on a common theme. Information must be segregated into separate tables for each one-to-many data relationship. For example, one well may have many well screens with unique top and bottom depth values; each well screen constitutes one record. Tables are linked by key fields. The well id field is the primary key field for every table in the BRACS Database. For each one-to-many relationship at least one additional key field is required.

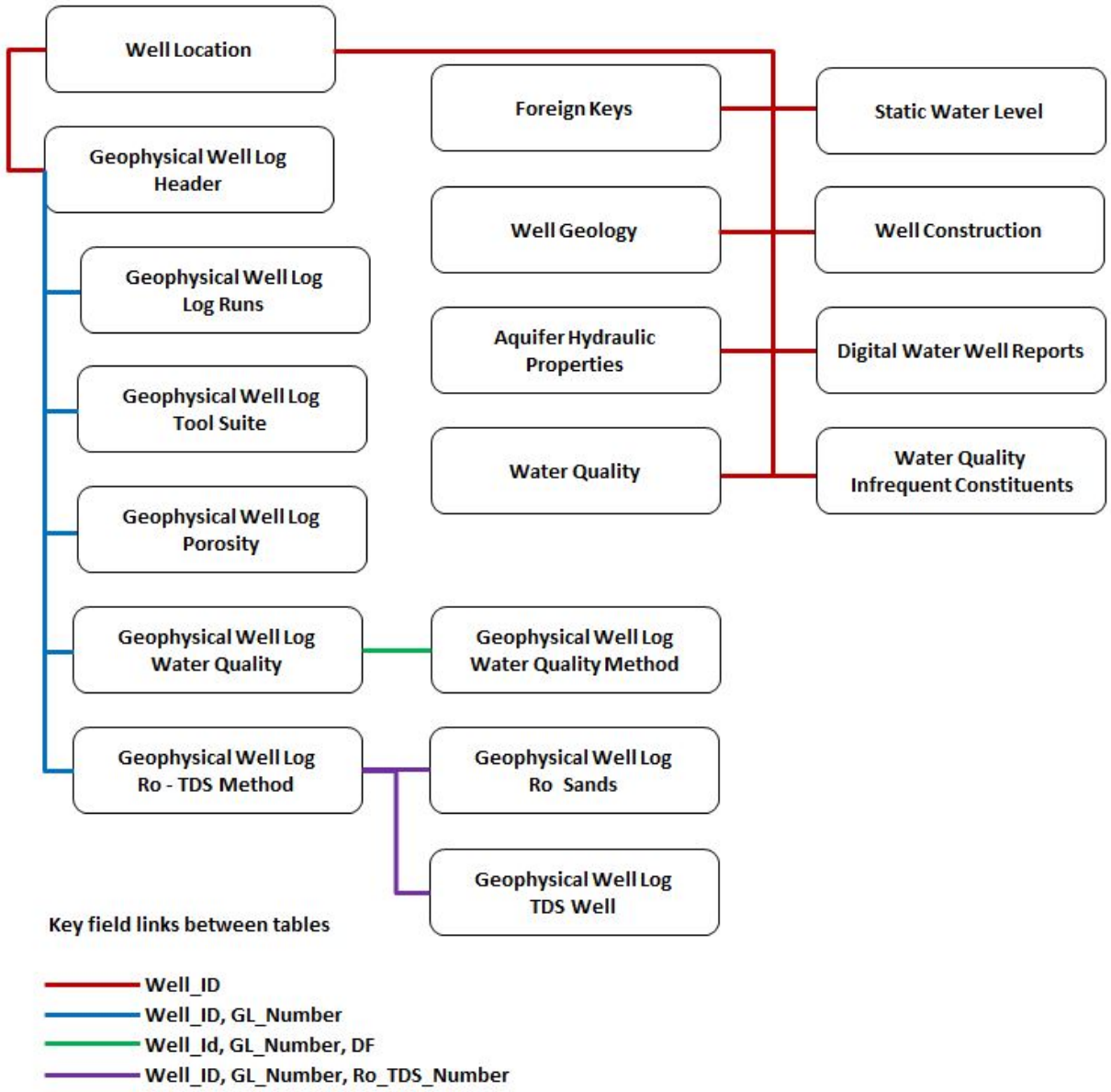

Figure 20.2-1. Table relationships in the BRACS Database. Each rectangle represents a primary data table. The lines connecting the tables represent key fields: red represents the primary key well_id, blue represents the second key, green represents the third key, and purple represents the fourth key. New well records must be appended to the well location table to set the unique well_id. The tables, fields, and key fields are described in more detail in Meyer (2017).

Well locations

The table called tblWell_Location contains one record for each well record in the BRACS Database and is assigned a unique well_id as the key field. The well_id field links all the tables together. This table contains information such as well owner, well depth(s), location attributes (such as latitude, longitude, and elevation), source of well information, county name, and date drilled.

Foreign keys

The table called tblBracs_ForeignKey has zero to many unique well identification names or numbers assigned to it (for example, state well number and American Petroleum Institute number). These identifiers, also known as foreign keys, permit database linkage to the supporting databases developed from external agencies and other TWDB project databases with geophysical well logs and stratigraphic pick information.

Digital well reports

The table called tblBracsWaterWellReports contains zero to many records for digital copies of water well reports and miscellaneous records including oil and gas well scout tickets. The purpose of this table is to track the digital file names, file types, and hyperlinks to the documents.

Geophysical well logs

Information on the digital geophysical well logs is recorded in the table called tblGeophysicalLog_Header. This includes the type of digital file, digital file name, data hyperlink to the log image, and well log parameters such as depth. The well log parameters are only recorded if the well log is to be used for resistivity analysis for interpreted total dissolved solids.

Each geophysical well log may have one or more tools used to record subsurface parameters. This information is recorded in the table tblGeophysicalLog_Suite. Each tool name and its start and bottom depth values in units of feet below ground surface are recorded in this table.

A geophysical well log may be collected during different drilling stages (runs) within specific depth intervals. Each log run will usually have different drilling mud and temperature parameters. These parameters are recorded in the table called tblGeophysicalLog_Header_LogRuns.

The results from resistivity analysis for interpreted total dissolved solids are recorded in several tables. Evaluating more than one depth interval per well necessitated designing the table tblGeophysicalLog_WQ to hold the depth of formation, temperature, and resistivity of the mud filtrate values for that interval. Evaluating more than one resistivity technique per depth interval dictated designing one table, tblGeophysicalLog_WQ_Method, to hold the analysis results including interpreted total dissolved solids, log correction values, method used, geophysical well log used, and a multitude of intermediate values.

One log analysis technique, the Ro-TDS Method, involves the comparison of log resistivity versus total dissolved solids concentration. This information is placed in the following tables: tblBRACS_GL_Analysis_Ro_TDS_Main, tblBRACS_GL_Analysis_Ro_Sands, and tblBRACS_GL_Analysis_TDS_Well. These tables record the final data pairs, the sands and their respective resistivity values, and the total dissolved solids concentration sample results for all wells used in the analysis.

Geophysical well log analysis is used to determine the porosity of specific geologic intervals. This information is recorded in the table called tblGeophysicalLog_Porosity.

Well geology

The descriptions of rock types reported on drillers' well logs, simplified lithologic descriptions, stratigraphic picks, and hydrochemical zones are all contained in the table called tblWell_Geology. Each record contains a top and bottom depth, thickness of the unit, top and bottom elevations, source of data, and a value for type of geologic pick (for example, lithologic, stratigraphic, or hydrogeologic). The latter field permits the storage of all this information in one table and the ability to view the information in one form.

Well construction

Well casing and screen information is contained in the table called tblBracs_Casing. This table design is similar to the well-casing table in the TWDB Groundwater Database and contains top and bottom depths for casing and screen.

Water quality

Two tables contain the results of water quality analyses recorded for wells that are not in the TWDB Groundwater Database: tblBracsWaterQuality and tblBracsInfrequentConstituents. The table designs are similar to those in the TWDB Groundwater Database.

All water quality records used to develop the maps and tables in Section 11 of the report were appended to the table called tblBRACS_Lipan_MasterWaterQuality. This table includes records obtained from the TWDB Groundwater Database and records obtained from research for wells in the BRACS Database.

Static water level

Static water level information is contained in the table called tblBRACS_SWL. The table is similar to its equivalent in the TWDB Groundwater Database. Information on dates, water levels, and source of measurement are recorded in the table. Static water levels for all wells in the study area were compiled into a custom table called tblBRACS_Lipan_SWL.

Aquifer hydraulic properties

Information from existing aquifer tests conducted for all BRACS studies is contained in the table called tblBRACS_AquiferTestInformation. The table contains fields for hydraulic conductivity, transmissivity, specific yield, storage coefficient, drawdown, pumping rate, specific capacity, the types of units for each measurement, date of analysis, source of information, and remarks. If an analysis included the top and bottom depths of the screen, well depth, and static water level, it was captured in this table in case the values differed from what is presented in the casing table (test may have been performed before total depth of the well was reached). The length of aquifer tests, values for drawdown versus recovery, pumping and static water levels, and two analysis remarks fields complete the table design. A custom table for this study area is named tblBRACS_Lipan_Aquifer_Test.

Aquifer determination

The results of the aquifer determination for well records described in Section 9 are presented in the table called tblBRACS_Lipan_AquiferDetermination. This table includes fields for the new aquifer decision, TWDB Groundwater Database aquifer code assigned to the well (if any), well

and screen depths, whether the well has multiple screens, well owner, and latitude/longitude coordinates. Fields for geological formation top and bottom depths derived from GIS geological formation datasets are listed.

20.3 Geographic information system datasets

Many GIS datasets were created during the course of this study. The GIS techniques used to build the files are explained in the following sections and noted in the GIS file metadata. ArcGIS® 10.0 and the Spatial Analyst® extension software by Environmental Systems Research Institute, Inc. (ESRI) were used to create the GIS files. Each of the GIS files prepared for this BRACS study is available for download from the TWDB website (www.twdb.texas.gov/innovativewater/bracs/studies.asp).

Each point file is in the ArcGIS® shape file format. Point files of well control used for general purposes have a geographic projection and the North American Datum 1983 as the horizontal datum. Point files used for GIS surface (raster) creation have an Albers projection and the North American Datum 1983 as the horizontal datum.

All surface files are in the ArcGIS® raster integer grid file format with an Albers projection and the North American Datum 1983 as the horizontal datum. All raster files are snapped to the project snap grid raster with a cell size of 250 by 250 feet.

Polygon and polyline files are in the ArcGIS® shape file format with an Albers projection and the North American Datum 1983 as the horizontal datum.

All well records are managed in Microsoft® Access® databases. Well records are queried from the database and imported into ArcGIS® for spatial analysis. When new attributes are added to a well using ArcGIS®, the information is imported into Microsoft® Access®, and the well records updated.

Every well record in each database used for this study contains latitude and longitude coordinates in the format of decimal degrees with a North American Datum of 1983. All of these well records were imported into ArcGIS® and georeferenced in a geographic coordinate system, North America, North American Datum 1983 projection. A point shapefile was then saved in a working directory. Every well record then had an elevation assigned from the U.S. Geological Survey seamless 30-meter digital elevation model using the ArcGIS® ArcToolbox (Spatial Analyst® Tools, Extraction, and Extract Values to Points). The dbase file from each shapefile was then imported into Microsoft® Access® and the elevation data updated to each well record, along with date, method, vertical datum, and agency attributes. Each well record also recorded the kelly bushing height when available.

In many cases, new wells were plotted in ArcGIS® and the latitude, longitude, and elevation were determined and appended to the database tables manually. The Original Texas Land Survey obtained from the Railroad Commission of Texas was the principal base map used to plot well locations; county highway maps and topographic maps were used on occasion.

GIS file name codes

ArcGIS® raster files are limited to 12 characters, necessitating the development of a file naming scheme for all GIS files created for BRACS studies. The full list of naming codes can be found in the BRACS Database in the table called tblGisFile_NamingConventions, and a shortened list of codes is presented in Table 20.3-1.

Each code is separated from the next code with an underscore character. For example, the code le_t_d refers to the Lueders formation top depth.

Table 20.3-1. GIS file naming codes applied to the Lipan Aquifer study area.

Code	Code type	Code position	Code description
Lipan or lip	BRACS Project	1	Lipan Aquifer project
le	Stratigraphic	1	Lueders Formation
ay	Stratigraphic	1	Arroyo Formation
vl	Stratigraphic	1	Vale Shale member
bw	Stratigraphic	1	Bullwagon Dolomite
tb	Stratigraphic	1	Tubb member
ch	Stratigraphic	1	Upper Choza member
sg	Stratigraphic	1	San Angelo Formation
sa	Stratigraphic	1	San Andres Formation
gy	Stratigraphic	1	Greyburg Formation
q	Stratigraphic	1	Queen Formation
sr	Stratigraphic	1	Seven Rivers Formation
ya	Stratigraphic	1	Yates Formation
ta	Stratigraphic	1	Tansill Formation
rsc	Stratigraphic	1	Rustler-Salado formations
dl	Stratigraphic	1	Dewey Lake Formation
ld	Stratigraphic	1	Dockum Group (Lower Dockum)
tg	Stratigraphic	1	Trinity Group
qt	Stratigraphic	1	Quaternary and Neogene sediments
ss	Salinity zone	1	Slightly saline water
ms	Salinity zone	1	Moderately saline water
vs	Salinity zone	1	Very saline water
swl	Value	1	Static water level
t	Surface position	2	Top
b	Surface position	2	Bottom
e	Value	3	Elevation above mean sea level (units: feet)
d	Value	3	Depth below ground surface (units: feet)
tk	Value	3	Thickness (units: feet)
con	Data type	4	Contour
ext	Data type	4	Extent
pt	Data type	4	Point
pl	Data type	4	Polyline

Code	Code type	Code position	Code description
pg	Data type	4	Polygon
25	Contour interval	5	Contour interval of 25 feet (units: feet)
50	Contour interval	5	Contour interval of 50 feet (units: feet)
100	Contour interval	5	Contour interval of 100 feet (units: feet)
250	Contour interval	5	Contour interval of 250 feet (units: feet)
400	Contour interval	5	Contour interval of 400 feet (units: feet)
500	Contour interval	5	Contour interval of 500 feet (units: feet)

Project support GIS files

Unique GIS datasets representing administrative, geologic, and well control features were developed for the project. The filenames associated with these datasets are presented in Table 20.3-2.

Table 20.3-2. Project support GIS files.

File type	Point file name	Polyline file name	Polygon file name	Raster file name
Project snap grid				lip_snap250
Project elevation				dem_i_250
Project boundary		Lipan_Study_Bound_line	Lipan_Study_Bound_poly	
Project well control	BRACS_GIS _Lipan			
Aquifer determination	Lipan_AQD			
Surface geology			Lipan_GAT_clip_dissolve	
Master water quality			Lipan_Master_WQ	
Public water supply boundary			Lipan_PWS_clip	
Texas counties			Lipan_County _Clip	
Texas cities			Lipan_City_Clip	
U.S. Highways		Lipan_US_Highway_Clip		

File type	Point file name	Polyline file name	Polygon file name	Raster file name
Texas groundwater conservation districts			Lipan_GCD_Clip	
Texas groundwater management areas			TWDB_GMAs	
Texas regional water planning areas			TWDB_RWPAs	
Class II injection wells	Lipan_UIC _ClassII_Wells			
Geologic cross-section	Lipan _Cross_Section _Points	Lipan_Cross_Section_Line		
Surface water		Lipan_Streams_Clip	Lipan_Major_Reservoirs	
Figure feathering			Lipan_Feather_Mask	
Aquifer test data	Lipan_AT_ Select			

Geologic formation GIS files

Raster GIS datasets representing the mapped geologic structural features in the study area are presented in Table 20.3-3.

Table 20.3-3. Geological formation GIS files.

Unit name	Raster surface file name	Polygon file name	Raster extent file name
Lueders Formation	le_t_d	le_ext_pg	le_ext
	le_t_e		
Arroyo Formation	ay_t_d	ay_ext_pg	ay_ext
	ay_t_e		
	ay_tk		
Vale Shale member	vl_t_d	vl_ext_pg	vl_ext
	vl_t_e		
	vl_tk		

Unit name	Raster surface file name	Polygon file name	Raster extent file name
Bullwagon Dolomite	bw_t_d	bw_ext_pg	bw_ext
	bw_t_e		
	bw_tk		
Tubb member	tb_t_d	tb_ext_pg	tb_ext
	tb_t_e		
	tb_tk		
Upper Choza member	ch_t_d	ch_ext_pg	ch_ext
	ch_t_e		
	ch_tk		
San Angelo Formation	sg_t_d	sg_ext_pg	sg_ext
	sg_t_e		
	sg_tk		
San Andres Formation	sa_t_e	sa_ext_pg	sa_ext
	sa_t_d		
	sa_tk		
Grayburg Formation	gy_t_d	gy_ext_pg	gy_ext
	gy_t_e		
	gy_tk		
Queen Formation	q_t_d	q_ext_pg	q_ext
	q_t_e		
	q_tk		
Seven Rivers Formation	sr_t_d	sr_ext_pg	sr_ext
	sr_t_e		
	sr_tk		
Yates Formation	ya_t_d	ya_ext_pg	ya_ext
	ya_t_e		
	ya_tk		

Unit name	Raster surface file name	Polygon file name	Raster extent file name
Tansill Formation	ta_t_d	ta_ext_pg	ta_ext
	ta_t_e		
	ta_tk		
Rustler-Salado formations	rsc_t_d	rsc_ext_pg	rsc_ext
	rsc_t_e		
	rsc_tk		
Dewey Lake Formation	dl_t_d	dl_ext_pg	dl_ext
	dl_t_e		
	dl_tk		
Dockum Group	dol_t_d	dol_ext_pg	dol_ext
	dol_t_e		
	dol_tk		
Trinity Group	tg_b_e	tg_ext_pg	tg_ext
	tg_tk		
Quaternary and Neogene sediments	qt_b_e	qt_ext_pg	qt_ext
	qt_tk		

Salinity zones raster files

Raster GIS datasets representing the mapped salinity zone surfaces in the study area are presented in Table 20.3-4.

Table 20.3-4. Salinity zone raster files.

Salinity zone	Raster surface file name
Slightly Saline	ss_t_d
	ss_t_e
Moderately Saline	ms_t_d
	ms_t_e
Very Saline	vs_t_d_
	vs_t_e

20.4 Water quality well summary

We used 918 calculated or measured water quality samples to develop all of our water quality zones within the Permian formations. Data on these samples are tabulated below. The data was generated either using Alger-Harrison Method interpretations of geophysical well logs or measurements from actual water samples. Latitudes and longitudes are in North American Datum of 1983 (NAD 83).

Table 20.4-1. Permian formation water quality sample summary.

State well number	BRACS well id	Formation	Latitude	Longitude	TDS (mg/L)	Method
	16967	Lueders	31.258406	-100.011360	4711	Alger Harrison
	16968	Lueders	31.192280	-100.040213	5229	Alger Harrison
	16978	Lueders	31.310039	-99.944605	4957	Alger Harrison
	16980	Lueders	31.524238	-100.078050	43846	Alger Harrison
	17000	Lueders	31.198571	-100.110850	7808	Alger Harrison
	17062	Lueders	31.343286	-100.031832	16765	Alger Harrison
	18840	Lueders	31.616946	-100.151194	14615	Alger Harrison
	18849	Lueders	31.603704	-100.179536	30000	Alger Harrison
	23156	Lueders	31.998302	-101.067511	71250	Alger Harrison
	24736	Lueders	31.551085	-100.513121	71250	Alger Harrison
	24744	Lueders	31.428755	-100.160580	9194	Alger Harrison
	24754	Lueders	31.547039	-100.349678	30000	Alger Harrison
	24756	Lueders	31.391699	-100.452771	5182	Alger Harrison
	24971	Lueders	31.488928	-100.206702	8381	Alger Harrison
4312903	25724	Lueders	31.768179	-100.540247	30000	Alger Harrison
	25746	Lueders	31.767280	-100.780087	20357	Alger Harrison
	26130	Lueders	31.416940	-100.186871	6477	Alger Harrison
	26747	Lueders	31.740011	-101.105129	15000	Alger Harrison
	26819	Lueders	31.736161	-101.134080	19000	Alger Harrison
	26935	Lueders	31.042560	-100.515493	6129	Alger Harrison
	27000	Lueders	31.760639	-101.168551	8382	Alger Harrison
	27035	Lueders	31.756725	-101.145281	9828	Alger Harrison
	27113	Lueders	31.812097	-100.974954	43846	Alger Harrison
	27114	Lueders	31.326624	-100.453610	10179	Alger Harrison
	27134	Lueders	31.783869	-101.129950	7703	Alger Harrison
	27383	Lueders	31.710253	-101.104552	6477	Alger Harrison
	27383	Lueders	31.710253	-101.104552	6786	Alger Harrison
	27386	Lueders	31.728821	-101.133670	9500	Alger Harrison
	27447	Lueders	31.705179	-101.036072	5534	Alger Harrison
	27785	Lueders	31.538677	-101.157729	19556	Alger Harrison

State well number	BRACS well id	Formation	Latitude	Longitude	TDS (mg/L)	Method
	27959	Lueders	31.794067	-101.207502	8906	Alger Harrison
	28110	Lueders	31.791977	-101.123064	10000	Alger Harrison
	28112	Lueders	31.781719	-101.143621	15833	Alger Harrison
	28197	Lueders	31.756456	-101.052521	6628	Alger Harrison
	28604	Lueders	31.300435	-100.721659	9048	Alger Harrison
	28744	Lueders	31.780859	-101.163011	12667	Alger Harrison
	29166	Lueders	31.738238	-101.052882	6333	Alger Harrison
	29308	Lueders	31.774400	-101.066539	24783	Alger Harrison
	29768	Lueders	31.880645	-101.173602	12391	Alger Harrison
	29841	Lueders	31.740682	-101.065509	23750	Alger Harrison
	29878	Lueders	31.866645	-101.192122	9344	Alger Harrison
	30284	Lueders	31.693683	-100.117215	22800	Alger Harrison
	30677	Lueders	31.848176	-101.184512	8143	Alger Harrison
	30857	Lueders	31.836070	-101.145734	6333	Alger Harrison
	30878	Lueders	31.968134	-100.985169	17600	Alger Harrison
	31067	Lueders	31.651239	-100.032031	6000	Alger Harrison
	32652	Lueders	31.802076	-101.225033	10755	Alger Harrison
	32775	Lueders	31.655623	-100.590218	18387	Alger Harrison
	32775	Lueders	31.655623	-100.590218	20000	Alger Harrison
	32781	Lueders	31.099638	-100.339207	7917	Alger Harrison
	32783	Lueders	31.383863	-100.184251	12571	Alger Harrison
	32787	Lueders	31.427686	-100.482211	30000	Alger Harrison
	32788	Lueders	31.462631	-100.269613	15405	Alger Harrison
	32790	Lueders	31.421155	-100.273114	10000	Alger Harrison
	32792	Lueders	31.556768	-100.144445	5278	Alger Harrison
	32796	Lueders	31.420053	-100.228682	3149	Alger Harrison
	32799	Lueders	31.383220	-100.307365	19000	Alger Harrison
	32800	Lueders	31.108047	-100.499164	51818	Alger Harrison
	32805	Lueders	31.352206	-100.525198	8906	Alger Harrison
	32806	Lueders	31.399977	-100.684287	5229	Alger Harrison
	32808	Lueders	31.302859	-100.461553	7125	Alger Harrison
	32814	Lueders	31.514450	-100.444722	18387	Alger Harrison
	33111	Lueders	31.639387	-100.111214	19655	Alger Harrison
	34486	Lueders	31.112499	-100.036712	3413	Alger Harrison
	34601	Lueders	31.677053	-100.035443	43846	Alger Harrison
	35381	Lueders	31.210412	-100.481005	10179	Alger Harrison
	35561	Lueders	31.455673	-100.618163	19655	Alger Harrison

State well number	BRACS well id	Formation	Latitude	Longitude	TDS (mg/L)	Method
	35563	Lueders	31.465803	-100.589194	16286	Alger Harrison
	35809	Lueders	31.923467	-100.874297	15405	Alger Harrison
	36282	Lueders	31.457230	-100.048028	13571	Alger Harrison
4343601	37961	Lueders	31.296855	-100.641823	19000	Alger Harrison
	37974	Lueders	31.546184	-100.432327	8507	Alger Harrison
	37975	Lueders	31.512490	-100.381069	38000	Alger Harrison
	37977	Lueders	31.279513	-100.436529	4524	Alger Harrison
	38262	Lueders	31.619595	-100.516255	38000	Alger Harrison
	47564	Lueders	31.256367	-100.735358	20357	Alger Harrison
	47609	Lueders	31.431211	-100.985135	10000	Alger Harrison
	47858	Lueders	31.503295	-100.697688	10556	Alger Harrison
	51650	Lueders	31.200276	-100.539197	13571	Alger Harrison
	51672	Lueders	31.542921	-100.901953	10962	Alger Harrison
4352407	51891	Lueders	31.195660	-100.590356	11176	Alger Harrison
4320105	53709	Lueders	31.720326	-100.614950	15000	Alger Harrison
4310901	53713	Lueders	31.788703	-100.758778	7917	Alger Harrison
4310503	53730	Lueders	31.800084	-100.796123	19000	Alger Harrison
4302903	53737	Lueders	31.891535	-100.785607	95000	Alger Harrison
4321106	53774	Lueders	31.734940	-100.463144	17273	Alger Harrison
	54502	Lueders	31.291304	-100.511095	1738	Alger Harrison
	54508	Lueders	31.492880	-100.506374	14615	Alger Harrison
	55188	Lueders	31.537764	-100.660755	18387	Alger Harrison
	55188	Lueders	31.537764	-100.660755	14250	Alger Harrison
	55188	Lueders	31.537764	-100.660755	25909	Alger Harrison
	55203	Lueders	31.461285	-100.381017	18387	Alger Harrison
	55207	Lueders	31.353511	-100.488535	28500	Alger Harrison
	55220	Lueders	31.431533	-100.254143	8906	Alger Harrison
	55221	Lueders	31.148304	-100.637771	12128	Alger Harrison
	55225	Lueders	31.422830	-100.371988	33529	Alger Harrison
	55227	Lueders	31.400305	-100.540771	10556	Alger Harrison
	55228	Lueders	31.521243	-100.226309	22800	Alger Harrison
	55235	Lueders	31.224487	-100.661647	21923	Alger Harrison
	55240	Lueders	31.115071	-100.234607	7703	Alger Harrison
	55256	Lueders	31.300295	-100.380127	21923	Alger Harrison
	55262	Lueders	31.444116	-100.340034	6628	Alger Harrison
	55267	Lueders	31.521707	-100.687579	16286	Alger Harrison
	55267	Lueders	31.521707	-100.687579	10962	Alger Harrison

State well number	BRACS well id	Formation	Latitude	Longitude	TDS (mg/L)	Method
	55271	Lueders	31.505700	-100.596876	9194	Alger Harrison
	55271	Lueders	31.505700	-100.596876	17812	Alger Harrison
	55271	Lueders	31.505700	-100.596876	19000	Alger Harrison
	55271	Lueders	31.505700	-100.596876	31667	Alger Harrison
	55281	Lueders	31.332853	-100.137059	16765	Alger Harrison
	55296	Lueders	31.212865	-100.589465	9048	Alger Harrison
	55300	Lueders	31.621898	-100.393097	10179	Alger Harrison
	55304	Lueders	31.220066	-100.363786	15833	Alger Harrison
	55306	Lueders	31.137044	-100.590618	5534	Alger Harrison
	55318	Lueders	31.268958	-100.554217	12128	Alger Harrison
	55319	Lueders	31.244158	-100.576827	4191	Alger Harrison
	55336	Lueders	31.191478	-100.606837	9828	Alger Harrison
	55338	Lueders	31.224076	-100.623007	8462	Alger Harrison
	55340	Lueders	31.245330	-100.618482	22800	Alger Harrison
	55351	Lueders	31.126329	-100.501252	21923	Alger Harrison
	55360	Lueders	31.420102	-100.127310	11633	Alger Harrison
	55361	Lueders	31.624130	-100.457540	8769	Alger Harrison
	55362	Lueders	31.658302	-100.633439	16286	Alger Harrison
	55362	Lueders	31.658302	-100.633439	30000	Alger Harrison
	55382	Lueders	31.639943	-100.619228	15833	Alger Harrison
	55384	Lueders	31.662079	-100.559102	6552	Alger Harrison
	55385	Lueders	31.677209	-100.662452	12128	Alger Harrison
	55428	Lueders	31.571589	-100.210934	15000	Alger Harrison
	55688	Lueders	31.143217	-100.368527	25909	Alger Harrison
	55692	Lueders	31.158984	-100.538909	9048	Alger Harrison
	55699	Lueders	31.195538	-100.653457	19000	Alger Harrison
	55700	Lueders	31.568457	-100.163715	18387	Alger Harrison
	55704	Lueders	31.557770	-100.232381	4254	Alger Harrison
	55706	Lueders	31.402332	-100.525024	33529	Alger Harrison
	55707	Lueders	31.249595	-100.228910	6264	Alger Harrison
	55711	Lueders	31.130599	-100.620426	8382	Alger Harrison
	55716	Lueders	31.647943	-100.622598	12955	Alger Harrison
	55725	Lueders	31.543810	-100.308467	15833	Alger Harrison
	55730	Lueders	32.000690	-101.215894	57000	Alger Harrison
	55737	Lueders	31.237837	-100.506252	9500	Alger Harrison
	55756	Lueders	31.599846	-100.496584	17959	Alger Harrison
	55761	Lueders	31.154799	-100.629646	6404	Alger Harrison

State well number	BRACS well id	Formation	Latitude	Longitude	TDS (mg/L)	Method
	55762	Lueders	31.400269	-100.498751	23750	Alger Harrison
	55815	Lueders	31.324434	-100.265912	4351	Alger Harrison
	55923	Lueders	31.168158	-100.472501	8636	Alger Harrison
	58520	Lueders	31.052059	-100.373988	14615	Alger Harrison
	55144	Lueders	31.577000	-100.027000	3953	Measured
	55146	Lueders	31.500000	-100.033000	1902	Measured
	55147	Lueders	31.455000	-100.011000	6049	Measured
	18840	Arroyo	31.616946	-100.151194	17273	Alger Harrison
	18849	Arroyo	31.603704	-100.179536	27143	Alger Harrison
	23156	Arroyo	31.998302	-101.067511	16286	Alger Harrison
	24736	Arroyo	31.551085	-100.513121	33529	Alger Harrison
	24744	Arroyo	31.428755	-100.160580	15833	Alger Harrison
	24754	Arroyo	31.547039	-100.349678	15405	Alger Harrison
	24756	Arroyo	31.391699	-100.452771	15405	Alger Harrison
	24971	Arroyo	31.488928	-100.206702	23750	Alger Harrison
4312903	25724	Arroyo	31.768179	-100.540247	20357	Alger Harrison
	25746	Arroyo	31.767280	-100.780087	7703	Alger Harrison
	26130	Arroyo	31.416940	-100.186871	6786	Alger Harrison
	26747	Arroyo	31.740011	-101.105129	20357	Alger Harrison
	26755	Arroyo	31.818349	-101.168217	14615	Alger Harrison
	26819	Arroyo	31.736161	-101.134080	9048	Alger Harrison
	26935	Arroyo	31.042560	-100.515493	12391	Alger Harrison
	27024	Arroyo	31.764369	-101.152701	21111	Alger Harrison
	27024	Arroyo	31.764369	-101.152701	13902	Alger Harrison
	27035	Arroyo	31.756725	-101.145281	33529	Alger Harrison
	27113	Arroyo	31.812097	-100.974954	11400	Alger Harrison
	27113	Arroyo	31.812097	-100.974954	10962	Alger Harrison
	27113	Arroyo	31.812097	-100.974954	17812	Alger Harrison
	27114	Arroyo	31.326624	-100.453610	12955	Alger Harrison
	27134	Arroyo	31.783869	-101.129950	11633	Alger Harrison
	27383	Arroyo	31.710253	-101.104552	5876	Alger Harrison
	27386	Arroyo	31.728821	-101.133670	7125	Alger Harrison
	27447	Arroyo	31.705179	-101.036072	5938	Alger Harrison
	27785	Arroyo	31.538677	-101.157729	27500	Alger Harrison
	27959	Arroyo	31.794067	-101.207502	5938	Alger Harrison
	28110	Arroyo	31.791977	-101.123064	12667	Alger Harrison
	28112	Arroyo	31.781719	-101.143621	13256	Alger Harrison

State well number	BRACS well id	Formation	Latitude	Longitude	TDS (mg/L)	Method
	28744	Arroyo	31.780859	-101.163011	4318	Alger Harrison
	29166	Arroyo	31.738238	-101.052882	8382	Alger Harrison
	29308	Arroyo	31.774400	-101.066539	19655	Alger Harrison
	29768	Arroyo	31.880645	-101.173602	10755	Alger Harrison
	29841	Arroyo	31.740682	-101.065509	21923	Alger Harrison
	29878	Arroyo	31.866645	-101.192122	13902	Alger Harrison
	30284	Arroyo	31.693683	-100.117215	15405	Alger Harrison
	30677	Arroyo	31.848176	-101.184512	8769	Alger Harrison
	30857	Arroyo	31.836070	-101.145734	6628	Alger Harrison
	30878	Arroyo	31.968134	-100.985169	10732	Alger Harrison
	32743	Arroyo	31.785080	-100.107017	7500	Alger Harrison
	32775	Arroyo	31.655623	-100.590218	13902	Alger Harrison
	32775	Arroyo	31.655623	-100.590218	13538	Alger Harrison
	32781	Arroyo	31.099638	-100.339207	5089	Alger Harrison
	32783	Arroyo	31.383863	-100.184251	15172	Alger Harrison
	32787	Arroyo	31.427686	-100.482211	31667	Alger Harrison
	32788	Arroyo	31.462631	-100.269613	27143	Alger Harrison
	32790	Arroyo	31.421155	-100.273114	19000	Alger Harrison
	32792	Arroyo	31.556768	-100.144445	1373	Alger Harrison
	32796	Arroyo	31.420053	-100.228682	12667	Alger Harrison
	32799	Arroyo	31.383220	-100.307365	27143	Alger Harrison
	32800	Arroyo	31.108047	-100.499164	35625	Alger Harrison
	32805	Arroyo	31.352206	-100.525198	11176	Alger Harrison
	32806	Arroyo	31.399977	-100.684287	5481	Alger Harrison
	32808	Arroyo	31.302859	-100.461553	9500	Alger Harrison
	32814	Arroyo	31.514450	-100.444722	21923	Alger Harrison
	33111	Arroyo	31.639387	-100.111214	17812	Alger Harrison
	35381	Arroyo	31.210412	-100.481005	6404	Alger Harrison
	35509	Arroyo	31.509118	-100.342155	27143	Alger Harrison
	35561	Arroyo	31.455673	-100.618163	10179	Alger Harrison
	35563	Arroyo	31.465803	-100.589194	17812	Alger Harrison
	35809	Arroyo	31.923467	-100.874297	11633	Alger Harrison
	35809	Arroyo	31.923467	-100.874297	27143	Alger Harrison
4343601	37961	Arroyo	31.296855	-100.641823	19655	Alger Harrison
	37974	Arroyo	31.546184	-100.432327	16765	Alger Harrison
	37975	Arroyo	31.512490	-100.381069	7500	Alger Harrison
	37977	Arroyo	31.279513	-100.436529	5644	Alger Harrison

State well number	BRACS well id	Formation	Latitude	Longitude	TDS (mg/L)	Method
	38262	Arroyo	31.619595	-100.516255	31667	Alger Harrison
	47564	Arroyo	31.256367	-100.735358	15000	Alger Harrison
	47609	Arroyo	31.431211	-100.985135	11633	Alger Harrison
	47858	Arroyo	31.503295	-100.697688	9500	Alger Harrison
	51650	Arroyo	31.200276	-100.539197	21923	Alger Harrison
	51672	Arroyo	31.542921	-100.901953	13571	Alger Harrison
4329301	51781	Arroyo	31.622197	-100.413971	6404	Alger Harrison
4352407	51891	Arroyo	31.195660	-100.590356	19655	Alger Harrison
4320105	53709	Arroyo	31.720326	-100.614950	7703	Alger Harrison
4310901	53713	Arroyo	31.788703	-100.758778	5000	Alger Harrison
4310503	53730	Arroyo	31.800084	-100.796123	17273	Alger Harrison
4302903	53737	Arroyo	31.891535	-100.785607	21923	Alger Harrison
4321106	53774	Arroyo	31.734940	-100.463144	22800	Alger Harrison
	54502	Arroyo	31.291304	-100.511095	2080	Alger Harrison
	54508	Arroyo	31.492880	-100.506374	15833	Alger Harrison
	55188	Arroyo	31.537764	-100.660755	10556	Alger Harrison
	55203	Arroyo	31.461285	-100.381017	19000	Alger Harrison
	55207	Arroyo	31.353511	-100.488535	28500	Alger Harrison
	55220	Arroyo	31.431533	-100.254143	20357	Alger Harrison
	55221	Arroyo	31.148304	-100.637771	10179	Alger Harrison
	55225	Arroyo	31.422830	-100.371988	16286	Alger Harrison
	55227	Arroyo	31.400305	-100.540771	15405	Alger Harrison
	55228	Arroyo	31.521243	-100.226309	31667	Alger Harrison
	55235	Arroyo	31.224487	-100.661647	10962	Alger Harrison
	55240	Arroyo	31.115071	-100.234607	5700	Alger Harrison
	55256	Arroyo	31.300295	-100.380127	23750	Alger Harrison
	55262	Arroyo	31.444116	-100.340034	4318	Alger Harrison
	55267	Arroyo	31.521707	-100.687579	11400	Alger Harrison
	55271	Arroyo	31.505700	-100.596876	31667	Alger Harrison
	55296	Arroyo	31.212865	-100.589465	7403	Alger Harrison
	55300	Arroyo	31.621898	-100.393097	12391	Alger Harrison
	55304	Arroyo	31.220066	-100.363786	8906	Alger Harrison
	55306	Arroyo	31.137044	-100.590618	14250	Alger Harrison
	55318	Arroyo	31.268958	-100.554217	15833	Alger Harrison
	55319	Arroyo	31.244158	-100.576827	9661	Alger Harrison
	55336	Arroyo	31.191478	-100.606837	7500	Alger Harrison
	55338	Arroyo	31.224076	-100.623007	8906	Alger Harrison

State well number	BRACS well id	Formation	Latitude	Longitude	TDS (mg/L)	Method
	55340	Arroyo	31.245330	-100.618482	8636	Alger Harrison
	55351	Arroyo	31.126329	-100.501252	30000	Alger Harrison
	55360	Arroyo	31.420102	-100.127310	12391	Alger Harrison
	55361	Arroyo	31.624130	-100.457540	12391	Alger Harrison
	55382	Arroyo	31.639943	-100.619228	9048	Alger Harrison
	55385	Arroyo	31.677209	-100.662452	11400	Alger Harrison
	55413	Arroyo	31.184239	-100.196578	16286	Alger Harrison
	55428	Arroyo	31.571589	-100.210934	51818	Alger Harrison
	55683	Arroyo	31.097479	-100.569498	20357	Alger Harrison
	55688	Arroyo	31.143217	-100.368527	12128	Alger Harrison
	55692	Arroyo	31.158984	-100.538909	8507	Alger Harrison
	55699	Arroyo	31.195538	-100.653457	16765	Alger Harrison
	55700	Arroyo	31.568457	-100.163715	43846	Alger Harrison
	55704	Arroyo	31.557770	-100.232381	33529	Alger Harrison
	55706	Arroyo	31.402332	-100.525024	51818	Alger Harrison
	55707	Arroyo	31.249595	-100.228910	5938	Alger Harrison
	55711	Arroyo	31.130599	-100.620426	25909	Alger Harrison
	55716	Arroyo	31.647943	-100.622598	17812	Alger Harrison
	55725	Arroyo	31.543810	-100.308467	17273	Alger Harrison
	55730	Arroyo	32.000690	-101.215894	63333	Alger Harrison
	55731	Arroyo	31.291575	-100.542113	16765	Alger Harrison
	55756	Arroyo	31.599846	-100.496584	15439	Alger Harrison
	55756	Arroyo	31.599846	-100.496584	30345	Alger Harrison
	55761	Arroyo	31.154799	-100.629646	28500	Alger Harrison
	55762	Arroyo	31.400269	-100.498751	19655	Alger Harrison
	55815	Arroyo	31.324434	-100.265912	12128	Alger Harrison
	55923	Arroyo	31.168158	-100.472501	15405	Alger Harrison
	58520	Arroyo	31.052059	-100.373988	7308	Alger Harrison
4339602		Arroyo	31.426388	-100.141666	1955	Measured
4339602		Arroyo	31.426388	-100.141666	1997	Measured
4339602		Arroyo	31.426388	-100.141666	1892	Measured
4339304		Arroyo	31.473888	-100.125832	4094	Measured
4339304		Arroyo	31.473888	-100.125832	3211	Measured
4347301		Arroyo	31.361944	-100.157500	1511	Measured
4348402		Arroyo	31.303333	-100.115277	2359	Measured
4324301		Arroyo	31.709166	-100.008333	1272	Measured
4324301		Arroyo	31.709166	-100.008333	979	Measured

State well number	BRACS well id	Formation	Latitude	Longitude	TDS (mg/L)	Method
4324301		Arroyo	31.709166	-100.008333	1492	Measured
4332305		Arroyo	31.592221	-100.039444	1481	Measured
4332305		Arroyo	31.592221	-100.039444	2279	Measured
4332305		Arroyo	31.592221	-100.039444	2279	Measured
4332305		Arroyo	31.592221	-100.039444	2223	Measured
4332305		Arroyo	31.592221	-100.039444	1874	Measured
	55140	Arroyo	31.689000	-100.039000	3801	Measured
	55145	Arroyo	31.573000	-100.015000	1539	Measured
	55148	Arroyo	31.393000	-100.166000	1519	Measured
4331602		Arroyo	31.580555	-100.160278	986	Measured
4332403		Arroyo	31.555001	-100.118889	1552	Measured
4340104		Arroyo	31.464723	-100.091111	1054	Measured
4340402		Arroyo	31.443056	-100.098611	1350	Measured
4348101		Arroyo	31.355834	-100.091111	820	Measured
4348101		Arroyo	31.355834	-100.091111	849	Measured
4348401		Arroyo	31.312778	-100.113612	2126	Measured
	23156	Bullwagon Dolomite	31.998302	-101.067511	51818	Alger Harrison
	24736	Bullwagon Dolomite	31.551085	-100.513121	22800	Alger Harrison
	24736	Bullwagon Dolomite	31.551085	-100.513121	17273	Alger Harrison
	24754	Bullwagon Dolomite	31.547039	-100.349678	11176	Alger Harrison
	24756	Bullwagon Dolomite	31.391699	-100.452771	15833	Alger Harrison
4312903	25724	Bullwagon Dolomite	31.768179	-100.540247	11633	Alger Harrison
	25746	Bullwagon Dolomite	31.767280	-100.780087	6951	Alger Harrison
	26747	Bullwagon Dolomite	31.740011	-101.105129	7215	Alger Harrison
	26755	Bullwagon Dolomite	31.818349	-101.168217	5089	Alger Harrison
	26819	Bullwagon Dolomite	31.736161	-101.134080	5044	Alger Harrison
	26935	Bullwagon Dolomite	31.042560	-100.515493	5044	Alger Harrison
	27000	Bullwagon Dolomite	31.760639	-101.168551	19000	Alger Harrison
	27035	Bullwagon Dolomite	31.756725	-101.145281	20357	Alger Harrison
	27114	Bullwagon Dolomite	31.326624	-100.453610	5534	Alger Harrison
	27134	Bullwagon Dolomite	31.783869	-101.129950	13571	Alger Harrison
	27383	Bullwagon Dolomite	31.710253	-101.104552	6129	Alger Harrison
	27386	Bullwagon Dolomite	31.728821	-101.133670	12128	Alger Harrison
	27959	Bullwagon Dolomite	31.794067	-101.207502	5135	Alger Harrison
	28197	Bullwagon Dolomite	31.756456	-101.052521	11176	Alger Harrison
	28603	Bullwagon Dolomite	31.422247	-100.917424	31667	Alger Harrison
	28744	Bullwagon Dolomite	31.780859	-101.163011	12391	Alger Harrison

State well number	BRACS well id	Formation	Latitude	Longitude	TDS (mg/L)	Method
	29166	Bullwagon Dolomite	31.738238	-101.052882	8507	Alger Harrison
	29308	Bullwagon Dolomite	31.774400	-101.066539	18387	Alger Harrison
	29768	Bullwagon Dolomite	31.880645	-101.173602	28500	Alger Harrison
	29841	Bullwagon Dolomite	31.740682	-101.065509	8028	Alger Harrison
	29878	Bullwagon Dolomite	31.866645	-101.192122	12128	Alger Harrison
	30677	Bullwagon Dolomite	31.848176	-101.184512	15405	Alger Harrison
	30857	Bullwagon Dolomite	31.836070	-101.145734	4957	Alger Harrison
	30878	Bullwagon Dolomite	31.968134	-100.985169	11429	Alger Harrison
	32361	Bullwagon Dolomite	31.426817	-100.913211	7500	Alger Harrison
	32652	Bullwagon Dolomite	31.802076	-101.225033	10755	Alger Harrison
	32775	Bullwagon Dolomite	31.655623	-100.590218	9828	Alger Harrison
	32775	Bullwagon Dolomite	31.655623	-100.590218	9670	Alger Harrison
	32781	Bullwagon Dolomite	31.099638	-100.339207	5278	Alger Harrison
	32787	Bullwagon Dolomite	31.427686	-100.482211	43846	Alger Harrison
	32799	Bullwagon Dolomite	31.383220	-100.307365	6333	Alger Harrison
	32800	Bullwagon Dolomite	31.108047	-100.499164	38000	Alger Harrison
	32805	Bullwagon Dolomite	31.352206	-100.525198	6404	Alger Harrison
	32808	Bullwagon Dolomite	31.302859	-100.461553	7125	Alger Harrison
	32814	Bullwagon Dolomite	31.514450	-100.444722	6786	Alger Harrison
	35049	Bullwagon Dolomite	31.437403	-100.840957	4790	Alger Harrison
	35381	Bullwagon Dolomite	31.210412	-100.481005	8143	Alger Harrison
	35563	Bullwagon Dolomite	31.465803	-100.589194	8507	Alger Harrison
	35809	Bullwagon Dolomite	31.923467	-100.874297	5644	Alger Harrison
	35809	Bullwagon Dolomite	31.923467	-100.874297	5644	Alger Harrison
4343601	37961	Bullwagon Dolomite	31.296855	-100.641823	23750	Alger Harrison
	37975	Bullwagon Dolomite	31.512490	-100.381069	43846	Alger Harrison
	37977	Bullwagon Dolomite	31.279513	-100.436529	1252	Alger Harrison
	38262	Bullwagon Dolomite	31.619595	-100.516255	18387	Alger Harrison
	47542	Bullwagon Dolomite	31.374111	-100.804242	6129	Alger Harrison
	47564	Bullwagon Dolomite	31.256367	-100.735358	7040	Alger Harrison
	47609	Bullwagon Dolomite	31.431211	-100.985135	15172	Alger Harrison
	47858	Bullwagon Dolomite	31.503295	-100.697688	11176	Alger Harrison
	51650	Bullwagon Dolomite	31.200276	-100.539197	7808	Alger Harrison
4352407	51891	Bullwagon Dolomite	31.195660	-100.590356	3497	Alger Harrison
4320105	53709	Bullwagon Dolomite	31.720326	-100.614950	7808	Alger Harrison
4310503	53730	Bullwagon Dolomite	31.800084	-100.796123	12955	Alger Harrison
4302903	53737	Bullwagon Dolomite	31.891535	-100.785607	21923	Alger Harrison

State well number	BRACS well id	Formation	Latitude	Longitude	TDS (mg/L)	Method
4321106	53774	Bullwagon Dolomite	31.734940	-100.463144	25143	Alger Harrison
	54502	Bullwagon Dolomite	31.291304	-100.511095	1738	Alger Harrison
	54508	Bullwagon Dolomite	31.492880	-100.506374	3986	Alger Harrison
	55188	Bullwagon Dolomite	31.537764	-100.660755	9194	Alger Harrison
	55203	Bullwagon Dolomite	31.461285	-100.381017	18387	Alger Harrison
	55207	Bullwagon Dolomite	31.353511	-100.488535	25909	Alger Harrison
	55220	Bullwagon Dolomite	31.431533	-100.254143	13256	Alger Harrison
	55221	Bullwagon Dolomite	31.148304	-100.637771	4831	Alger Harrison
	55225	Bullwagon Dolomite	31.422830	-100.371988	57000	Alger Harrison
	55227	Bullwagon Dolomite	31.400305	-100.540771	6628	Alger Harrison
	55235	Bullwagon Dolomite	31.224487	-100.661647	11400	Alger Harrison
	55267	Bullwagon Dolomite	31.521707	-100.687579	9828	Alger Harrison
	55296	Bullwagon Dolomite	31.212865	-100.589465	8507	Alger Harrison
	55300	Bullwagon Dolomite	31.621898	-100.393097	19655	Alger Harrison
	55304	Bullwagon Dolomite	31.220066	-100.363786	7403	Alger Harrison
	55306	Bullwagon Dolomite	31.137044	-100.590618	7917	Alger Harrison
	55318	Bullwagon Dolomite	31.268958	-100.554217	16286	Alger Harrison
	55319	Bullwagon Dolomite	31.244158	-100.576827	5588	Alger Harrison
	55338	Bullwagon Dolomite	31.224076	-100.623007	1821	Alger Harrison
	55340	Bullwagon Dolomite	31.245330	-100.618482	2111	Alger Harrison
	55351	Bullwagon Dolomite	31.126329	-100.501252	6196	Alger Harrison
	55361	Bullwagon Dolomite	31.624130	-100.457540	12667	Alger Harrison
	55362	Bullwagon Dolomite	31.658302	-100.633439	14615	Alger Harrison
	55382	Bullwagon Dolomite	31.639943	-100.619228	6628	Alger Harrison
	55384	Bullwagon Dolomite	31.662079	-100.559102	9194	Alger Harrison
	55385	Bullwagon Dolomite	31.677209	-100.662452	9661	Alger Harrison
	55683	Bullwagon Dolomite	31.097479	-100.569498	10962	Alger Harrison
	55688	Bullwagon Dolomite	31.143217	-100.368527	8906	Alger Harrison
	55692	Bullwagon Dolomite	31.158984	-100.538909	4014	Alger Harrison
	55699	Bullwagon Dolomite	31.195538	-100.653457	5588	Alger Harrison
	55706	Bullwagon Dolomite	31.402332	-100.525024	6404	Alger Harrison
	55711	Bullwagon Dolomite	31.130599	-100.620426	21923	Alger Harrison
	55716	Bullwagon Dolomite	31.647943	-100.622598	10000	Alger Harrison
	55725	Bullwagon Dolomite	31.543810	-100.308467	30000	Alger Harrison
	55730	Bullwagon Dolomite	32.000690	-101.215894	81429	Alger Harrison
	55756	Bullwagon Dolomite	31.599846	-100.496584	18333	Alger Harrison
	55756	Bullwagon Dolomite	31.599846	-100.496584	21463	Alger Harrison

State well number	BRACS well id	Formation	Latitude	Longitude	TDS (mg/L)	Method
	55762	Bullwagon Dolomite	31.400269	-100.498751	21111	Alger Harrison
	55923	Bullwagon Dolomite	31.168158	-100.472501	4634	Alger Harrison
4347203		Bullwagon Dolomite	31.374721	-100.193610	1363	Measured
4347203		Bullwagon Dolomite	31.374721	-100.193610	1208	Measured
4331203		Bullwagon Dolomite	31.598610	-100.170277	947	Measured
4331203		Bullwagon Dolomite	31.598610	-100.170277	798	Measured
4331203		Bullwagon Dolomite	31.598610	-100.170277	879	Measured
4331203		Bullwagon Dolomite	31.598610	-100.170277	928	Measured
4331203		Bullwagon Dolomite	31.598610	-100.170277	1253	Measured
4331203		Bullwagon Dolomite	31.598610	-100.170277	1114	Measured
4331203		Bullwagon Dolomite	31.598610	-100.170277	1164	Measured
4331203		Bullwagon Dolomite	31.598610	-100.170277	1014	Measured
4331203		Bullwagon Dolomite	31.598610	-100.170277	1404	Measured
4331203		Bullwagon Dolomite	31.598610	-100.170277	1117	Measured
4331203		Bullwagon Dolomite	31.598610	-100.170277	1134	Measured
4331203		Bullwagon Dolomite	31.598610	-100.170277	1175	Measured
4331807		Bullwagon Dolomite	31.541389	-100.178611	2377	Measured
4331807		Bullwagon Dolomite	31.541389	-100.178611	2420	Measured
	23156	Tubb	31.998302	-101.067511	12128	Alger Harrison
	24736	Tubb	31.551085	-100.513121	11176	Alger Harrison
	24754	Tubb	31.547039	-100.349678	16765	Alger Harrison
	24756	Tubb	31.391699	-100.452771	4872	Alger Harrison
4312903	25724	Tubb	31.768179	-100.540247	16286	Alger Harrison
	25746	Tubb	31.767280	-100.780087	5644	Alger Harrison
	26747	Tubb	31.740011	-101.105129	10962	Alger Harrison
	26755	Tubb	31.818349	-101.168217	15000	Alger Harrison
	26819	Tubb	31.736161	-101.134080	16765	Alger Harrison
	26935	Tubb	31.042560	-100.515493	3654	Alger Harrison
	27000	Tubb	31.760639	-101.168551	14250	Alger Harrison
	27113	Tubb	31.812097	-100.974954	11400	Alger Harrison
	27113	Tubb	31.812097	-100.974954	11400	Alger Harrison
	27113	Tubb	31.812097	-100.974954	9048	Alger Harrison
	27114	Tubb	31.326624	-100.453610	12128	Alger Harrison
	27134	Tubb	31.783869	-101.129950	8769	Alger Harrison
	27383	Tubb	31.710253	-101.104552	8769	Alger Harrison
	27386	Tubb	31.728821	-101.133670	12128	Alger Harrison
	27440	Tubb	31.608987	-101.070468	8507	Alger Harrison

State well number	BRACS well id	Formation	Latitude	Longitude	TDS (mg/L)	Method
	27440	Tubb	31.608987	-101.070468	16765	Alger Harrison
	27447	Tubb	31.705179	-101.036072	8261	Alger Harrison
	27785	Tubb	31.538677	-101.157729	22000	Alger Harrison
	27959	Tubb	31.794067	-101.207502	7037	Alger Harrison
	28110	Tubb	31.791977	-101.123064	10755	Alger Harrison
	28112	Tubb	31.781719	-101.143621	9344	Alger Harrison
	28197	Tubb	31.756456	-101.052521	11633	Alger Harrison
	28603	Tubb	31.422247	-100.917424	25909	Alger Harrison
	28604	Tubb	31.300435	-100.721659	5588	Alger Harrison
	28744	Tubb	31.780859	-101.163011	5534	Alger Harrison
	29166	Tubb	31.738238	-101.052882	11176	Alger Harrison
	29308	Tubb	31.774400	-101.066539	21923	Alger Harrison
	29768	Tubb	31.880645	-101.173602	19655	Alger Harrison
	29841	Tubb	31.740682	-101.065509	16765	Alger Harrison
	29878	Tubb	31.866645	-101.192122	8507	Alger Harrison
	30677	Tubb	31.848176	-101.184512	14615	Alger Harrison
	30857	Tubb	31.836070	-101.145734	7500	Alger Harrison
	30878	Tubb	31.968134	-100.985169	12055	Alger Harrison
	32361	Tubb	31.426817	-100.913211	9048	Alger Harrison
	32461	Tubb	31.431536	-101.006333	13256	Alger Harrison
	32652	Tubb	31.802076	-101.225033	7500	Alger Harrison
	32775	Tubb	31.655623	-100.590218	10556	Alger Harrison
	32775	Tubb	31.655623	-100.590218	11733	Alger Harrison
	32775	Tubb	31.655623	-100.590218	12391	Alger Harrison
	32775	Tubb	31.655623	-100.590218	10115	Alger Harrison
	32787	Tubb	31.427686	-100.482211	15833	Alger Harrison
	32805	Tubb	31.352206	-100.525198	15000	Alger Harrison
	32806	Tubb	31.399977	-100.684287	4597	Alger Harrison
	32808	Tubb	31.302859	-100.461553	6196	Alger Harrison
	32814	Tubb	31.514450	-100.444722	6786	Alger Harrison
	35049	Tubb	31.437403	-100.840957	7917	Alger Harrison
	35381	Tubb	31.210412	-100.481005	9500	Alger Harrison
	35561	Tubb	31.455673	-100.618163	7500	Alger Harrison
	35561	Tubb	31.455673	-100.618163	8382	Alger Harrison
	35563	Tubb	31.465803	-100.589194	21111	Alger Harrison
	35809	Tubb	31.923467	-100.874297	2794	Alger Harrison
	35809	Tubb	31.923467	-100.874297	7500	Alger Harrison

State well number	BRACS well id	Formation	Latitude	Longitude	TDS (mg/L)	Method
	37974	Tubb	31.546184	-100.432327	5758	Alger Harrison
	37975	Tubb	31.512490	-100.381069	10179	Alger Harrison
	37977	Tubb	31.279513	-100.436529	1129	Alger Harrison
	38262	Tubb	31.619595	-100.516255	19655	Alger Harrison
	47564	Tubb	31.256367	-100.735358	15833	Alger Harrison
	47609	Tubb	31.431211	-100.985135	27143	Alger Harrison
	47858	Tubb	31.503295	-100.697688	11633	Alger Harrison
	51672	Tubb	31.542921	-100.901953	15405	Alger Harrison
4329301	51781	Tubb	31.622197	-100.413971	6786	Alger Harrison
4352407	51891	Tubb	31.195660	-100.590356	7808	Alger Harrison
4320105	53709	Tubb	31.720326	-100.614950	10755	Alger Harrison
4310901	53713	Tubb	31.788703	-100.758778	7917	Alger Harrison
4310503	53730	Tubb	31.800084	-100.796123	15000	Alger Harrison
4302903	53737	Tubb	31.891535	-100.785607	22800	Alger Harrison
4321106	53774	Tubb	31.734940	-100.463144	27143	Alger Harrison
	54502	Tubb	31.291304	-100.511095	2088	Alger Harrison
	55188	Tubb	31.537764	-100.660755	15833	Alger Harrison
	55188	Tubb	31.537764	-100.660755	12667	Alger Harrison
	55207	Tubb	31.353511	-100.488535	28500	Alger Harrison
	55221	Tubb	31.148304	-100.637771	6404	Alger Harrison
	55225	Tubb	31.422830	-100.371988	16765	Alger Harrison
	55227	Tubb	31.400305	-100.540771	13571	Alger Harrison
	55235	Tubb	31.224487	-100.661647	24783	Alger Harrison
	55267	Tubb	31.521707	-100.687579	7308	Alger Harrison
	55267	Tubb	31.521707	-100.687579	9194	Alger Harrison
	55271	Tubb	31.505700	-100.596876	19000	Alger Harrison
	55296	Tubb	31.212865	-100.589465	9344	Alger Harrison
	55300	Tubb	31.621898	-100.393097	10179	Alger Harrison
	55306	Tubb	31.137044	-100.590618	6628	Alger Harrison
	55318	Tubb	31.268958	-100.554217	12391	Alger Harrison
	55319	Tubb	31.244158	-100.576827	10962	Alger Harrison
	55336	Tubb	31.191478	-100.606837	5429	Alger Harrison
	55338	Tubb	31.224076	-100.623007	4957	Alger Harrison
	55340	Tubb	31.245330	-100.618482	12391	Alger Harrison
	55361	Tubb	31.624130	-100.457540	12955	Alger Harrison
	55362	Tubb	31.658302	-100.633439	5377	Alger Harrison
	55362	Tubb	31.658302	-100.633439	21923	Alger Harrison

State well number	BRACS well id	Formation	Latitude	Longitude	TDS (mg/L)	Method
	55382	Tubb	31.639943	-100.619228	13571	Alger Harrison
	55384	Tubb	31.662079	-100.559102	7808	Alger Harrison
	55384	Tubb	31.662079	-100.559102	7808	Alger Harrison
	55385	Tubb	31.677209	-100.662452	9500	Alger Harrison
	55683	Tubb	31.097479	-100.569498	5876	Alger Harrison
	55692	Tubb	31.158984	-100.538909	2192	Alger Harrison
	55693	Tubb	31.338945	-100.496427	3931	Alger Harrison
	55699	Tubb	31.195538	-100.653457	9048	Alger Harrison
	55706	Tubb	31.402332	-100.525024	15405	Alger Harrison
	55711	Tubb	31.130599	-100.620426	22800	Alger Harrison
	55716	Tubb	31.647943	-100.622598	21111	Alger Harrison
	55725	Tubb	31.543810	-100.308467	19655	Alger Harrison
	55730	Tubb	32.000690	-101.215894	63333	Alger Harrison
	55756	Tubb	31.599846	-100.496584	17255	Alger Harrison
	55756	Tubb	31.599846	-100.496584	15172	Alger Harrison
	55762	Tubb	31.400269	-100.498751	19000	Alger Harrison
4338602		Tubb	31.448055	-100.256666	1300	Measured
4338602		Tubb	31.448055	-100.256666	1246	Measured
4339114		Tubb	31.468332	-100.225277	1356	Measured
4339114		Tubb	31.468332	-100.225277	1559	Measured
	55152	Tubb	31.514000	-100.184000	2322	Measured
	55153	Tubb	31.516000	-100.215000	1463	Measured
	55155	Tubb	31.535000	-100.250000	2639	Measured
	55164	Tubb	31.333000	-100.267000	4197	Measured
4331204		Tubb	31.590556	-100.193611	1827	Measured
4331407		Tubb	31.570000	-100.230833	1448	Measured
4338910		Tubb	31.383611	-100.262223	2344	Measured
4339408		Tubb	31.418333	-100.243334	1405	Measured
4339408		Tubb	31.418333	-100.243334	1337	Measured
4339408		Tubb	31.418333	-100.243334	1848	Measured
4346208		Tubb	31.373611	-100.307223	1308	Measured
4346208		Tubb	31.373611	-100.307223	1545	Measured
4346208		Tubb	31.373611	-100.307223	1260	Measured
4346208		Tubb	31.373611	-100.307223	1382	Measured
4346215		Tubb	31.370555	-100.302501	1864	Measured
	23156	Choza	31.998302	-101.067511	10000	Alger Harrison
	24736	Choza	31.551085	-100.513121	25909	Alger Harrison

State well number	BRACS well id	Formation	Latitude	Longitude	TDS (mg/L)	Method
	24736	Choza	31.551085	-100.513121	20357	Alger Harrison
4312903	25724	Choza	31.768179	-100.540247	15000	Alger Harrison
	25746	Choza	31.767280	-100.780087	5135	Alger Harrison
	26755	Choza	31.818349	-101.168217	11176	Alger Harrison
	26819	Choza	31.736161	-101.134080	10755	Alger Harrison
	27000	Choza	31.760639	-101.168551	10755	Alger Harrison
	27024	Choza	31.764369	-101.152701	19000	Alger Harrison
	27035	Choza	31.756725	-101.145281	23750	Alger Harrison
	27113	Choza	31.812097	-100.974954	12391	Alger Harrison
	27113	Choza	31.812097	-100.974954	16765	Alger Harrison
	27113	Choza	31.812097	-100.974954	16765	Alger Harrison
	27134	Choza	31.783869	-101.129950	8636	Alger Harrison
	27383	Choza	31.710253	-101.104552	7125	Alger Harrison
	27386	Choza	31.728821	-101.133670	10755	Alger Harrison
	27440	Choza	31.608987	-101.070468	11875	Alger Harrison
	27785	Choza	31.538677	-101.157729	22564	Alger Harrison
	27959	Choza	31.794067	-101.207502	15833	Alger Harrison
	28110	Choza	31.791977	-101.123064	11875	Alger Harrison
	28110	Choza	31.791977	-101.123064	6628	Alger Harrison
	28112	Choza	31.781719	-101.143621	5876	Alger Harrison
	28197	Choza	31.756456	-101.052521	27143	Alger Harrison
	28603	Choza	31.422247	-100.917424	16765	Alger Harrison
	28604	Choza	31.300435	-100.721659	7600	Alger Harrison
	29166	Choza	31.738238	-101.052882	15000	Alger Harrison
	29308	Choza	31.774400	-101.066539	15000	Alger Harrison
	29768	Choza	31.880645	-101.173602	24783	Alger Harrison
	29841	Choza	31.740682	-101.065509	22800	Alger Harrison
	29878	Choza	31.866645	-101.192122	12128	Alger Harrison
	30677	Choza	31.848176	-101.184512	8636	Alger Harrison
	30878	Choza	31.968134	-100.985169	15172	Alger Harrison
	32361	Choza	31.426817	-100.913211	12667	Alger Harrison
	32461	Choza	31.431536	-101.006333	23750	Alger Harrison
	32652	Choza	31.802076	-101.225033	13902	Alger Harrison
	32775	Choza	31.655623	-100.590218	13571	Alger Harrison
	32775	Choza	31.655623	-100.590218	13538	Alger Harrison
	32787	Choza	31.427686	-100.482211	7125	Alger Harrison
	32805	Choza	31.352206	-100.525198	14615	Alger Harrison

State well number	BRACS well id	Formation	Latitude	Longitude	TDS (mg/L)	Method
	32806	Choza	31.399977	-100.684287	7703	Alger Harrison
	34825	Choza	31.641391	-100.788573	4972	Alger Harrison
	35049	Choza	31.437403	-100.840957	8769	Alger Harrison
	35563	Choza	31.465803	-100.589194	12955	Alger Harrison
	35809	Choza	31.923467	-100.874297	7308	Alger Harrison
4343601	37961	Choza	31.296855	-100.641823	7808	Alger Harrison
	37974	Choza	31.546184	-100.432327	10556	Alger Harrison
	37975	Choza	31.512490	-100.381069	9048	Alger Harrison
	38262	Choza	31.619595	-100.516255	28500	Alger Harrison
	47542	Choza	31.374111	-100.804242	11176	Alger Harrison
	47545	Choza	31.428441	-100.802794	15000	Alger Harrison
	47564	Choza	31.256367	-100.735358	12667	Alger Harrison
	47609	Choza	31.431211	-100.985135	21111	Alger Harrison
	47858	Choza	31.503295	-100.697688	23750	Alger Harrison
	51650	Choza	31.200276	-100.539197	12128	Alger Harrison
	51672	Choza	31.542921	-100.901953	10962	Alger Harrison
4329301	51781	Choza	31.622197	-100.413971	3931	Alger Harrison
4352407	51891	Choza	31.195660	-100.590356	8769	Alger Harrison
4320105	53709	Choza	31.720326	-100.614950	11633	Alger Harrison
4310901	53713	Choza	31.788703	-100.758778	8507	Alger Harrison
4310503	53730	Choza	31.800084	-100.796123	8906	Alger Harrison
4302903	53737	Choza	31.891535	-100.785607	23750	Alger Harrison
4321106	53774	Choza	31.734940	-100.463144	11400	Alger Harrison
	54502	Choza	31.291304	-100.511095	1748	Alger Harrison
	54505	Choza	31.152371	-100.671089	9344	Alger Harrison
	55188	Choza	31.537764	-100.660755	21111	Alger Harrison
	55221	Choza	31.148304	-100.637771	13256	Alger Harrison
	55235	Choza	31.224487	-100.661647	31667	Alger Harrison
	55267	Choza	31.521707	-100.687579	16923	Alger Harrison
	55267	Choza	31.521707	-100.687579	15405	Alger Harrison
	55271	Choza	31.505700	-100.596876	21111	Alger Harrison
	55271	Choza	31.505700	-100.596876	19000	Alger Harrison
	55296	Choza	31.212865	-100.589465	9194	Alger Harrison
	55300	Choza	31.621898	-100.393097	12955	Alger Harrison
	55306	Choza	31.137044	-100.590618	2639	Alger Harrison
	55319	Choza	31.244158	-100.576827	5182	Alger Harrison
	55336	Choza	31.191478	-100.606837	10962	Alger Harrison

State well number	BRACS well id	Formation	Latitude	Longitude	TDS (mg/L)	Method
	55338	Choza	31.224076	-100.623007	12128	Alger Harrison
	55340	Choza	31.245330	-100.618482	13902	Alger Harrison
	55361	Choza	31.624130	-100.457540	3585	Alger Harrison
	55362	Choza	31.658302	-100.633439	5000	Alger Harrison
	55382	Choza	31.639943	-100.619228	11176	Alger Harrison
	55384	Choza	31.662079	-100.559102	13902	Alger Harrison
	55385	Choza	31.677209	-100.662452	11400	Alger Harrison
	55437	Choza	31.560584	-100.808842	11176	Alger Harrison
	55693	Choza	31.338945	-100.496427	4318	Alger Harrison
	55699	Choza	31.195538	-100.653457	6867	Alger Harrison
	55711	Choza	31.130599	-100.620426	21923	Alger Harrison
	55716	Choza	31.647943	-100.622598	31667	Alger Harrison
	55730	Choza	32.000690	-101.215894	51818	Alger Harrison
	55756	Choza	31.599846	-100.496584	13333	Alger Harrison
	55756	Choza	31.599846	-100.496584	5500	Alger Harrison
	55771	Choza	31.173190	-100.586029	5876	Alger Harrison
	55797	Choza	31.246397	-100.649597	14250	Alger Harrison
	51449	Choza	31.239721	-100.612222	67470	Measured
4338703		Choza	31.414444	-100.334444	2091	Measured
4338703		Choza	31.414444	-100.334444	2129	Measured
4338305		Choza	31.491666	-100.287777	2465	Measured
	55154	Choza	31.472000	-100.326000	1035	Measured
	55159	Choza	31.526000	-100.410000	2948	Measured
	55160	Choza	31.393000	-100.383000	1741	Measured
	55161	Choza	31.407000	-100.396000	2673	Measured
	55162	Choza	31.407000	-100.395000	2213	Measured
	55163	Choza	31.406000	-100.390000	3778	Measured
	55165	Choza	31.346000	-100.426000	1320	Measured
	55166	Choza	31.371000	-100.432000	2451	Measured
	55167	Choza	31.374000	-100.433000	2423	Measured
	55168	Choza	31.384000	-100.432000	3694	Measured
	55170	Choza	31.384000	-100.433000	3661	Measured
	55171	Choza	31.378000	-100.442000	3975	Measured
	55172	Choza	31.376000	-100.447000	3520	Measured
	55174	Choza	31.375000	-100.473000	4207	Measured
4323703		Choza	31.626667	-100.212223	818	Measured
4323801		Choza	31.636111	-100.194445	1068	Measured

State well number	BRACS well id	Formation	Latitude	Longitude	TDS (mg/L)	Method
4330303		Choza	31.610556	-100.264445	567	Measured
4330604		Choza	31.574444	-100.286945	2264	Measured
4330604		Choza	31.574444	-100.286945	3029	Measured
4330702		Choza	31.534445	-100.350278	676	Measured
4331104		Choza	31.610556	-100.247222	502	Measured
4331105		Choza	31.611112	-100.240556	635	Measured
4331408		Choza	31.576111	-100.238056	1665	Measured
4337209		Choza	31.458889	-100.426944	1932	Measured
4337210		Choza	31.458889	-100.429722	1448	Measured
4337501		Choza	31.455001	-100.421389	2925	Measured
4337509		Choza	31.454445	-100.422500	2330	Measured
4337511		Choza	31.451945	-100.432778	2131	Measured
4337603		Choza	31.437500	-100.391111	1626	Measured
4337603		Choza	31.437500	-100.391111	1741	Measured
4337702		Choza	31.380555	-100.476389	852	Measured
4337905		Choza	31.398056	-100.406667	4820	Measured
4337906		Choza	31.391111	-100.379444	2049	Measured
4337907		Choza	31.379167	-100.404445	1795	Measured
4337909		Choza	31.390834	-100.385834	1703	Measured
4337909		Choza	31.390834	-100.385834	1832	Measured
4337910		Choza	31.390834	-100.379167	2069	Measured
4338204		Choza	31.478611	-100.303334	5317	Measured
4338214		Choza	31.493334	-100.304167	2208	Measured
4338214		Choza	31.493334	-100.304167	1388	Measured
4338705		Choza	31.382778	-100.358889	1668	Measured
4338705		Choza	31.382778	-100.358889	1751	Measured
4345104		Choza	31.372500	-100.472222	2080	Measured
4345106		Choza	31.375000	-100.474444	4483	Measured
4345201		Choza	31.374722	-100.434445	2710	Measured
	21323	San Angelo	31.472488	-100.703703	13902	Alger Harrison
	21326	San Angelo	31.440819	-100.709463	16765	Alger Harrison
	21337	San Angelo	31.215104	-100.690742	10962	Alger Harrison
	23156	San Angelo	31.998302	-101.067511	23750	Alger Harrison
	24736	San Angelo	31.551085	-100.513121	12955	Alger Harrison
4312903	25724	San Angelo	31.768179	-100.540247	11875	Alger Harrison
	25746	San Angelo	31.767280	-100.780087	9828	Alger Harrison
	26747	San Angelo	31.740011	-101.105129	8636	Alger Harrison

State well number	BRACS well id	Formation	Latitude	Longitude	TDS (mg/L)	Method
	26755	San Angelo	31.818349	-101.168217	13256	Alger Harrison
	26819	San Angelo	31.736161	-101.134080	5816	Alger Harrison
	27000	San Angelo	31.760639	-101.168551	9194	Alger Harrison
	27035	San Angelo	31.756725	-101.145281	17812	Alger Harrison
	27113	San Angelo	31.812097	-100.974954	13902	Alger Harrison
	27113	San Angelo	31.812097	-100.974954	12391	Alger Harrison
	27115	San Angelo	31.815259	-101.070459	15405	Alger Harrison
	27134	San Angelo	31.783869	-101.129950	11633	Alger Harrison
	27383	San Angelo	31.710253	-101.104552	9344	Alger Harrison
	27386	San Angelo	31.728821	-101.133670	7703	Alger Harrison
	27447	San Angelo	31.705179	-101.036072	6264	Alger Harrison
	27785	San Angelo	31.538677	-101.157729	12754	Alger Harrison
	27959	San Angelo	31.794067	-101.207502	5644	Alger Harrison
	28110	San Angelo	31.791977	-101.123064	8636	Alger Harrison
	28110	San Angelo	31.791977	-101.123064	10755	Alger Harrison
	28112	San Angelo	31.781719	-101.143621	7600	Alger Harrison
	28197	San Angelo	31.756456	-101.052521	7703	Alger Harrison
	28744	San Angelo	31.780859	-101.163011	4222	Alger Harrison
	29166	San Angelo	31.738238	-101.052882	11875	Alger Harrison
	29308	San Angelo	31.774400	-101.066539	28500	Alger Harrison
	29768	San Angelo	31.880645	-101.173602	11875	Alger Harrison
	29841	San Angelo	31.740682	-101.065509	11875	Alger Harrison
	29878	San Angelo	31.866645	-101.192122	6706	Alger Harrison
	29878	San Angelo	31.866645	-101.192122	7125	Alger Harrison
	30677	San Angelo	31.848176	-101.184512	5229	Alger Harrison
	30857	San Angelo	31.836070	-101.145734	8028	Alger Harrison
	30878	San Angelo	31.968134	-100.985169	22000	Alger Harrison
	32361	San Angelo	31.426817	-100.913211	12955	Alger Harrison
	32461	San Angelo	31.431536	-101.006333	17812	Alger Harrison
	32652	San Angelo	31.802076	-101.225033	9828	Alger Harrison
	32775	San Angelo	31.655623	-100.590218	11176	Alger Harrison
	32775	San Angelo	31.655623	-100.590218	10864	Alger Harrison
	32793	San Angelo	31.351065	-100.606029	16765	Alger Harrison
	32806	San Angelo	31.399977	-100.684287	7808	Alger Harrison
	34825	San Angelo	31.641391	-100.788573	7719	Alger Harrison
	34825	San Angelo	31.641391	-100.788573	15439	Alger Harrison
	35049	San Angelo	31.437403	-100.840957	5534	Alger Harrison

State well number	BRACS well id	Formation	Latitude	Longitude	TDS (mg/L)	Method
	35123	San Angelo	31.588329	-100.846288	10000	Alger Harrison
	35123	San Angelo	31.588329	-100.846288	16286	Alger Harrison
	35344	San Angelo	31.821594	-100.730633	31667	Alger Harrison
	35344	San Angelo	31.821594	-100.730633	43846	Alger Harrison
	35563	San Angelo	31.465803	-100.589194	15833	Alger Harrison
	35809	San Angelo	31.923467	-100.874297	17273	Alger Harrison
4343601	37961	San Angelo	31.296855	-100.641823	6552	Alger Harrison
	47542	San Angelo	31.374111	-100.804242	5135	Alger Harrison
	47564	San Angelo	31.256367	-100.735358	8906	Alger Harrison
	47609	San Angelo	31.431211	-100.985135	11400	Alger Harrison
	47774	San Angelo	31.224901	-100.779088	16765	Alger Harrison
	47858	San Angelo	31.503295	-100.697688	19000	Alger Harrison
4329301	51781	San Angelo	31.622197	-100.413971	4750	Alger Harrison
4352407	51891	San Angelo	31.195660	-100.590356	7500	Alger Harrison
4320105	53709	San Angelo	31.720326	-100.614950	7600	Alger Harrison
4310901	53713	San Angelo	31.788703	-100.758778	11875	Alger Harrison
4310503	53730	San Angelo	31.800084	-100.796123	12955	Alger Harrison
4302903	53737	San Angelo	31.891535	-100.785607	51818	Alger Harrison
4321106	53774	San Angelo	31.734940	-100.463144	10364	Alger Harrison
4321106	53774	San Angelo	31.734940	-100.463144	10755	Alger Harrison
	54505	San Angelo	31.152371	-100.671089	12391	Alger Harrison
	55188	San Angelo	31.537764	-100.660755	11176	Alger Harrison
	55221	San Angelo	31.148304	-100.637771	4672	Alger Harrison
	55235	San Angelo	31.224487	-100.661647	11875	Alger Harrison
	55267	San Angelo	31.521707	-100.687579	10962	Alger Harrison
	55296	San Angelo	31.212865	-100.589465	6786	Alger Harrison
	55306	San Angelo	31.137044	-100.590618	2227	Alger Harrison
	55336	San Angelo	31.191478	-100.606837	2096	Alger Harrison
	55338	San Angelo	31.224076	-100.623007	3239	Alger Harrison
	55340	San Angelo	31.245330	-100.618482	15405	Alger Harrison
	55361	San Angelo	31.624130	-100.457540	4101	Alger Harrison
	55362	San Angelo	31.658302	-100.633439	12128	Alger Harrison
	55364	San Angelo	31.649109	-100.861884	6951	Alger Harrison
	55382	San Angelo	31.639943	-100.619228	8906	Alger Harrison
	55385	San Angelo	31.677209	-100.662452	11400	Alger Harrison
	55414	San Angelo	31.545795	-100.789102	8382	Alger Harrison
	55414	San Angelo	31.545795	-100.789102	6129	Alger Harrison

State well number	BRACS well id	Formation	Latitude	Longitude	TDS (mg/L)	Method
	55437	San Angelo	31.560584	-100.808842	9344	Alger Harrison
	55438	San Angelo	31.568043	-100.819452	10556	Alger Harrison
	55438	San Angelo	31.568043	-100.819452	15000	Alger Harrison
	55686	San Angelo	31.763053	-100.857990	14250	Alger Harrison
	55690	San Angelo	31.630700	-100.855884	10364	Alger Harrison
	55693	San Angelo	31.338945	-100.496427	696	Alger Harrison
	55699	San Angelo	31.195538	-100.653457	6867	Alger Harrison
	55711	San Angelo	31.130599	-100.620426	11176	Alger Harrison
	55716	San Angelo	31.647943	-100.622598	19000	Alger Harrison
	55730	San Angelo	32.000690	-101.215894	23750	Alger Harrison
	55756	San Angelo	31.599846	-100.496584	15439	Alger Harrison
	55771	San Angelo	31.173190	-100.586029	4191	Alger Harrison
	55797	San Angelo	31.246397	-100.649597	15405	Alger Harrison
	55822	San Angelo	31.976691	-101.229964	10556	Alger Harrison
	51449	San Angelo	31.239721	-100.612222	7040	Measured
	51449	San Angelo	31.239721	-100.612222	7637	Measured
	55158	San Angelo	31.514000	-100.453000	2900	Measured
4329801		San Angelo	31.539167	-100.438056	1679	Measured
4337204		San Angelo	31.470278	-100.432500	673	Measured
4344301		San Angelo	31.371667	-100.512223	2154	Measured
2862707	17558	Queen	32.017239	-101.364117	8143	Alger Harrison
	21323	Queen	31.472488	-100.703703	8636	Alger Harrison
	21326	Queen	31.440819	-100.709463	14615	Alger Harrison
	21337	Queen	31.215104	-100.690742	3677	Alger Harrison
	21606	Queen	31.419725	-100.748328	9344	Alger Harrison
4312903	25724	Queen	31.768179	-100.540247	7215	Alger Harrison
	25746	Queen	31.767280	-100.780087	15833	Alger Harrison
	27113	Queen	31.812097	-100.974954	27143	Alger Harrison
	27115	Queen	31.815259	-101.070459	15000	Alger Harrison
	27440	Queen	31.608987	-101.070468	15405	Alger Harrison
	27447	Queen	31.705179	-101.036072	10000	Alger Harrison
	32053	Queen	31.607063	-100.726051	16286	Alger Harrison
	32361	Queen	31.426817	-100.913211	9661	Alger Harrison
	32461	Queen	31.431536	-101.006333	8261	Alger Harrison
	32775	Queen	31.655623	-100.590218	8769	Alger Harrison
	32775	Queen	31.655623	-100.590218	8462	Alger Harrison
	32806	Queen	31.399977	-100.684287	10755	Alger Harrison

State well number	BRACS well id	Formation	Latitude	Longitude	TDS (mg/L)	Method
	34828	Queen	31.605382	-100.762362	9828	Alger Harrison
	35344	Queen	31.821594	-100.730633	40714	Alger Harrison
	35809	Queen	31.923467	-100.874297	9048	Alger Harrison
	35809	Queen	31.923467	-100.874297	11176	Alger Harrison
	35809	Queen	31.923467	-100.874297	6786	Alger Harrison
	35974	Queen	31.486148	-100.626744	3701	Alger Harrison
	47542	Queen	31.374111	-100.804242	6196	Alger Harrison
	47564	Queen	31.256367	-100.735358	3701	Alger Harrison
	47609	Queen	31.431211	-100.985135	13571	Alger Harrison
	47774	Queen	31.224901	-100.779088	9661	Alger Harrison
	47947	Queen	31.336231	-100.717167	7600	Alger Harrison
	51672	Queen	31.542921	-100.901953	14615	Alger Harrison
4320105	53709	Queen	31.720326	-100.614950	7125	Alger Harrison
4310901	53713	Queen	31.788703	-100.758778	10000	Alger Harrison
4310503	53730	Queen	31.800084	-100.796123	12667	Alger Harrison
4310305	53734	Queen	31.836250	-100.764699	21923	Alger Harrison
4302903	53737	Queen	31.891535	-100.785607	81429	Alger Harrison
	55267	Queen	31.521707	-100.687579	7215	Alger Harrison
	55364	Queen	31.649109	-100.861884	11633	Alger Harrison
	55364	Queen	31.649109	-100.861884	8382	Alger Harrison
	55364	Queen	31.649109	-100.861884	22800	Alger Harrison
	55414	Queen	31.545795	-100.789102	4597	Alger Harrison
	55437	Queen	31.560584	-100.808842	7500	Alger Harrison
	55438	Queen	31.568043	-100.819452	10556	Alger Harrison
	55438	Queen	31.568043	-100.819452	10556	Alger Harrison
	55686	Queen	31.763053	-100.857990	17812	Alger Harrison
	55690	Queen	31.630700	-100.855884	11875	Alger Harrison
	55699	Queen	31.195538	-100.653457	2689	Alger Harrison
	55730	Queen	32.000690	-101.215894	114000	Alger Harrison
	55797	Queen	31.246397	-100.649597	13902	Alger Harrison
	55822	Queen	31.976691	-101.229964	24783	Alger Harrison
2862707	17558	Seven Rivers	32.017239	-101.364117	5588	Alger Harrison
	21323	Seven Rivers	31.472488	-100.703703	5327	Alger Harrison
	21337	Seven Rivers	31.215104	-100.690742	3631	Alger Harrison
	21606	Seven Rivers	31.419725	-100.748328	6867	Alger Harrison
	25746	Seven Rivers	31.767280	-100.780087	9661	Alger Harrison
	27113	Seven Rivers	31.812097	-100.974954	21923	Alger Harrison

State well number	BRACS well id	Formation	Latitude	Longitude	TDS (mg/L)	Method
	27115	Seven Rivers	31.815259	-101.070459	25909	Alger Harrison
	27447	Seven Rivers	31.705179	-101.036072	8636	Alger Harrison
	32053	Seven Rivers	31.607063	-100.726051	16286	Alger Harrison
	32461	Seven Rivers	31.431536	-101.006333	15833	Alger Harrison
	32806	Seven Rivers	31.399977	-100.684287	8769	Alger Harrison
	34828	Seven Rivers	31.605382	-100.762362	10556	Alger Harrison
	35123	Seven Rivers	31.588329	-100.846288	12955	Alger Harrison
	35123	Seven Rivers	31.588329	-100.846288	10000	Alger Harrison
	35344	Seven Rivers	31.821594	-100.730633	19655	Alger Harrison
	35809	Seven Rivers	31.923467	-100.874297	20357	Alger Harrison
	35809	Seven Rivers	31.923467	-100.874297	18387	Alger Harrison
	35974	Seven Rivers	31.486148	-100.626744	1827	Alger Harrison
	47542	Seven Rivers	31.374111	-100.804242	4790	Alger Harrison
	47609	Seven Rivers	31.431211	-100.985135	21923	Alger Harrison
	47774	Seven Rivers	31.224901	-100.779088	10364	Alger Harrison
	47947	Seven Rivers	31.336231	-100.717167	5000	Alger Harrison
	51672	Seven Rivers	31.542921	-100.901953	9828	Alger Harrison
4352407	51891	Seven Rivers	31.195660	-100.590356	3725	Alger Harrison
4310503	53730	Seven Rivers	31.800084	-100.796123	19655	Alger Harrison
4310305	53734	Seven Rivers	31.836250	-100.764699	27143	Alger Harrison
4302903	53737	Seven Rivers	31.891535	-100.785607	47500	Alger Harrison
	54505	Seven Rivers	31.152371	-100.671089	5429	Alger Harrison
	55267	Seven Rivers	31.521707	-100.687579	8382	Alger Harrison
	55267	Seven Rivers	31.521707	-100.687579	7500	Alger Harrison
	55686	Seven Rivers	31.763053	-100.857990	11875	Alger Harrison
	55699	Seven Rivers	31.195538	-100.653457	2984	Alger Harrison
	55730	Seven Rivers	32.000690	-101.215894	43846	Alger Harrison
	55797	Seven Rivers	31.246397	-100.649597	10556	Alger Harrison
	55822	Seven Rivers	31.976691	-101.229964	21111	Alger Harrison
4327304		Seven Rivers	31.616943	-100.661666	625	Measured
4327302		Seven Rivers	31.610277	-100.659722	563	Measured
4327302		Seven Rivers	31.610277	-100.659722	597	Measured
4327313		Seven Rivers	31.593055	-100.656388	614	Measured
4327313		Seven Rivers	31.593055	-100.656388	645	Measured
4328212		Seven Rivers	31.614722	-100.581110	413	Measured
4328212		Seven Rivers	31.614722	-100.581110	453	Measured
	55156	Seven Rivers	31.581000	-100.590000	2119	Measured

State well number	BRACS well id	Formation	Latitude	Longitude	TDS (mg/L)	Method
	55175	Seven Rivers	31.586000	-100.646000	1354	Measured
	55176	Seven Rivers	31.375000	-100.618000	4910	Measured
	55177	Seven Rivers	31.352000	-100.610000	1986	Measured
	55178	Seven Rivers	31.358000	-100.609000	6492	Measured
	55179	Seven Rivers	31.356000	-100.609000	3959	Measured
4327309		Seven Rivers	31.613334	-100.660556	725	Measured
4336701		Seven Rivers	31.411112	-100.604445	984	Measured
4336701		Seven Rivers	31.411112	-100.604445	835	Measured
4343301		Seven Rivers	31.367500	-100.628889	772	Measured
2862707	17558	Yates	32.017239	-101.364117	5534	Alger Harrison
	25746	Yates	31.767280	-100.780087	7215	Alger Harrison
	27113	Yates	31.812097	-100.974954	22800	Alger Harrison
	27115	Yates	31.815259	-101.070459	16286	Alger Harrison
	27115	Yates	31.815259	-101.070459	25909	Alger Harrison
	27437	Yates	32.025389	-101.193241	24783	Alger Harrison
	27440	Yates	31.608987	-101.070468	6477	Alger Harrison
	27447	Yates	31.705179	-101.036072	10179	Alger Harrison
	32053	Yates	31.607063	-100.726051	14250	Alger Harrison
	32461	Yates	31.431536	-101.006333	21111	Alger Harrison
	34828	Yates	31.605382	-100.762362	5044	Alger Harrison
	35344	Yates	31.821594	-100.730633	14615	Alger Harrison
	35344	Yates	31.821594	-100.730633	21111	Alger Harrison
	35809	Yates	31.923467	-100.874297	3202	Alger Harrison
	35809	Yates	31.923467	-100.874297	5377	Alger Harrison
	47609	Yates	31.431211	-100.985135	31667	Alger Harrison
4310503	53730	Yates	31.800084	-100.796123	12667	Alger Harrison
4310305	53734	Yates	31.836250	-100.764699	27143	Alger Harrison
4302903	53737	Yates	31.891535	-100.785607	31667	Alger Harrison
	55730	Yates	32.000690	-101.215894	16286	Alger Harrison
	55822	Yates	31.976691	-101.229964	6264	Alger Harrison
4319701		Yates	31.659444	-100.710277	1390	Measured
4319701		Yates	31.659444	-100.710277	1450	Measured
4319701		Yates	31.659444	-100.710277	1022	Measured
4319701		Yates	31.659444	-100.710277	1082	Measured
4319701		Yates	31.659444	-100.710277	1124	Measured
4319702		Yates	31.658889	-100.710001	1588	Measured
4319804		Yates	31.655278	-100.704445	1771	Measured

Notes: TDS = total dissolved solids; mg/L = milligrams per liter.